Assessing the impact of climate change on water resources in Upper Kabul River Basin, Afghanistan

PhD. Thesis

Tooryalay Ayoubi, M.Sc.

Year: 2024

Assessing the impact of climate change on water resources in Upper Kabul River Basin, Afghanistan

A Dissertation

Submitted in partial fulfilment of the

requirements for the doctoral degree ***Dr. rer. nat.***

To the Department of Earth Sciences,

Institute of Geographical Sciences, Applied Physical Geography, Environmental Hydrology and Resource Management,

Freie Universität Berlin

Submitted by

Tooryalay Ayoubi

B.Sc Faculty of Geoscience, Kabul University, Afghanistan

M.Sc. Information Engineering and Science, University of the Ryukyu, Japan

March 2024

First Examiner

Prof. Dr. Achim Schulte

Department of Earth Sciences, Institute of Geographical Sciences, Applied Physical Geography, Environmental Hydrology and Resource Management, Freie Universität Berlin.

Berlin, Germany

Second Examiner

Prof. Dr. Brigitta Schütt

Department of Earth Sciences, Institute of Geographical Science, division of Physical Geography, Freie Universität Berlin,

Berlin, Germany

Date of defense: 11.07.2024

Declaration of independence: I hereby declare that I have completed this disertation independently and have not used any sources or aids other than those specified. This research received the funds from the German Academic exchange Service (Deutscher Akademischer Austauschdienst, DAAD) scholarship. The Freie Universität Berlin provided the environment for this research.

Printed and/or Published with the support of the German Academic Exchange Service, and the Freie Universitätes Berlin.

This page is intentionally left blank

ACKNOWLEDGMENT

I would like to express my gratitude to the individuals who played a crucial role in assisting me in the completion of this research project. First, I am deeply thankful and extend my appreciation to my supervisor, Prof. Dr. Achim Schulte for his guidance, patience and encouraging throughout this extensive undertaking work. His ability to motivate me to seek answers to seemingly insurmountable questions has been invaluable. I also could not have undertaken this journey without my defense committee members, who generously provided knowledge and expertise during the review of this work, and provided their valuable comments. Additionally, this endeavor would not have been possible without the generous support from Dr. Christian Reinhardt -Imjela, which his contribution and valuable comments in completing this Ph.D work is invaluable. The support of my colleagues in Institute of Geographical Sciences, Applied Physical Geography, Environmental Hydrology and Resource Management has been immeasurable acknowledged. Similarly, I am deeply thankful to my family, especially my parents, siblings, relatives, and friends for their support, encouragement and love during completing of this work. A special thanks to my wife, whose unwavering love and support have been instrumental in this journey.

Furthermore, I wish to express my gratitude to the colloquies and authorities at Ministry of Energy and water (MEW), and Ministry of Agriculture, Irrigation and livestock (MAIL) in Afghanistan for providing the crucial weather and streamflow data for this study. I would like to also acknowledge that this work is done based on funding provided by the German Academic Exchange Service (Deutscher Akademischer Austauschdienst/DAAD) scholarship from 10. 2019 to 03. 2024. The findings, conclusions, or recommendations expressed in this study are solely those of the author(s) and do not necessarily reflect the views of the German Academic Exchange Service. Lastly, I want to thank from Freie Universität Berlin (FUB) to facilitate the office and space to complete this work.

تقدیم و قدردانی پایان نامه !

این پایان نامه را ضمن تشکر و سپاس بیکران و در کمال افتخار و امتنان محضر پدر عزیزم و مادر مهربانم بخاطر همه تلاش های محبت آمیزی که در دوران مختلف زنده گی ام انجام داده اند و با مهربانی زنده گی کردن و زیستن را به من آموخته اند؛ تقدیم می نمایم.

TABLE OF CONTENTS

LIST OF FIGURES

LIST OF TABLES

LIST OF ABBREVIATIONS

APHRODITE	Asian Precipitation – Highly Resolved Observational Data Integration
95PPU	95 Percent Probability Uncertainty
a.s.l	Above Sea Level
ARB	Amu River Basin
CMhyd	Climate Model data for hydrologic modelling
CMIP3	Couple Model Intercomparison Project Phase 3
CMIP5	Couple Model Intercomparison Project Phase 5
DACCAR	Danish Committee for Aid to Afghan Refugees
DEM	Digital Elevation Model
ESGF	Earth System Grid Federation
FAO	Food and Agricultural Organization of the United Nations
GCM	Global Climate Model
GIS	Geographic Information System
GLOFs	Glacial Lake Outburst Floods
HKKH	Hindu Kush-Karakoram- Himalaya
HMRB	Harirud-i-Murghab River Basin
HRB	Helmand River Basin
HRU	Hydrological Response Unit
ICIMOD	International Centre for Integrated Mountain Development
IDW	Inverse Distance Interpolation method
IPCC	Intergovernmental Panel on Climate Change
IWRM	Integrated Water Resources Management
KGE	Kling-Gupta efficiency
KRB	Kabul River Basin
MAIL	Ministry of Agriculture, Irrigation and Livestock
MEW	Ministry of Energy and Water
MUSLE	Modified Universal Soil Loss Equation
NRB	North River Basin
NSE	Nash-Sutcliffe Efficiency
OAT	One-at-a-time (sampling method in sensitivity analysis)

PBIAS	Percent bias
RCM	Regional Climate Model
RCP	Representative Concentration Pathway
SA-CORDEX	South Asia domain- Coordinated Regional Downscaling Experiment
SCS-CN	Soil Conservation Service- Curve Number
SRTM	Shuttle Radar Topographic Mission
SWAT	Soil and Water Assessment Tool
SWATCUP	SWAT Calibration and Uncertainty Programs
UKRB	Upper Kabul River Basin
UNCF	United Nations Children's Fund
USDA	United States Department of Agriculture
UTM	Universal Transverse Mercator "coordinate system"

ABSTRACT

The climate change is expected to have significant impacts on the water resources in Afghanistan, which could exacerbate existing challenges related to water availability, water quality, and water management in the future. Therefore, this study investigated the impact of climate change on water availability in Upper Kabul River Basin (UKRB) in Afghanistan by analyzing the past and future streamflow dynamics and hydrology related parameters (e.g., water balance components). A hydrological model was developed in UKRB using the Soil and Water Assessment Tool (SWAT) from 2009-2019, calibrated from 2010-2016 and validated from 2017-2018. The model was built, calibrated and validated on daily and on monthly time intervals to provide a comprehensive analysis of the model's accuracy. The performance of SWAT hydrological model is done by comparing the simulated results to the observed runoff in the Upper Kabul River Basin. SWAT was capable of estimating surface runoff with satisfactory to very good accuracy in 6 observation station across the UKRB during calibration and validation. Four regional climate models (RCMs) were used to project the climate change impact scenarios for the baseline (1986-2005), and future periods of 2030-2049 (hereafter 2040s), and 2080-2099 (hereafter 2090s). The future hydrology projections were built under RCP4.5 and RCP8.5 scenarios. The precipitation and temperature from the RCMs were bias corrected using three bias correction methods including the linear scaling (Ls), delta change (Dc) and empirical quantile mapping (Eqm). The bias corrected results in the baseline period were validated with APHRODTE precipitation and temperature data which is used as observations in the absence of in situ measurements. The precipitation and temperature outputs from bias correction methods were analyzed based on monthly, seasonal and annual intervals, and then the outputs from the linear scaling method were used in SWAT model for further climate change impact analysis.

The results indicated that all three bias correction methods improved the raw data of climate model outputs (RMCs), reduced the biases in precipitation and temperature variables based on APHRODITE datasets. However, the outputs from linear scaling performed better than empirical quantile mapping in capturing the distribution of precipitation, maximum temperature (Tmax) and minimum temperature (Tmin) in the historical period. Therefore, the Linear method was selected for further water availability assessment in the study area. According to the bias correction results, under the RCP4.5 scenario, the annual temperature is expected to increase by 1.9 °C in the 2040s and 2.3 °C in the 2090s. However, under the RCP8.5 scenario, the increase in mean annual

temperature is projected to be more severe, with an increase of 3.1 °C in the 2040s and 6.1 °C in the 2090s. In addition, this study also examined how the extremes in temperature and precipitation might change in the future, specifically looking at six indices: annual total wet day precipitation (PRCPTOT), extremely wet days (R99p), monthly minimum value of daily minimum temperature (TNn), monthly maximum value of daily maximum temperature (TXx), warm nights and warm days over the course of the 21st century (2006-2100) in UKRB.

Results showed that temperatures increased in all seasons, with earlier peaks occurring in June instead of July in both periods of 2040s and 2090s. The results also show that, there was a significant increase in extremes of maximum and minimum temperature's trend indicating that the future temperature is getting hotter. The future mean annual precipitation observed to be increase in the 2040s and 2090s compared to the baseline, however, an insignificant decreasing trend of annual precipitation observed during 2006-2100. The future mean annual precipitation will increase by 5 % in 2040s and 1 % 2090s under RCP4.5 over the study area. Moreover, under RCP8.5, the mean annual precipitation is expected to increase by 9 % in 2040s and almost + 2% in 2090s compared to the baseline. The annual spatial precipitation changes range from -3 % to +27 % in the 2040s and from -8 % to + 17% in the 2090s under RCP4.5. Similarly, under RCP8.5, it ranges from -3 % to +44 % in the 2040s and from -10 % to +27 % in the 2090s. The future hydrological results show that there will be an increase in mean annual runoff and mean annual total water yield in the 2040s and 2090s compared to the baseline period in UKRB. The results of our study also revealed a backward shift in the annual discharge peaks from May and June to March and April in Tang-i-Gulbahar and Shukhi stations, while in Tang-i-Saidan station, the runoff peak shifted from April to March in both periods of 2040s and 2090s in UKRB due to climate change. The results also show that there has been a significant increase in the future actual evapotranspiration (ET) and potential evapotranspiration (PET) in the UKRB under both RCP4.5 and RCP8.5 scenarios. However, decreases in mean annual snowfall, snowmelt, sublimation, percolation and ground water recharge is expected in the future under both RCP4.5 and RCP8.5 scenarios. The decrease in snowmelt and glacier melt could also lead to changes in the timing and volumes of river flow which can impact the water availability for agriculture, urban use, and hydropower generation. Overall, this study contributes to the growing body of knowledge on climate change impacts on water resources and emphasizes the need for continued research in this field.

ABSTRACT (DEUTSCH)

Es wird erwartet, dass der Klimawandel erhebliche Auswirkungen auf die Wasserressourcen in Afghanistan haben wird, so dass sich die bestehenden Herausforderungen in Bezug auf Wasserverfügbarkeit, Wasserqualität und Wassermanagement in Zukunft noch verschärfen könnten. Daher wurden in dieser Studie die Auswirkungen des Klimawandels auf die Wasserverfügbarkeit im Einzugsgebiet des Oberen Kabul Flusses (UKRB) in Afghanistan untersucht, wobei die vergangene und künftige Abflussdynamik sowie der Einfluss auf die Wasserhaushaltskomponenten analysiert wurden. Mit dem Soil and Water Assessment Tool (SWAT) wurde für den Zeitraum 2009-2019 ein hydrologisches Modell entwickelt, von 2010-2016 kalibriert und von 2017-2018 validiert. Das Modell wurde in täglichen und monatlichen Zeitschritten erstellt, kalibriert und validiert, um eine umfassende Analyse der Genauigkeit des Modells zu ermöglichen. Die Güte des hydrologischen Modells wird durch den Vergleich der simulierten Ergebnisse mit dem beobachteten Abfluss im Einzugsgebiet des Oberen Kabul bewertet. SWAT war während der Kalibrierung und Validierung in der Lage, den Oberflächenabfluss an 6 Beobachtungsstationen im gesamten UKRB mit zufriedenstellender bis sehr gute Genauigkeit zu simulieren. Im Anschluss wurden die Daten von vier regionalen Klimamodellen (RCMs) wurden, um die hydrologischen Auswirkungen des Klimawandels für die Basisperiode (1986-2005) und die zukünftigen Zeiträume 2030-2049 (im Folgenden 2040er) und 2080-2099 (im Folgenden 2090er) abzuschätzen. Die zukünftigen Projektionen wurden auf Basis der Szenarien RCP4.5 und RCP8.5 erstellt. Der Niederschlag und die Temperatur aus den RCMs wurden mit Hilfe von drei Methoden einer Bias-Korrektur unterzogen (Linear Scaling Ls; Delta-Change, Dc; Empirical Quantile Mapping, Eqm). Die Bias korrigierten Ergebnisse für den Basiszeitraum wurden mit APHRODITE-Niederschlags- und Temperaturdaten validiert, die in Ermangelung von In-situ-Messungen als Beobachtungen verwendet werden. Die Ergebnisse der Bias-Korrektur wurden auf der Grundlage monatlicher, saisonaler und jährlicher Zeitschritte evaluiert, wobei die Ergebnisse der Ls Methode in SWAT für weitere Analysen der Auswirkungen des Klimawandels verwendet wurden.

Die Ergebnisse zeigten, dass alle drei Methoden zur Bias-Korrektur die Rohdaten der Klimamodell-Outputs (RMCs) verbesserten und den Bias der Niederschlags- und Temperaturreihen auf der Grundlage der APHRODITE-Datensätze reduzierten. Die Ergebnisse der Ls-Methode zeigten bessere Ergebnisse bei der Korrektur von Niederschlag,

Maximaltemperatur (Tmax) und Minimaltemperatur (Tmin) im historischen Zeitraum als die Eqm Methode. Daher wurde die lineare Methode für die weitere Analyse der Wasserverfügbarkeit im Untersuchungsgebiet ausgewählt. Nach den Ergebnissen der Bias-Korrektur wird unter dem RCP4.5-Szenario ein Anstieg der Jahrestemperatur um 1,9 °C in den 2040er Jahren und um 2,3 °C in den 2090er Jahren erwartet. Unter dem RCP8.5-Szenario wird der Anstieg der mittleren Jahrestemperatur jedoch mit einem Anstieg von 3,1 °C in den 2040er Jahren und 6,1 °C in den 2090er Jahren voraussichtlich stärker ausfallen. Außerdem wurde in dieser Studie anhand von sechs Indizes (jährlicher Gesamtniederschlag an Regentagen, PRCPTOT; extrem feuchte Tage, R99p; monatliches Minimalwert der täglichen Minimaltemperatur, TNn; monatlicher Maximalwert der täglichen Maximaltemperatur (TXx), warme Nächte und warme Tage im Laufe des 21. Jahrhunderts (2006-2100)), untersucht, wie sich Temperatur- und Niederschlagextreme in der Zukunft verändern könnten.

Die Ergebnisse zeigten, dass die Temperaturen in allen Jahreszeiten anstiegen, wobei die Spitzenwerte in beiden Zeiträumen (2040 und 2090) eher im Juni als im Juli auftraten. Gleichzeitig war ein signifikanter Anstieg der Extremwerte der Maximal- und Minimaltemperaturen zu verzeichnen, was darauf hindeutet, dass die Temperaturen in Zukunft heißer werden. Der künftige mittlere Jahresniederschlag nimmt in den 2040er und 2090er Jahren im Vergleich zum Basisszenario zu, wobei jedoch im Zeitraum 2006-2100 ein geringer Rückgang des Jahresniederschlags zu beobachten ist. Der künftige mittlere Jahresniederschlag wird unter RCP4.5 im Untersuchungsgebiet in den 2040er Jahren um 5 % und in den 2090er Jahren um 1 % zunehmen. Darüber hinaus ist unter RCP8.5 zu erwarten, dass der mittlere Jahresniederschlag in den 2040er Jahren um 9 % und in den 2090er Jahren um fast 2 % gegenüber dem Ausgangswert zunehmen wird. Die jährlichen räumlichen Niederschlagsänderungen reichen von -3 % bis +27 % in den 2040er Jahren und von -8 % bis + 17 % in den 2090er Jahren unter RCP4.5. Unter RCP8.5 reicht die Spanne von -3 % bis +44 % in den 2040er Jahren bis -10 % bis +27 % in den 2090er Jahren. Die hydrologischen Ergebnisse zeigen, dass der mittlere jährliche Abfluss und der mittlere jährliche Gesamtwasserertrag in den 2040er und 2090er Jahren im Vergleich zum Basiszeitraum im UKRB ansteigen werden.

Die Ergebnisse unserer Studie zeigen auch eine Verlagerung der jährlichen Abflussmaxima von Mai /Juni auf März/April in den Stationen Tang-i-Gulbahar und Shukhi, während sich in der Station Tang-i-Saidan die Abflussspitze in beiden Zeiträumen der 2040er und 2090er Jahre im

UKRB aufgrund des Klimawandels von April auf März verschiebt. Die Ergebnisse zeigen auch, dass es einen signifikanten Anstieg der zukünftigen tatsächlichen Evapotranspiration (ET) und der potenziellen Evapotranspiration (PET) im UKRB sowohl unter dem RCP4.5 als auch dem RCP8.5 Szenario geben kann. Es wird jedoch erwartet, dass der mittlere jährliche Schneefall, die Schneeschmelze, die Sublimation, die Perkolation und die Grundwasserneubildung sowohl unter dem RCP4.5- als auch unter dem RCP8.5-Szenario zurückgehen werden. Der Rückgang der Schneeschmelze und der Gletscherschmelze könnte auch zu Veränderungen des Zeitpunkts und der Menge des Abflusses führen, was sich auf die Verfügbarkeit von Wasser für die Landwirtschaft, die urbane Nutzung und die Wasserkrafterzeugung auswirken kann. Insgesamt trägt diese Studie zum wachsenden Wissen über die Auswirkungen des Klimawandels auf die Wasserressourcen bei und unterstreicht den Bedarf an weiterer Forschung in diesem Bereich.

1 INTRODUCTION

Climate change is increasingly acknowledged as a critical global issue, exerting significant impacts on hydrological processes, including precipitation, evapotranspiration, and runoff (Sediqi and Komori, 2023). These changes pose significant challenges to the sustainability of water resources worldwide (Shiru *et al.*, 2020; Sediqi and Komori, 2023). Moreover, the climate change can have negative consequences on the natural ecosystem, as well as a severe impact on social life and economic development (Calvin *et al.*, 2023). In developing countries like Afghanistan, which is characterized by its arid and semi-arid climate, the impacts of climate change are particularly critical and acute. The Kabul River Basin (KRB) is one of the five major river basins in Afghanistan is crucial to the socio-economic stability of the country and the neighboring country Pakistan, is increasingly vulnerable to the risks and disruptions caused by the impact of climate change. The KBR which (Figure 1-1) generates 40 % of the country's total runoff serves as the main water source for millions of people in both Afghanistan and Pakistan, providing essential water for domestic use, agriculture, and hydropower generation (Ahmad and Wasiq, 2004). However, recent research indicates that the hydrological dynamics of the KRB are being profoundly changed by the impact of climate change, raising concerns about the future water availability in the basin.

1.1 Overview of climate change in Afghanistan

Afghanistan is categorized as a semi-arid area and is a landlocked country with a total area of 652,864 sq.km. It is located at crossroads of Central Asia and South Asia between latitudes 29.5°N - 38.5° N and longitudes 60.5°E - 75°E. The country extends 1,300 km from northeast to southwest, and about 600 km from north to south. Afghanistan is introduced with a high mountainous terrain which the Hindu Khush, the westernmost extension of the Karakorum and the Himalayas, and Pamir ranges are the famous rising over 7000 m from see level. Afghanistan shares the border with six counties including Tajikistan, Uzbekistan, Turkmenistan, Pakistan, Iran and China. Afghanistan has abundant water resources, more than 80 percent derived from snow and glaciers melt in the Hindu Kush mountains (Ahmad and Wasiq, 2004). Water resources endowment in Afghanistan is significant on an annual per capita basis with five major river basins (MEW and JICA, 2019) including the Kabul River Basin (KBR), Helmand River Basin (HRB), Harirud-i-Murghab River Basin (HMRB), North River Basin (NRB) and Amu River Basin (ARB), Figure 1-1. Annual

available water resource is said to be 75 billion m^3 (Surface water: 57 billion m^3, Groundwater: 18 billion m^3) as total for the entire country (MEW and JICA, 2019).

Afghanistan is among the countries most vulnerable to the impacts of climate change, primarily due to its geographical location, socio-economic conditions (e.g., low adaptive capacity), and the past/ongoing conflicts which hampers effective climate adaptation strategies (Kreft *et al.*, 2015; Aich, N. Akhundzadah, *et al.*, 2017). The key sectors, including water, energy, and agriculture are among the most vulnerable to climate change in Afghanistan (Aich, N. Akhundzadah, *et al.*, 2017). The Sixth Assessment Report of the Intergovernmental Panel on Climate Change (IPCC, 2021) identifies South Asia, including Afghanistan as a climate hotspot, where rising temperatures, shifting precipitation patterns, and increased the frequency of extreme weather events are expected to have severe consequences in the future. Studies show that Afghanistan has already experienced a warming of approximately 1.8°C since the mid-20th century, a trend that is expected to continue, with the projections indicating a further air temperature increase of 2.5°C to 3°C by the mid-21st century (2050s) under a high-emission/RCP8.5 scenario (IPCC, 2021). This temperature warming trend is particularly concerning for Afghanistan's water resources, which are heavily dependent on snowmelt and glaciers from the Hindu Kush mountain range. The glaciers and snowpack's in the country act as natural reservoirs, gradually releasing water into the Rivers, thereby sustaining the river's flow during the dry seasons. However, studies have shown that the accelerated melting of glaciers, coupled with reduced snowfall, is leading to a decline in the volume and timing of surface runoff in the in rivers, particularly in the KRB (Shroder et al., 2016). This in fact shows that Afghanistan's average annual precipitation is expected to become more erratic, with longer dry spells interspersed with intense rainfall events, increasing the likelihood of both droughts and floods (Shahid, 2018).

The precipitation of the country has been estimated around 300 mm per year, while in the north overall, annual precipitation averages 400 mm per year (Ahmad and Wasiq, 2004). This precipitation hardly satisfies the incremental water demand of the country, while precipitation varies geographically (MEW and JICA, 2019). The country has a harsh climate of the continental type and the severity of winter is accentuated by the range of high mountain altitudes. Winter and spring are the seasons of most variable weather, where most of the annual precipitation occurs in these seasons (December to May) (Mills, 2013). Additionally, more than 80% of the annual rainfall is in the form of snow at the highlands of above 2,500 m in elevation. The snow line is between 4,000-5,000 m, so there is little permanent snow and there are few glaciers (Ahmad and Wasiq,

2004). The snow melt starts in March, peaks in May and lasts until June or July. Summers in Afghanistan are warm, and there is no rainfall during the summer months. As a result, droughts are frequent, creating food security problems for many Afghans. Runoff from the mountains into the rivers is heavy for a brief period during the spring thaw, sometimes causing floods and landslides. For the rest of the year, runoff tends to be irregular and low. Particularly in summer, there is no or low stream flow in rivers, except those feds by snow and glaciers. Agriculture is the mainstay of Afghanistan's economy, with approximately 80% of the population engaged in it. However, since most of the irrigation facilities were destroyed by years of war, the occurrences of floods and erosion are increasing due to devastated river basins and deteriorating water-retaining capacity, causing damage to downstream irrigation systems (MEW, 2019).

Afghanistan has a population of 29 million, with 79% living in rural areas (HydrateLife, 2012). Only 27% of the population has access to improved water resources, dropping to 20% in rural areas (HydrateLife, 2012). The situation is even worse regarding access to improved sanitation facilities, with only 5% of the population having access nationwide, and just 1% in rural areas, ranking Afghanistan among the worst in the world (HydrateLife, 2012). According to a survey by the United Nations Children's Fund (UNCF), the lack of clean drinking water has been fatal to Afghanistan's children, with 102 out of every 1,000 children born dying before reaching the age of five. One major reason for these appalling statistics is that infrastructure has been destroyed by years of war. As a post-conflict country, Afghanistan faces significant challenges in securing reliable water for drinking, agriculture, and food security.

1.2 The Kabul River Basin and its Importance

The Kabul River Basin (KRB) is located in the eastern part of Afghanistan (Figure1-1). The KBR is a critical water source for Afghanistan, particularly for the densely populated regions around Kabul city and the agricultural heartlands of Nangarhar province (Favre & Kamal, 2004). The basin covers approximately 70,000 square kilometers, encompassing a diverse range of ecosystems from high-altitude glaciers to arid plains (Favre & Kamal, 2004). The river, which is 700 km long, flows 460 km in Afghanistan and 240 km in Pakistan, receiving substantial flows from several tributaries. The river's flow is primarily fed by snowmelt from the Hindu Kush, making it highly sensitive to temperature fluctuations. The KRB generates almost 40% of Afghanistan's total runoff and drains 12% of its area. It has the highest annual flows (24 bcm) but the smallest area (79,000 km²), followed by the Amu Darya Basin (17 bcm) with an area of about

242,000 km², and the Helmand River Basin (14 bcm) with the largest area (320,000 km²) (Ahmad and Wasiq, 2004). The basin's hydrology is complex, with significant seasonal variations driven by the melting of snow in the spring and summer, which coincides with the peak agricultural demand for water. Surface water resources supply approximately 28% of the total irrigated area (Mills, 2013; Mohammad Tayib Bromand, 2015) and account for 35% of Afghanistan's population. The basin includes the Kabul urban area, which is one of the biggest engines of economic growth and has the fastest population growth rate in the country. The KRB is divided into eight sub-basins, as shown in Figure 1-1, based on climate, hydrology, and physiography according to the IWRM procedure of 2011. The significance of the KRB extends beyond Afghanistan's borders, as the river flows into Pakistan, where it merges with the Indus River. This transboundary nature of the river adds another layer of complexity to water management in the region, with potential implications for regional security. As water scarcity becomes more pronounced due to climate change, the competition for water resources between Afghanistan and Pakistan is likely to intensify, potentially leading to conflicts (Mustafa et al., 2018). The strategic importance of the KRB, therefore, cannot be overstated, as it underpins both national and regional stability.

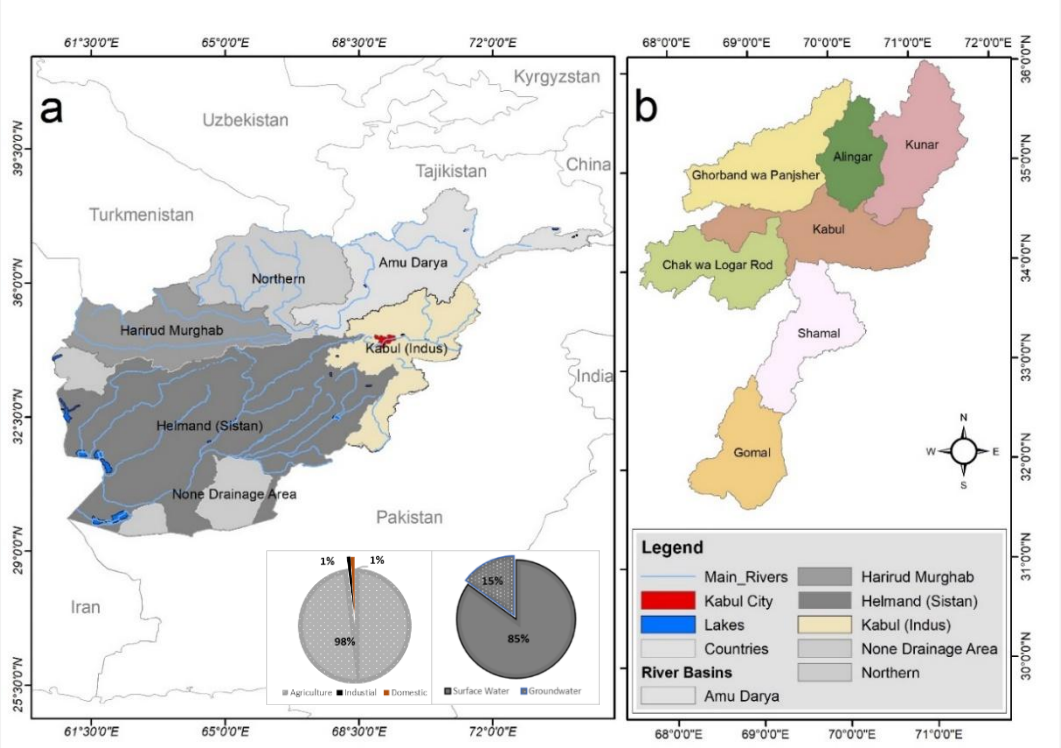

Figure 1-1: Major river basin in Afghanistan (a), and the major division of watersheds in KRB (b). (Source: National Atlas of Afghanistan and MEW 2011).

1.3 Impact of climate change on the Kabul River Basin

Recent hydrological studies and climate models have provided a grim outlook for the future of the KRB. Ahmad et al. (2023) conducted an analysis using global climate models to project the future flow of the Kabul River under various climate scenarios. Their findings suggest a potential reduction in the average annual flow by up to 20% by 2050, driven by reduced snow cover and earlier snowmelt Ahmad et al. (2023). This reduction in flow is expected to have severe consequences for water availability during the critical summer months when demand for irrigation and drinking water is highest. Moreover, the timing of water flow is also projected to shift, with peak flows occurring earlier in the year due to earlier snowmelt, which may result in water shortages later in the summer (Ahmad et al., 2023). This seasonal mismatch between water availability and demand poses a significant challenge for water resource management in the KRB. Additionally, the increased frequency of extreme weather events, such as heavy rainfall and floods, threatens to disrupt the already fragile water infrastructure in the region, further complicating the management of water resources (Ilyas et al., 2022). As a result of climate change, a decline in water availability would directly impact agricultural productivity, exacerbating food insecurity in the region already struggling with high levels of poverty and malnutrition. Water scarcity in the KRB could also exacerbate existing social tensions and contribute to conflict. Afghanistan has a history of localized disputes over water resources, and as climate change reduces the availability of water, these conflicts are likely to become more frequent and intense (Gioli et al., 2014). Moreover, the transboundary nature of the Kabul River adds an international dimension to these challenges, as both Afghanistan and Pakistan depend on its waters. The lack of a comprehensive bilateral agreement on water sharing between the two countries could lead to increased tensions as water becomes scarcer (Mustafa et al., 2018). As the climate change impact continues to alter the region's hydrological regime, the implications for water resources and water security, agriculture, energy, and regional stability are profound.

The key objective of the study is to analyze the current water availability, and the potential changes in future water resources (e.g., runoff, snowmelt, groundwater recharge, actual evapotranspiration, potential evapotranspiration) under climate change in the Upper Kabul River Basin (UKRB), under RCP4.5 and RCP8.5 scenarios for the period of 2040s (2030-2049) and 2090s (2080-2099). Therefore, this study aims to analyze the current water availability, and the climate-induced potential impacts on future water resources in Upper Kabul River Basin (UKRB) which includes three watersheds; the Logar watershed, the medium Kabul river watershed, and the

Ghorband & Panjshir watershed using the SWAT hydrological model and the Regional Climate Models (RCMs) under RCP4.5 and RCP8.5 scenarios for the period of 2040s (2030-2049) and 2090s (2080-2099). By understanding the specific vulnerabilities and risks associated with climate change in the KRB, stakeholders can develop more effective strategies to safeguard this critical water resource for future generations.

1.4 Problem statement

Currently, the Kabul River Basin (KRB) faces severe water resource challenges, particularly in Kabul city, where groundwater levels are rapidly declining due to population growth, groundwater pollution, and climate change, Table 1-1 (Mills, 2013). The basin's population has tripled since the last century, increasing water demand as surface water supplies diminish and groundwater consumption rises, leading to aquifer depletion (Bromand, 2015). In Kabul, 85% of the population relies on groundwater, primarily from shallow aquifers (Figure 1-2). Recent studies show a significant decline in groundwater levels, with drops of over 15 meters in parts of the city between 2003 and 2016 (Zaryab et al., 2017). Groundwater levels are decreasing at an annual rate of 1.7 meters (Zaryab et el., 2017), driven by the growing population, which has doubled since the 1990s. Many shallow wells, springs, and karizes have dried up, making sustainable water management crucial for urban and rural communities.

Figure 1-2: A child is filling his pots with a hand pump in Kabul city (a) (Source: newslens.pk), and the hand-pump made by DACAAR to support the drought and conflict-affected communities in Afghanistan (b) (Source: DACAAR, 2021).

Table 1.1: Decrease in ground water level in the last 34 years in the KRB [6].

Year	Water Level change (m)	Decline (m/year)
1982-2003	6	0.28
2003-2016	15	1.15

Other studies confirm this alarming trend. For example, (Brati, Ishihara and Higashi, 2019) reported a 0.77 meters/year decline in groundwater levels over the past decade (Figure 1-3). Mack, et. al., (2013) observed a similar decline in Kabul, despite some improvement in rural areas due to normal precipitation after the early 2000s drought (Figure 1-3). Some of the key issues in the KRB include:

1. Increasing water deman due to rapid population growth, especially in Kabul.
2. Loss of water recharge zones and increased floods due to climate change, urbanization and deforestation.
3. Water scarcity exacerbated by climate change which disrupting weather patterns.
4. Increasing the gaps between water supply and demand due to climate change impacts.
5. Declining groundwater levels and reduced access to safe water for domestic, agricultural, and environmental needs.

The impact of climate change on water resources and water availability is significant, specially for surface runoff and ground water recharge. To explore the relationship between climate change and water availability, we want to develop the SWAT hydrological model and perform bias corrections of the RCMs output under RCP4.5 and RCP8.5 in the UKRB. threfore, this study addresses the following research questions:

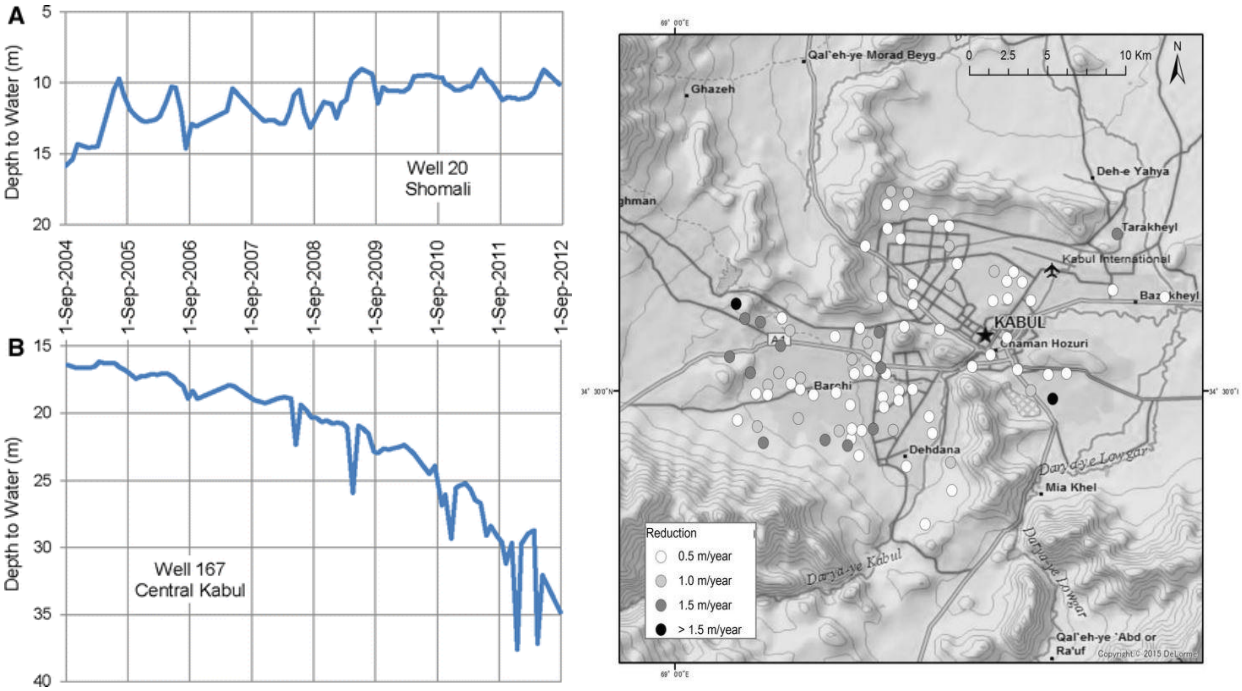

Figure 1-3: Left graphs: Monthly depth to water at Afghanistan Geological Survey wells; a 20 wells at shomali, and b 167 wells in center of Kabul city, from September 2004 to 2012 in the Kabul Basin-Afghanistan (Mack, Chornack and Taher, 2013), Right map: Location of ground water wells in Kabul city.

1.5 Research Questions

In this study, the main research questions that will be considered are:.

1. How has climate (e.g., precipitation and temperature) changed in recent decades, and what will be the change in future climate over time compared to the baseline?

   Under this question, the sub questions are addressed:

   - How have annual precipitation and temperature trends changed from the baseline period (1986-2005) to the 2040s and 2090s in Upper Kabul River Basin.
   - What are future projections of the temperature and precipitation magnitude under RCP4.5 and RCP8.5 scenarios compared to the baseline?
   - How do bias correction techniques (e.g., linear scaling, quantile mapping, and delta change) improve precipitation and temperature in climate models against APHRODITE data?

2. How will the climate change impact water availability in the UKRB under RCP4.5 and RCP8.5 in 2040s and 2090s?

   Under this question, the sub questions are addressed:

- How will climate (temperature and precipitation) influence the hydrology (e.g., surface runoff, evapo-transpiration, and groundwater recharge)?
- How do climate change-induced shifts in temperature and precipitation influence the shift in runoff regimes (peaks) to earlier or future months?
- Can a SWAT hydrological model be developed for future climate studies and water availability in data-poor regions like the KRB?

1.6 Objective of study

The key objective of the study is to analyze the current water availibility, and the potential changes in future water resources (e.g., runoff, snowmelt, groundwater recharge, actual evapotranspiration, potential evapotranspiration) under climate change impact in the Upper Kabul River Basin under RCP4.5 and RCP8.5 scenarios for the period of 2040s (2030-2049) and 2090s (2080-2099).

The comprehensive study and management of water resource for now and late 21st century will lead to more sustainable water resources in the basin and even in the country. One of the main solutions to evaluate the current water resources is to take a modeling approach in which the restricted data available are used for model calibration and validation, but then if the model is deemed valid, model predictions can be used to provide a deeper understanding of the runoff drivers in the basin. Therefore, this study will contribute to the overall understanding of the hydrological characteristics in the UKRB through the evaluation of the SWAT (Soil and Water Assessment tool) model's performance. Moreover, the study will provide a comprehensive analyze in the impact of climate change on future water resources in UKRB, considering multiple aspects such as precipitation, temperature, runoff, and groundwater recharge. The study will also contribute to provide actionable information for effective water resource management and adaptation strategies in the KRB. The key objectives of this study summarized as following:

1. Estimation of presend and future surface runoff and water balance by utilizing the Soil and Water Assessment Tool (SWAT) hydrological model in UKRB.
2. Assessment of the future (2040s, 2090s) precipitation and temperature variation, compared to the historical period (1986-2005) and performing of three bias correction methods.
3. Projection of the future climate change impacts on surface runoff and total water availability under RCP4.5 and RCP8.5 scenarios.

2 LITERATURE REVIEW

Climate change is increasingly acknowledged as a critical global issue, exerting significant effects on hydrological processes, including precipitation, evapotranspiration, and runoff (Sediqi and Komori, 2023). These changes pose significant challenges to the sustainability of water resources worldwide (Shiru *et al.*, 2020; Sediqi and Komori, 2023). Also, the climate change can have negative consequences on the natural ecosystem, as well as a severe impact on social life and economic development (Calvin *et al.*, 2023).

The Intergovernmental Panel on Climate Change (Calvin *et al.*, 2023) report shows that the global surface temperature in 2011-2020 was 1.1 °C higher than 1850–1900, with larger increases over lands (1.59°C) than over oceans (0.88 °C) (Masson-Delmotte *et al.*, 2021; Calvin *et al.*, 2023). Also, the global surface temperature between 2001–2020 increased 0.99 °C compared to the period of 1850-1900 (Masson-Delmotte *et al.*, 2021). Changes observed in the earth's climate since the early 20th century are primarily driven by human activities (e.g., burning fossil fuel and agriculture), and natural processes especially anthropogenic factors that cause increase in greenhouse gas level in the earth's atmosphere, raising the earth's average surface temperature (Calvin *et al.*, 2023; Intergovernmental Panel on Climate Change (IPCC), 2023). The rise in global temperature is highly related to change in hydro-climatic variables and sea-level rise (Tadese, Kumar and Koech, 2020; Hoegh-Guldberg *et al.*, 2022).

Hydrological systems, especially snow and glaciers can be impacted by global climate change, altering the timing and amount of runoff in mountainous areas (Arian *et al.*, 2016). The Hindu Kush-Karakoram- Himalaya (HKKH) region has the highest density of glaciers outside the poles and feed many larger rivers in Asia, which Indus river is one of them (Bokhari *et al.*, 2018). Previous studies showed that, the HKKH region is expected to see a higher rate of mean surface temperature rise towards 2100 than the global average (Ahmad *et al.*, 2015; Iqbal *et al.*, 2018). Increasing temperature will change the precipitation pattern, consequently, the runoff in river and the water cycle will be significantly affected in the region (Iqbal *et al.*, 2018) including the KRB being one of the major tributary for the Indus river. A study showed that, an increase of 0.39 °C was observed in temperature of Central Asia from 1979 to 2011 (Hu *et al.*, 2014). While, studies predicted a mean temperature increase of up to 6.5 °C compared to the pre-industrial period by the end of this century across Central Asia (Kreft *et al.*, 2015; Reyer *et al.*, 2017). Ridley et al. (2013) found that the Karakorum will receive more precipitation due to an increase of westerly

disturbances. This is confirmed by (Mukhopadhyay and Khan, 2014) which projects warming up to 2 °C and a slight increase of precipitation (8–10%) until 2050 for the Upper Indus River Basin including the Hindukush region.

Afghanistan is categorized as a semi-arid country in terms of climate; the annual average precipitation of the country has been estimated about 300mm, which hardly satisfies the incremental water demand of the whole country, although precipitation varies geographically (MEW and JICA, 2019). The key sectors, including water, energy, and agriculture, are among the most vulnerable to climate change in Afghanistan (Aich, N. A. Akhundzadah, *et al.*, 2017a). Winter precipitation accounts for 80 % of the country's total water resources while in summer, water resources are not enough to satisfy crop's water demand (Akhtar *et al.*, 2021). The temporal gap between precipitation and peak demand is currently more or less closed by the fact that a high share of precipitation is snow melting in late spring or summer. It is expected that this rather advantageous pattern will change due to climate change, with the basin receiving less snow but more rainfall, resulting in the tendency for a quicker response of the basin on rainfall. Consequently, there would be an increased mismatch between water availability and water demand, which would widen the gap.

The country frequently experienced severe weather conditions or climatic events, resulting in significant economic and human losses (Aich, N. A. Akhundzadah, *et al.*, 2017a; UC Louvain, 2020). For example, the deadliest disaster event recorded between 2000 and 2018 was a cold spell occurring in January and February 2008, which resulted in 1,317 fatalities (UC Louvain, 2020). However, the main disaster types affecting the country are floods and drought. Moreover, between 2000 and 2018, Afghanistan experienced 66 floods, accounting for nearly 56 % of recorded disasters, resulting in a total of 2,374 deaths (34.4% of total fatalities). However, a drought impacted 8,710,000 people over the same period (UC Louvain, 2020). The most impactful disaster event in terms of affected population in Afghanistan was a drought in year 2000, where more than 2.5 million people suffered from water shortages and famine (UC Louvain, 2020).

The snow and glaciers in Afghanistan are at high risk, especially in summer season the snow and glacier cover is retreated and high melting occurs due to climate change (Arian *et al.*, 2016). Afghanistan has 3,940 glaciers covering an overall area of 2,677 km². So far, almost 13.8% of the glacier area was lost from 1990 to 2015, Figure 2-1, and this reduction is expected to continue (ICIMOD, 2018; Maharjan *et al.*, 2021). The glacier area lost was 3.6 % between 1990 and 2000; 4.7 % between 2000 and 2010; and nearly 6 % from 2010 to 2015 (Maharjan *et al.*, 2021). This

shows that the loss percentage has been greater in recent decades. Figure 2-2 shows the variations in loss of glacier's area at different elevations. The analyses by (Maharjan *et al.*, 2021) indicated that, the maximum area loss was at elevations from 4,700 m to 5,200 m from see level (m.s.l). The largest glacial area loss was 47 Km^2 at elevations from 4,900 m to 5,000 m.s.l and above that there have been no significant changes in glacial areas. Whereas, the investigations showed that glacial areas below 3200 m.s.l have completely disappeared in Afghanistan (Maharjan et al., 2021).

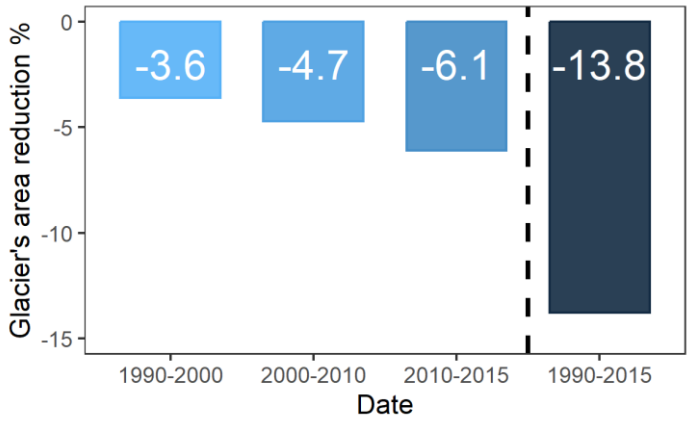

Figure 2-1: The change in glaciers area in Afghanistan (Source: S.B. Maharjan et al., 2021).

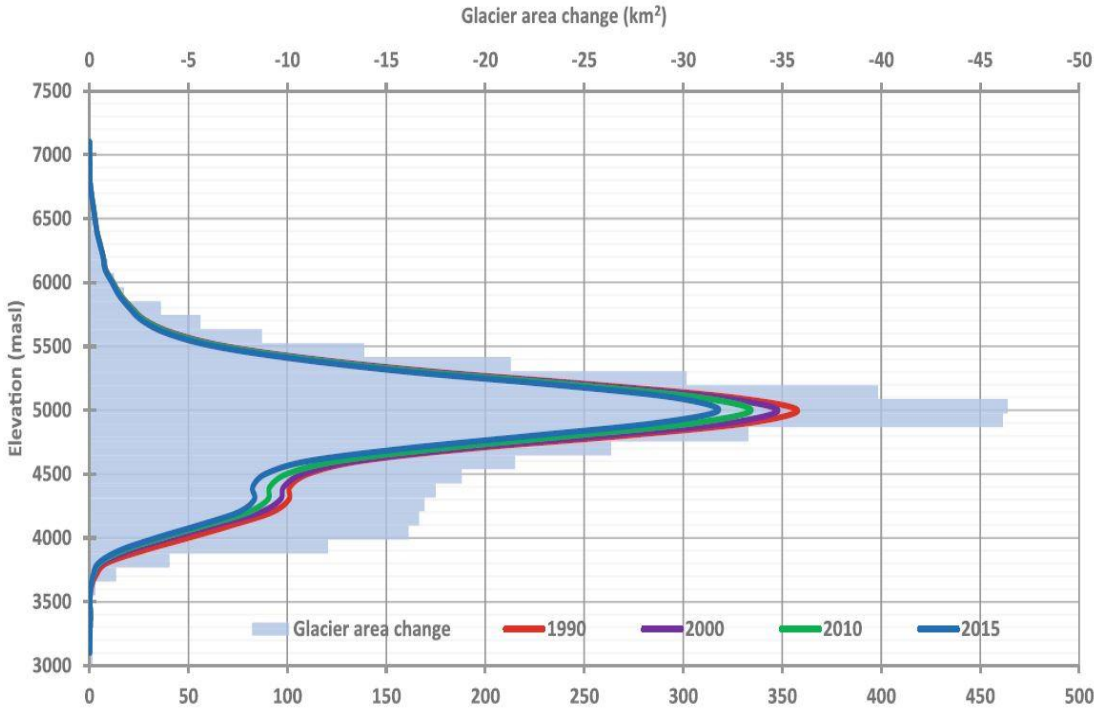

Figure 2-2: Distribution of glacial area and changes in area from 1990 to 2015 at 100 m elevation zone (Source: S.B. Maharjan et al., 2021).

Glaciers play a critical role in the supply of drinking water and irrigation. Currently, the early melting of glaciers, combined with spring precipitation, is triggering catastrophic floods laden with rocks. Research by the International Centre for Integrated Mountain Development and Ministry of Energy and Water (ICIMOD/MEW) indicated that in some regions of Afghanistan, the number of glaciers and glacial lakes has increased. This is likely due to larger glaciers breaking up because of climate change (Bjelica, 2021). Glacial Lake Outburst Floods (GLOFs) often come from these new glacial lakes. For instance, in a recent incident on 12 July 2018, flash floods originating from a glacial lake at an elevation of 4,500 m traveled approximately 14 km down a tributary in Panjshir province (ICIMOD, 2018). This event caused the loss of at least 10 lives, destruction of infrastructures, damage of fertile agricultural lands, and the closure of major roads (ICIMOD, 2018). About 85% of Afghanistan's total agricultural yield is produced by irrigation, which consumes 98 % of the water used. However, irrigation performance at the basin level is poor (Akhtar *et al.*, 2018, 2021). Kabul River Basin (KRB), which covers more than 12% of Afghanistan's territory, generates approximately 26 % of the country's total annual stream-flow. The basin accounts for 35 % of population, and has the fastest population growth rate in the country, plays a key role in developing the country's economic growth.

Recently Sidiqi et al. (2018) conducted a study on climate change projections in the Kabul River Basin (KRB) using three Global Climate Models (GCMs). Their findings indicated that the mean annual temperature is projected to increase by 1.8 °C, 3.5 °C, and 4.8 °C by the 2020s, 2050s, and 2090s, respectively. Their results also indicated a projected increase in mean annual precipitation. Other study was conducted on climate change and its implications for stream flow in the KRB (Wi et al., 2015). The study utilized GCMs to project the mean annual temperature for the future period (2050s). Their results indicated that under RCP4.5 and RCP8.5 scenarios, the mean annual temperature is expected to increase by 2.2 °C and 2.8 °C, respectively. However, the study does not identify a clear trend in precipitation (Wi et al., 2015). Moreover, a study conducted by McSweeney et al. (2010) indicate an increase of 0.6 °C in mean annual temperature since 1961. Their results also revealed a slight decrease in mean annual precipitation, averaging 2 % per decade. However, it is important to note that the analysis of past data in this study relied on station data with significant data gaps. Additionally, in this study, the explanatory power of the projections is limited due to the coarse resolution of the CMIP3 global models, which have a resolution of 2.5 degrees, particularly given the extremely mountainous character of the country.

Valentin Aich (2016) used reanalysis data from Global Soil Wetness Project Phase 3 (GSWP3)

to identify changes in the past and an ensemble of 12 downscale Regional Climate Models (RCMs) for future projections. They found that the climate models projected an increase in future temperature trend, with the magnitude depending on the global carbon emissions. Their results also indicated projected temperature increases ranges by 1.7 °C (RCP 4.5), and 2.3 °C (RCP 8.5) for the period of 2006 to 2050, while for the longer time frames of 2006 to 2099, the projected temperature increases ranges by 2.7 °C (RCP 4.5), and 6.4 °C (RCP 8.5) (Aich and Khoshbeen, 2016; Aich, N. A. Akhundzadah, *et al.*, 2017b). The mentioned events and studies highlight Afghanistan's vulnerability to climate change, indicating insufficient adaptation to both current and future challenges. The findings demonstrate that temperatures are projected to rise in the country, while the trends in precipitation show both increases and decreases without a clear pattern. Although few studies exist (e.g., McSweeney et al. 2010; Mukhopadhyay & Khan 2014; Aich et al. 2017) related to climate change in Afghanistan, there is a limitation in terms of the lack of bias correction and/or downscaling for the GCMs and RCMs data, specifically in the KRB. However, the basin serves as a crucial water source for domestic and agriculture. Recently, a study examined the climate change impacts on water resources in the Kabul River Basin (Akhtar *et al.*, 2021), but neglected bias correction and uncertainty associated with global climate models, and also only used one RCM for future water evaluations.

Previous studies have focused either on the whole KBR, using Global Climate Models (GCMs) (Sidiqi, Shrestha and Ninsawat, 2018) or on the lower section of the basin (Wi *et al.*, 2015), but there is not a specific study on the Upper Kabul River Basin using Regional Climate Models (RCMs). Therefore, to develop sustainable plans for managing water resources against climate change, preparing for the recurring natural hazards (e.g., floods and droughts), and to prevent financial losses and causalities under climate change, there is a high demand to evaluate the present and possible future water availability in the UKRB. On the other hand, the region analyzed in this study has not been holistically covered in the scientific literatures. This fact adds more to the importance of this study. Additionally, temperature and precipitation are very significant weather elements with significant impacts on hydrology. Therefore, the bias correction of precipitation and temperature is essential before applying any climate or hydrological impact studies. Thus, the main objective of this study is to provide a robust evaluation of climate change impacts on water availability in the UKRB. We evaluated the historical (1986-2005) and future periods of 2040s and 2090s. This assessment includes the evaluation of three bias correction techniques for precipitation and temperature data from the RCMs of CORDEX South Asia datasets.

2.1 SWAT hydrological model

The Soil and Water Assessment Tool (SWAT) has been widely used, and is a semi-distributed hydrological model designed to simulate the impact of land use and climate changes on water resources (Arnold *et al.*, 1998). The SWAT model (Arnold *et al.*, 1998; Neitsch *et al.*, 2011) is a distributed parameter and continuous time simulation model, developed by Dr. Jeff Arnold for the United States Department of Agriculture and Agriculture Research Services (USDA and ARS). The SWAT model has been developed to predict the hydrological response of un-gauged catchments to natural inputs as well as the manmade interventions. Both the water quantity and quality, and the sediment transportation can be assessed by this model. The model is; (a) physically based, (b) uses readily available inputs, (c) is computationally efficient to operate, and (d) is continuous time and capable of simulating long terms for computing the effects of land use management and the climate changes. The SWAT operates on a daily time step and is designed to predict the impact of land use change and climate change on water resources, sediment transportation, and agricultural chemical yields (Arnold *et al.*, 1998; Abbaspour, 2015). The model is capable of simulating a high level of spatial details by dividing the watershed into a large number of sub-watersheds and the hydrologic response unit (HRU). Major model components include weather, hydrology, soil temperature, plant growth, nutrients, pesticides, and land management. The water balance of each HRU in SWAT is represented by four storage volumes, including: snow, soil profile (0-2 m), shallow aquifer (typically 2-20 m), and deep aquifer (> 20 m). Flow generation, sediment yield, and non-point-source loadings from each HRU in a sub-watershed are summed, and the resulting loads are routed through the channels, streams, ponds, and/or reservoir to the watershed outlet. The hydrological cycle which simulated by SWAT model is based on the water balance equation, which considers the shallow aquifer and unsaturated zone above the impermeable layer as a unit. The hydrologic processes are based on the following water balance equation (1):

$$\mathrm{SW}_t = SW_0 + \sum_{i=1}^{n} (R_{day} - Q_{surf} - E_a - W_{seep} - Q_{gw}) \quad (1)$$

Where, SW_t is the final soil water content ($mm\ H_2O$), SW_0 is Initial soil water content ($mm\ H_2O$), R_{day} is the amount of precipitation on day i ($mm\ H_2O$), Q_{surf} is the amount of surface runoff on day i ($mm\ H_2O$), E_a is the amount of evapotranspiration on day i ($mm\ H_2O$), W_{seep} is the amount of water percolation or amount of water entering the vadose zone from soil profile on day i ($mm\ H_2O$), Q_{gw} is the amount of return flow on day i ($mm\ H_2O$), and t is time in days.

The soil profile is subdivided into multiple layers that support soil water processes, including infiltration, evaporation, plant uptake, lateral soil flow, and percolation to lower layers in the SWAT model (Arnold *et al.*, 1998). The soil percolation component of SWAT uses a storage routing technique to predict flow through each soil layer in the root zone. Downward flow occurs when field capacity of a soil layer is exceeded and the layer below is not saturated. Percolation from the bottom of the soil profile recharges the shallow aquifer (Neitsch *et al.*, 2011). If the temperature in a particular layer is less or equal to 0 ºC, no percolation is allowed from that layer. Lateral subsurface flow in the soil profile is calculated simultaneously with percolation. The contribution of groundwater flow to the total stream flow is simulated by routing a shallow aquifer storage component to the stream (Arnold, Allen and Bernhardt, 1993). SWAT also simulates the sediment and nutrients dynamics. Sediment yield is calculated based on the Modified Universal Soil Loss Equation (MUSLE) in this model (Williams, 1975). The total amounts of nitrates in runoff and subsurface flow is calculated from the volume of water in each pathway with the average concentration. Phosphorus however is assumed to be a relatively less mobile nutrient, with only the top 10 mm of soil considered in estimating the amount of soluble phosphorus removed in runoff. A loading function is used to estimate the phosphorus load bound to sediments (McElroy *et al.*, 1976). SWAT calculates the number of algae, amount of dissolved oxygen and carbonaceous biological oxygen demand (CBOD - the amount of oxygen required to decompose the organic matter transported in surface runoff) entering the main channel with surface runoff (Thomann, R.V. and Mueller, 1987).

In comparison of SWAT to other hydrological models such as the Hydrologic Engineering Center's Hydrological Modeling System (HEC-HMS) and MIKE SHE, multiple sources highlights their defferent applications and strengths. HEC-HMS is a lumped model primarily used for flood simulation and lacks the detailed spatial variability that SWAT offers (Aawar and Khare, 2020). MIKE SHE, on the other hand, provides a fully integrated approach to surface and groundwater modeling but is more data-intensive and computationally demanding compared to SWAT (Ougahi, Karim and Mahmood, 2022). In contrast to these models, SWAT’s strengths lie in its flexibility and ability to simulate various land-use and agricultural practices alongside hydrological processes. This feature is particularly important, where land-use changes, such as deforestation and urban expansion, significantly affect water resources. Moreover, SWAT's relatively low data requirement compared to MIKE SHE makes it more feasible for use in data-scarce regions like the KRB. Also, the integration of SWAT with GIS and its modular structure allows for greater flexibility in

modeling land use, soil types, and climatic factors, making it particularly suited for regions with diverse topography and limited data availability (Ougahi, Karim and Mahmood, 2022).

2.2 Global and regional application of SWAT in Climate Change Impact Studies

The SWAT model widely used in many studies for different purpose globally and regionally to assess the impact of climate change on water resources, including the streamflow, water quality, and the sediment transports.. Some examples are the use of SWAT model in continental-scale hydrology and water quality assessment for Europe (Abbaspour, 2015), water resource management and water balance assessment (Ayoubi and Dongshik, 2016; Adib *et al.*, 2020; Nasiri, Ansari and Ziaei, 2020), snowpack and snow melt changes assessment in Himalayas (Singh *et al.*, 2017; Tuo *et al.*, 2018; Liu, Cui and Li, 2020), and the climate change impacts on water resources and hydrology (Mohanty *et al.*, 2012; Narsimlu, Gosain and Chahar, 2013; Giang *et al.*, 2014; Iqbal *et al.*, 2018; Forero-Ortiz, Martínez-Gomariz and Monjo, 2020).

Globally, numerus studies have employed the SWAT to simulate hydrological responses to various climate change scinarios, for instance, research conducted in the United States, Europe, and the Asia has demonstrated the model's ability to integrate climate change ouputs (e.g., GCMs or RCMs) with localized lund use and soil data (Ficklin *et al.*, 2009; Arnold *et al.*, 2012). These studies generally indicate that climate change leads to altered precipitation patterns, increased frequency of extreme events, and significant shifts in water availability across regions. For example, Mississippi River Basin and the Rhine Basin has highlighted the risk of increased flooding and water scarcity under future climate scenarios, showcasing SWAT's utility in assessing water-related climate vulnerabilities (Jha *et al.*, 2006; Guse, Reusser and Fohrer, 2014). The major advantage of SWAT is that this model can evaluate the hydrological parameters in ungagged watersheds, assess the relative impact of alternative inputs (e.g. changes in climate parameters, vegetation etc.) on water quality and quantity. The model has gained a wide global acceptability and currently more than hundreds of peer-reviewed research papers have been published based on SWAT model application.

Regionally, SWAT has been applied to more localized watersheds in Africa, South America, and Asia, espicailly in Afghanistan where water management challenges are often more pronounced due to limited infrastructure and data. In African basins like the Blue Nile, studies using SWAT have illustrated potential reductions in streamflow due to projected decreases in rainfall and rising temperatures (Mengistu and Sorteberg, 2012). Similarly, in South Asia,

particularly the Ganges and Brahmaputra river basins, the model has been employed to assess the impacts of glacier retreat and monsoon variability on water resources (Immerzeel, van Beek and Bierkens, 2010).

Recent studies using the SWAT model have highlighted significant climate change impacts on water resources in the KRB. The SWAT model has been applied to simulate the basin's hydrological responses to projected climate scenarios, showing substantial shifts in streamflow and water availability due to rising temperatures and changing precipitation patterns. Research by (Sidiqi and Shrestha, 2021) indicates that increased temperatures in the KRB are accelerating snowmelt from the surrounding Hindu Kush mountains, which leads to higher runoff during spring but a significant reduction in water availability in the summer months when demand is highest. Additionally, a study by Ahmadzai et al. (2021) found that under future climate scenarios, due to warming trend, the snowmelt will intensify in mountains that feed the Kabulr River, potentially increase streamflow in short term but cuasing longterm water shortages. As a consequence, the frequency and intensity of extreme weather events such as floods and droughts are likely to increase, placing further strain on water management in the KRB. Further, research by Sharifi et al. (2021) highlights that the seasonal variability in water availability in the Kabul River Basin is projected to increase. The winter months, which traditionally receive snowfall that contributes to spring and summer runoff, may see reduced snowpack, while the summer months could experience increased glacial melt. This leads to a mismatch between water supply and demand, especially during the agricultural growing season when irrigation is most needed. Bromand (2015) utilized SWAT to simulate streamflow changes under various climate scenarios. These studies highlighted that future precipitation and temperature changes could lead to shifts in runoff patterns, which would exacerbate the already stressed water availability in the basin. A study (Ougahi, Karim and Mahmood, 2022) analysed the climate change impacts on water balance in the KRB under RCP4.5 and RCP8.5 scenarios. The study demonstrated that climate change could lead to significant reductions in water availability in the KRB, particularly during dry seasons, which is critical for planning sustainable water management practices in this semi-arid area. This research also highlighted the importance of incorporating both climate and land use changes in hydrological assessments. These studies underline the value of using the SWAT model to assess the complex hydrological impacts of climate change in the KRB and to inform adaptive water resource management strategies. Therefore, this study also selected SWAT to build a hydrologic model and estimate the impact of climate change on water resource in UKRB.

3 STUDY AREA

3.1 Location

The Kabul River originates from the Paghman mountains on the west and Koh-e-Safi mountains on the east of Kabul province. The Kabul River is 700 km long (435 miles) is part of the Indus catchment (Houben and Tunnermeier, 2005). The Kabul River Basin (KRB) lies in the north-east quarter of Afghanistan which contains all Afghan rivers that join the Indus River in Pakistan. The Kabul basin accounts for 35 % of the population's water supply, and has the fastest population growth in Afghanistan (Ghulami et al., 2022). The upper part of KBR (Figure 1-1 and Figure 3-1) comprises three primary river systems: the Ghorband & Panjshir river, the Logar river, and the Kabul river. The study covers an area of 26,043 km^2, located at a latitude of (33.6° – 35.9° N) and longitude of (67.63° – 70.30° E). The north and northeast part of the basin is situated in the highlands of the Hindukush mountains which are drained by the Ghurband and Panjshir rivers and are the main source of water for agriculture and domestic consumptions.

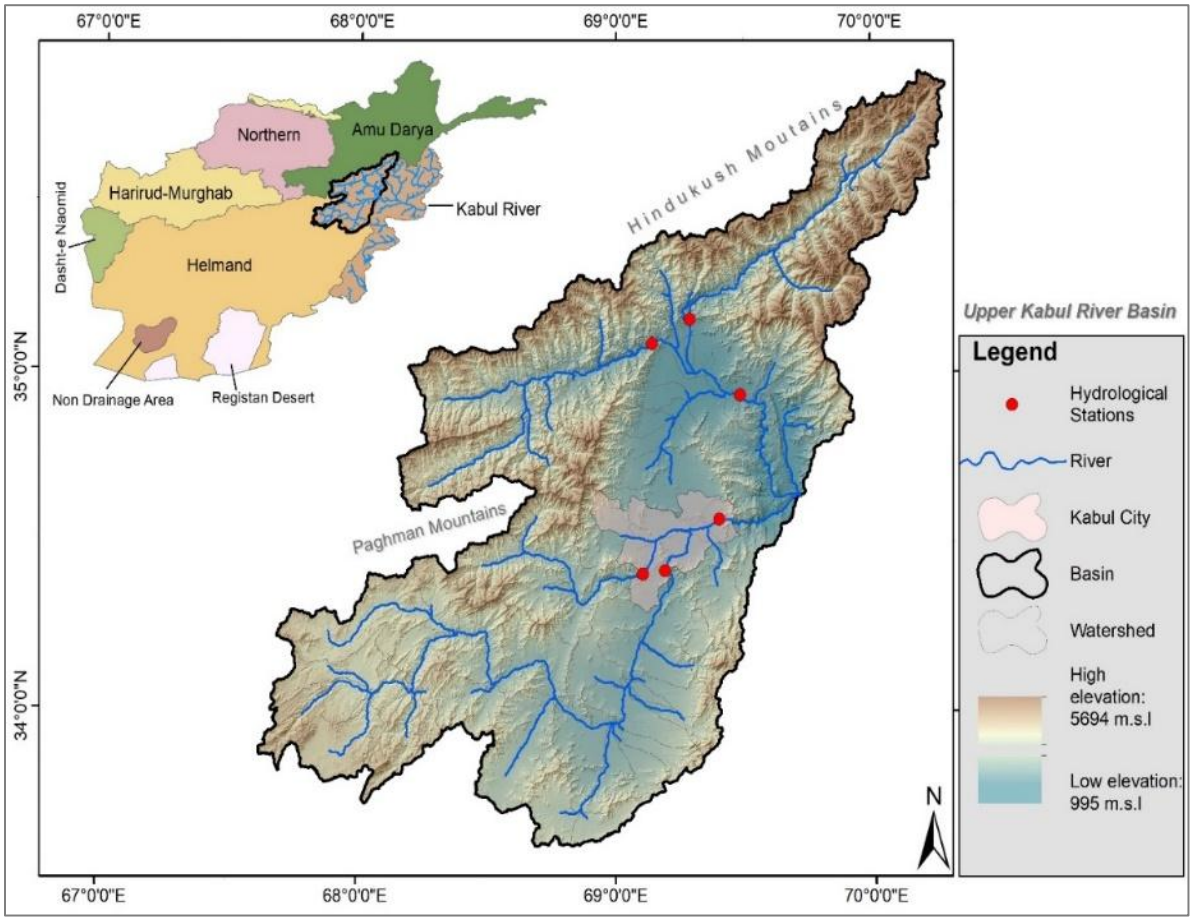

Figure 3-1: Location of study area (The Upper Kabul River Basin).

3.2 Topography

The elevation of the basin varies from of 995 m to 5,694 m above sea level (msl), and shown in figure 3-1. Topography of the study area is alpine with the steep slopes. The northern areas consisting high mountains with rocks, sharp peaks and heavy slopes, while the southern portions include mainly low mountain ranges, foothills, and plain areas. Some of the north mountain's peaks have permanent snow caps and glaciers.

3.3 Geology

The Kabul river is situated at intersection of three major translational and extensional fault systems that have enabled and shaped three interconnected, largely fluvial aquifers (Logar, Kabul, Paghman) that are 20 -70 m thick and composed of course sand to gravelly colluvial detritus (Eqrar and Shroder, 2016). The higher permeability occur where the coarse clastic are uncemented, but deeper buried clastic may be slightly cemented to produce lower permeability (Eqrar and Shroder, 2016). The surface of KRB is host to groups or regions of largely mountain runoff-fed tributaries that collectively from the river system, which is subdivided into a number of sub basin of greater or lesser importance.

3.4 Climate

The climate of the Kabul River Basin is characterized by cold winters and hot summers, with less or no precipitation and streamflow in the summer, except the rivers and streams fed by snowmelt and glaciers (Sidiqi, Shrestha and Ninsawat, 2018). June to August experiences the highest temperatures in the KRB with July being the warmest month (38°C), and the coldest months occur from November to February with a minimum in January -11°C) in the study area (UKRB). The average monthly temperature is recorded 34.2 °C in Naghlu station, 24 °C in Payin Qargha station, 20.3 °C in Pul-i-Surkh station, 25.2 °C in Pul-i-Ashawa station, and 28 °C in Tang-i-Gulbahar station in the KRB (Figure 3-2). The lower part of the basin is warmer than the upper parts of the basin. The annual potential evapotranspiration (PET) is approximately 1600 mm in the Kabul river basin (Akhtar, 2017). Precipitation is the main driver of variability in the water balance over a space and at a time. Changes in precipitation have very important implications in hydrology and water resources (Bruce, 2017). Hydrological variability over time is influenced by variations in precipitation over daily, seasonal, annual and decadal time scales in a watershed/basin (Cao *et al.*, 2021). The precipitation amount and type vary significantly due to elevations and season in the

basin, figure 3-2. The mean annual precipitation for the period 1986-2005 is 428 mm, while the average annual temperature is 7.6 °C based on 20 years of APHRODITE dataset over the UKRB. Based on ground observations, the annual precipitation records show 350 mm from 2009 to 2019 in UKRB. Higher precipitation occurs in winter and early spring seasons (December to May), while less or no precipitation occurs in summer. February and March have the higher precipitation compared to other months in a year.

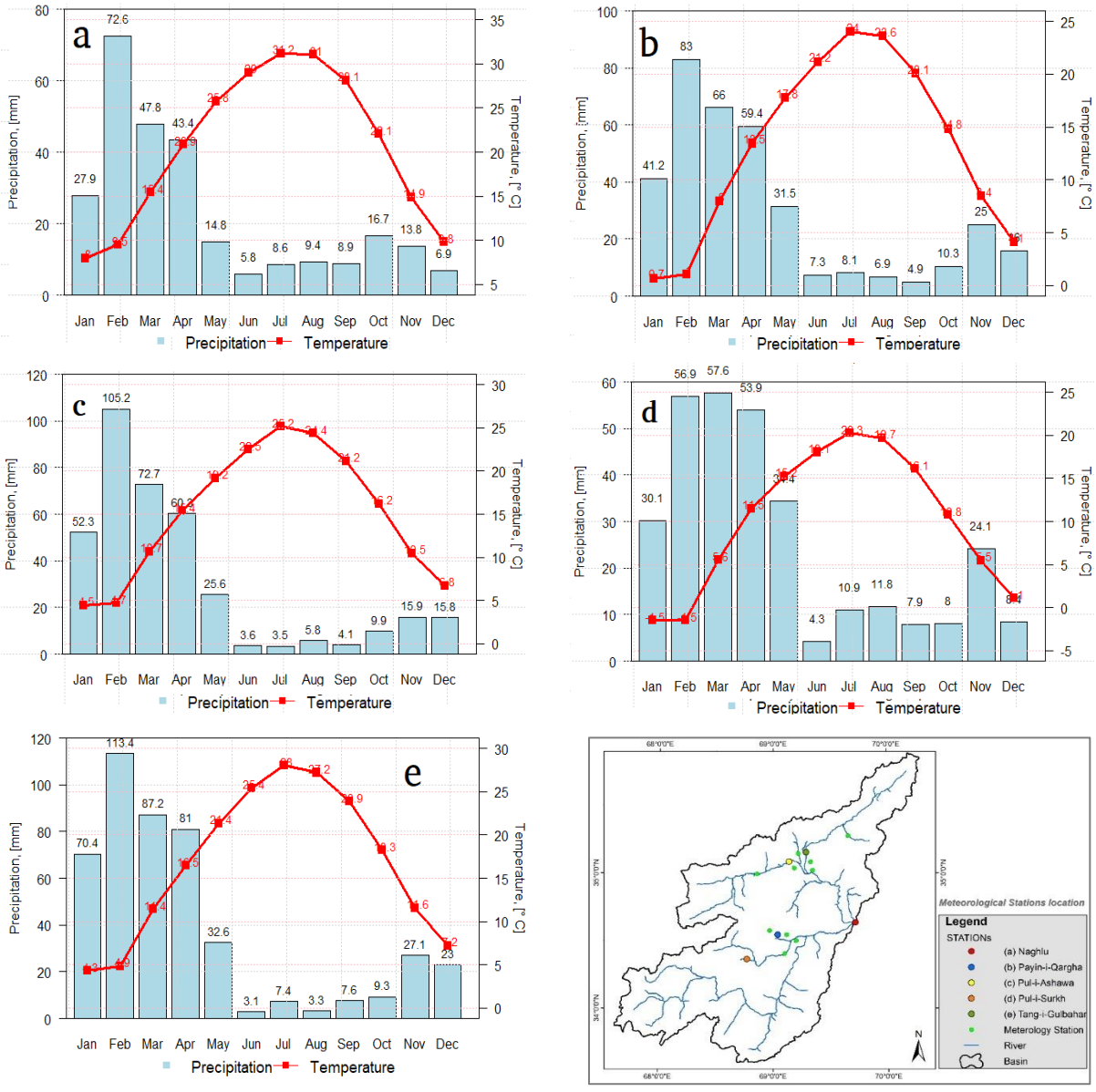

Figure 3-2: The climograph of Naghlu (a), Payin Qargh (b), Pul-i-Surkh (c), Pul-i-Ashawa (d), and Tang-i-Gulbahar (e) stations in the UKRB. The map showed in the upper left corner shows the location of the meteorological stations in the UKRB.

3.5 Hydrology

The schematic hydrology representation of KRB is shown in figure 3-3, provided by (World Bank, 2010). Topographic map with stations location and rivers network is shown also in the figure 3-3. The high elevation in the KRB is almost 6,200 msl and the lowest elevation is 380 msl (Figure 3-3). The current study includes three main rivers; including the Kabul River, the Logar River, and the Ghorband & Panjshir River. Naghlu reservoir is the outlet point of the basin. More details about the rivers explained in the below sections. The annual average water flow is around 140 Million m^3 (Mm^3) at Maidan station, 490 Mm^3 at Tang-i-Gharu station, and 3,400 Mm^3 at Naghlu station in the Kabul river. Only 15% of flow at Naghlu is contributed by the Kabul River (Mills, 2013). The water-flow contribution originates from the northern tributaries which are largely fed by snowmelt and glaciers. The glaciers represent a long-term asset that stabilizes the water supply in summer months and are the source of steady streamflow.

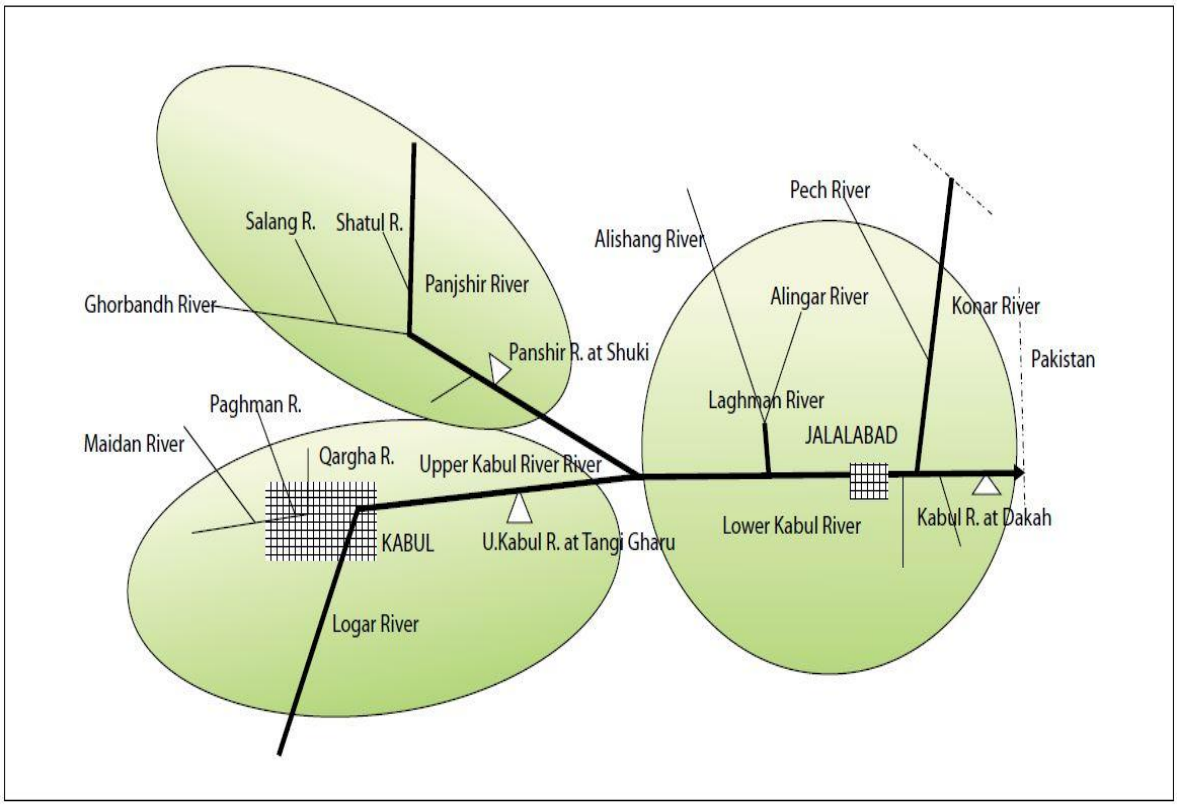

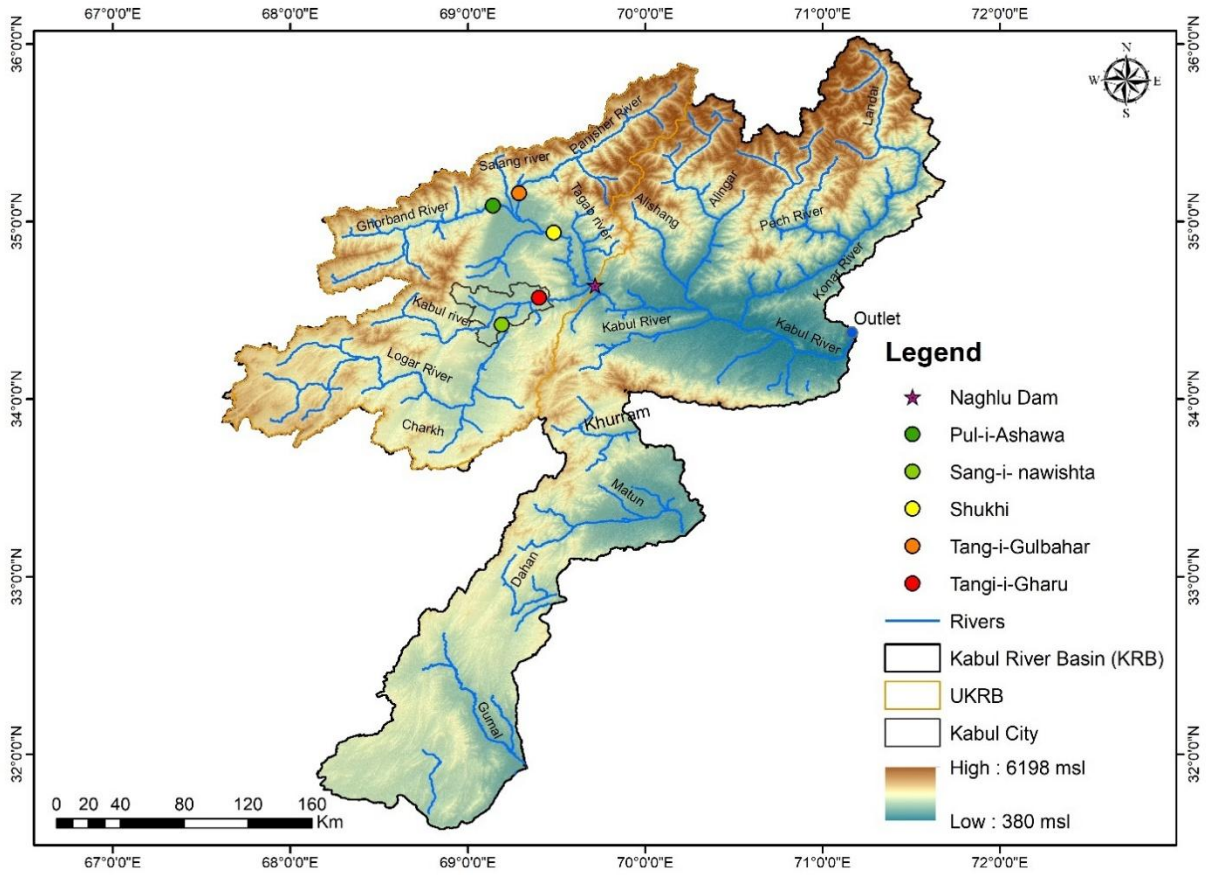

Figure 3-3: Schematic Diagram of the Kabul River Sub-basins: (1) Logar and Upper Kabul sab-basin; (2) Panjshir sub-basin; (3) Lower Kabul sub-basin (World Bank, 2010), and (B) Topographic map with stations location and river networks in the Kabul River Basin.

3.5.1 Kabul River

The Kabul sub basin include three small rivers which enters the Kabul city region are; the Maidan river, Paghman river, and Qargha river shown in Figure 3-3 (Zaryab *et al.*, 2017). The Kabul river also called medium river. All three rivers originate from the high mountain ranges located upstream of Kabul city. These rivers join at different confluences throughout Kabul city and flow through the center of Kabul. The Maidan river is formed by numerous small streams in west of Kabul city. The River changes its name to Kabul river before it enters the city and flows across the city where joining the Paghman and Qargha tributaries and then flows further until Naghlu dam where it joins into Panjshir river (Mills, 2013; Eqrar and Shroder, 2016). The main water projects and users of the Kabul river are Qargha reservoir, Shatoot irrigation and water supply to Maidan Shar and Tang-i-Saidan. When the Maidan river reaches Kabul city it has little or no water due to high water withdrawal for irrigation. After the confluence with the Panjshir river, the

river continues and called as Kabul River (Mills, 2013)**.** The historical monthly flow in Tang-i-Gharu station located in Kabul river is shown in the Figure 3-4.

3.5.2 Logar River

The Logar sub basin drains a dry and hilly watershed south of the Kabul city and comprises approximately 75 % of the drainage area of the Logar-Kabul area. There is modest but significant irrigated agriculture along the Logar river valleys in upstream of Kabul city. The main water users from Logar rivers are: Chak-e-Wardak dam for hydro power production, the irrigated agricultural lands along the river, and the Kol-e-Hasmat Khan wetland located in south of Kabul city. The average annual flow recorded almost 230 Million m3 at Kajab and 300 Mm3 at Sang-i-Naweshta stations (Figure 3-4).

3.5.3 Ghorband and Panjshir rivers

Ghorband river which is 130 km long originate from the Hindu Kush mountains, flowing through Parwan province. The river forms the Ghorband basin until it joins the Panjshir river. The Salang river which is 438 km long is the tributary of the Ghorband river. The average annual flow is about 730 Mm^3 at Pule Ashawa station, situated in this river (Figure 3-4). The river joins with the Panjshir river in Baghram district of Charikar province (Favre and Kamal, 2004) and then the river (Mills, 2013).

The Panjshir River takes its source near the Anjuman Pass and flows southward through the Hindu Kush mountains. After its confluence with Ghorband river, this river called Panjshir river. It has 150 kilometers long and joins the Kabul River at town of Surobi distruct (Favre and Kamal, 2004). The Panjshir watershed is formed by the Panjshir river and it's tributary; Ghorband, Salang, and Shatul rivers. The upper portion of this watershed consists of steep mountain valleys in the Hindu Kush mountain range, which reaches over 6,000 m.s.l and remains snow covered throughout the year. The southern portion of the Panjshir watershed opens into the broad and gently sloping fertile Shomali Plain which has some of the most important irrigated lands. Although the drainage area of the Panjshir River at Shukhi is smaller at approximately 84% compared with the Kabul river, but it's average annual streamflow is larger almost 6 times than Kabul river. The mean annual water flow of Panjshir river is 1,710 Mm3 at Gulbahar station (Figure 3-4). The combined flow from above two rivers is 3,080 Mm3 observed at Sukhi stations (Mills, 2013)**.** Panjshir and Ghurband rivers together provide roughly 14 % of annual flow of the whole Kabul river basin

(Ayoubi, 2017). The Waterflow contributions from the Ghurband & Panjshir Rivers are primarily due to snow and glaciers melt (Eqrar and Shroder, 2016).

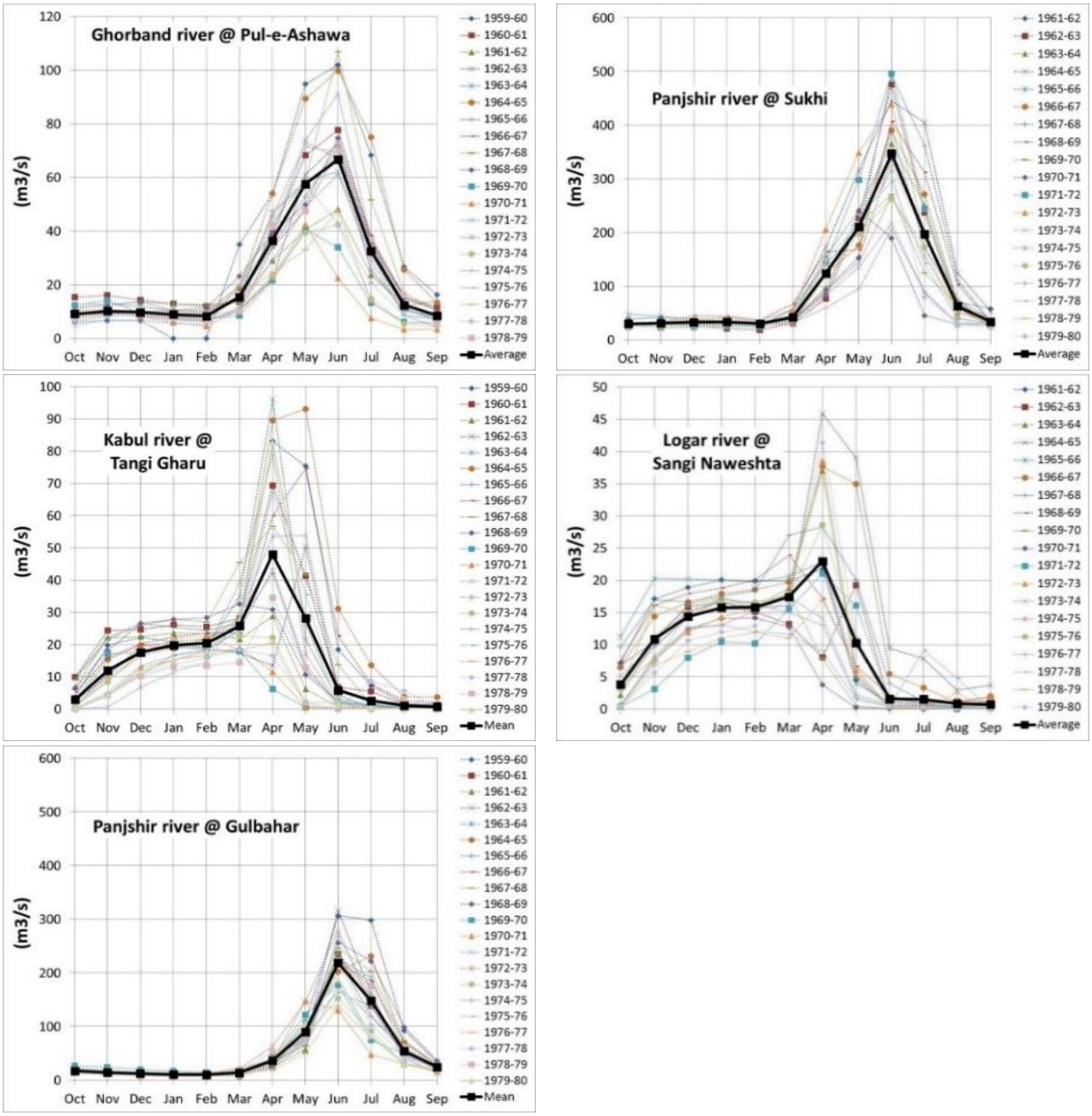

Figure 3-4: Historical hydrographs (1959 -1979) in Tang-i-Gharu station on Kabul river, Sangi-Nawishta on Logar river, Pul-Ashawa on Ghorband river, Gulbahar station on Panjshir river, and Shukhi station on Panjshir river of the Kabul river basin (Source: AWARD, 2013).

3.6 Land use and land cover classification

The land cover data obtained from Food and Agriculture Organization (FAO) in Afghanistan (FAO, 2010). The land use map of UKRB includes thirteen major classes which includes intensively agricultural area, rainfed area, fruit trees, vineyard, barren land/sand cover, forest close and needle leaved areas, rangeland, marshland, urban area, irrigated agricultural land (marginal irrigation), forest with undifferentiated areas, shrubs with degenerated forests, and water bodies. The dominant land cover in UKRB is the rangeland, which covers 75 % of the study area, Table 3-1. Land use change has a major impact on runoff and evapotranspiration due to changes in land area allocation for settlement or urbanization, cutting forests, removing trees and plants, changing agricultural areas to rangelands or barren lands. Table 3-1 shows the land cover classification area in the UKRB in Afghanistan. The Kabul River Basin presents a diverse pattern of land use, shaped by its topography, hydrographic characteristics, and settlement patterns (Ougahi, Karim and Mahmood, 2022). This basin, which extends across both highland and lowland areas, is defined by its rugged mountainous regions in the north and northeast and low-lying plains and valleys in the south. In northern Hindukush mountains, due to limited accessibility and defficult terrain, agriculture is largly confined to terraced farming along the river valleys. These regions are often characterized by rangelands and areas of forest**,** though forest cover has significantly declined due to deforestation. The lower basin, featuring flatter terrain and proximity to water sources supports extensive agriculture, especially irrigated crops like wheat, maize, rice and barley. Rapid urbanization, especially around Kabul, has led to significant land-use changes, impacting both agriculture and natural water systems (Khatiwada, Pradhananga and Nepal, 2024). The mid-elevation regions are dominated by grazing lands and pasture, while the upper basin marked by mountainous areas, consists primarily of forests and rangelands. These land use patterns are influenced by both natural and human-induced factors like deforestation, population growth, and climate change impacts (Khatiwada, Pradhananga and Nepal, 2024). As the population continues to grow, sustainable land and water management are crucial to balance development needs with environmental conservation.

The land use data was sub divided into thirty-one classes. The land use map was prepared based on SWAT requirements and reclassified into thirteen major classes, Figure 3-5. The land use data preprocessed and was projected to UTM Zone 42 N using the raster projection in ArcMap before it was used in SWAT. Land use is a major factor in hydrological modeling for streamflow and evapotranspiration estimation in the basin.

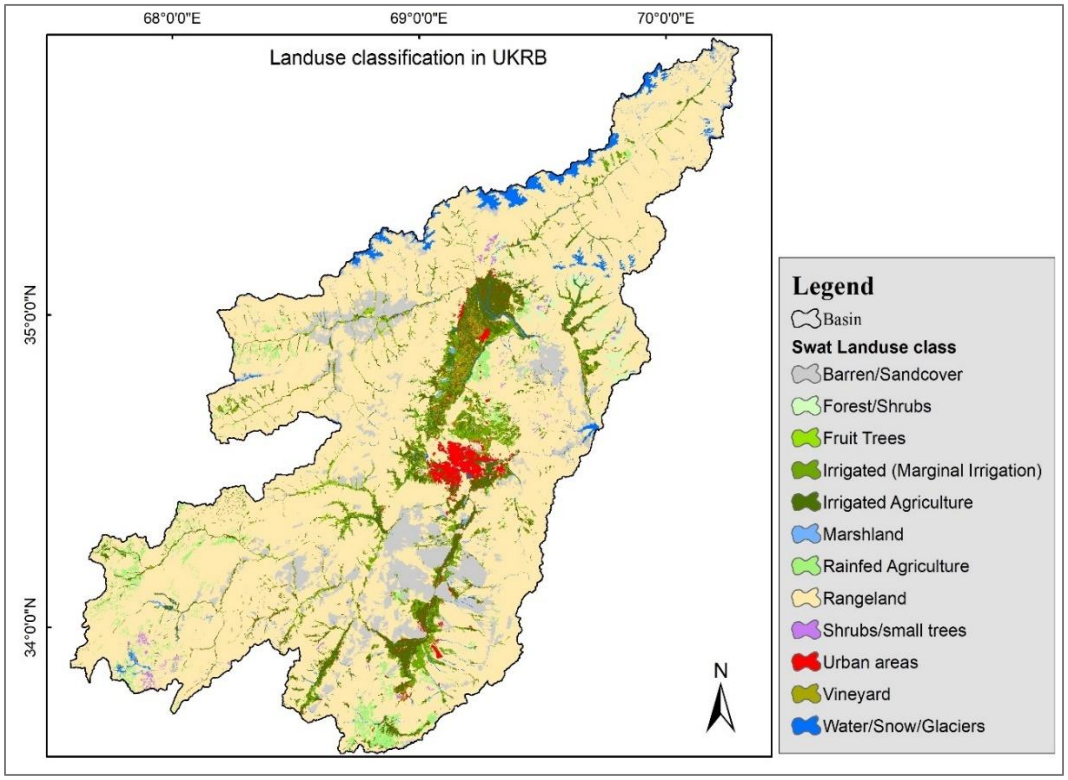

Figure 3-5:The spatial variation of Land use and Land cover types in UKRB ((FAO, 2010)).

Table 3.1:Shows Land use classifications in the UKRB ((FAO, 2010)*).*

No	Land cover Types	Area (Km^2)	Area (%)
1	Intensively cultivated (1 or 2 crop/yr)	1552.0	6.0
2	Rainfed Ag. land	521.5	2.0
3	Fruit trees	259.1	1.0
4	Vineyard	189.7	0.72
5	Barren/sand cover	2050.9	7.9
6	Forest close and open needle leaved	160.5	0.6
7	Rangeland	19534.2	`75.0
8	Marshland	78.1	0.3
9	Urban areas	445.8	1.7
10	Irrigated Ag. land (marginal irrigation)	638.8	2.5
11	Forest undifferentiated	10.8	0.01
12	Shrubs/degenerated forest	72.4	0.3
13	Water/snow	529.0	2.0
	Total	*26,043*	*100*

3.7 Soil characteristics and discription

Soil profile has great effects on water flow due to its infiltration rates. Soil texture describes the proportion of different sized mineral particles that are found in a soil (Jones, Caon and Yigini, 2023). The main particle size classes are broadly clay (<0.002mm), silt (0.02-0.63mm) and sand (0.063-2.0mm). Texture is measured by sieving, or by feeling the grains by rubbing the soil between your fingers. Particle size classifications may vary in different countries. Furthermore, large sand particles can be described as coarse, medium and fine. The Kabul River Basin has diverse soil types due to its varied topography, climate, and geological history. The main soil texture in study area is loam with hydrologic soil group of class c and d (Table 3-2). A description of the specified soil types within this region is as below:

- *Lithosols-Cambisols-Rankers:* Lithosols are shallow soils found on steep slopes, often characterized by a lack of significant soil development due to limited depth and high rock content. Lithosols are typically found in mountainous regions and are prone to erosion (Schad, 2016). The Cambisols are with limited horizon development, often found in areas where soil formation processes are relatively young or interrupted (Schad, 2016). They are moderately weathered soils, found in a variety of landscapes including slopes and valleys, and are typically fertile enough to support agriculture, especially when well-drained. The Rankers are shallow, acidic soils typically found on steep slopes, formed from non-calcareous parent material. Rankers are usually found in upland areas with cool climates and are characterized by a thin organic layer overlying rock (Schad, 2016). The combination of Lithosols, Cambisols, and Rankers in the KRB indicates areas with varied topography, where soil development is influenced by the erosion processes and parent rock material. These soils are common in mountainous regions of Afghanistan, where steep slopes and rugged terrain dominate.
- *Xerosols:* are soils found in arid and semi-arid regions, characterized by low organic matter content and limited leaching (Jones, Caon and Yigini, 2023). These soils are often calcareous and exhibit a coarse texture. They are associated with desert or semi-desert climates and support drought-resistant vegetation. The Lithosols-Xerosols combination in the KRB indicates areas with arid to semi-arid conditions, likely in the lower elevations or regions receiving limited precipitation. These soils reflect the dry climate and the erosional forces acting on the landscape.

- *Calcaric Fluvisols:* Fluvisols are young, fertile soils typically found in river valleys and floodplains, formed from alluvial deposits (ICIMOD, 2012). Fluvisols are characterized by layers of sediments deposited by flooding rivers, making them rich in nutrients and suitable for agriculture. Moreover, Calcaric term indicates the presence of calcium carbonate in the soil, which often results from the weathering of calcareous rocks or the deposition of calcareous sediments (ICIMOD, 2012). Calcaric Fluvisols are therefore fertile, well-drained soils found in areas with significant alluvial activity. In the KRB, Calcaric Fluvisols are likely found along the riverbanks and floodplains, where the periodic flooding deposits fertile sediments. These soils are crucial for agriculture in the region, supporting crops due to their nutrient richness (ICIMOD, 2012).
- *Glacial Soils:* Soils associated with glaciers are typically poorly developed, consisting of a mixture of unsorted glacial till, including rock fragments, sand, silt, and clay (Shroder, Ahmadzai and Ellis, 2007). Glaciers contribute to the formation of various landforms like moraines, outwash plains, and glacial valleys. The soils in glacial regions are often young and lack well-defined horizons due to the recent deposition of material by retreating glaciers (Shroder, Ahmadzai and Ellis, 2007). The Glaciers in the KRB are primarily found in the high mountain ranges, such as the Hindu Kush ranges.

The soil physical properties such as soil texture, available water content, hydraulic conductivity, soil bulk density and organic carbon content for different layers of each soil type are required when modeling the hydrology of a basin by SWAT. Soil type has great effects on surface runoff due to its infiltration rate. In this study, soil data obtained from FAO/UNESCO website (FAO, 1971)**.** The digitized soil map of the world, at 1:5,000,000 scale was in the geographic projection and converted to UTM projections (WGS1984, UTM Zone 42N) using the raster projection in Arc-map before using in SWAT. Figure 3-6 shows the soil classification type in the UKRB.

Table 3.2: Shows area of soil class. SHG is soil hydrologic group.

ID	Soil Type	Area Km^2	Area (%)	Texture	SHG
1	Lithosols- Cambisols-Rankers	9484.7	36.4	Loam	C
2	Lithosols- Xerosols	12271.0	47.1	Loam	D
3	Calcaric Flurisols	4005.7	15.4	Loam	D
4	Glaciers	281.5	1.1	UWD	D
	Total	26042.9	100		

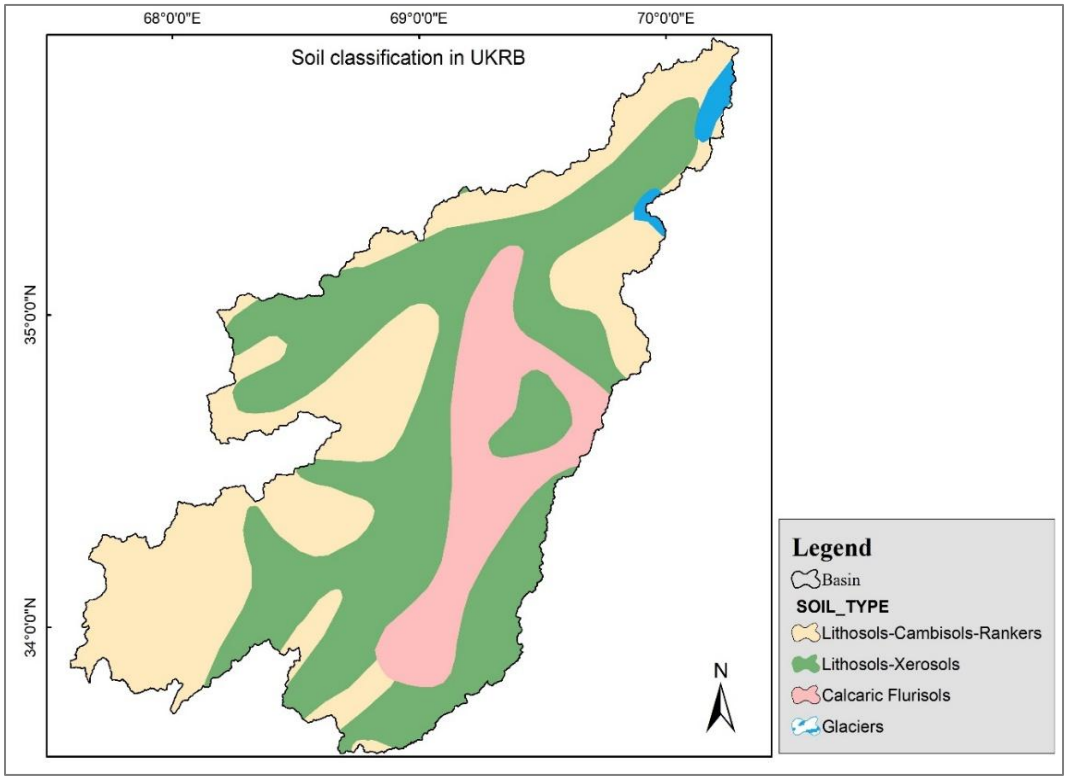

Figure 3-6: Soil classification type in study area (FAO, 1971).

3.8 Weather Data

The weather data is among the most important inputs required for the SWAT to estimate the hydrology of a basin. It is good to have a meteorological station within the watershed of interest, but sometimes obtaining representative weather data for watershed-scale hydrological modelling can be difficult and time consuming (Fuka *et al.*, 2014). The daily precipitation, Tmax, and Tmin covering the period from 1st January 2009 to 31st December 2019 was collected from 21 meteorological stations within UKRB in Afghanistan. Figure 3-7 shows the location of meteoritical stations in UKRB. Among these meteorological stations, the daily precipitation and temperature data of 13 stations were obtained from National Water Affairs Regulation Authority (NAWARA) and only daily precipitation of 8 stations were obtained from Ministry of Agriculture, Irrigation and Livestock (MAIL) in Afghanistan (Table 3-3). The remaining weather parameters, i.e. wind speed, relative humidity and solar radiation were not available for the study area, therefore, the Hargreaves method used in the SWAT modeling.

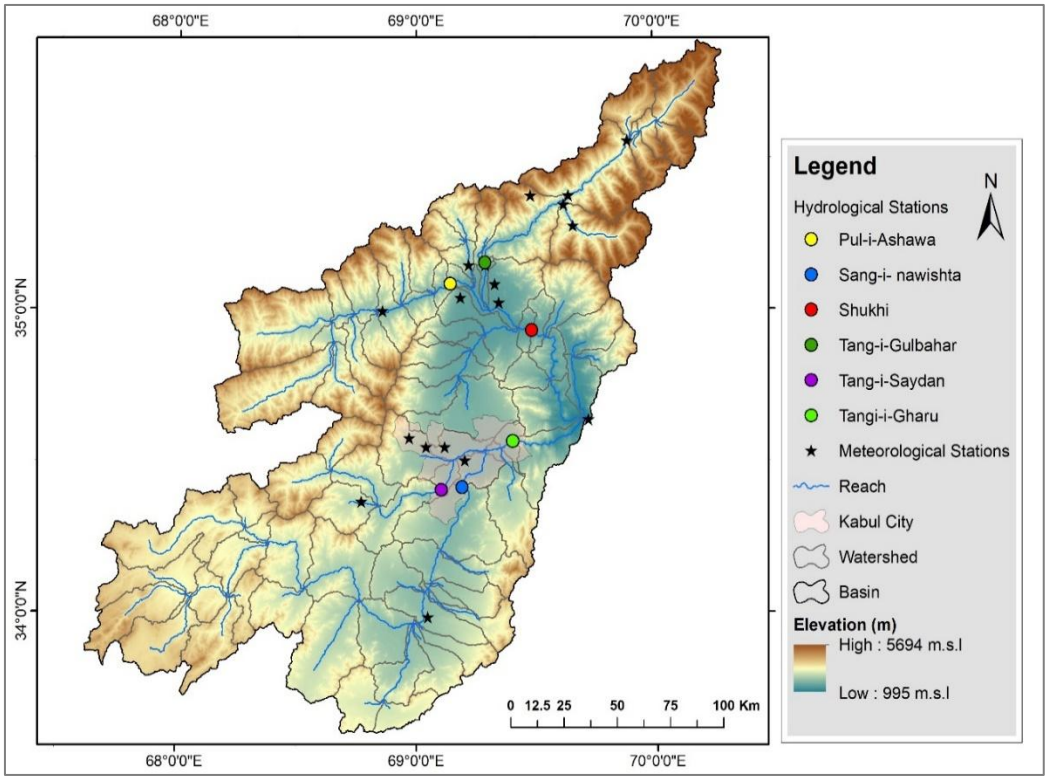

Figure 3-7: Locations of the meteorological and hydrological stations in UKRB.

Table 3.3: Shows the stations name, elevation and data availability in UKRB (MAIL, 2019; NAWARA, 2019).

No	Name	Lat	Long	Elev (m)	Owner	Precipitation	Temperature
1	Bagh-i-Lala	35.15	69.22	1698	NAWARA	Yes	Yes
2	Bagh-i-Omomi	35.15	69.29	1587	NAWARA	Yes	Yes
3	Doabi	35.35	69.62	2059	NAWARA	Yes	Yes
4	Keraman	35.28	69.66	2232	NAWARA	Yes	Yes
5	Khawak	35.56	69.89	2405	NAWARA	Yes	Yes
6	Naghlu	34.64	69.72	998	NAWARA	Yes	Yes
7	Omarz	35.38	69.64	2042	NAWARA	Yes	Yes
8	Pul-i-Ashawa	35.09	69.14	1624	NAWARA	Yes	Yes
9	Pul-i-Surkh	34.37	68.77	2216	NAWARA	Yes	Yes
10	Payin-i-Qargha	34.55	69.04	1970	NAWARA	Yes	Yes
11	Qala-i-Malik	34.58	68.97	2211	NAWARA	Yes	Yes
12	Tang-i-Gulbahar	35.16	69.29	1625	NAWARA	Yes	Yes
13	Tang-i-Saydan	34.41	69.1	1870	NAWARA	Yes	No
14	Badam Bagh	34.55	69.118	1803	MAIL	Yes	No
15	Gul Khana	34.506	69.202	1793	MAIL	Yes	No

16	Kapisa Agri	35.026	69.346	1471	MAIL	Yes	No
17	Kohestan	35.088	69.329	1536	MAIL	Yes	No
18	Logar	33.988	69.046	1922	MAIL	Yes	No
19	Dashtak	35.38	69.48	3401	MAIL	Yes	No
20	Charikar	35.043	69.185	1559	MAIL	Yes	No
21	Seya Gerd	34.999	68.858	1848	MAIL	Yes	No

Note: *NAWARA= National Water Affairs Regulation Authority, MAIL: Ministry of Agriculture, Irrigation and Livestock.*

3.9 Gap filling (observed precipitation and temperature)

Most of the hydro-meteorological stations have missing values (gaps) for months or even for years, due to the past several years of war and the technical problems in KRB. So, to fill the gaps of the precipitation and temperature data, the Inverse Distance Weighting (IDW) interpolation method is used in GIS. The IDW was selected based on stations elevation and distance. The average values from nearest stations calculated to extract the value for target station. For some stations which their closest stations also had gaps in the same period of time, the average of all past years (e.g., 2009-2019) calculated for that station and were used in the model. The maximum and minimum temperature data were available only for 12 stations inside the basin which belongs to NAWARA, but the temperature data from 11 station were used in the modeling because Tang-i-Saidan station had gaps for many years, therefore excluded in this study. Table 3-3 shows the station details including coordinates, elevation, and data availability in the study area. The Hargreaves method was chosen for estimation of Potential Evapotranspiration (PET), because this method use the minimum, maximum and mean air temperatures only for calculation of PET (Neitsch *et al.*, 2011)**.**

3.10 Hydrology (discharge) data

Daily observed discharge data from January 2010 to September 2018 in 6 hydrological stations installed on different tributaries in KRB were acquired from NAWARA. The discharge data were used during calibration and validation process of the SWAT model. The choice of these stations was made in a way to make sure that there were no storage areas or reservoirs or any major diversions that could possibly influence the discharge at the monitoring points. Table 3-4 shows characteristics of the selected hydrologic stations used in calibration and validation.

Table 3.4: Shows the observed flow stations used during calibration and validation periods.

No	Stations	Latitude	Longitude	Elevation (m)	Location	Drainage area (Km^2)
1	Pul-i-Ashawa	35.0888	69.141886	1624	Gurband river	4008
2	Sang-i-nawishta	34.41818	69.191130	1813	Logar river	9718
3	Shukhi	34.93616	69.484394	1374	Panjshir river	10840
4	Tang-i-Gulbahar	35.15932	69.288683	1625	Panjshir river	3527
5	Tang-i-Saydan	34.40897	69.104411	1870	Maidan river	1642
6	Tangi-i-Gharu	34.56988	69.402169	1775	Kabul river	12810

4 METHODOLOGICAL APPROACH USED

The methodology adopted in this study includes the application of Soil and Water Assessment Tool (SWAT) for current water availability analysis, bias corrections of precipitation and temperature from four RCMs, and the impact of climate change on hydrology in the Upper Kabul River Basin (UKRB) in Afghanistan. A detailed description of method is given in the following sections.

4.1 Development of SWAT hydrological model for UKRB

A distributed hydrologic model can be used for analyzing hydrologic process, planning, and managing water resources, investigating water quality, and predicting climate change. Thus, the Soil and Water Assessment Tool (SWAT 2012, VER 2018/Rev 670) (Arnold *et al.*, 1998; Srinivasan *et al.*, 1998; Winchell *et al.*, 2013) is used to estimate the runoff, analyze the components of water balance, and to predict the impacts of climate change on water availability in the UKRB.

During the modeling setup, the first procedure performed was the watershed delineation. The basin was delineated using the Geographic Information System (GIS) tool. The SWAT model is able to divide the basin to sub-basins and Hydrologic Response Units (HRUs). Therefore, after completing watershed delineation, three spatial datasets like; slope, land use, and soil type were used to determine HRUs. The input data were preprocessed before using in the model. Using the HRU as a basis, all the components of water balance can be determined for similar lands having the same topography, land use, and soil types, assuming that similar lands would share similar hydrologic characteristics (Ayoubi and Dongshik, 2016; Kouchi *et al.*, 2017; Mengistu, van Rensburg and Woyessa, 2019). The details of procedure for a basin delineation and HRUs can be found in (Neitsch *et al.*, 2011; Winchell *et al.*, 2013). Afterwards, the preprocessed climatic data were fed to the model, containing rainfall, minimum temperature and maximum temperature. The data gaps were filled using the Inverse Distance Interpolation method (IDW) in meteorology stations, and the SWAT weather generator (WGEN) process. The runoff generation method was set to be estimated with the Soil Conservation Curve Number (SCS-CN) method, and the potential evapotranspiration was estimated using Hargreaves equation (2), (Neitsch *et al.*, 2011). The Hargreaves equation used in SWAT was published in 1985 as temperature-based method (Hargreaves and Samani, 1985).

$$\lambda E_0 = 0.0023 \,.\, H_0 \,.\, (T_{max} - T_{min})^{0.5} \,.\, \left(\bar{T}_{ave} + 17.8 \right) \quad (2)$$

Where, λ is the latent heat of vaporization (MJ Kg -1), E_0 is potential evapotranspiration (mm day^{-1}), H_0 is the extra-terrestrial radiation (MJ M^{-2} day $^{-1}$), Tmax is the maximum air temperature for a given day (^{0}C), Tmin is the minimum air temperature for a given day (^{0}C), and $\bar{T}_{ave}$ is the mean air temperature for a given day (^{0}C). The channel water routing was simulated by variable storage routing, and the rainfall distribution was simulated by mixed exponential method. After all the above processes were completed, the SWAT simulation was activated.

The SWAT model was set to run continuously on daily base, and on monthly intervals from 1st January 2009 till 31st December 2019 (11 years), and a one-year warm-up period (2019) was selected to stabilize the model. Thus, a 10-year period of hydrologic variables was simulated for the studied basin (excluding the warm-up period). Most researchers in hydrology related studies have used the Nash-Sutcliffe Efficiency (NSE) and R^2 to assess the model accuracy and applicability. Hence, the NS equation is selected in our study during calibration and validation process. During winter, the Kabul Basin receives and stores a substantial amount of snowfall, and during summer the snow melts from the high altitudes. Therefore, the snowmelt has been considered during development and calibration of the SWAT model for UKRB. Equation (3) illustrates how snowmelt is calculated in SWAT:

$$SNO_{mlt} = b_{mlt} * sno_{cov} * \frac{T_{snow} + T_{max}}{2} - T_{mlt} \quad (3)$$

Where, SNO_{mlt} is the amount of snow melt per day (mm water equivalent), b_{mlt} is the melt factor (mm day-1 °C-1), sno_{cov} is the fraction of the hydrological response unit's area covered by snow, T_{snow} is the temperature below which precipitation is considered as snow fall (°C), Tmax is the maximum temperature on a given day (°C), and T_{mlt} is the base temperature above which snow melt is allowed. The model incorporates the leap year in its calculations automatically. The Equation (4) can be used to estimate the snow melt factor or b_{mlt}.

$$b_{mlt} = \frac{b_{mlt6} + bmlt_{12}}{2} + \frac{b_{mlt6} - bmlt_{12}}{2!} Sin \left[\frac{2\pi}{365} (d_n - 81) \right] \quad (4)$$

Where, b_{mlt} is the snow melt factor (mm day-1 °C-1), b_{mlt6} is the melt factor for 21 June (mm day-1 °C-1), b_{mlt12} is the melt factor for 21 December (mm day-1 °C-1), and d_n is the day number of the year, where 1 is for 1st of January and 365 is for 31st December (Winchell *et al.*, 2013; Iqbal *et al.*, 2018).

After calibration and validation of the model, the bias corrected precipitation and temperature data added to analyze the future climate change impact on runoff and water availability in UKRB. The framework, showing the major procedures in the simulation process is summarized in Figure 4-1. The following paragraphs describes the details related to the data input processing used for the simulation of the hydrology in the UKRB.

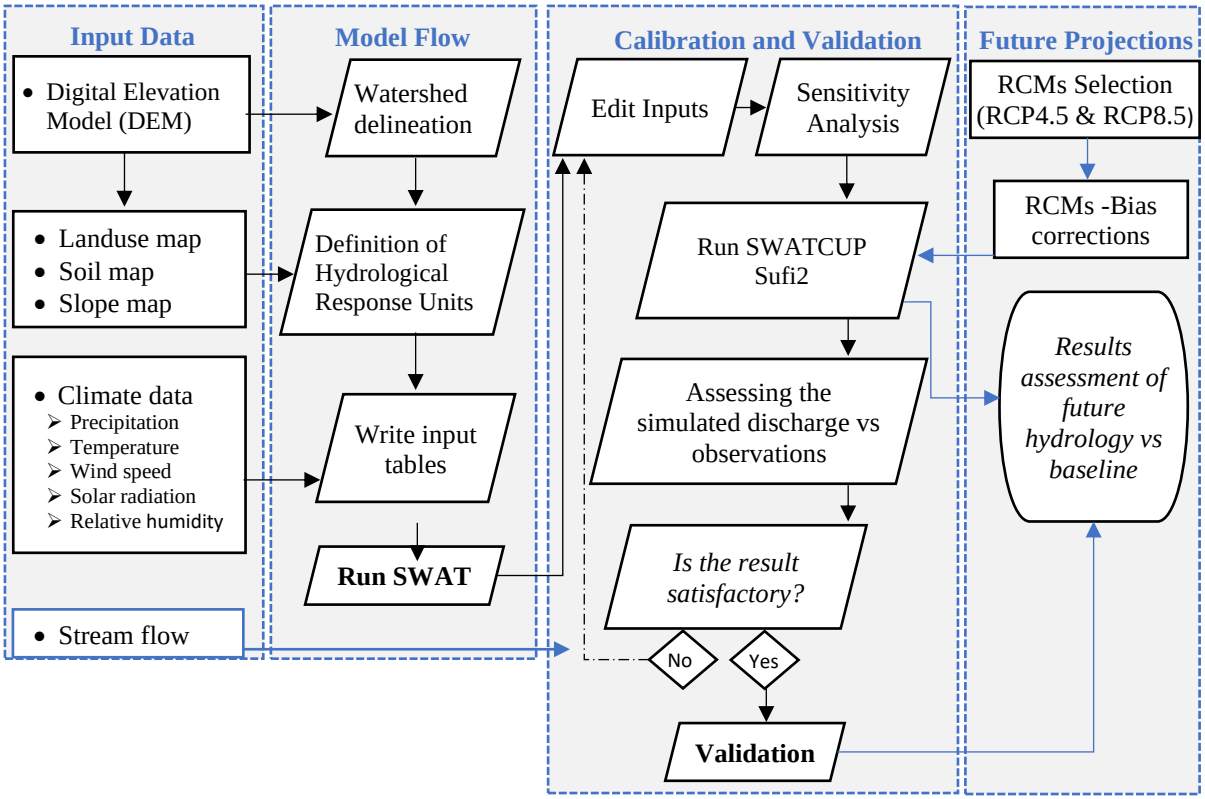

Figure 4-1: Flowchart for the processing of data, model setup, calibration and validation in UKRB.

4.2 Input Data for SWAT

Data gathering and processing is the main important and first step in hydrological modeling and climate change impact assessment. The spatial data required for SWAT includes Digital Elevation Model (DEM), land cover and land use, and soil characteristics. In addition, the meteorological data is required to model the basin includes daily rainfall, maximum temperature, minimum temperature, relative humidity, wind speed, and solar radiation. The hydrology data is required for calibration and validation steps. In this study, the data collected, preprocessed and used to estimate the water availability in the UKRB includes:

1. Digital Elevation Model (*DEM*) obtained from (U.S. Geological Survey, 2014).
2. Land use and land cover data obtained from Food and Agriculture Organization in Afghanistan (FAO, 2010). See more details is in section 3.6.
3. Soil data obtained from FAO-website and is available worldwide (FAO, 1971). See more details is in section 3.7.Daily precipitation and temperature obtained from the National Water Affairs Authority (*NAWARA*) and from Ministry of Agriculture, Irrigation and Livestock (*MAIL*) in Afghanistan (MAIL, 2019; NAWARA, 2019). See more details is in section 3.8.
4. To project the future climate change impacts, the precipitation and temperature data obtained from South Asia Domain of Coordinated Regional Downscaling Experiment (SA-CORDEX), and their corresponding CMIP5 driving GCMs hosted by the German Climate Computing Centre (DKRZ) (CMIP5-DKRZ, 2021). See more details is in section 4.7.2.

The data source with their spatial and temporal resolutions used in the SWAT are depicted in the Table 4-1. The SWAT hydrological model integrates data with different spatial resolutions, such as soil, land cover, and elevation by using a structured modeling approach. This ensures that these datasets, despite their varying scales, contribute effectively to simulating water flow, sediment transport, and nutrient cycling (Srinivasan and Arnold, 1994; Neitsch *et al.*, 2011). The SWAT starts with DEM to delineate the watershed into multiple sub-basins (Srinivasan and Arnold, 1994).

Table 4.1: Sources of data used for the present and future simulations of runoff in the UKRB. The data description includes, data type, time period the data used and the provider of the data.

Data Type	Name	Resolution	Period	Source
Spatial data	DEM	30 m	-	USGS Website, https://earthexplorer.usgs.gov
	Land use	30 m	-	FAO/MAIL,https://www.fao.org/publications/card/en/c/21ba617f-cbaa-498f-a8cd-0ec49daea6ab/
	Soil type	1:5000,000, or 50 km	-	Harmonized world soil database v1.2 | FAO SOILS PORTAL | Food and Agriculture Organization of the United Nations
Meteorological data	Precipitation, Temperature	Daily	2009-2019	NAWARA, MAIL
Hydrological data	Discharge	Monthly	2010-2018	NAWARA
Historical and future data				
APHRODITE data	Precipitation, Temperature	0.25°	1986-2005	https://www.chikyu.ac.jp/precip/english/products.html
RCMs output (RCP4.5 & RCP8.5)	Precipitation, Temperature	0.44°	2030-2049 2080-2099	https://esgf-data.dkrz.de/search/cmip5-dkrz/

The DEM is usually at a finer resolution (e.g., 30m or 90m) and determines topography, drainage networks, and flow direction. The DEM is usually at a finer resolution (e.g., 30m or 90m) and determines topography, drainage networks, and flow direction (Srinivasan and Arnold, 1994). SWAT further divides sub-basins into Hydrologic Response Units (HRUs). The HRUs are homogeneous land units created by overlaying soil, land use, and slope classes which allows SWAT to simulate water and nutrient cycles for specific land characteristics (Neitsch *et al.*, 2011). This is how SWAT integrates the different resolutions of input data such as landcover, soil and slope classes. SWAT defines different slope categories within sub-basins, which allows it to capture variation in runoff due to terrain steepness. The overlay of these datasets leads to the creation of HRUs, each of which has a unique combination of soil type, land cover, and slope class. Each HRU behaves homogeneously with respect to hydrological processes, meaning it has consistent infiltration, runoff, evapotranspiration, and nutrient dynamics (X. Zhang, R. Srinivasan and M. Van Liew, 2008).

To combine datasets of different resolutions effectively, SWAT uses the following approaches: 1) resampling and aggregation method which coarser datasets like landcover may be resampled or aggredated to match the DEM or to fit within the sub-basin boundaries. For example, land cover data at 1km resolution might be averaged or reclassified into fewer categories to align with the smaller sub-basins created from a higher-resolution DEM., and 2) the dominant or threshold approach during defining the HRUs (Gassman *et al.*, 2007). So, in this study, we used the threshold-based method in the SWAT for overlaying of the datasets and creating the HRUs. After simulating processes at the HRU level, SWAT aggregates results back up to the sub-basin and watershed level. This approach allows the model to produce meaningful watershed-scale outputs despite the initial variation in data resolution (Abbaspour *et al.*, 2015).

4.3 Digital Elevation Model (DEM)

Digital Elevation Model (DEM) is used to define the topography of study area, delineate the sub-basin and stream networks in the modelling process. The resolution of the DEM is the most critical input parameter when developing a SWAT model (Gassman *et al.*, 2007)**.** In general, the quality of the DEM strongly has impacts on final output of the hydrological model (Chaubey *et al.*, 2005; Ayoubi, 2017). Therefore, it is wise to use the finest available DEM data for model application, if available. In this research the Shuttle Radar Topographic Mission (SRTM) DEM

with 30 m resolution obtained from USGS website (https://earthexplorer.usgs.gov) (U.S. Geological Survey, 2014). To prepare the DEM of the study area, 9 tiles of DEM were obtained, merged and then clipped in Arc GIS. These tiles are in 30m x 30m resolution and 1 x 1-degree latitude and longitude wide. The DEM was filled in the ArcMap using the raster editor tool and converted from geographic coordinate system (GCS) to Universal Transverse Mercator (UTM) coordinate system before using in SWAT. The statistical parameters of sub basin such as, slope gradient, slope length, and stream network characteristics (for instance: primary, secondary, mean rivers) calculated and derived from DEM during the model construction. The maximum elevation ranges to 5,694m and the minimum elevation ranges to 995m from see level in the UKRB (Figure 3-1 in chapter 3).

4.4 Model calibration

The successful application of a hydrologic model is highly dependent on the calibration, sensitivity and uncertainty analysis of parameters (Abbaspour, 2015; Mengistu, van Rensburg and Woyessa, 2019). In this study, two steps were used for calibration of the model; 1) the manual calibration helper in SWAT for parameterizations until a convenient result of simulated discharge obtained and; 2) the automatic calibration approach using the Sequential Uncertainty Fitting version-2 (Sufi-2) algorithm in the SWAT-CUP (SWAT Calibration and Uncertainty Program) (Abbaspour, Johnson and van Genuchten, 2004; Abbaspour, 2015). Sufi-2 is one of the stochastic calibration programs in SWAT-CUP and is a semi-automated inverse modelling procedure based on Latin Hypercube Sampling. A detailed description of SUFI-2 can be found in (Abbaspour, Johnson and van Genuchten, 2004; Abbaspour, 2015). In this study first the daily calibration, following the monthly calibration was performed using discharge at 6 gauging stations. The calibration performed from January 2010 to December 2016 (i.e., 7 years) in the UKRB. SUFI2 has many options of model performance indicators. For this study, the Nash-Sutcliffe coefficient (NS) was used as a major objective function in the calibration and validation process (Nash and Sutcliffe, 1970). The coefficient of determination (R^2), percent bias (PBIAS) (Yapo, Gupta and Sorooshian, 1996), and Kling-Gupta efficiency (KGE) coefficient (Gupta *et al.*, 2009) were also additional criteria used for the evaluation. Equations (5), (6), (7), (8) were used to calculate the performance indices by comparing the observations and estimated discharge in 6 stations.

$$NS = 1 - \frac{\sum_i (Q_{o,i} - Q_{s,i})^2}{\sum_i (Q_{o,i} - \overline{Q}_s)^2} \quad (5)$$

$$R^2 = \frac{\sum_i[(Q_{o,i}-\overline{Q}_o)(Q_{s,i}-\overline{Q}_s)]^2}{\sum_i(Q_{o,i}-\overline{Q}_s)\sum_i(Q_{s,i}-\overline{Q}_s)^2} \quad (6)$$

$$PBIAS = \frac{\sum_{i=1}^{n}(Q_{o,i}-Q_{s,i})*100}{\sum_{i=1}^{n}(Q_{o,i})} \quad (7)$$

$$KGE = 1 - \sqrt{(r-1)^2 + \left(\frac{\sigma s}{\sigma O}-1\right)^2 + \left(\frac{\mu s}{\mu o}-1\right)^2} \quad (8)$$

Where in equations (5-8), Q is discharge, $\overline{Q}$ is mean of discharge, o and s are observed and simulated, i is the i^{th} observed or simulated value, r is the linear scaling correlation between observed and simulated, σ is the standard deviation and μ is the mean.

Generally, the model simulations are called satisfactory if NSE > 0.50, the R^2 > 0.60 and the PBIAS is to be in range of approximately ± 25% (D. N. Moriasi *et al.*, 2007). A higher efficiency value indicates a more accurate prediction of observations, that's why authors tend to prefer higher values over lower ones (i.e., KGE = 1). Negative values of PBIAS indicate that the model overestimates flow while the positive values of PBIAS indicate underestimated flow (D. N. Moriasi *et al.*, 2007).

4.5 Sensitivity and Uncertainty analysis

The sensitivity analysis conducted based on One-at-a-time (OAT) sampling method to see the impact of parameters independently to streamflow. Then, the sensitivities of all parameters selected by one-at-a-time option were further prioritized by global sensitivity analysis option in SWAT-CUP. To prioritize the sensitive parameters, the p-value and t-state of global sensitivity procedure were used (Abbaspour *et al.*, 2015; Mengistu, van Rensburg and Woyessa, 2019). The sources of model uncertainty could be from driving variables (e.g. inputs), the conceptual model itself, the uncertainty in measured data, or the uncertainty during parametrization (Abbaspour *et al.*, 2015; Mengistu, van Rensburg and Woyessa, 2019). The propagation of all sources of model uncertainty to parameters and model outputs is expressed as the 95 % probability distributions. The 95 % probability distribution were calculated at the 2.5 % and 97.5 % levels of cumulative distribution of an output variable and it is called 95 % prediction uncertainty (95PPU) (Abbaspour *et al.*, 2015)**.** SWAT-CUP uses two statistical indicators to quantify all the sources of uncertainty includes the p-factor which is the percentage of observed data enveloped by the modelling results (95PPU), and the R-factor which is the thickness of the 95PPU envelop.

4.6 Model Validation

Validation is essential to trust the model's performance (D. N. Moriasi *et al.*, 2007)**.** The observed daily discharge was available from January 2017 to December 2018 (i.e. 1 year & 9 months) and have been used to validate the SWAT model at daily and monthly time scales in upper Kabul river basin.

4.7 Bias correction of temperature and precipitation from RCMs

Bias correction is the process of removing the systematic biases in the RCMs output with reference to the observed data for the historical period and applying the developed method for bias correction of future data (Dutta and Bhattacharjya, 2022). Tow types of data were used for bias corrections and climate change analysis: (1) the global APHRODITE (Asian Precipitation – Highly Resolved Observational Data Integration Toward Evaluation) precipitation and temperature dataset, available publicly; (2) Regional Climate Models (RCM) datasets (Table 4-2). The different data types used in this study, methods and tools used for performing bias corrections are explained in the sections bellow.

4.7.1 Historical data description (APHRODITE)

Due to lacking access of historical observations of daily precipitation and temperature in Kabul river basin, analyzing the climate data based on ground station is complicated and couldn't be possible. Therefore, the global APHRODITE (Asian Precipitation – Highly Resolved Observational Data Integration Towards Evaluation) precipitation and temperature grid datasets which are available in the public domain are used and accepted as observations for baseline period (Table 4-2). According to Ghulami (2017) the APHRODITE precipitation and temperature dataset is more suitable and was already validated based on ground station's for the Kabul river basin, so in the lack of sufficient surface observations, these data were used as a baseline reference to perform bias correction and to validate the RCMs dataset. Figure 4-2 shows the location of *APHRODITE* grid stations selected in this study.

The APHRODITE daily data cover a long period of more than 50 years (1951–2007) with a spatial resolution of 0.25° that is based on a dense network of rain-gauge data for Asia, including the Himalayas, South and Southeast Asia and mountainous areas in the Middle East. The grid datasets are created primarily with data obtained from a rain-gauge observation network using an interpolation scheme (Yatagai et al., 2012).

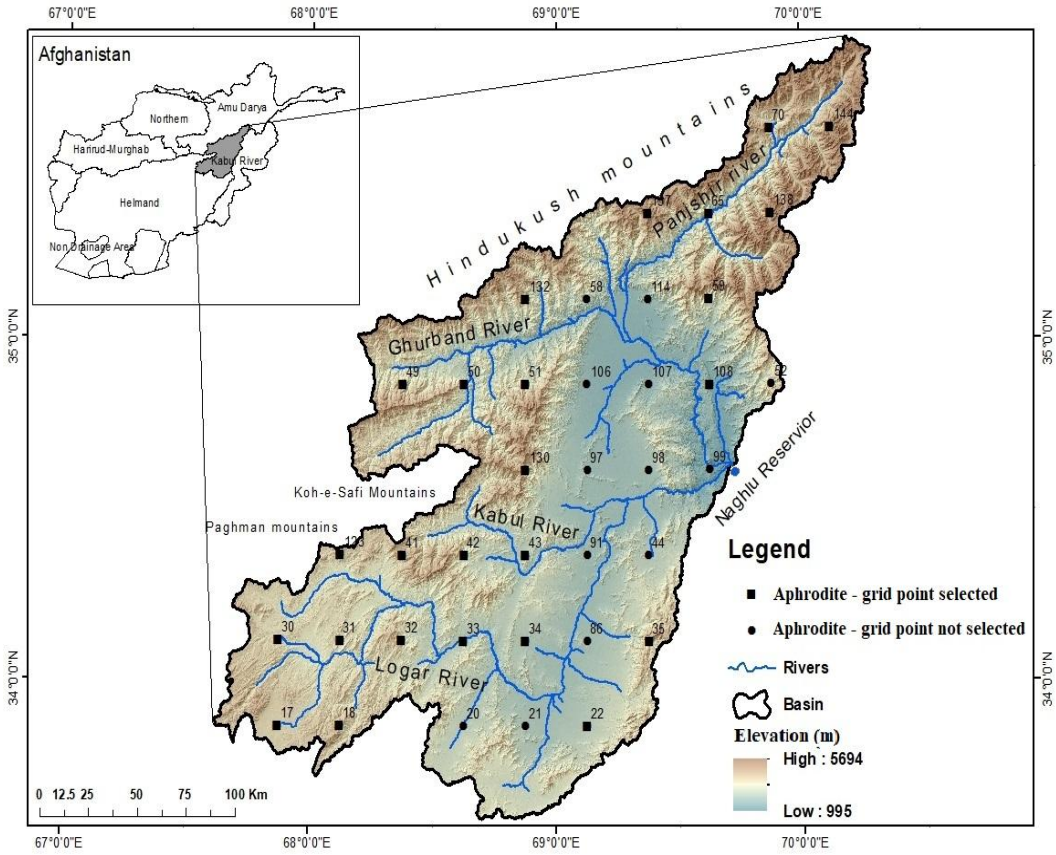

Figure 4-2: Location of selected Aphrodite climate grid stations in the upper Kabul river basin.

4.7.2 Climate projection experiments (SA-CORDEX)

Temperature and precipitation data were obtained from the Regional Climate Models (RCMs) of the South Asia domain of CORDEX (Coordinated Regional Downscaling Experiment) hosted by the German Climate Computing Centre (DKRZ) (CMIP5-DKRZ, 2021). CORDEX focuses on high-resolution climate information produced by different dynamical and statistical downscaling techniques, and aims to provide coordinated sets of high-resolution regional climate projections worldwide. Most of the CORDEX-RCM simulations are openly available through the Earth System Grid Federation (ESGF) and through regional data portals that are widely used for vulnerability, impacts, and adaptation (VIA) studies, which in turn guide decision-making at regional and local levels (Nikulin and Legutke, 2016). Four RCM models under RCP4.5 and RCP8.5 were used in the study (Table 4-2). The CORDEX RCM's data is presented on a 0.44° x 0.44° grid resolution; however, it still required bias correction before analysis.

In order to use the gridded precipitation and temperature products as inputs for hydrological applications and climate impact studies, it is necessary to assess the accuracy of these products

against the reference datasets. The RCM's data was selected based on its availability for Afghanistan and considering the previous climate change studies (Aich, N. A. Akhundzadah, *et al.*, 2017b; Ghulami, Babel and Shrestha, 2017; Sidiqi, Shrestha and Ninsawat, 2018). The future analysis was performed in two periods; the 2040s (2030-2049), and the 2090s (2080-2099) which were then compared with the baseline period of 1986-2005 to summarize the results.

Table 4.2: Description of the Aphrodite data and the regional climate models selected for this study.

Precipitation and temperature gridded dataset						
Name of product		Resolution	Domain	Institution	Availability	Reference
APHRODITE MAV1101R1		0.25°x 0.25°	Monsoon Asia 60° E-150° E, 15°S-55°N	Japan Meteorological Agency (JMA)	1951-2007	https://www.chikyu.ac.jp/precip/english/products.html
CORDEX SA RCMs (Regional Climate Models)						
Model	RCMs	Driving GCMs	Institution	Domain	Resolution	Reference
1	RCA4	CCCMa-CanESM2	SMHI	WAS-44	0.44° x 0.44°	https://esgf-data.dkrz.de/search/cmip5-dkrz/
2	RegCM4-4	NOAA-GFDL-ESM2M	IITM	WAS-44	0.44° x 0.44°	
3	REMO2009	MPI-M-MPI-ESM-LR	MPI-CSC	WAS-44i	0.44° x 0.44°	
4	RCA4	MIROC-MIROC5	SMHI	WAS-44	0.44° x 0.44°	

WAS: Stands for South Asia domain, 44 is the grid resolution, and suffix i mean regular grid; SMHI: Swedish Meteorological and Hydrological Institute, Rossby Centre (Sweden); IITM: Indian Institute of Tropical Meteorology (India); and MPI-CSC: Max Planck Institute for Meteorology - Climate Service Center at Germany.

4.7.3 Bias correction Methods

Temperature and precipitation in the RCMs often shows significant biases due to systematic model error or discretization and spatial averaging within grid cells which prevents the use of RCM's data as direct input for hydrological modeling (Teutschbein and Seibert, 2012). Therefore, bias correction procedures are essential to minimize the biases between simulated variables with the observations. Following the evaluation of bias correction methods in previous studies (Teutschbein & Seibert 2012; Mendez et al. 2020), three bias correction methods were used to adjust the biases in historical and future daily precipitation and temperature over UKRB, including the linear scaling (Ls), Delta change (Dc) and the Empirical quantile mapping (Eqm) methods. The Ls and Dc methods were performed using the CMhyd (Climatic Model data for hydrologic

modeling) tool (Rathjens *et al.*, 2016). However, the Eqm method was performed using the Q-map package (functions: 'fitQmapQUANT' and 'doQmapQUANT') in the R programming language (Lukas, 2016). The Eqm method was selected because the previous studies showed that this method yielded the best results for precipitation bias correction (Gudmundsson *et al.*, 2012a; Enayati *et al.*, 2021). The present study applied a variety of evaluation techniques, including visual comparison of simulations against APHRODITE data and the application of quantitative performance metrics. Standard deviation and correlations were also compared to assess the performance of each RCM and each bias correction method using Taylor diagrams. More details related to methods used are described in the following sections.

4.7.4 CMhyd (Climatic Model data for hydrologic modeling) Tool

CMhyd is designed to extract and perform bias corrections for each station. The underlying idea is to identify biases between observed and simulated historical climate variables to parametrize a bias correction algorithm that is used to correct simulated historical climate data. Figure 4-3 shows the methodology used for bias correction of Ls and Dc using CMhyd in this study. Bias correction procedures employ a transformation algorithm for adjusting climate model output (Rathjens *et al.*, 2016).

Several bias correction methods have been incorporated for temperature and precipitation bias-correction in CMhyd with the ability to analyze on a daily timescale. These methods are Linear scaling (Ls), Delta change (Dc), Distribution mapping (Dm), Local intensity scaling (Li) for precipitation, Power transformation (Pt) for precipitation, and Variance scaling (Vs) for temperature (Teutschbein and Seibert, 2012; Rathjens *et al.*, 2016). Bias correction methods are assumed to be stationary, i.e. the correction algorithm and its parametrization for current climate conditions are assumed to be valid for future conditions as well. Thus, the same correction algorithm is applied to the future climate data. However, it is unknown how well a bias correction method performs for conditions different from those used for parametrization (Rathjens *et al.*, 2016). A good performance during the evaluation period does not guarantee a good performance under changed future conditions. A previous study (Teutschbein and Seibert, 2012) provided mathematical descriptions for all these methods. Following the evaluation of bias correction methods in previous studies (Teutschbein and Seibert, 2012; Mendez *et al.*, 2020), the Ls and Dc methods were selected to adjust the temperature and precipitation for the baseline and future scenarios using CMhyd tool.

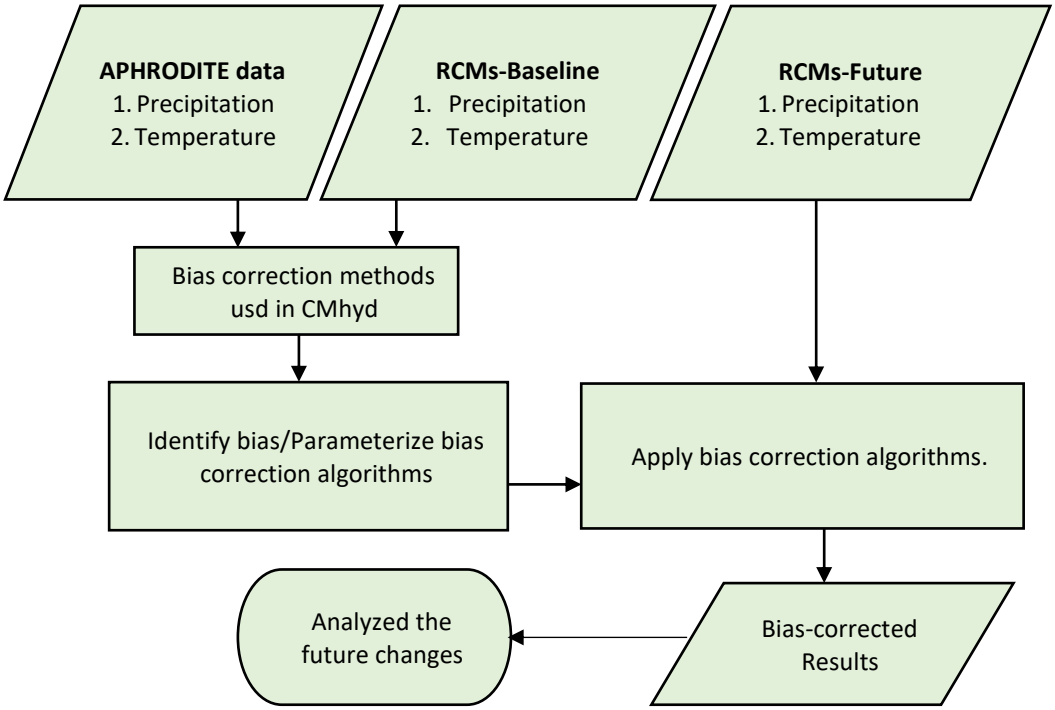

Figure 4-3: Method used for delta change and linear scaling approach using CMhyd tool.

4.7.5 Linear Scaling (Ls) method:

Linear scaling (Ls) is the most straightforward bias correction approach used in several studies (Teutschbein and Seibert, 2012; Shrestha, Acharya and Shrestha, 2017; Selvakumar and Gunavathi, 2021). Ls adjusts the mean monthly values with a perfect agreement with the mean monthly observations. Precipitation is corrected with a factor based on the ratio of long-term monthly mean observed and control data. Temperature is corrected with help of an additive term based on the difference of long-term monthly mean observed and control data, (Teutschbein and Seibert, 2012). The applied correction factors and addends are assumed to remain unvaried even for future conditions (Teutschbein and Seibert, 2012). However, the Ls approach can correctly adjust the climatic factors only when the monthly mean values are included (Selvakumar and Gunavathi, 2021). The method can be expressed in the equations 9-12.

$$P^{*}_{Cont}(i) = P_{raw}\ (i)\ \times \left[\ \frac{\mu_m\ (P_{obs}\ (i))}{\mu_m\ (P_{raw}\ (i))}\ \right] \tag{9}$$

$$P^{*}_{Scen}(i) = P_{raw}\ (i)\ \times \left[\ \frac{\mu_m\ (P_{obs}\ (i))}{\mu_m\ (P_{raw}\ (i))}\ \right] \tag{10}$$

$$T^{*}_{Cont}(i) = T_{raw}(i) + \mu m\left(T_{obs}(i)\right) - \mu m\left(T_{raw}(i)\right) \quad (11)$$

$$T^{*}_{Scen}(i) = T_{raw}(i) + \mu m\left(T_{obs}(i)\right) - \mu m\left(T_{raw}(i)\right) \quad (12)$$

Where, P* and T* represent the final bias-corrected precipitation and temperature, *Cont* and *Scen* shows the control (historical) and future periods, P_{raw} and T_{raw} shows raw precipitation and temperature from RCMs, respectively. (i) is time interval (daily), P_{obs}, T_{obs} is the observed precipitation & temperature, and μ_m is the mean values for the month.

4.7.6 Delta Change (Dc) method:

Delta change method is comparatively simple and widely used in future climate change projections (Selvakumar and Gunavathi, 2021). This method computes differences between current and future RCM simulations and adds these changes to the observed time series. Applying the Dc method assume that GCM/RCM simulate relative changes more reliably than absolute values (Ghulami *et al.*, 2022). The advantage of Dc approach is to consider the relative changes, and therefore these changes can be applied to the baseline observations any time they become available (Ghulami *et al.*, 2022). The Dc method was used for precipitation and temperature data using equations (13-14); more details about the Dc could be found in (Teutschbein and Seibert, 2012; Rathjens *et al.*, 2016) respectively.

$$P_{Corr}(i) = P_{obs}(i) * \frac{\mu m\,(P_{Corr}(i))}{\mu m(P_{raw}(i))} \quad (13)$$

$$T_{Corr}(i) = T_{obs}(i) + \mu m\left(T_{corr}(i)\right) - \mu m(T_{raw}(i)) \quad (14)$$

Where P_{obs}, P_{raw} and P_{corr} denote observed, raw and corrected precipitation, while T_{obs}, T_{raw} and T_{corr} are observed, raw and corrected temperature on the day (i^{th}) of the month (m) respectively, and μm denotes the monthly mean values.

4.7.7 Empirical quantile mapping (Eqm)

In general, the quantile mapping (Qm) methods implement statistical transformation for post-processing of climate modeling outputs. There are several *Qm* methods for adjusting the precipitation and temperature bias correction methods, and may not necessarily have a similar capability in the correction of biases in the RCM's output (Enayati *et al.*, 2021). These methods include the Empirical quantile mapping (Eqm), Empirical robust quantile mapping (*ERQM*),

Parametric transformation functions (PTF), Distribution derived transformation (*DIST*), Smoothing splines (*SSPLIN*), and Quantile delta mapping (*QDM*). The *Eqm* method was selected in this study because the previous studies showed that the this method performed the best results in bias correction (Gudmundsson *et al.*, 2012a; Enayati *et al.*, 2021). Eqm is a non-parametric method using the non-parametric transformation function (Qian and Chang, 2021). Eqm estimates values of the empirical cumulative distribution functions (CDFs) of observed and modeled time series for regularly spaced quantile levels (0, 0.01…, 0.99, 1.00). Accordingly, Eqm uses the linear interpolations to adjust a datum with unavailable quantile values (Enayati *et al.*, 2021). The bias corrected future projection at time-t via quantile mapping can be mathematically expressed as below equation.

$$x^{\circ}(t) = F_{o,h}^{-1}\left[F_{m,f}\left(x_{m,f}(t)\right)\right] \quad (15)$$

Where, $x°$ (t) denote the estimated future observation at time t during the projection period. This is obtained by bias correcting future model simulation via a transfer function g ( ), such that $x°$ (t) = g [$x_{m,f}$(t)]. $F_{o,h}^{-1}$ is inverse of CDF for the historical observations, $F_{m,f}$ is CDF of the future climate models, and $x_{m,f}(t)$ is future climate model data at time t.

4.7.8 Taylor Diagrams

Taylor diagrams are used for evaluation of the results against the observations, and designed to graphically show which of several approximate representations (in this case, a collection of climate models) is most realistic or how close a set of patterns match observations (Taylor, 2001). This diagram, facilitates the comparative assessment of different models. It is used to quantify the degree of correspondence between the modeled and observed variables (in our case precipitation and temperature) in terms of three statistics: the Pearson correlation coefficient (*R*), the root-mean-square error (*RMSE*), and the standard deviation (*Std*). The *R* should be as close to 1 as possible. *RMSE* should be as small as possible and close to zero, and the *Std* of the model results should be as close as possible to the *Std* of the observations.

Taylor diagrams have been primarily used to evaluate models designed to study climate change and other aspects of Earth's environment (Sun *et al.*, 2018). Taylor also noted the geometric connection between correlation, standard deviation, and the central pattern *RMSE*, and found that all three could be plotted simultaneously (Taylor, 2001). Generally, the plotted values are derived from climatological monthly, seasonal, or annual means. Because the different variables (e.g.,

precipitation and temperature) may have widely varying numerical values, the results are normalized by the reference variables. The ratio of the normalized variances indicates the relative amplitude of the model and observed variations. Taylor diagram combines various statistical indicators for multiple models on a single quadrant: The correlation coefficient values, the x-axis, the y-axis, delimit arcs with standard deviation values, and the internal semi-circles correspond to the RMSE values. The statistical indicators show the performance of the individual models in comparison with the observations. The RMSE measures the differences between values predicted by a model or estimator and the values observed. It is a good measure of accuracy. Meanwhile, the correlation coefficient is a measure of the correlation (linear dependence) between two variables. Taylor diagrams can be constructed with a number of different open source and commercial software packages, including: MATLAB, Python and R programming language.

4.7.9 Need for Taylor Diagrams

When we need to check the quality of several simulated models vs. the observations with different statistical tests, we should first compute the statistical analyses between the observations and future model's data, then check each of the results and decide that one of the applied models has the better result in compare to the observations. This process is not easy when we have several models under various scenarios and for multiple parameters simultaneously. In this situation, the best method to achieve and analyses the best results in a short time will be the using of Taylor diagrams.

4.7.10 How to compute Taylor Diagram?

In general, the Taylor diagram characterizes the statistical relationship between two fields, a test field (a field simulated by a model) and a reference field (observations) Taylor (2005). The reason that each point in the two-dimensional space of the Taylor diagram can represent three different statistics simultaneously (i.e., the centered RMS difference, the correlation, and the standard deviation) is that these statistics are related by the following formula:

$$E'^2 = \sigma_{f^2} + \sigma_{r^2} - 2\sigma_f \sigma_r R \qquad (16)$$

Where R is the correlation coefficient between the test and reference fields, E' is the centered RMS difference between the fields, and σ_{f^2} and σ_{r^2} are the variances of the test and reference

fields, respectively. The construction of the diagram (with the correlation given by the cosine of the azimuthal angle) is based on the similarity of the above equation and the Law of Cosines:

$$c^2 = a^2 + b^2 - 2ab\cos\emptyset \tag{17}$$

5 RESULT AND PERFORMANCE EVALUATION

5.1 Calibration and validation of SWAT (current scenario)

Model performance is usually evaluated by measuring the simulated result versus the observations (e.g., discharge, precipitation, temperature, sediment, etc…) in a study area. In this section, the results from SWAT is described in a daily and subsequently in a monthly time period for assessment of water availability in UKRB.

5.1.1 Daily flow results

The daily hydrologic model of UKRB was calibrated for the period of 2010-2016 and validated for 2017-2018 based on observed discharge availability. The daily graphical comparison of simulated and observed streamflow during calibration and validation is shown in Figure 5-1. Model performance was satisfactory to good across the basin with worse results being obtained in dry areas (e.g. Sangi-i-Nawishta station in Logar river) in Table 5-1. Meanwhile, the uncertainty was recorded at maximum range in the peaks simulated by SWAT. There is an underestimation of the flow peak for some years in calibrated stations. The simulated baseflow was in a very reasonable fit in all stations, except for Pul-i-Ashawa, where the falling limb shows higher baseflow in August and September compared to the observations. Total drainage area of UKRB is almost 26,000 km^2 and the terrain is differing from a very mountainous to flat areas with dissimilar climatic conditions. Therefore, to account the orographic effects, precipitation laps rate (mm H2O/Km) and temperature laps rate (°C/Km) were adjusted by adding the elevation bands in the sub-basins (95 sub-basin) (Neitsch *et al.*, 2011; Arnold *et al.*, 2012).

The statistics of model performance indicators for daily calibration and validation are shown in Figures 5-2 and 5-3. The main objective function used was the Nash-Sutcliffe (NS) coefficient. For Tangi Gulbarhar, the daily results of NS statistics showed a very good correlation, which was 0.85 during calibration and 0.90 during validation, respectively. The NS was 0.73 and 0.68 for Shukhi station, 0.59 and 0.03 for Pul-i-Ashawa, 0.58 and 0.70 for Tang-i-Gharu, 0.63 and 0.57 for Tang-i-Saidan during calibration and validation, respectively. Whereas, the NS was 0.44, 0.14 at Sang-i-Nawishta station and was satisfactory over the calibration and validation period, respectively.

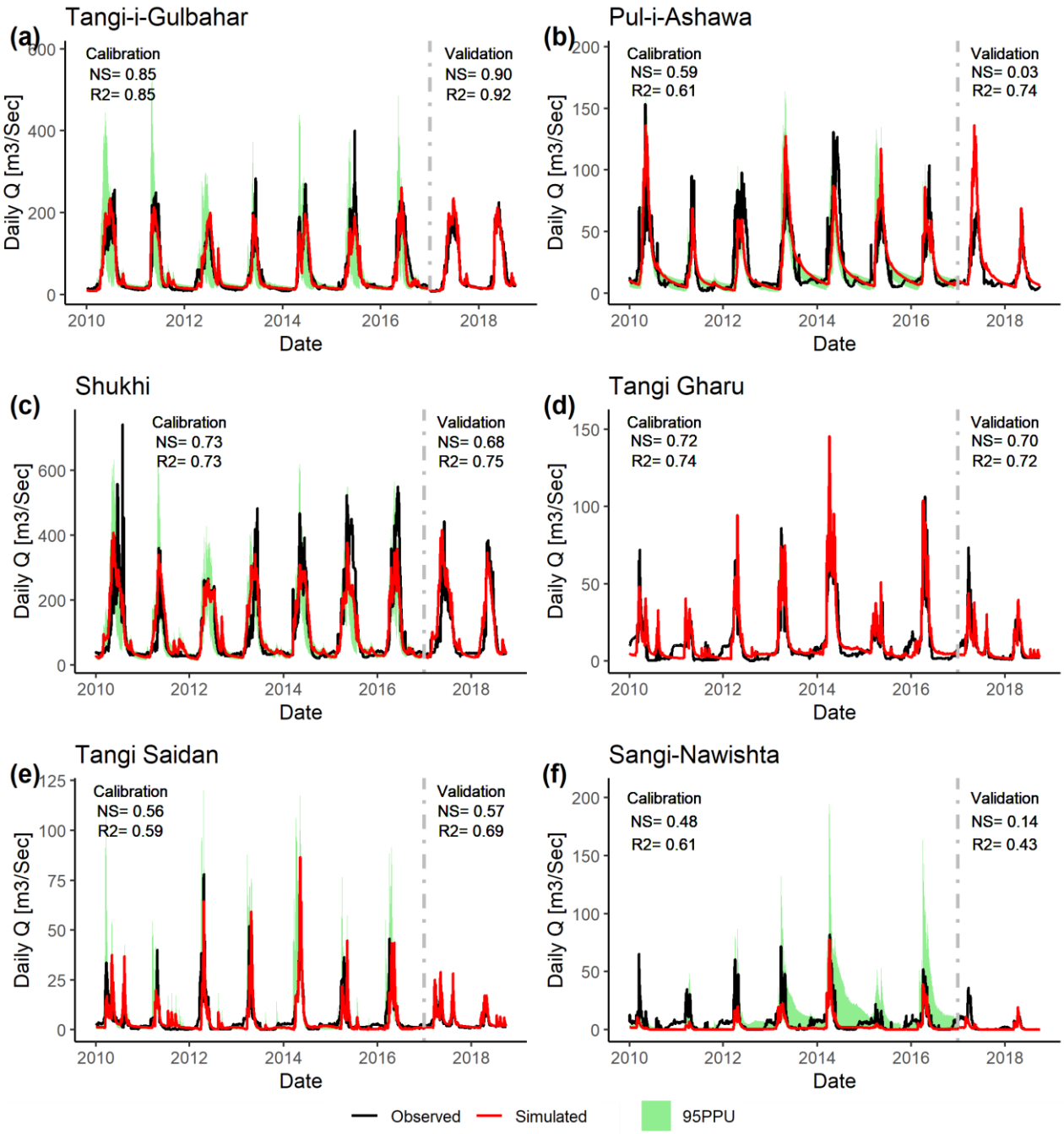

Figure 5-1: Comparison of daily observed and simulated streamflow during calibration (2010-2016) and validation (2017-2018) at Tangi-gulbahar, Pul-i-ashawa, Shukhi, Tang-i-gharu, Tang-i-saidan, and Sang-i-Nawishta stations located in UKRB. 95PPU shows the 95 percent prediction uncertainty.

Table 5.1: Daily statistical results during calibration and validation in 6 stations of UKRB. Cal= calibration, Val= validation in the table.

	Tang-i-Gulbahar		Pul-i-Ashawa		Shukhi		Tang-i-Gharu		Tang-i-Saidan		Sang-i-Nawishta	
	Cal	**Val**	**Cal**	**Val**	**Cal**	**Val**	**Cal**	**Val**	**Cal**	**Val**	**Cal**	**Val**
p-factor	0.83	0.47	**0.74**	**0.3**	**0.73**	**0.19**	**0.16**	**0.20**	**0.38**	**0.23**	**0.64**	**0.07**
r-factor	1.00	0.00	**0.74**	**0.00**	**0.75**	**0.00**	**0.09**	**0.12**	**0.90**	**0.06**	**1.71**	**0.00**
R^2	0.85	0.92	**0.61**	**0.74**	**0.73**	**0.75**	**0.74**	**0.72**	**0.59**	**0.69**	**0.61**	**0.43**
NS	0.85	0.9	**0.59**	**0.03**	**0.73**	**0.68**	**0.72**	**0.70**	**0.56**	**0.57**	**0.48**	**0.14**
PBIAS %	5.1	-4.7	**2.5**	**-36.3**	**-3.7**	**-16.2**	**3.30**	**10.1**	**24.8**	**-14.2**	**0.55**	**69.5**
	Very good		good		Very good		good		good		satisfactory	

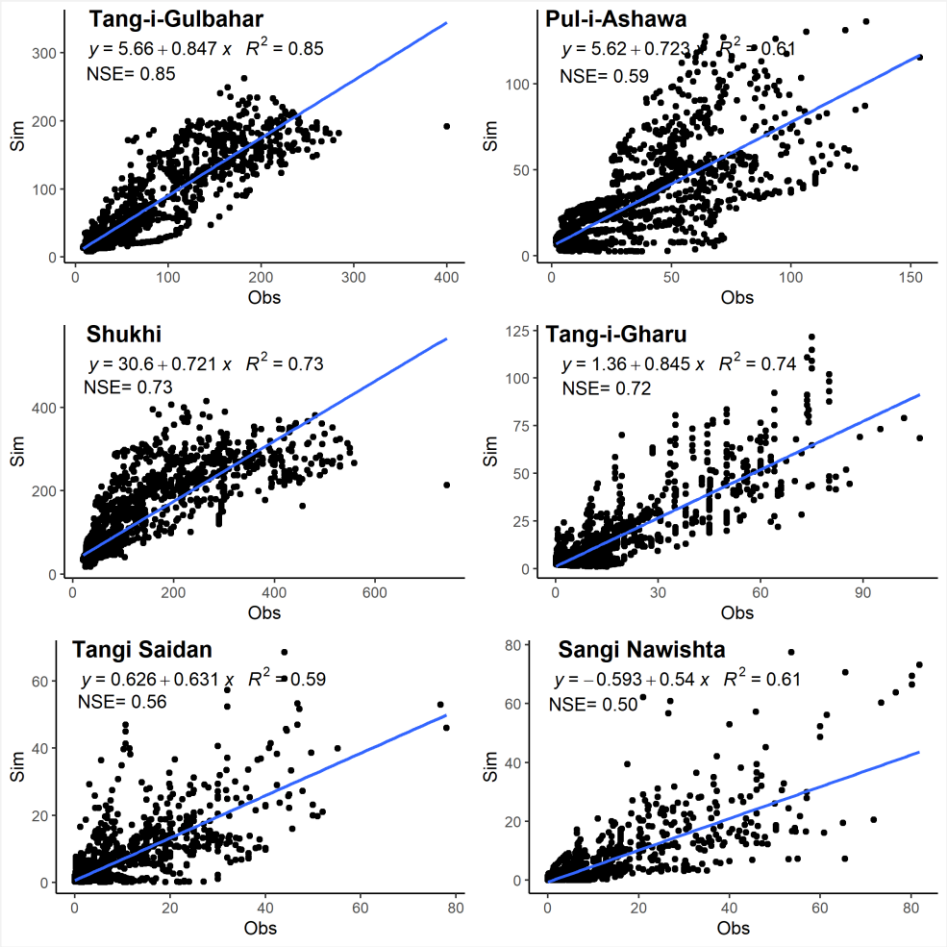

Figure 5-2: Comparison of observed and simulated daily discharge by scatter plots, and its statistical results during calibration period (01.2010- 12. 2016) in 6 station of UKRB.

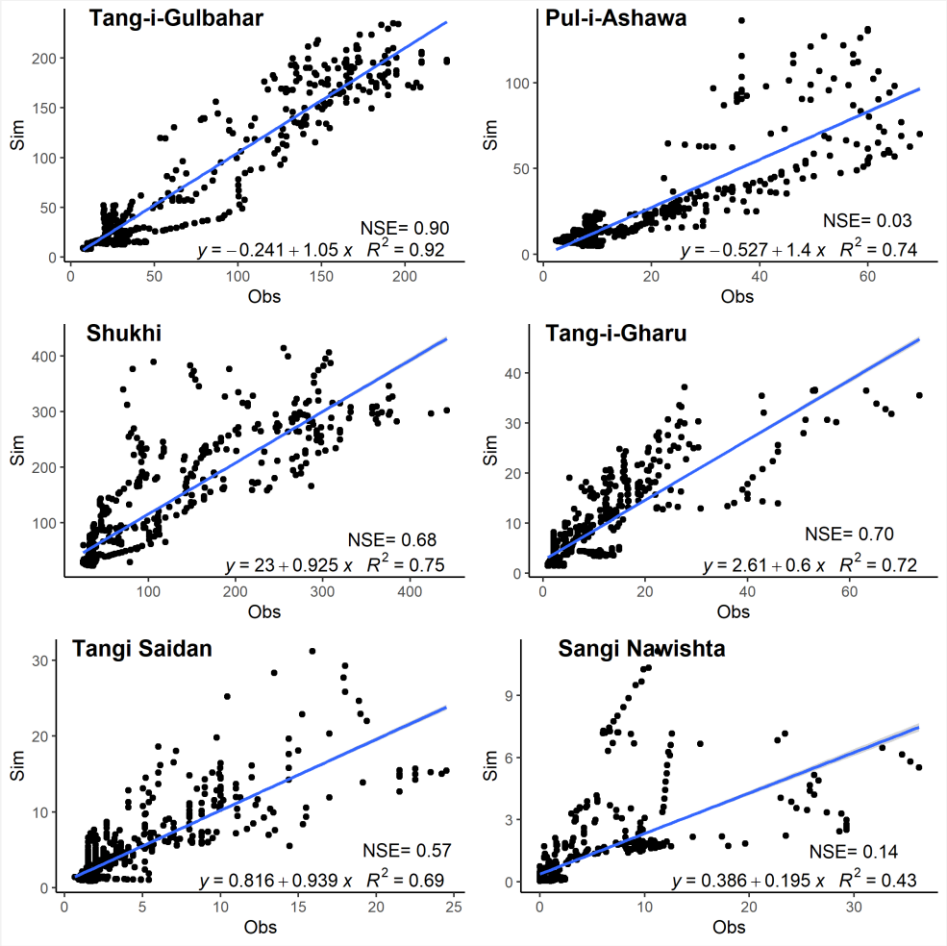

Figure 5-3: Comparison of observed and simulated daily discharge by scatter plots, and its statistical results during validation period (01. 2017- 09. 2018) in 6 station of UKRB.

To further evaluate the daily runoff results of the SWAT in UKRB, the water volumes of two station from deferent watersheds (from upstream and downstream) were analyzed and compared. The difference in the daily streamflow volume of Tang-i-Gulbahar station at Panjshir river, and Tang-i-Saidan station at Kabul river are summarized in Table 5-2. The volume of runoff at Panjshir River is about 10 times greater than the volume of runoff at the Kabul river. The Logar river and Kabul rivers in UKRB derive their flow from winter and spring precipitation. While, the flow in the Panjshir river is mainly from snowmelt and glacier melt. The base flow of the Logar and Kabul sub-basin during the summer months is very low when the demand for irrigation water is greatest, whereas there is a substantial base flow in the Panjshir watershed.

Table 5.2: Comparison of UKRB Subbasins at two-gauge stations from (2010-2018).

Station	DA (Km^2)	AF (m^3/Sec)	AAF (Mm^3/yr)	Yield (m^3/sec/Km^2)	Yield (l/sec/Km^2)	Yield/TA (Mm^3/yr/km^2)
Tang-i-Gulbahar station at Panjshir river.	2703	50	1,590	0.0182	18.17	65.88
Tang-i-Saidan station at Kabul river.	1642	5	150	0.0024	2.38	5.28

Note: DA= Drainage area, AF= Average Flow, AAF= Annual Average flow, TA= Total Area

5.1.2 Monthly calibration results

The SWAT was calibrated for monthly runoff from 2010 to 2016, and validated from 2017 to 2018 for assessing the monthly hydrologic response in UKRB. The monthly runoff also shows that the model performance is quite satisfactory to good across the basin with worse results being obtained for Sangi-i-Nawishta station. The monthly graphical comparison of simulated and observed streamflow during calibration and validation is depicted in Figure 5-4.

The peaks in runoff shows underestimation for some years in all stations during calibration, (specifically is much lower for Sang-i-Nawishta at Logar river), while it is overestimated in some stations during validation. Although the timing of the discharge peaks is accurate for the calibration and validation periods, the PBIAS is still within the range in the results recorded for the UKRB. It is obvious from observed and simulated hydrographs (Figure 5-4) that the magnitude of water flow varies from year to year and usually is higher between May and August. The runoff peak starts in April followed by June and July each year and lasts until the end of August. Shukhi station at Panjshir river recorded the highest annual peak flows in June 2015 and 2016. Similar flow peaks can also be seen in the validation graphs (Figure 5-4). Generally, it can be seen that the SWAT model produced statistically satisfactory results in comparison with observations at various watersheds.

The percentage of bias (PBIAS) measures the average tendency of the simulated data to be larger or smaller than their observed counterparts (Golmohammadi *et al.*, 2014). The optimal value of PBIAS is 0.0, with low magnitude values indicating an accurate model simulation. Positive values indicate under-estimation bias, and negative values indicate over-estimation bias (Golmohammadi

et al., 2014). Moreover, the PBIAS is in a good range for all stations, except Sang-i-Nawishta. The PBIAS results showed as following during calibration and validation respectively.

- Tang-i-Gulbahar: 4.2 % underestimation in calibration, 4.8 % overestimation in validation.
- Pul-i-Ashawa: 2.6 % underestimation in calibration, 36 % overestimation in validation.
- Shukhi: 3.7 % and 16.2 % overestimation in calibration and validation, respectively.
- Tang-i-Gharu: 1.1 % and 10.5 % underestimation in calibration and validation, respectively.
- Tang-i-Saidan: 22 % underestimation in calibration, 14 % overestimation in validation.
- Sang-i-Nawishta: 58 % and 69 % underestimation in calibration and validation, respectively.

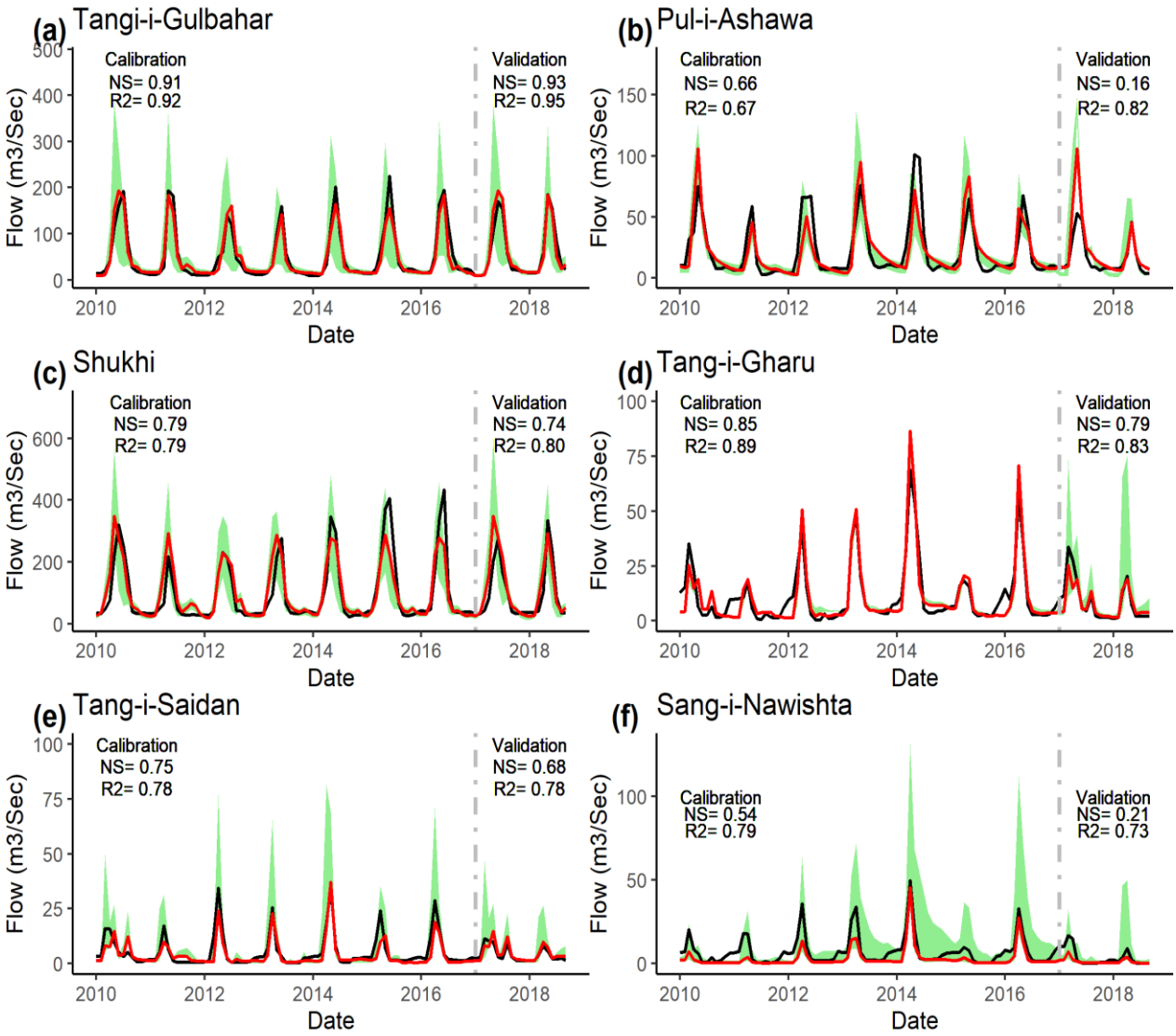

Figure 5-4: Comparison of monthly observed and simulated stream flow during calibration (2010-2016) and validation (2017-2018) at Tangi-gulbahar, Pul-i-ashawa, Shukhi, Tang-i-gharu, Tang-i-saidan, and Sang-i-Nawishta stations located in UKRB.

5.1.3 Monthly statistical results

The Nash-Sutcliffe (NS) coefficient was used as a main objective function during monthly calibration process. Three other objective functions were also selected and analyzed: namely the coefficient of determination (R^2), the percent bias (PBIAS) and Kling-Gupta efficiency (KGE). Table 5-3 shows the monthly statistical results from SWAT model. The monthly NS results was 91 % for Tangi Gulbarhar, 79 % for Shukhi, 66 % for Pul-i-Ashawa, 85 % for Tangi-Gharu, 75 % Tang-i-Saidan, and 54 % for Sang-i-Nawishta stations, respectively during calibration. All stations had good to very good agreements between simulated and observed runoff, except Sang-i-Nawishta which is satisfactory in this study.

The monthly validation results showed the NS of 0.93 for Tangi Gulbarhar, 0.74 for Shukhi, 0.16 for Pul-i-Ashawa, 0.79 for Tang-i-Gharu, 0.68 Tang-i-Saidan, and 0.21 for Sang-i-Nawishta stations, respectively in Table 5-3. The lower values of NS in Sang-i-Nawishta could be due to observed discharge error or the input precipitations in SWAT. The overall range of NS achieved in this study was in agreement with other similar studies performed at larger basins (Abbaspour *et al.*, 2015; Ayoubi and Dongshik, 2016; Akhtar *et al.*, 2021). In addition, good corresponding between other model outputs and measured data (soil moisture, evapotranspiration, etc.) might increase confidence in the model calibration.

Table 5.3: Monthly summary statistical results during calibration and validation in 6 stations of UKRB. Cal= calibration, Val= validation in the table.

	Tangi Gulbahar		**Puli Ashawa**		**Shukhi**		**Tangi Gharu**		**Tangi Saidan**		**Sangi Nawishta**	
	Cal	Val	Cal	Val	Cal	Val	Cal	Val	Cal	Val	Cal	Val
p-factor	0.83	0.47	0.74	0.3	0.73	0.19	0.42	0.11	0.38	0.19	0.64	0.05
r-factor	1.0	0.0	0.7	0.0	0.0	0.0	1.4	0.0	0.9	0.0	0.1	0.0
R2	0.92	0.95	0.67	0.82	0.79	0.8	0.89	0.83	0.78	0.78	0.79	0.73
NS	0.91	0.93	0.66	0.16	0.79	0.74	0.85	79	0.75	0.68	0.54	0.21
PBIAS	4.2	-4.8	2.6	-36.3	-3.7	-16.2	1.1	10.5	22.5	-13.9	58.1	69.6
KGE	0.89	0.88	0.80	0.27	0.82	0.78	0.85	0.71	0.69	0.76	0.34	0.017
	v. good		good		v. good		good		good		satisfactory	

In the calibration period, the mean and standard deviation values of simulated runoff versus observed runoff values are analyzed and shown in Table 5-4 for monthly interval. Based on the statistical results and the differences which were of small magnitude, it can be verified that the

SWAT model adequately simulated the runoff and hydrological parameters in UKRB, demonstrating its quality and potential as a numerical tool for water resources management.

Table 5.4: The mean and standard deviations of disrcharge in calibration and validation periods.

	Calibration (Discharge)				**Validation (Discharge)**			
Stations Name	Mean		Std-Dev		Mean		Std-Dev	
	Sim	Obs	Sim	Obs	Sim	Obs	Sim	Obs
Tang-i-Gulbahar	49.0	51.2	52.1	56.9	60.9	58.1	63.5	57.9
Pul-i-Ashawa	*21.6*	*22.2*	*21.7*	*23.3*	*22.2*	*16.3*	*24.0*	*14.8*
Shukhi	100.4	96.8	89.2	102.7	112.4	96.7	98.0	89.7
Tang-i- Gharu	11.1	11.3	15.7	13.8	7.8	8.7	6.8	9.1
Tang-i-Saidan	4.0	5.2	6.2	7.5	4.6	4.0	3.8	3.3
Sang-i-Nawishta	3.0	7.1	6.4	8.8	1.1	3.6	1.7	5.1

Sim= Simulation, Obs= Observed, Std = Standard Deviation

5.1.4 Monthly Flow Duration Curve (FDC)

It is essential to understand the hydrological behavior of watersheds to get more precise results for planning all demands for water use, through reference flow procedures Rosario *et al.*, (2017). One of the alternatives to determine water availability in a watershed is the construction of flow duration curves (FDC). Discharges with probability of exceedance equal to or over 90 % are essential in hydrological studies for planning water supply, since they indicate the quantity of water that can be guaranteed with the corresponding certainty level. Discharges with probability of exceedance of 50 % are important to evaluate the maximum possible flow to be regularized. The probability of exceedance equal to or lower than 10 % are applied in studies associated to extreme flood events (Oliveira et al., 2015).

Figure 5-5 illustrates the monthly simulated versus observed runoff duration curves in the period of 2010-2018 in the UKRB. By observing the FDC, it can be observed that the simulated flow frequency was same as observed in Tang-i-Gulbahar station at Panjshir river. The simulated flow frequency was underestimated compared to observed flow between 15 % - 20 %, and between 35% - 50% of probability of exceedance but in contrary the flow frequency was overestimated over 70% probability of exceedance in Pul-i-Ashawa station at Ghurband river.

In the Shukhi station at Panjshir river, the simulated flow was under estimated below 20% of probability of exceedance, while it was overestimated under 40% of probability of exceedance, and

as well as over 80% of probability of exceedance. Concerning the Kabul and Logar rivers, the simulated FDC shows underestimation between 30 % - 60 % of probability of exceedance, but overestimated over 80 % of probability of exceedance. In Tang-i-Saidan station, the simulated FDC was underestimated below 49 % and overestimated above 80 % of probability of exceedance. The Sang-i-Nawishta station, the simulated flow was underestimated compared to observed flow in below 80 % of probability of exceedance. The magnitude of difference was high in highest flow rates in most stations. Over 80% probability of exceedance level is considered safe for determining assured water supply in the basin.

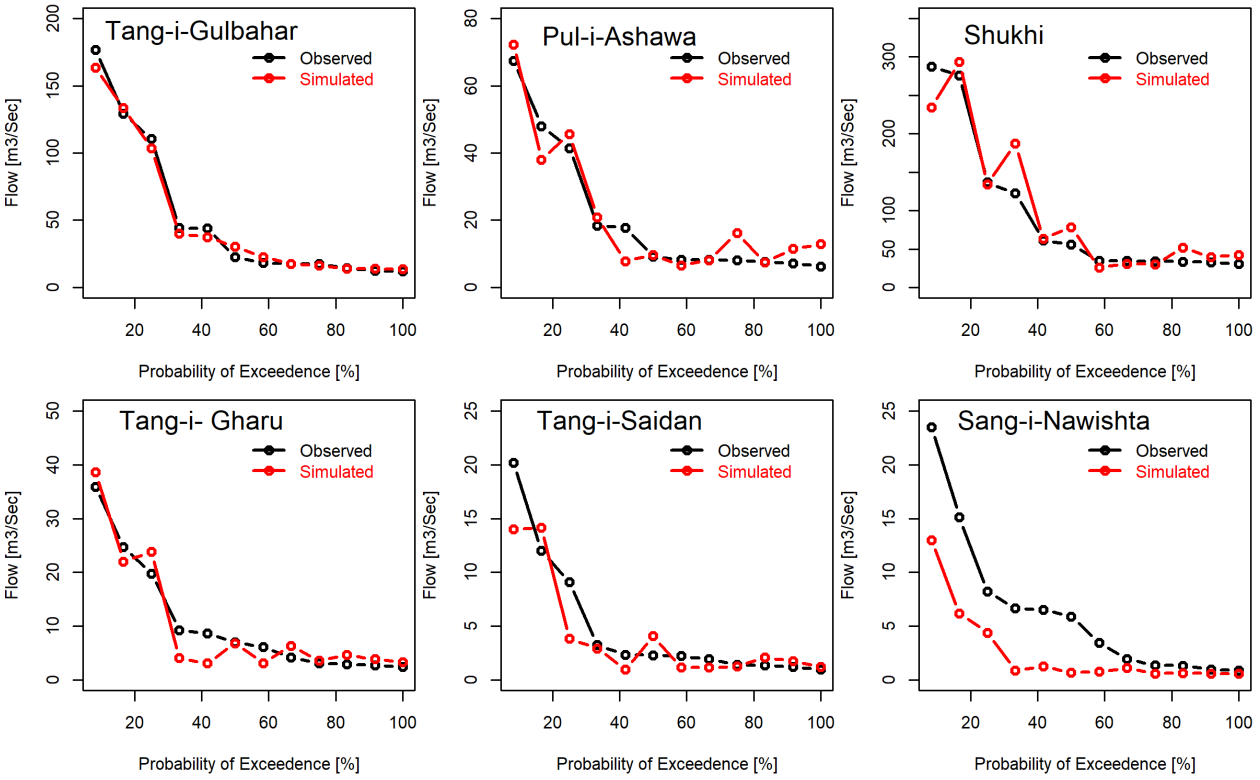

Figure 5-5: Flow duration curve of discharge in six hydrological stations in UKRB.

5.1.5 Monthly water balance

The outputs provided by the model are very exhaustive covering all the components of water balance, spatially and temporally. The sub components of the water balance that are more significant and were used for analyses include: precipitation, total water yield, actual evapotranspiration (ET). The water yield includes the surface runoff, lateral flow and base flow (or shallow groundwater). In other words, the total water yield is the equivalent depth in mm of flow

past the outlet of the watershed. These components are expressed in terms of monthly or annual depth of water in mm over the entire watershed area. The monthly water balance components including rainfall, water yield and evapotranspiration from 2010-2019 in the UKRB is depicted in the Figure 5-6. Average monthly total water yields (combined surface flow, lateral flow, and groundwater flow) supply the river flow with peaks starting in March and continues to August. Between February and July, the surface flow contributed more than lateral flow and groundwater flow with the high peaks 27 mm in May. This is due to contributions from rainfall and snow mostly in winter and spring months (December to May). The river flow also was mainly supplied by ground water (baseflow) all over the year with higher peaks between May and July. Between August to February, the figure obviously shows that the contribution of ground water flow was greater than surface runoff. Because in these months the occurrence of rain and snowfall was minimal, and it may be partly attributed to melt of snow and glaciers in the UKRB Figure 5-6. It can be seen that the water losses due to evapotranspiration are greater than water yield in UKRB.

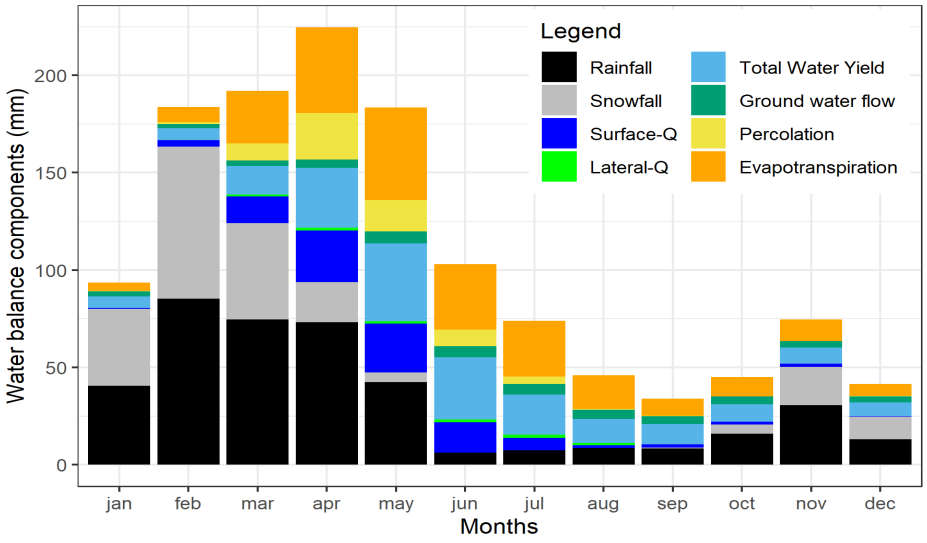

Figure 5-6: Simulated monthly water balance components in the UKRB.

5.1.6 Annual water balance

The temporal annual distribution of major water balance is depicted in the Figure 5-7, which includes the average annual precipitation, water yield, evapotranspiration and the groundwater recharge in UKRB. As shown in Figure 5-7 , the inter annual variation of rainfall for the period 2010 to 2019 was from 287 mm to 544 mm with minimum rainfall occurred in 2018 and maximum rainfall occurred in 2019. While the inter annual variation of water yield was from 113.8 mm to

199.5 mm for the same period. This shows that there is some degree of fluctuations in the rainfall and runoff pattern in the study area.

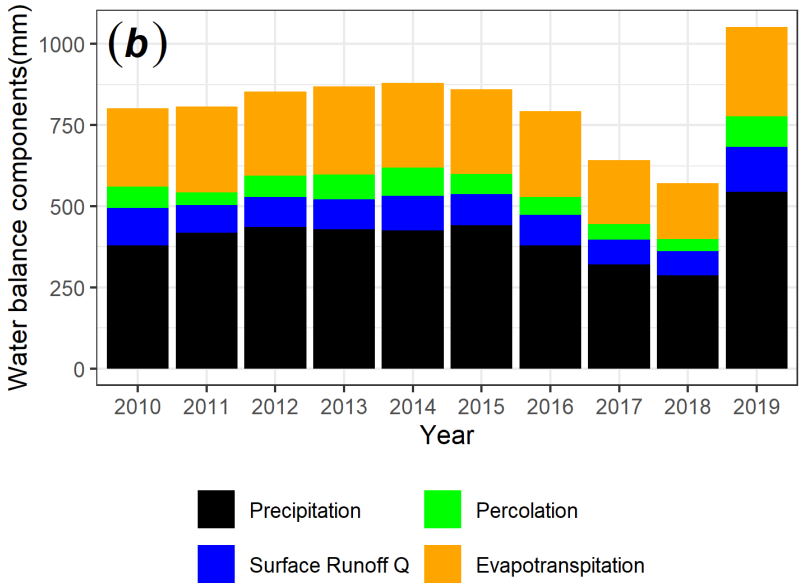

Figure 5-7: Simulated annual water balance components for UKRB (2010-2019).

By inserting an input of 406 mm average precipitation, the model simulation showed the output as 148 mm total water yield that accounts for 39 % of the basin water balance. While due to larger potential evapotranspiration of 1,790 mm, the average ET was estimated greater than the total water yields as 246.6 mm or 61 % of the total hydrological parameters that goes back to atmosphere. The surface runoff accounts for 24 % and the total aquifer recharge accounts 15.1 % of the annual hydrological cycle in UKRB, figure 5-8. Moreover, the soil characteristics of the basin allow percolation of 61 mm.

5.1.7 Annual cumulative runoff

The annual cumulative runoff calculated for each year and shows a very close result between observed and simulated runoff (Figure 5-9). From the cumulative runoff results, it is also indicated that model predicted runoff is in good agreement with observations, except the Sang-i-Nawishta station.

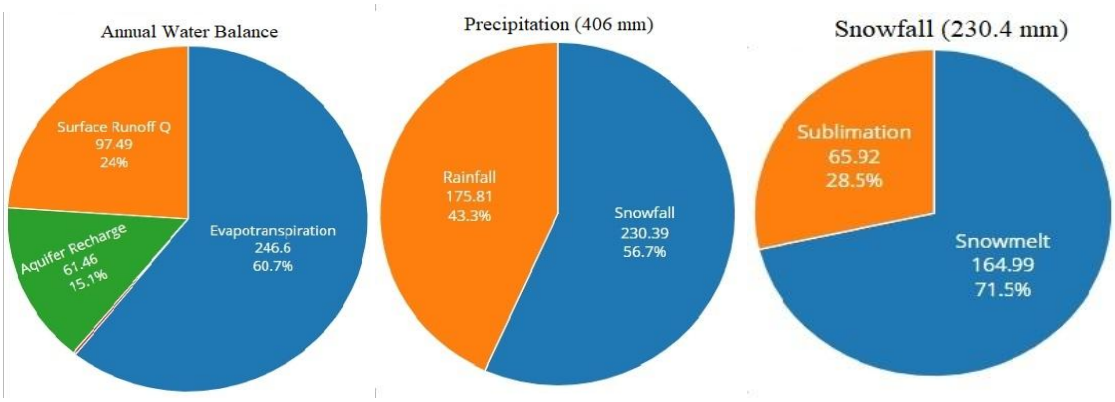

Figure 5-8: The annual water balance, precipitation and snowmelt outputs from SWAT in UKRB from 2010-2019.

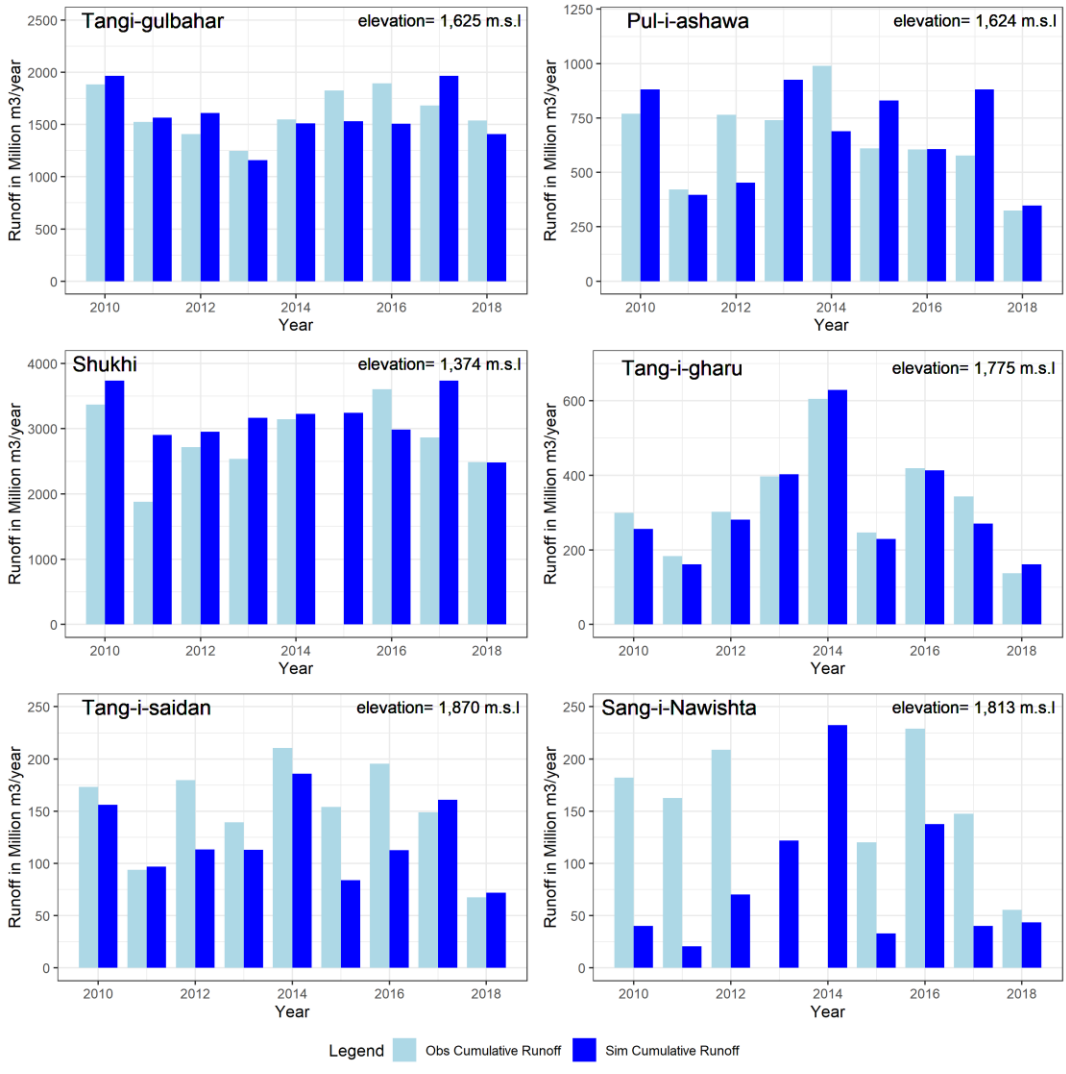

Figure 5-9: Annual cumulative of observed and simulated runoff from 2010 to 2018 at Six hydrologicalstations located in UKRB.

The total annual runoff from two stations; Tang-i-Gulbahar (TG) and Pul-i-Ashawa (PA) situated in the upper basins of study area were compared with Shukhi station which is located in the lower subbasins of the UKRB (Figure 5-10). The average annual total runoff from TG + PA together were estimated at 2,248 Million m3 per year, while there are 3,158 Million m3 per year of average annual runoff at the Shukhi station. The total runoff from January 2010 to September 2018 showed higher flow at Shukhi compared to the sum of the TG and PA stations. In addition, there are some other small river basins which contribute to the total runoff in Shukhi. This indicates that the model estimated the runoff and hydrology parameters well in UKRB.

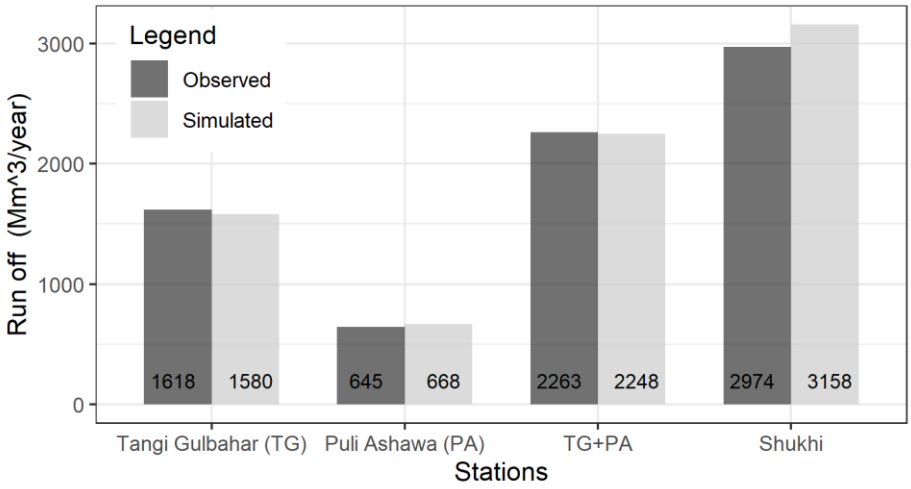

Figure 5-10: Comparison of annual runoff from 01.2010 to 09.2018 between Shukhi station and total of Tang-i-Gigabar (TG) and Pul-i-Ashawa (PA) stations. The Shukhi station located in lower sub-basin, while the TG and PA stations located in upper Subbasins.

5.1.8 Spatial hydrological outputs

The spatial hydrological outputs of the SWAT model, after calibration and validation, are presented in Figure 5-11 for the period 2010-2018. The spatial maps in Figure 5-11 include key parameters such as precipitation, snowmelt, surface runoff, soil available water content (SWAve), percolation, groundwater recharge (GW), evapotranspiration (ET), potential evapotranspiration (PET), total water yield (Total WYLD), and sediment yield (Sidm-YLD) for the sub-catchments within the Upper Kabul River Basin (UKRB). The elevation of the high mountains significantly influenced the spatial distribution of hydrological parameters across the UKRB. The northern part of the basin experiences higher precipitation and snowfall, whereas the southern regions exhibit considerably less rainfall and snowfall. Correspondingly, surface runoff, soil percolation,

groundwater contribution to streams and rivers, and total water yield are greater in the higher elevation catchments compared to the lower elevation ones. However, the soil available water content is higher in the southern, lower elevation catchments of the UKRB, as depicted in Figure 5-11.

The spatial maps also indicate that both ET and PET are greater in the southern and western parts of the basin, where higher temperatures contribute to increased water evaporation and evapotranspiration. This results in more water transitioning to the gaseous phase and water losses due to evapotranspiration in the lower elevation areas. Sediment yield is notably higher in the mountainous regions, particularly around the peaks, while most other sub-catchments exhibit sediment loadings of less than 50 tons per hectare within the UKRB. It is important to note that sediment transport along watercourses was outside the scope of this study and, therefore, was not calibrated as part of the SWAT model.

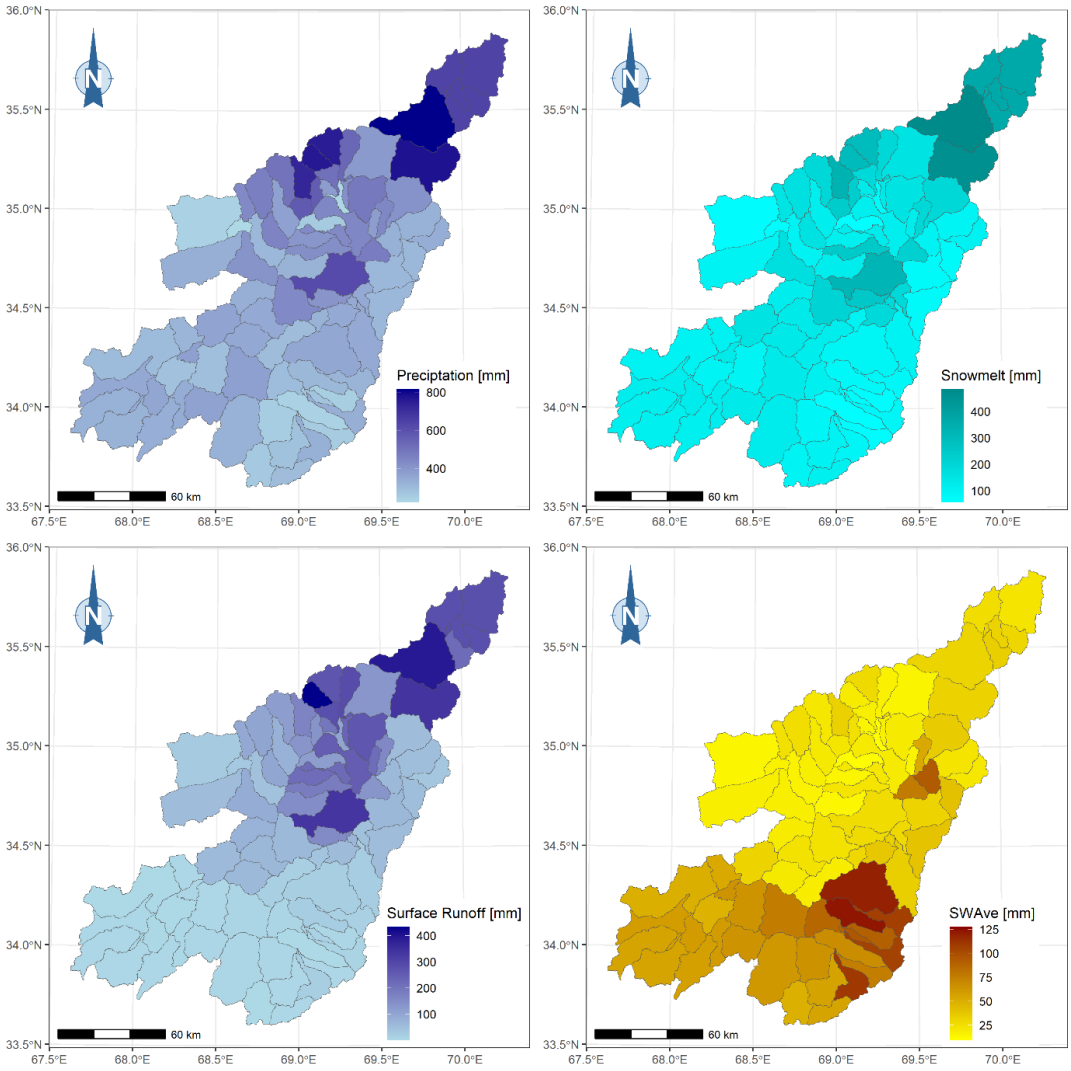

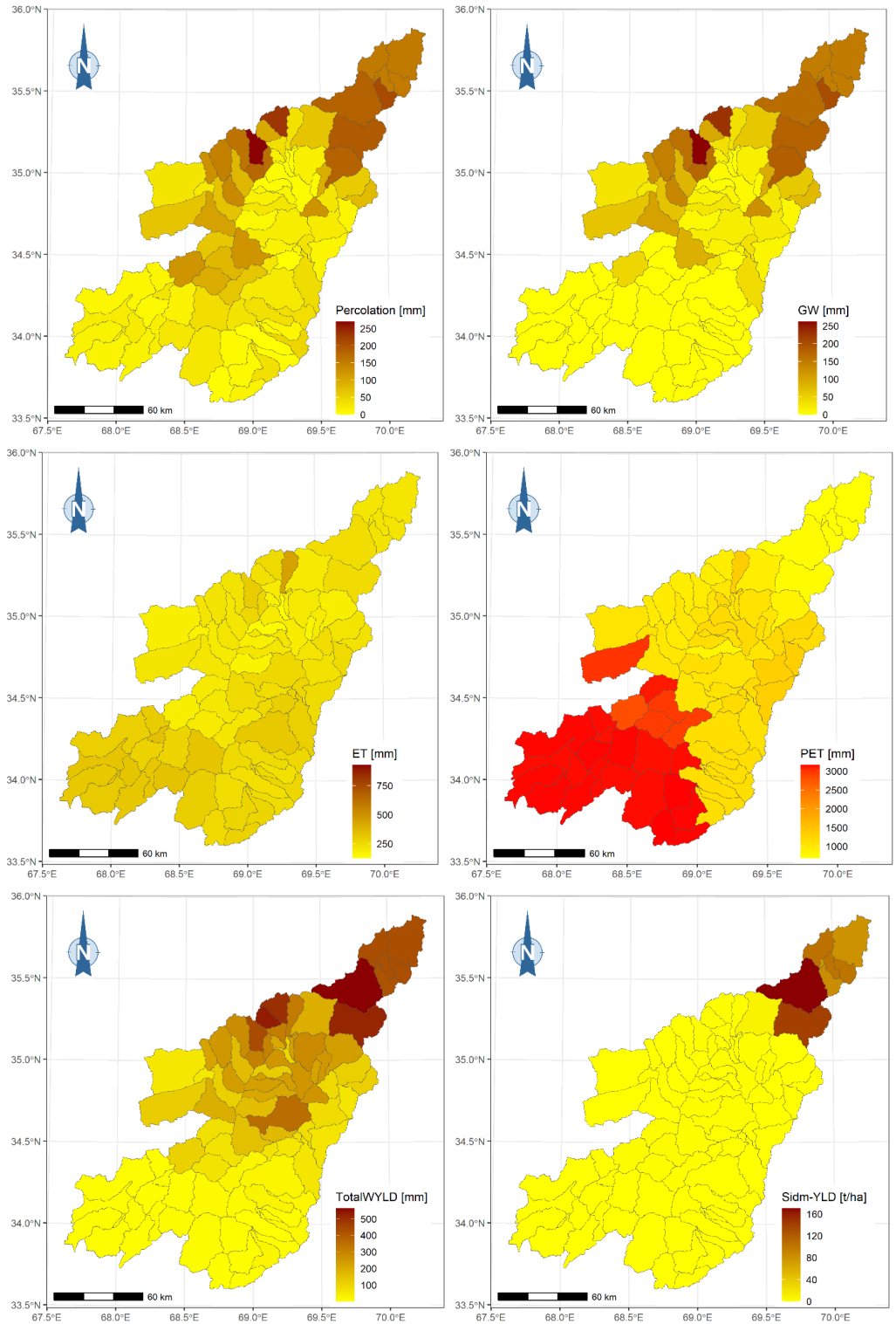

Figure 5-11: The spatial maps of hydrological parameters including the precipitation, snowmelt, surface runoff, soil available water content (SWAve), percolation, groundwater recharge (GW), evapotranspiration (ET), potential evapotranspiration (PET), total water availability or water yield (Total WYLD) and sediment yield (Sidm-YLD) in the UKRB.

5.1.9 Sensitivity parameter results

Identifying sensitive parameters enables us to focus only on those parameters which impacts most the model output during calibration process. However, during the calibration of SWAT model for runoff, 11 parameters (Table 5-5) out of 27-tested hydrology parameters (Table 5-6) were found to be the most sensitive for the runoff changes in UKRB. The five most sensitive parameters include SOL_AWC, GWQMN, PLAPS, SMFMX and ESCO. The sensitive parameters are ranked from top to bottom concerning the p-value and t-state. The rest of the parameters had either very small impacts or didn't had effects on runoff , thus removed from the further iterations during calibration of the model. Some previous studies (Mohammad Tayib Bromand, 2015; Akhtar, 2017; Ayoubi, 2017) in the Kabul river basin also adjusted some of these parameters.

Table 5.5: The most sensitive parameters contributing flow during calibration in UKRB.

Parameter Name	Details	Min	Max	Fitted	t-Stat	p-Value	S. Rank
v__SOL_AWC	Available water capacity of the soil layer (mm H2O/mm^{-1} soil)	0.0	0.2	0.1438	40.99	0.0000	1
v__GWQMN	Threshold depth of water in the shallow aquifer required for return flow to occur (mm H_2O)	700	900	888.33	7.697	0.0000	2
v__PLAPS.sub	Precipitation lapse rate (*mm/km)*	33	100	75.321	-7.395	0.0000	3
v__SUB_SMFMX	Maximum melt rate for snow during year (mm H2O°C^{-1}day^{-1})	0.0	5.0	1.5583	-6.880	0.0000	4
v__ESCO	Soil evaporation compensation factor	0.9	1.0	0.9424	-2.684	0.0077	5
v__SUB_TIMP	Snowpack temperature lag factor	0.0	1.0	0.8550	-2.581	0.0104	6
v__SMFMN	Minimum melt rate for snow during the year (mm H2O °C^{-1}day^{-1})	0.0	5.0	1.8583	2.539	0.0117	8
r__CN2.mgt	SCS runoff curve number	0.0	0.1	0.0454	-2.449	0.0150	9
v__SUB_SMTMP	Snowmelt base temperature (°C)	-5.0	5.0	-1.1167	1.696	0.0911	10
v__SUB_SFTMP	Snowfall temperature (°C)	2.0	4.0	3.9567	1.578	0.1157	11

v: existing parameter replaced by a given value, r: existing parameter multiplied by (1+ a given value).

Table 5.6: Shows the parameters range during calibration process in UKRB. The numbers with St are the stations number; e.g, St11=Tang-i-Gulbar), St 17= Pul-i-Ashawa, St 27=Shukhi, St 51=Tang-i-Gharu, St 62=Tang-i-Saidan, and St 65= Sang-i-Nawishta stations. Also, v, a, and r indicate that the existing parameter replaced by a given value, the value added to the existing parameter, and the existing parameter value is multiplied by (1+ a given value), respectively.

No	Parameter Name	Details of Abbreviations	Abs SWAT Value	SWAT Default		Calibrated Parameters Range					
			Min	*Max*		*St 11*	*St 17*	*St 27*	*St 51*	*St 62*	*St 65*
1	v__Plaps.sub	Precipitation lapse rate (mm/Km)	-1000	1000	0	210	210	180	20	0	75.32
2	v__Tlaps.sub	Temperature lapse rate (C/km)	-10	10	0	-4	-3.5	-2	-4	-4	-0.282
3	v__SFTMP.sno	Snowfall temperature	-20	20	1	-2.908333	-7.737	2.817	1.31875	-1.181	3.957
4	v__SMTMP.sno	Snowmelt base temperature	-20	20	0.5	4.355	1.8853	-0.45	0.787	-0.556	-3.512
5	v__SMFMX.sno	Maximum melt rate for snow during year (occurs on summer solstice)	0	20	4.5	4.408334	5.2486	2.958	4.0475	1.6148	2.425
6	v__SMFMN.sno	Minimum melt rate for snow during the year (occurs on winter solstice)	0	20	4.5	1.858333	0.1	0.5	4.1375	0.8639	1.558
7	v__TIMP.sno	Snowpack temperature lag factor	0	1	0.5	_	_	_	0.9075	_	0.027
8	v__SOL_AWC.sol	Available water capacity of soil	0	1	0.064	0.02	0.245	-0.04	0.16	0.05	0.2
9	v__SLSUBBSN.hru	Average slope length (m)	9	150	9.14	140	140	150	75.981514	140	140
10	v__HRU_SLP.hru	Average slope steepness (m/m)	0	1	0.72	0.08	0.002	0.005	0.004523	0.0209	0.005
11	v__OV_N.hru	Manning's "n" value for overland flow	0.01	35	0.15	5	5	5.293		7.4415	28
12	v__LAT_TTIME.hru	Lateral flow travel time (days)	0	180	0	150	150	150	69.416199	20	25
13	v__ESCO.hru	Soil evaporation compensation factor	0	1	0.95	0.8506	0.8665	0.762	0.581434	0.615	0.953
14	v__EPCO.hru	Plant uptake compensation factor	0	1	1	_	_	_	_	_	0.75
15	v__SURLAG.hru	Surface runoff lag time (days)	0.05	24	4	1	1	1	1	1	3
16	a__SHALLST.gw	Initial depth of water in the shallow aquifer (mm)	0	5000	1000	1500	300	_	_	500	538.8

17	a__DEEPST.gw	Initial depth of water in the deep aquifer (mm)	0	5000	2000	3000	500	_	_	1000	1797
18	v__GW_DELAY.gw	Groundwater delay (days)	0	500	31	584.5	180.25	200	200	270	153.3
19	v__ALPHA_BF.gw	Baseflow alpha factor (days)	0	1	0.048	0.7	0.5	0.5	0.5	0.5	
20	v__GWQMN.gw	Threshold depth of water in the shallow aquifer required for return flow to occur (mm)	0	5000	1000	669.583313	347.4	500	500	900	970.9
21	v__GW_REVAP.gw	Groundwater "revap" coefficient	0.02	0.2	0.02	0.03	0.02	0.02	0.02	0.1	0.038
22	v__REVAPMN.gw	Threshold depth of water in the shallow aquifer for "revap" to occur (mm)	0	1000	750	800	1000	950	950	600	500
23	v__RCHRG_DP.gw	Deep aquifer percolation fraction	0	1	0.05	0.0506	0.0201	1E-04	0.000101	0.0506	
24	r__CN2.mgt	SCS runoff curve number	35	98	79	0.051875	0.1902	0.166	-0.154945	0.0194	0.019
25	r__SOL_K(..).sol	Saturated hydraulic conductivity	0	2000	6.4	_	_	0.037	_	_	_
26	r__SOL_BD(..).sol	Moist bulk density	0.9	2.5	1.2	_	_	0.088	_	_	1.653
27	v__RCHRG_DP.gw	Deep aquifer percolation fraction	0	1	0.05	_	_	_	_	_	0.149

5.2 Bias Correction Results

5.2.1 Baseline Period – Statistical and graphical Results

Taylor diagrams have been used to analyses the monthly results of bias corrected precipitation and temperature over the historical period. The figure 5-12 and figure 5-13 show the results from each RCM, and the RCM's mean with the APHRODITE data by indicating the standard deviation (Std), correlation coefficient (r), and root mean square error (RMSE) in all three methods used. The observation point is indicated with a black point in the bottom line, which is a reference period. Based on the Taylor diagrams, the performance of all three methods were good and followed the similar pattern with the APHRODITE data.

The delta change method indicated the best correlation for all three variables of precipitation, Tmax and Tmin in our results (Figure 5-13), however, this approach does not adjust the RCM simulations but rather uses the observations and only the RCM change signals (Teutschbein and Seibert, 2012). So, this implies that the Dc method cannot be evaluated for the control/historical run because it corresponds to the observed climate and therefore gives the perfect simulation by definition. Therefore, the results of this method were also shown in this study but ignored in the further hydrologic evaluations. Between other two methods, the Ls results were closer to the observation for temperatures and precipitation (Figure 5-13), while commonly, the uncertainty is larger in precipitation of the climate models. The standard deviation of Ls method is closer to the standard deviation of APHRODITE observations compared to the Eqm method (Figure 5-13). The correlation coefficient (r^2) in Ls method is smaller than Eqm for precipitation which is 0.28 and 0.30, respectively. However, the r^2 of Ls is greater than Eqm method which is 0.95 for maximum and 0.96 for minimum temperatures, while in Eqm it is 0.93 for Tmax and 0.94 for Tmin, respectively.

The RMSE results shows a smaller value in Eqm method than Ls which is 26.6 and 29.6, respectively. As mentioned earlier that the Delta change (Dc) method results are same as observation in the historical period, therefore all the statistics of Dc and APHRODITE data are similar, therefore, it is ignored in this study. Additionally, we tried to show the result of Dc as well in order to see the differences of the methods and decrease the uncertainty in the model's output. But still all methods fit the observations of temperature and precipitation. Therefore, the Ls method is selected for future analyzing of precipitation and temperature in the UKRB. Table 5-7 describes statistical value of the three methods for precipitation, maximum temperature, and

minimum temperature over historical period against the APHRODITE data. The statistical result shows, all methods were able to reduce the MBE to zero or close to zero for Tmax and Tmin, and showed 0.56, 0.56 and 6.22, for Ls, Dc and Eqm methods respectively in precipitation. The Pearson correlation coefficient (r) is 0.53 for Ls and 0.55 for Eqm in precipitation, while in Tmax the (r) is 0.97 for both Ls and Eqm. Additionally, the (r) is 0.98 for Ls and 0.97 for Eqm in Tmin, respectively. The MAE and MSE is greater in Ls than Eqm in bias corrected precipitation, while both are smaller in Ls compared to Eqm method for the Tmax and Tmin.

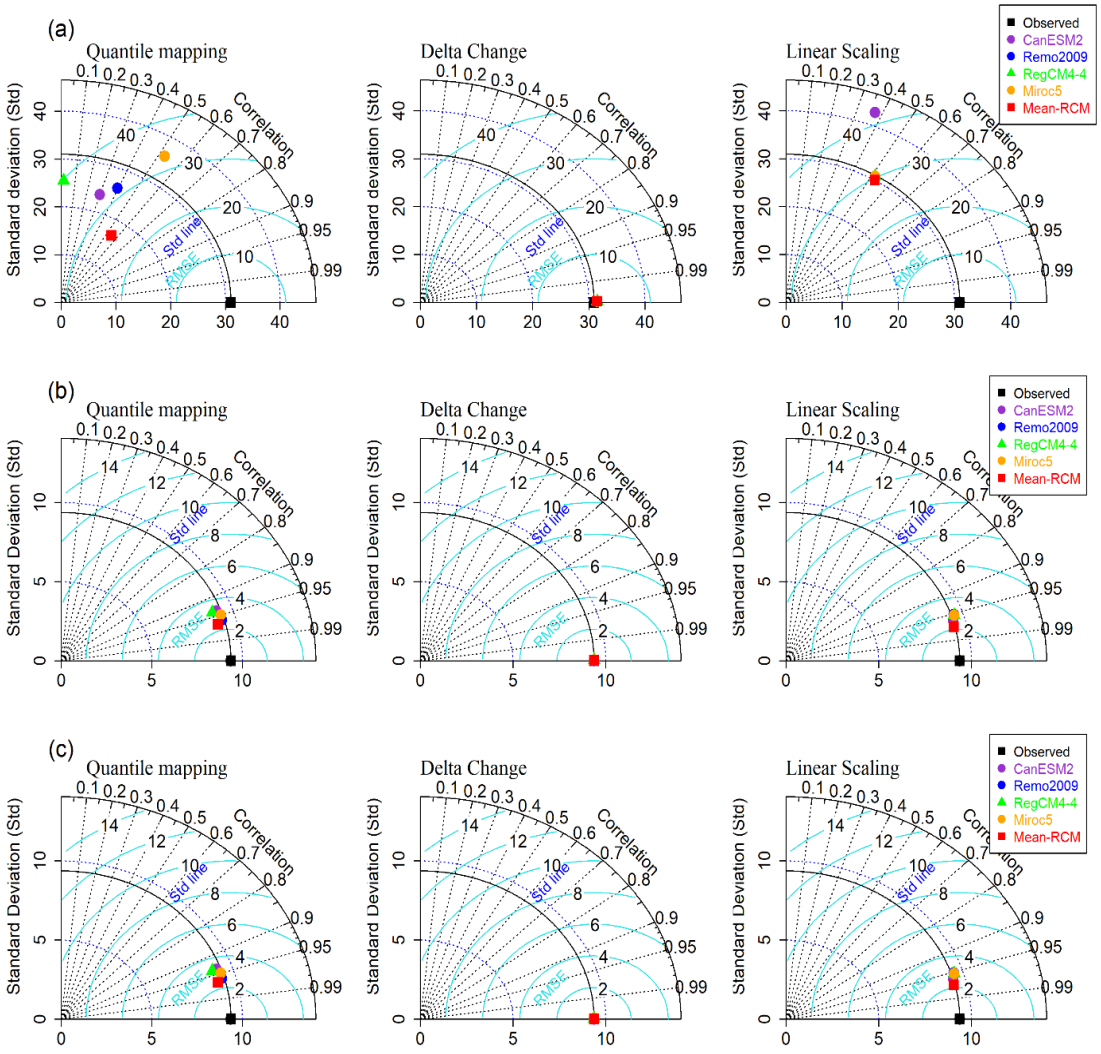

Figure 5-12: Taylor diagrams display a statistical comparison of bias-corrected; (a) precipitation, (b) Tmax, and (c) Tmin vs APHRODITE data for each climate model. The radial distance from the origin is represented by blue dashed lines showing the standard deviations (Std) line.

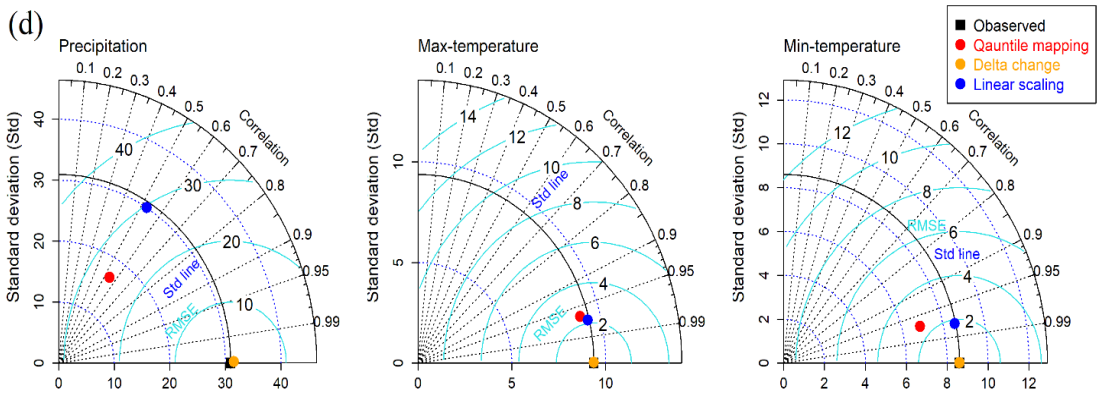

Figure 5-13: Taylor diagrams showing the comparison of methods for the RCM's mean vs APHRODITE-data for the monthly precipitation, Tmax and Tmin in the baseline period.

Table 5.7: Statistical results of the bias corrected precipitation, maximum temperature and minimum temperature from Ls, Dc and Eqm methods against the APHRODITE (accepted as observations) data.

		Precipitation			***T-max***			***T-min***		
No	***Errors***	***Ls***	***Dc***	***Qm***	***Ls***	***Dc***	***Qm***	***Ls***	***Dc***	***Qm***
1	ME	0.56	0.56	6.22	0.00	0.00	0.00	0.07	0.00	-0.95
2	MAE	21.09	0.57	20.86	1.69	0.00	1.87	1.43	0.00	2.30
3	MSE	878.88	0.71	709.55	4.68	0.00	5.88	3.29	0.00	7.42
4	RMSE	29.65	0.84	26.64	2.16	0.03	2.42	1.82	0.02	2.72
5	MBE	0.56	0.56	6.22	0.00	0.00	0.00	0.07	0.00	-0.95
6	PBIAS %	1.60	1.60	17.70	0.00	0.00	0.00	2.90	0.00	-39.50
7	r	0.53	1.00	0.55	0.97	1.00	0.97	0.98	1.00	0.97
8	r2	0.28	1.00	0.30	0.95	1.00	0.93	0.96	1.00	0.94
9	KGE	0.53	0.98	0.33	0.97	1.00	0.94	0.96	1.00	0.56
10	Std-O	31.01	31.01	31.01	9.39	9.39	9.40	8.62	8.62	8.62
11	Std-M	30.10	31.58	16.79	9.32	9.39	9.00	8.58	8.62	6.89

Mean Error (ME), Mean Absolute Error (MAE), Mean Squared Error (MSE), Root Mean Squared Error (RMSE), Mean Bias Error (MBE), Percent Bias (PBIAS%), Pearson Correlation coefficient (-1<= r <= 1), Coefficient of Determination (0<= r2 <= 1) gives the proportion of the variance of one variable that is predictable from the other variable, Kling-Gupta efficiency between simulation and observed (0<=KGE<=1), standard deviation of observed (Std-O), standard deviation of modelled (Std-M).

Figure 5-13 illustrate the long-term average of monthly precipitation and temperature over the historical period (1986-2005) using the Ls, Dc and Eqm methods to show the temporal differences between observations and the climate outputs. It can be seen that Eqm overestimates the mean monthly precipitation in dry months starting from May to January, while underestimated the precipitation in wetter months compared to the observations (Figure 5-14). While the Ls and Dc methods both shows the same results and is closer to the observations. The Eqm method also show over-estimation of Tmax values in the first half of the year (January to July), while indicated under-estimation values for the remaining months (August to December). The Tmin was under-estimated in all seasons compared to the observations using Eqm method. While the Ls and Dc methods again shows the best simulation estimations for both maximum and minimum temperatures compared to the baseline period (Figure 5-14). The annual comparison of bias corrected precipitation, Tmax and Tmin compared to the APHRODITE annual data is shown in the figure 5-15.

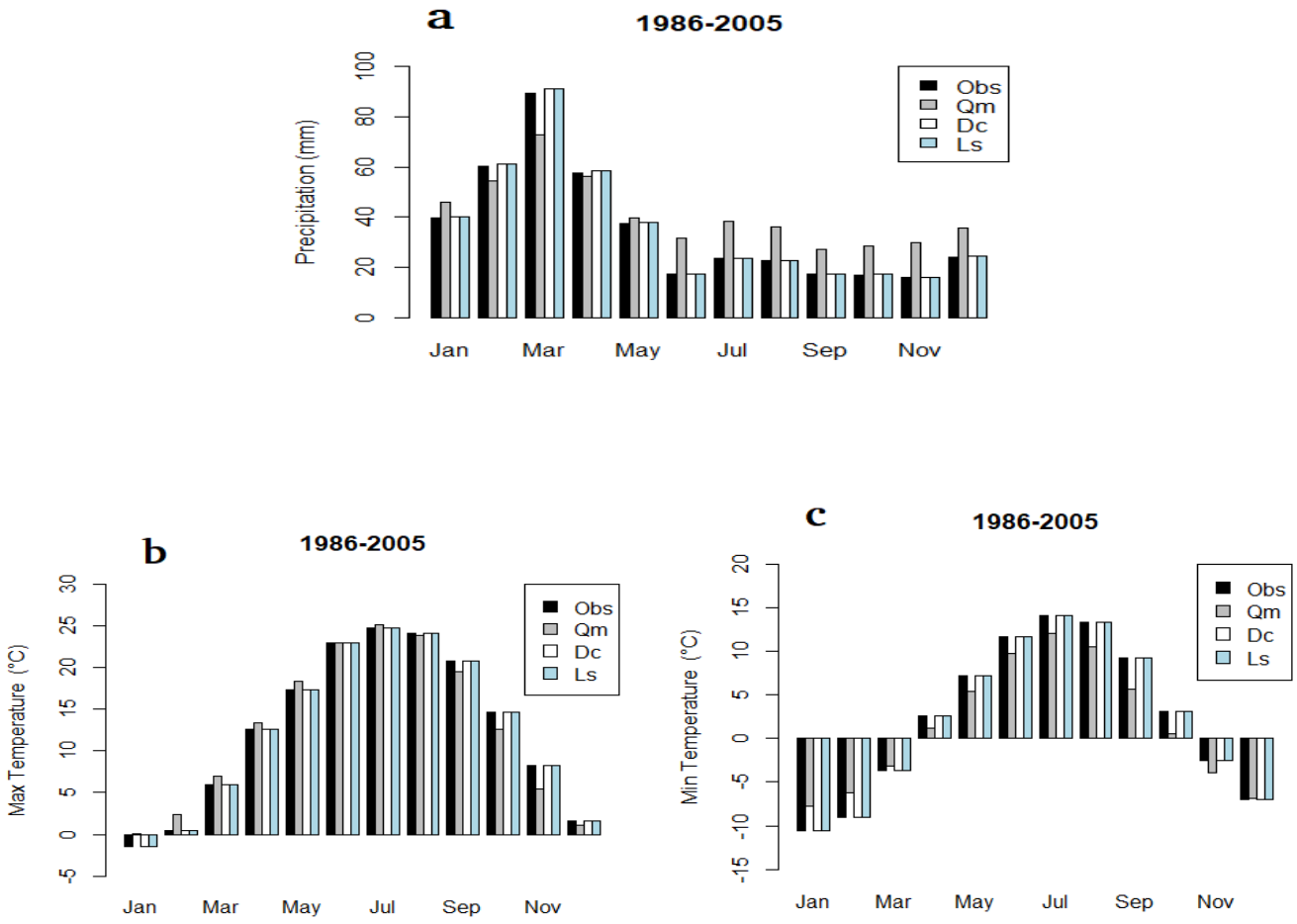

Figure 5-14: Mean monthly results using different bias correction methods over the historical period (1986-2005) for (a) precipitation, (b) Maximum temperature, and (c) minimum temperatures. The Obs indicates APHRODITE data, Qm indicates Quantile mapping, Dc shows Delta change and Ls shows Linear scaling results in the figures.

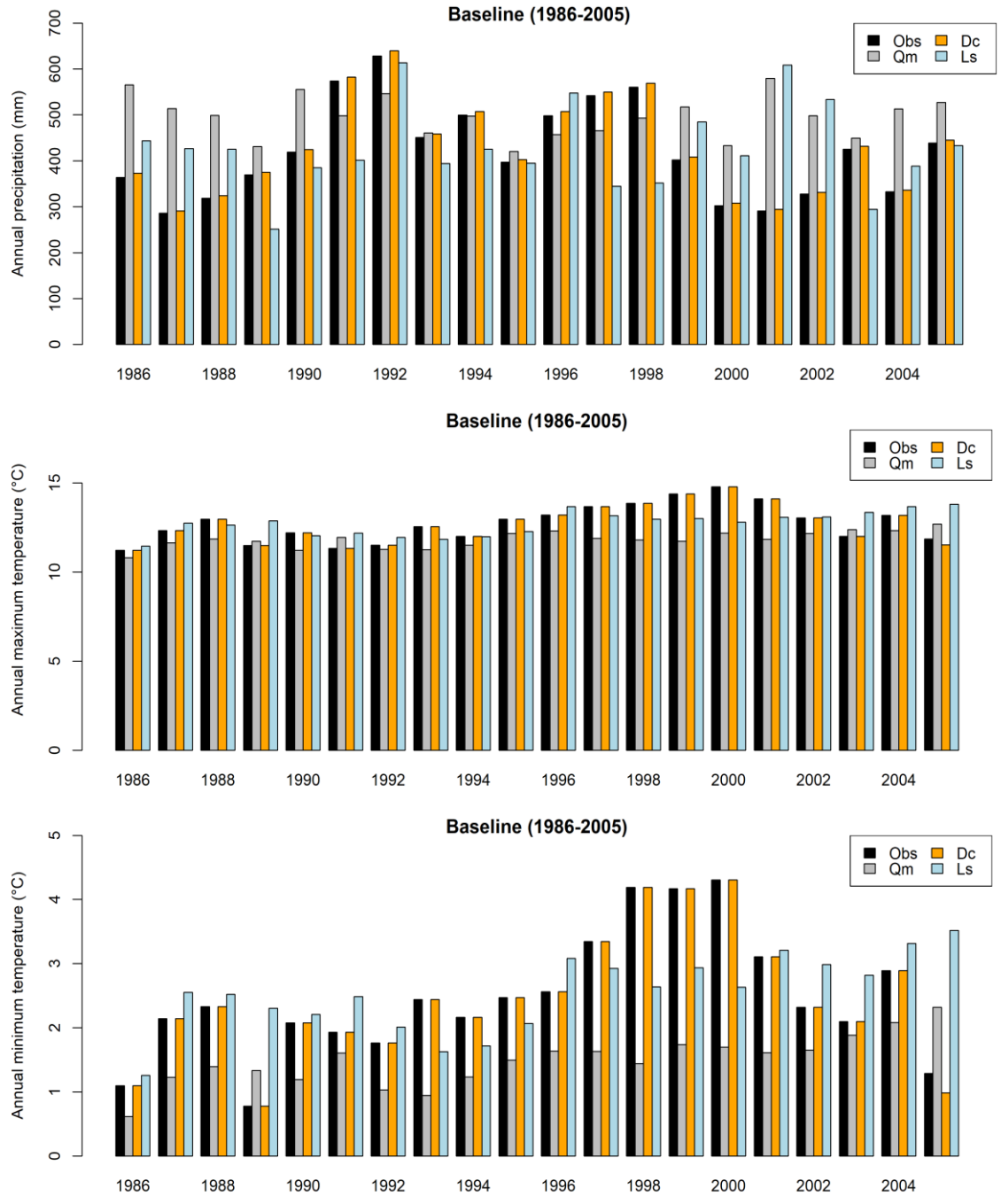

Figure 5-15: Show the annual bias-corrected precipitation, maximum temperature and minimum temperature in the baseline period over the UKRB. The Qm method under-estimated both the annual maximum temperature and annual minimum temperature compared to the observations.

5.2.2 Future Bias Corrected Precipitation

5.2.2.1 Monthly precipitation variations

Figure 5-15 indicates the future monthly precipitation variation compared to the baseline. To calculate the future monthly change over the baseline period, the future values of each model were compared with its baseline value for each month over the UKRB. The monthly precipitation change is different in every RCM which is typical for climate models in general. The black line in the Figure 5-15 shows the baseline or reference precipitation, while the red line shows the average of the RCM's precipitation. Based on the Ls method, in the 2040s, the future monthly precipitation shows a decrease in March, while show an increase in September and December in both RCP4.5 and RCP8.5. In 2090s, the monthly precipitation showed a decrease from March to June and shows an increase between Jun to December based on both RCP4.5 and RCP8.5, respectively.

In the 2040s, the future monthly precipitation difference compared to the baseline was between -10 mm (in March) to +12mm (December) based on RCPs 4.5. However, the future monthly precipitation difference compared to referenced period is -10 mm to +30 mm based on RCP8.5. Also, in the 2090s, the maximum monthly precipitation increases to 32 mm and 35 mm in RCP4.5 and RCP8.5, respectively. Meanwhile, both RCP4.5 and RCP8.5 shows a decrease of monthly precipitation in March (20 mm to 40 mm) compared to the baseline period. The future precipitation indicated a large variation between the RCM outputs, Figure 5-16. The bias-corrected precipitation shows very large daily variations in some stations located in the lowland areas, while there are fewer anomalies in the stations located in the high elevations of mountainous areas. Therefore, in this study, precipitation and temperature data from 25 grid-points were selected for analysis.

5.2.2.2 Seasonal precipitation variation

The seasonal precipitation variations are depicted in the Table 5-8. The table shows that the precipitation shows a decrease of -8 % and -12.3 % in spring season compared to the baseline in 2040s and 2090s respectively under RCP4.5. While it shows a drop of -2 % in near future (2040s) and -12 % in the far future (2090s) of the same season under RCP8.5 scenario. However, the precipitation shows an increase in other three seasons compared to the baseline period under both RCPs. The precipitation increases 6 to 35 % in 2040s and 0 to 18 % in 2090s of RCP4.5, while it

shows the increase of 9 % to 21 % in 2040s, and 12 % to 18 % in 2090s under RCP8.5 scenario.

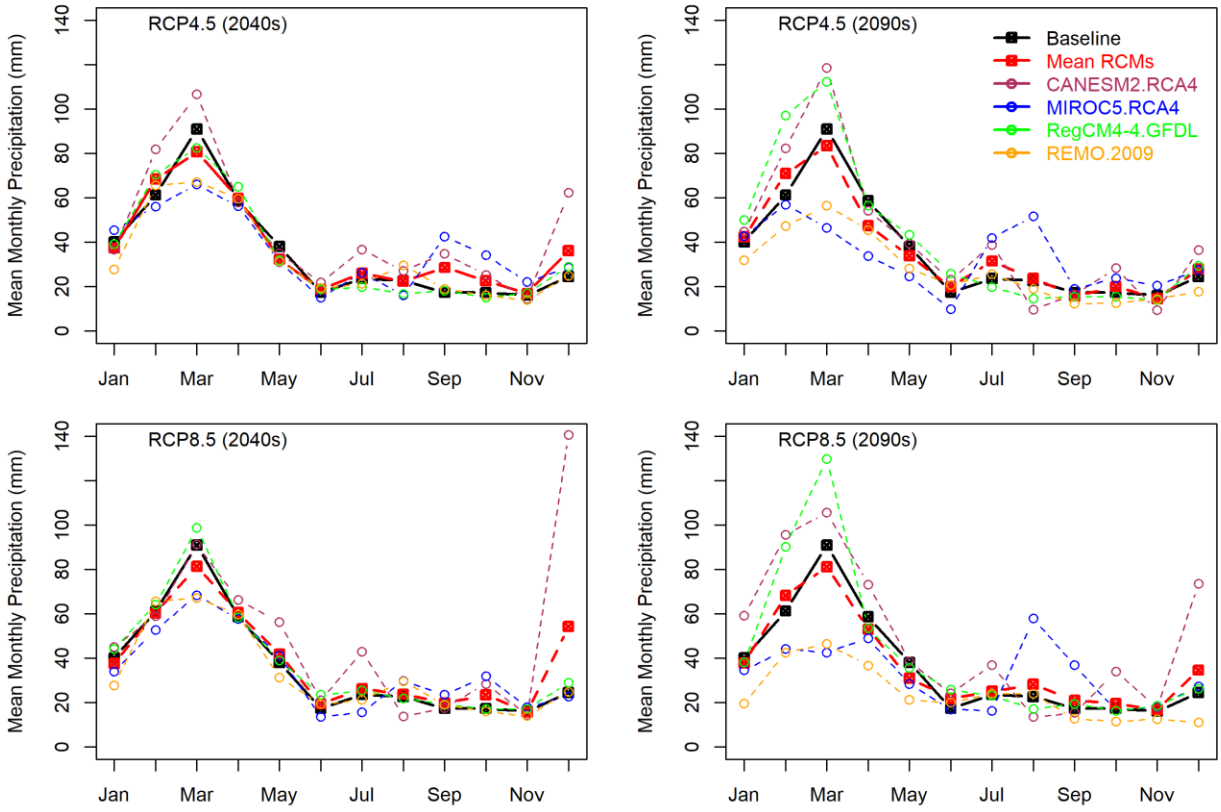

Figure 5-16: Monthly mean bias corrected precipitation from the RCMs output for the future period of 2040s and 2090s.

Table 5.8: Seasonal precipitation change in UKRB.

RCP (Period)	Change in	Spring (MAM)	Summer (JJA)	Autumn (SON)	Winter (DJF)
RCP4.5 (2040s)	Precipitation	-8%	6%	35%	13%
RCP4.5 (2090s)	Precipitation	-12.3%	18%	0%	12%
RCP8.5 (2040s)	Precipitation	-2%	9%	17%	21%
RCP8.5 (2090s)	Precipitation	-12%	18%	13%	12%

5.2.2.3 Annual precipitation variation

The boxplots in the Figure 5-17 show the future mean annual projected precipitation. To calculate the future annual precipitation, the changes were applied to the annual mean of the RCMs against the baseline period, which were 428 mm/year. The mean annual precipitation values under RCP4.5 range to 449 mm/year and 431 mm/year in 2040s and 2090s, and under RCP8.5 ranges to 458 mm/year and 438 mm/year for the 2040s and 2090s, respectively. The mean annual precipitation change show that under RCP4.5, there will be an increase in annual precipitation of about +5% (21mm) in 2040s, and an increase of about +1% (3.2 mm) in 2090s. Moreover, under RCP8.5, the annual precipitation is expected to increase by +9 % (37 mm) in 2040s, and about +2 % (10 mm) in 2090s compared to the baseline period (Table 5-9). The annual precipitation for whole period of 2006-2100 are shown is Figure 5-18.

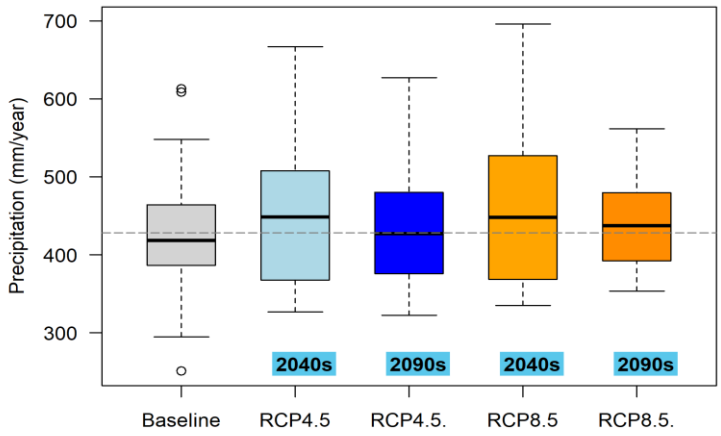

Figure 5-17: Future precipitation projections of the UKRB in Afghanistan.

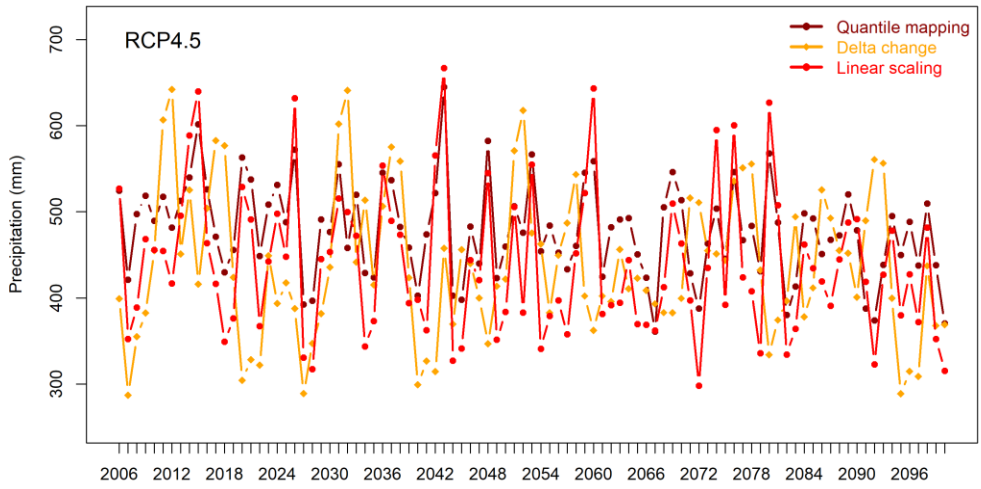

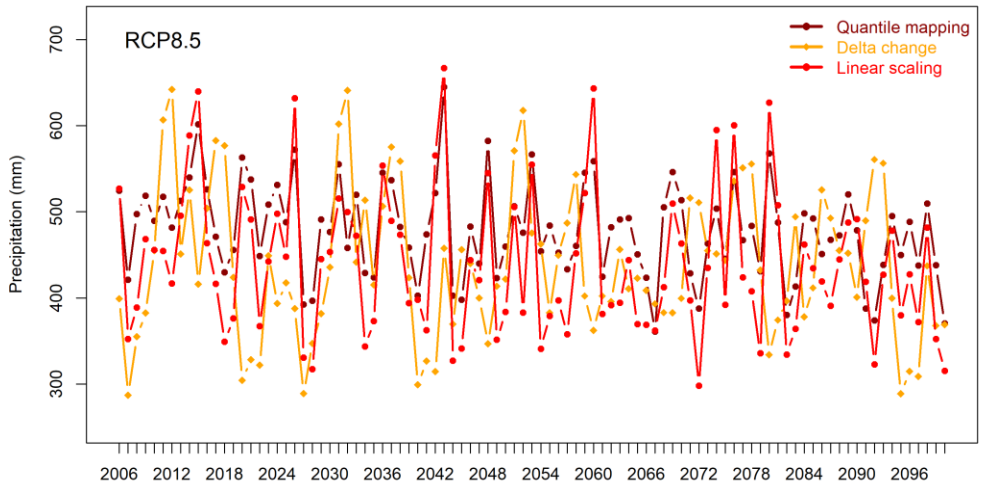

Figure 5-18: Future annual precipitation in the UKRB using the linear scaling, quantile mapping and the delta change methods.

Table 5.9: Annual mean precipitation changes in the UKRB.

		Values (mm)		**Abs Change (mm)**		**Change (%)**	
RCPs	Methods	2040s	2090s	2040s	2090s	2040s	2090s
RCP4.5	Linear Scaling	449	431	21	3	5%	1%
RCP8.5	Linear Scaling	458	438	30	10	6%	2%
RCP4.5	Quantile mapping	483	462	55	34	11%	7%
RCP8.5	Quantile mapping	498	452	70	24	14%	5%
RCP4.5	Delta change	447	422	19	-6	4%	-1%
RCP8.5	Delta change	461	466	33	38	7%	8%
	Baseline	428	428	_	_	_	_

5.2.3 Future Bias corrected Temperature

5.2.3.1 Monthly Temperature variations

Figure 5-19 shows the mean monthly projected temperature changes compared to the baseline in Upper Kabul River Basin (UKRB). The monthly temperature shows a higher temperature values compared to the baseline from January to July using all three methods (Ls, Dc, and Eqm). The temperature is even getting worse in 2090s of RCP8.5 in UKRB. Even though, the temperature values are different in all three methods but still the pattern is the same in all figures.

The monthly temperature shows an overestimation from December to July in both periods under RCP4.5, while in other months the changes are minimal. Additionally, the monthly temperature shows increase in all months for 2040s and 2090s under the RCP8.5 scenario. The monthly temperature peaks represent a one-month backward shift from July to June. Consequently, the future temperature will get warmer in all season, especially in spring, summer and winter seasons. This shift is expected to result in an earlier snowmelt in the high mountainous areas and accordingly affects the hydrological regime and the water resources in the region.

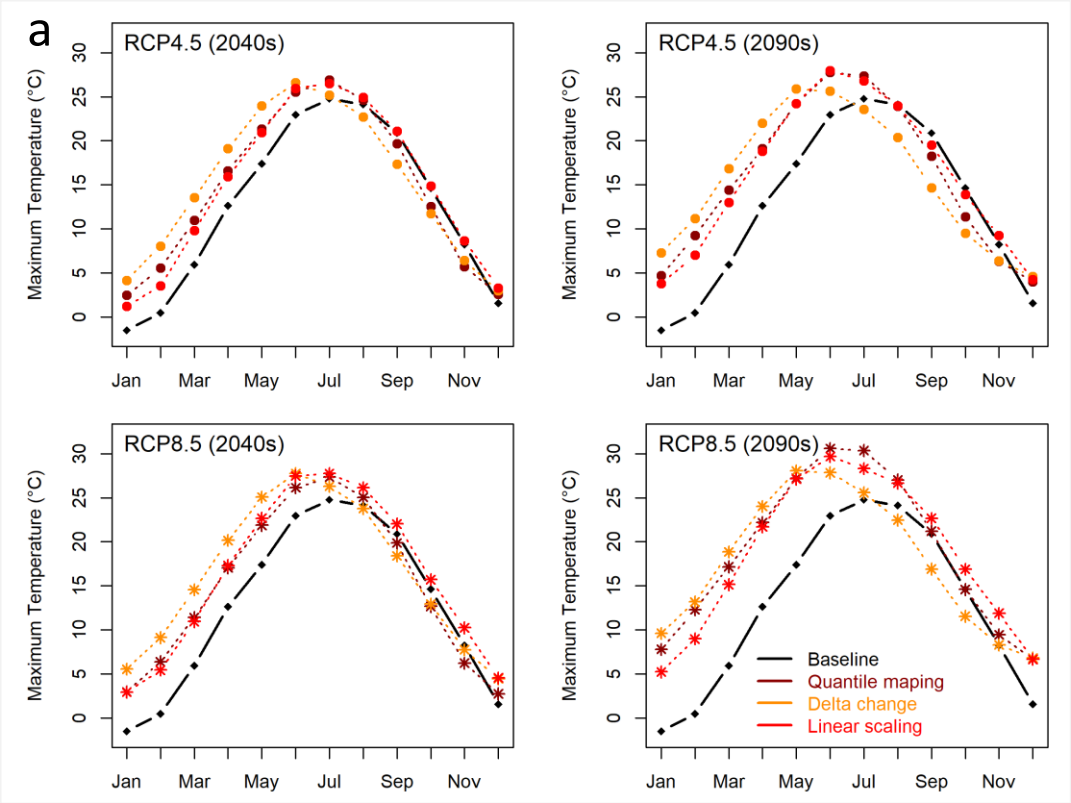

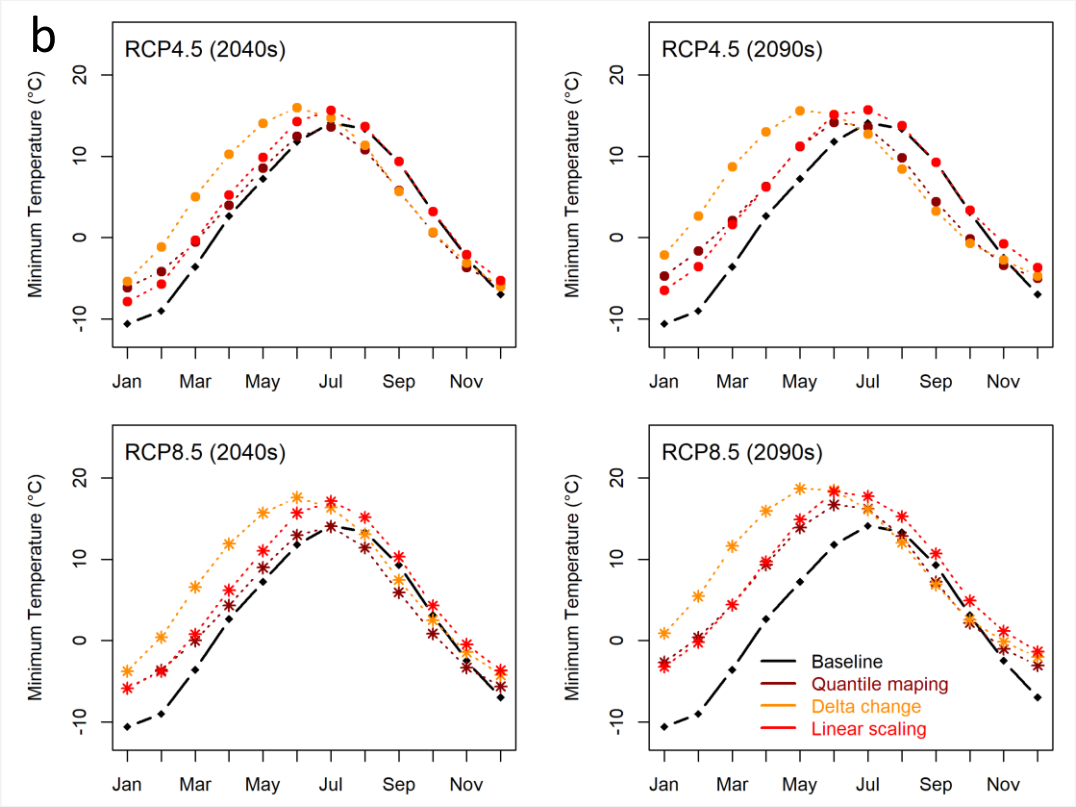

Figure 5-19: The future projections (a) Monthly maximum temperature, and (b) Monthly minimum temperature for the future period in 2040s and 2090s under RCP4.5 and RCP8.5 scenarios in UKRB.

Table 5-10 represents the monthly temperature absolute changes in °C from the baseline period. Based on the linear scaling results in 2040s, the average monthly temperature will increase between 0.2 °C to 3.6 °C based under RCP 4.5, and 1.1 °C to 5.1 °C based under RCP 8.5, respectively. Also, in 2090s, the average monthly temperature will increase from 0.1 °C to 6.1 °C based on RCP4.5, and 1.6 °C to 8.7 °C based on RCP 8.5, respectively. However, September and October of 2090s showed a negative temperature of -0.7 °C and -0.3 °C based on Rcp4.5. The results showed that a higher monthly temperature change rate is shown in spring and summer seasons (January–June) in the 2090s under RCP8.5 in all methods.

Table 5.10: Changes in future monthly temperature (°C) for the 2040s and 2090s comparted to the baseline period (1986-2005). The negative values show decreases in temperature.

2040s	Linear scaling		Delta change		Quantile mapping	
	Rcp4.5	Rcp8.5	Rcp4.5	Rcp8.5	Rcp4.5	Rcp8.5
Jan	2.7	4.6	5.4	6.9	4.2	4.6
Feb	3.2	5.1	7.7	9.0	5.0	5.6
Mar	3.6	4.7	8.1	9.4	4.1	4.5
Apr	3.0	4.1	7.0	8.4	2.7	3.1
May	3.1	4.5	6.7	8.1	2.6	3.1
Jun	2.8	4.2	3.9	5.3	1.6	2.2
Jul	1.6	3.0	0.5	1.9	0.8	1.2
Aug	0.6	1.9	-1.7	-0.3	-1.0	-0.5
Sep	0.2	1.1	-3.6	-2.2	-2.4	-2.2
Oct	0.2	1.1	-2.7	-1.2	-2.3	-2.1
Nov	0.4	2.0	-1.2	0.3	-1.9	-1.4
Dec	1.7	3.2	1.2	2.8	1.1	1.3

2090s	Linear scaling		Delta change		Quantile mapping	
	Rcp4.5	Rcp8.5	Rcp4.5	Rcp8.5	Rcp4.5	Rcp8.5
Jan	4.7	7.1	8.6	11.3	6.0	8.6
Feb	6.0	8.7	11.2	13.6	8.1	10.6
Mar	6.1	8.6	11.6	14.1	7.1	9.6
Apr	4.9	8.1	9.9	12.4	5.1	8.1
May	5.4	8.7	8.4	11.0	5.4	8.2
Jun	4.2	6.6	3.0	5.8	3.6	6.3
Jul	1.8	3.6	-1.3	1.4	1.1	3.8
Aug	0.1	2.2	-4.3	-1.5	-1.9	1.2
Sep	-0.7	1.6	-6.1	-3.2	-3.8	-0.9
Oct	-0.3	2.0	-4.5	-1.8	-3.3	-0.5
Nov	1.4	3.7	-1.1	1.2	-1.4	1.3
Dec	3.0	5.4	2.6	5.1	2.2	4.5

5.2.3.2 Seasonal temperature variations

The future seasonal variations of average temperature in upper Kabul river basin is depicted in the Figure 5-20 from the linear scaling method. The average temperature increases in all seasons, and in both periods under RCP4.5 and RCP8.5. In the 2090's, the changes in seasonal temperature is much greater than 2040s in both RCP4.5 than RCP8.5.

In 2040s, the seasonal temperature will increase from 0.2 °C in Autumn to 3.2 °C in spring under RCP4.5, while in 2090s, the seasonal temperature is expected to increase from 0.1 °C in Autumn to 5.5 °C Spring. Moreover, in 2040s, the seasonal temperature is expected to increase from 1.4 °C to 4.5 °C under RCP8.5, while in 2090s it would increase from 2.4 °C to 8.5 °C in the UKRB.

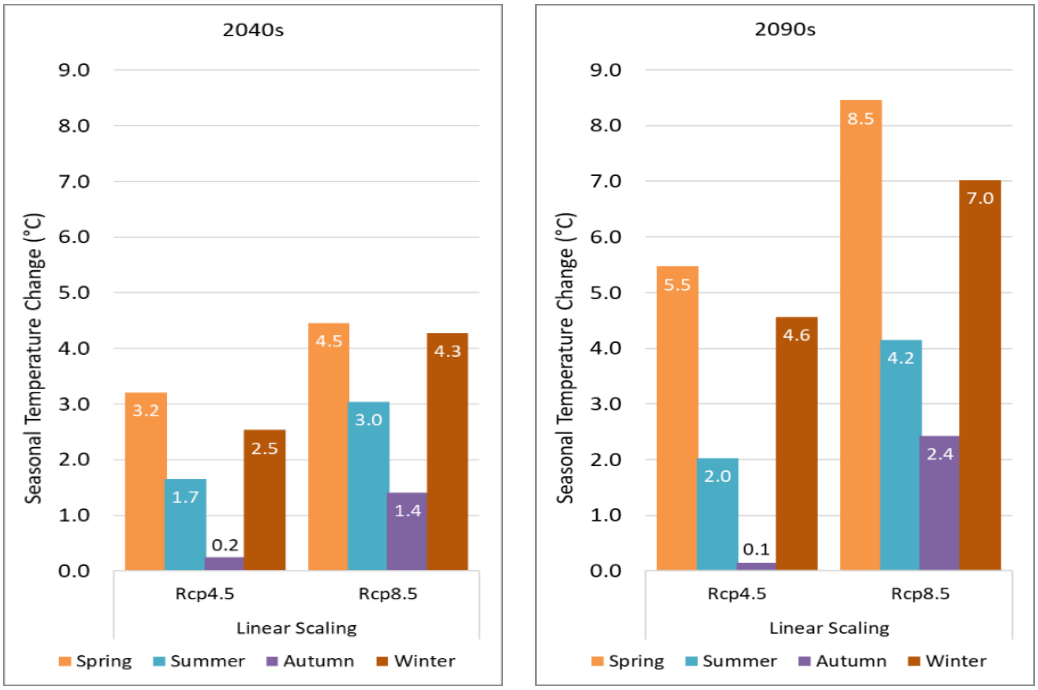

Figure 5-20: Seasonal mean temperature changes from the baseline in the UKRB. results from linear scaling method.

5.2.3.3 Annual temperature variations

The bias-corrected annual temperature from 2006 to 2100 are shown in Figure 5-21 for the linear scaling, quantile mapping and the delta change methods. The annual temperature changes pattern is increasing in all methods and showed the same pattern in all mentioned methods. The temperature gets worse under RCP8.5 compared to the RCP4.5 in the figures.

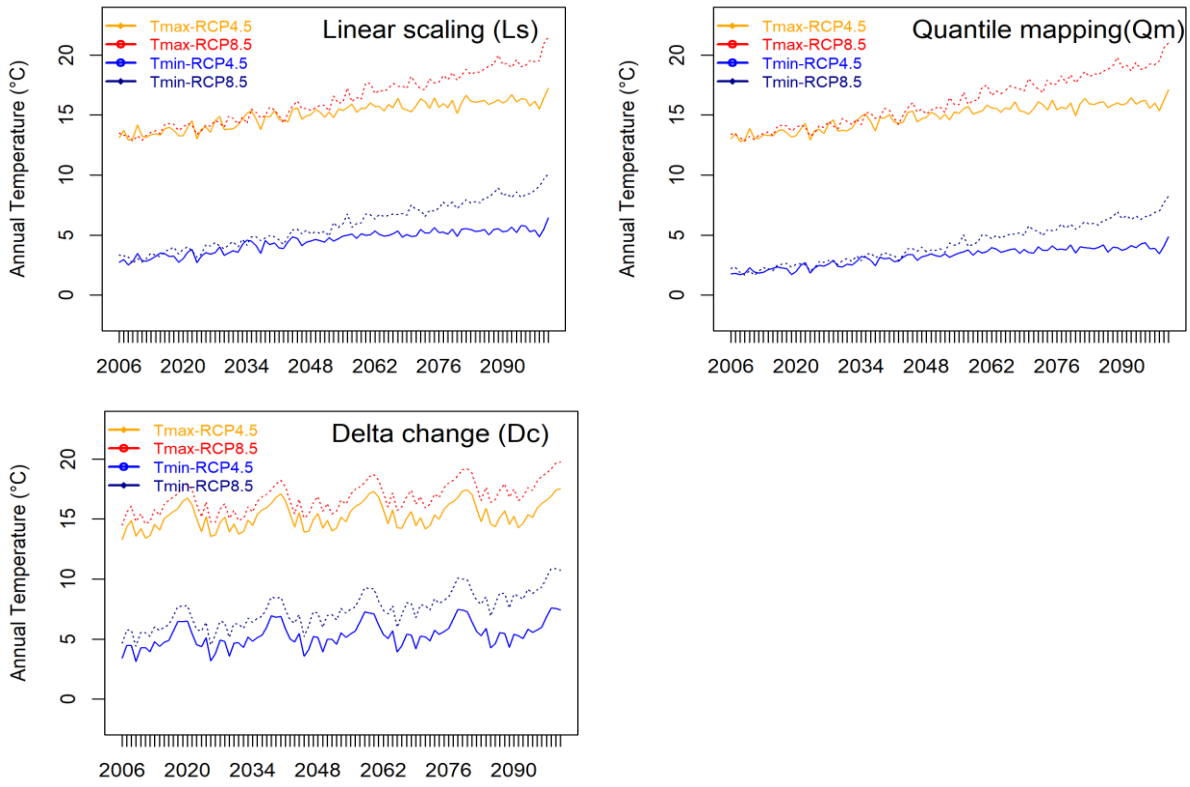

Figure 5-21: Future annual temperature in the UKRB using the linear scaling, delta change, empirical quantile mapping methods.

The future long-term mean annual temperature change compared to the baseline is depicted in the boxplots in Figure 5-22. The mean annual temperature in the baseline period is shown 7.6 °C. The future annual temperature under the RCP4.5 is predicted to 9.5 °C in 2040s, and 10.7 °C in 2090s based on linear scaling method. Under RCP8.5, the future annual temperature changes were projected to 10 °C and 13.7 °C for the 2040s and 2090s, respectively. The boxplots also show that the future mean annual temperature is getting worse in 2090s under RCP8.5. The annual projected temperature is depicted in Table 5-11. The mean annual temperature change shows an increase of +1.9 °C in 2040s and +3.1°C in 2090s under RCP4.5. Likewise, under RCP8.5, the mean annual temperature increases by +2.4 °C in 2040s and 6 °C in 2090s respectively.

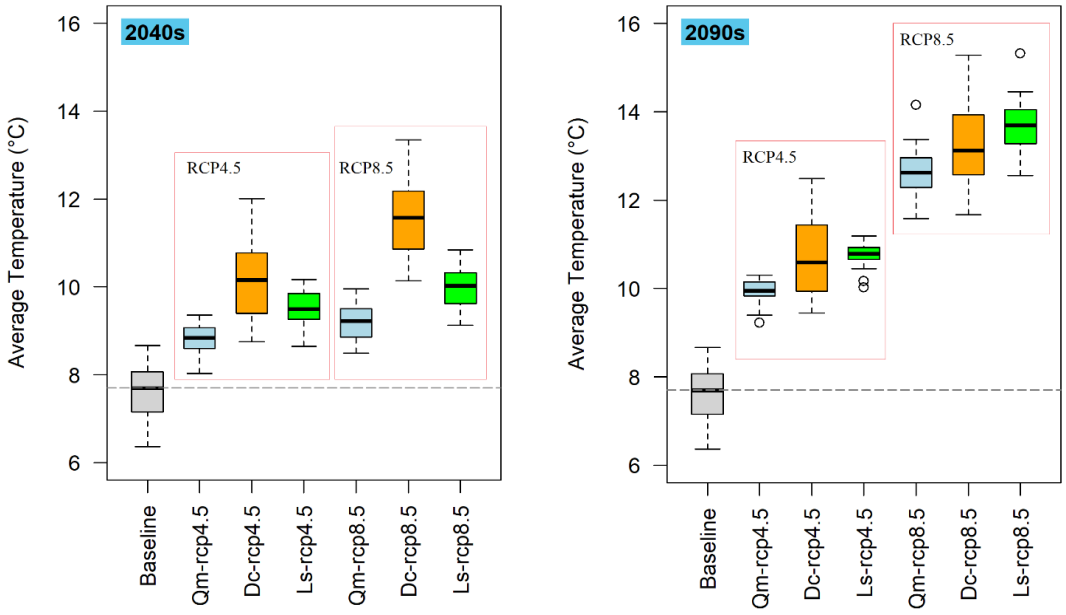

Figure 5-22: Means annual temperature changes compared to the baseline in UKRB.

Table 5.11: Future annual temperature changes compared to baseline in the UKRB.

	RCPs	Methods	2040s	2090s
1	RCP4.5	Linear scaling	+1.9 °C	+3.1 °C
2	RCP8.5	Linear scaling	+2.4 °C	+6.1 °C
3	RCP4.5	Quantile mapping	+1.2 °C	+2.3 °C
4	RCP8.5	Quantile mapping	+1.6 °C	+5.1 °C
5	RCP4.5	Delta change	+2.6 °C	+3.1 °C
6	RCP8.5	Delta change	+4.0 °C	+5.7 °C

5.2.4 Changes in spatial distribution

The spatial distribution of annual precipitation, Tmax and Tmin anomalies are depicted in the Figure 5-23 and Figure 5-25-26, respectively over the future periods using the Ls method. The results suggest that the spatial precipitation is likely to decrease in the north and northeast part of the basin (-3%, -3%), while it shows an increase in the southern part of the basin in 2040s (27% and 44%) under both RCP 4.5 and RCP 8.5. Likewise, in 2090s the annual spatial precipitation shows a decrease in some part of the north of the basin (-8%, -10%) under RCP4.5 and RCP8.5, while it shows a 17% and 27% increase of precipitation under both RCP4.5 and RCP8.5 respectively, in the UKRB (Figure 5-23). The Figure 5-24 illustrates the spatial changes in future

precipitation for each regional climate model (RCM) across the sub-catchments of the Upper Kabul River Basin during the 2040s, 2090s, and the baseline period (1986-2005), under RCP4.5 and RCP8.5 scenarios. According to the CanESM2 climate model, the maximum precipitation during the baseline period is approximately 650 mm. In the 2040s, this increases to between 800 mm and 1000 mm, and reaching nearly 1200 mm by the 2090s under both RCP scenarios. The minimum precipitation during the baseline period is 300 mm, which rises to between 400 mm and 450 mm in the 2040s, and nearly 500 mm in the 2090s, again under both RCP4.5 and RCP8.5. Based on CanESM2 projections, precipitation is expected to decrease in the northern sub-catchments while increasing in the southern part of the basin. Similarly, the Remo2009 model shows a baseline maximum precipitation of 650 mm. However, by the 2040s, precipitation decreases to 550 mm under both RCPs, with a slight increase to between 550 mm and 600 mm by the 2090s under RCP4.5 and RCP8.5. Unlike CanESM2, the Remo2009 model projects a clear decrease in precipitation in the southern part of the basin.

The RegCM4-4 model projects an increase in precipitation compared to the baseline period, rising from 650 mm to 700 mm in the future. This increase is observed in both the northern and southern parts of the basin. In contrast, the Miroc5 model shows a future decrease in precipitation compared to the baseline period. The maximum precipitation is projected to be around 550 mm in the 2040s under both RCPs, increasing slightly to between 550 mm and 600 mm by the 2090s. In summary, the results from the RCM ensemble indicate that precipitation is likely to decrease in the northern sub-catchments, while increasing in the southern and eastern parts of the UKRB. The contradictory behavior of precipitation changes in the Upper Kabul River Basin (UKRB), where annual precipitation decreases in higher elevation regions and increases in lower elevation areas under both the RCP 4.5 and RCP 8.5 climate scenarios, can be explained by several interrelated physical and meteorological processes.

5.2.4.1 Orographic Effects

In mountainous regions, moist air is forced to rise when it encounters high terrain (Minder, 2010). As the air rises, it cools and condenses, causing precipitation. In a warming climate, changes in temperature can alter how air masses interact with topography (Minder, 2010). In addition, Climate change may affect the sources of moisture (shift in moisture sources) and the prevailing wind patterns, leading to less moisture being available for uplift in higher elevations. Reduced snowfall or shifting atmospheric patterns might limit the amount of moisture reaching

high altitudes. Moreover, Higher elevations tend to experience stronger warming compared to lower areas (Prein et al., 2017).This is the case in the UKRB (Figure 5-23 and 5-24) which reduce snowfall and increase evaporation, leading to an overall reduction in precipitation at higher altitudes.

5.2.4.2 Regional Hydrological and Evaporation Changes

As temperatures increase, higher elevations may experience enhanced evaporation, especially from surface water bodies or soil, leading to a reduction in net precipitation (i.e., more moisture is lost than gained). Additionally, warmer temperatures can result in more intense precipitation events at lower elevations, causing higher runoff and potential localized increases in precipitation (Viviroli et al., 2011). This, combined with more efficient moisture recycling due to increased evapotranspiration from vegetation and soil, could explain the increased precipitation in the lower areas of the UKRB. Moreover, both scenarios RCP4.5 and RCP8.5 projects warming (Figures 5-23 and 5-24) but at different magnitudes. Under RCP 8.5 (a higher emissions scenario), the increased warming may exacerbate the processes described above, leading to even more pronounced reductions in precipitation in high-altitude areas due to stronger evaporation and atmospheric circulation shifts. At the same time, lowland areas might experience an increase in extreme rainfall events, boosting total annual precipitation. In summary, the contradictory behavior in precipitation patterns between high and low elevations in the UKRB can be attributed to complex interactions between temperature-driven changes, atmospheric dynamics, orographic processes, and evaporation patterns. Climate change may disrupt established precipitation regimes, causing less precipitation in mountain areas (due to reduced snow and altered storm tracks) and more in lower regions (due to increased convection and storm intensity).

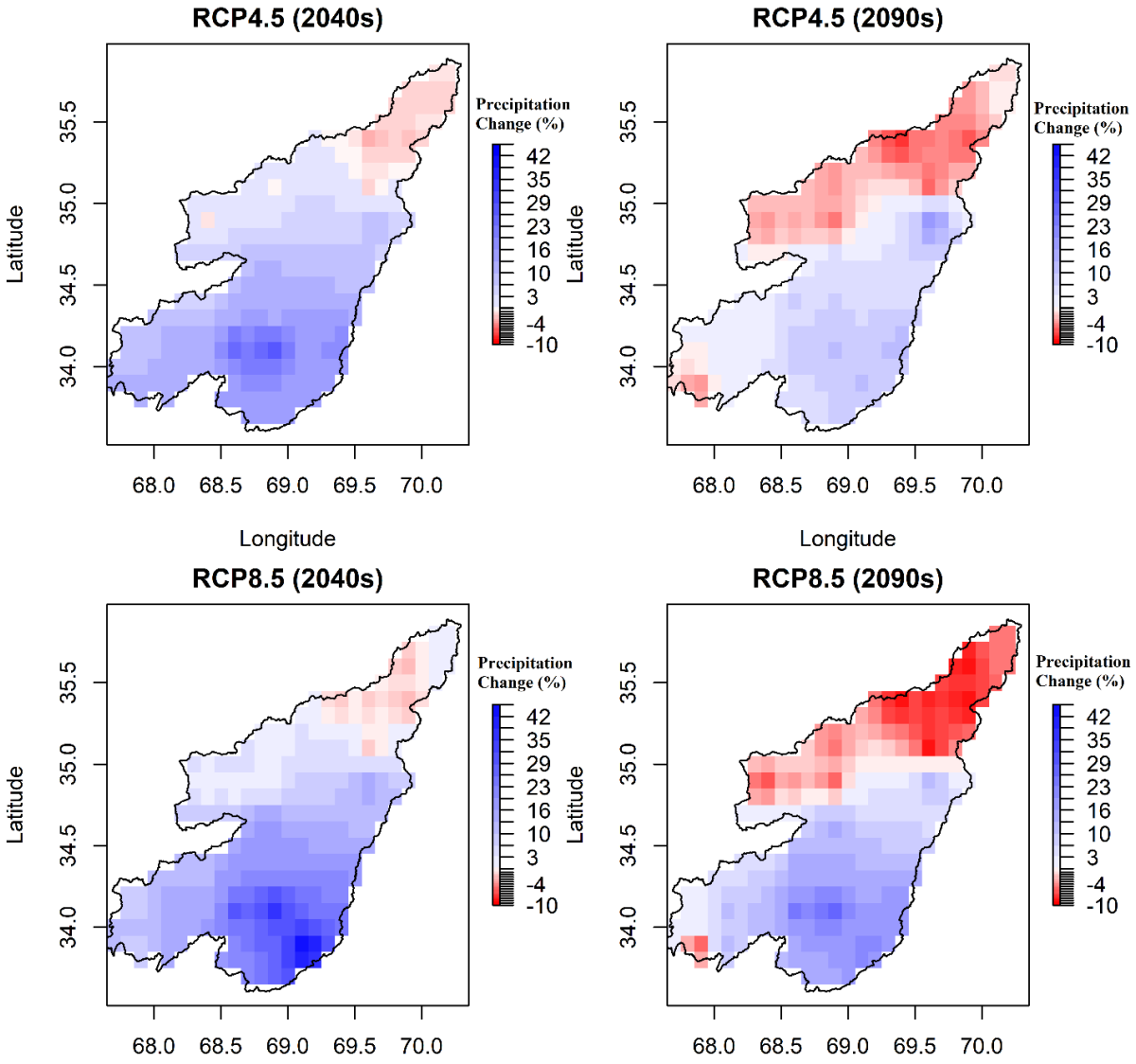

Figure 5-23: Future changes in spatial distribution of annual precipitation compared to the baseline period (1986–2005).

The temperature and precipitation anomaly calculation are a way to quantify the deviation of a given value from a reference value. It is commonly used in climatic science to assess the changes in over time. The precipitation equation can be expressed as follows:

$$Pr\ anomaly = 100^{*}\ (Baseline\ Pr - Future\ Pr)/\ Baseline\ Pr \qquad (18)$$

Where, the Pr is the precipitation values, and 100 is used to change the precipitation anomaly in percentage. The Precipitation anomaly represents the deviation from the reference. Observed Pr is the actual precipitation values at a specific time and location. While, the reference Pr is the baseline precipitation values used for comparison.

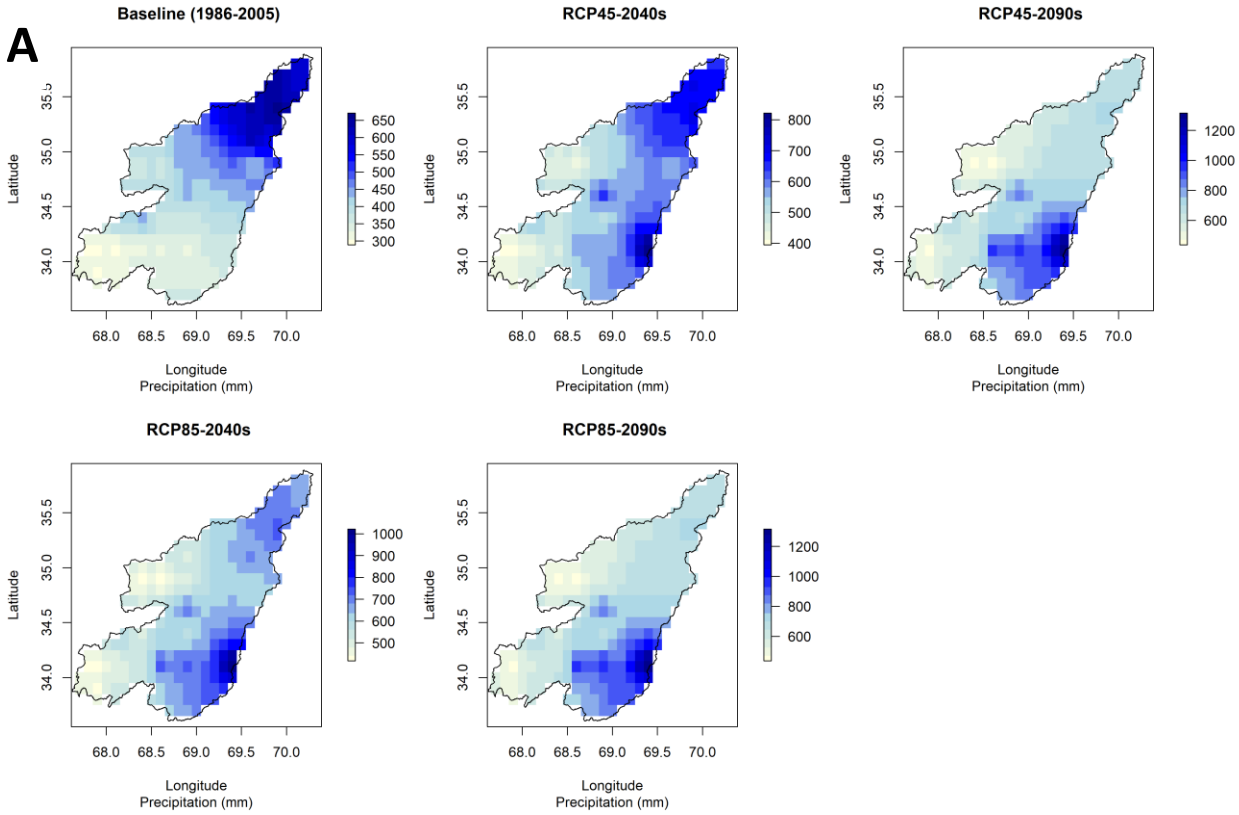
A
Baseline (1986-2005)
RCP45-2040s
RCP45-2090s
RCP85-2040s
RCP85-2090s
Latitude
Longitude
Precipitation (mm)

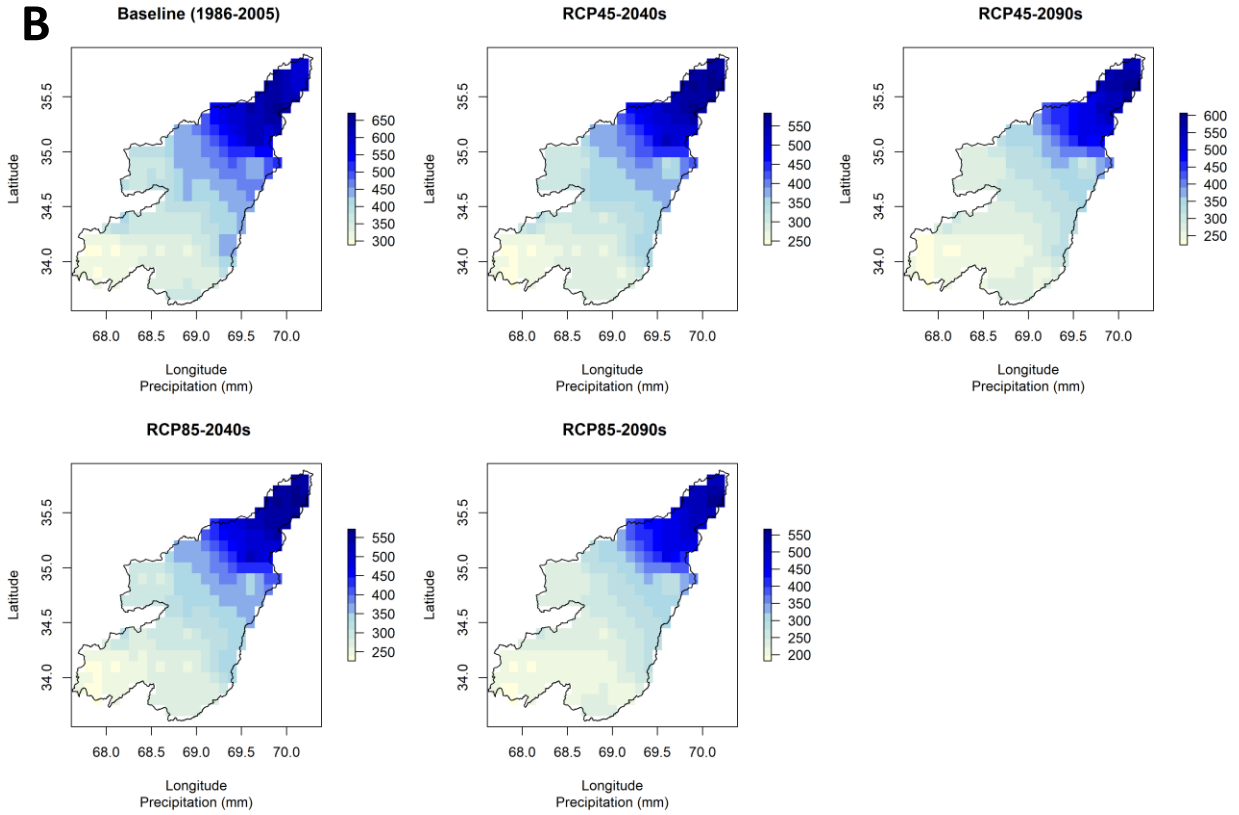
B
Baseline (1986-2005)
RCP45-2040s
RCP45-2090s
RCP85-2040s
RCP85-2090s
Latitude
Longitude
Precipitation (mm)

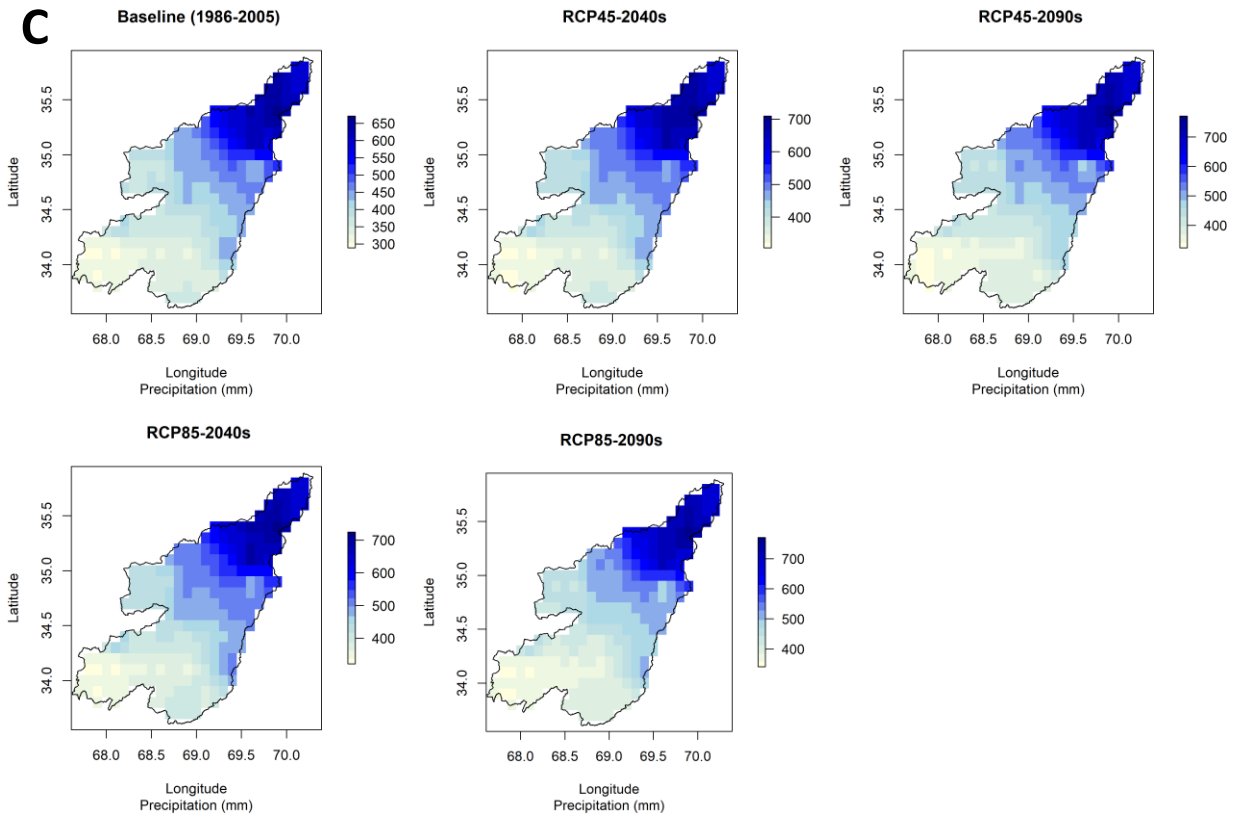
C
Baseline (1986-2005)
RCP45-2040s
RCP45-2090s
RCP85-2040s
RCP85-2090s
Latitude
Longitude
Precipitation (mm)

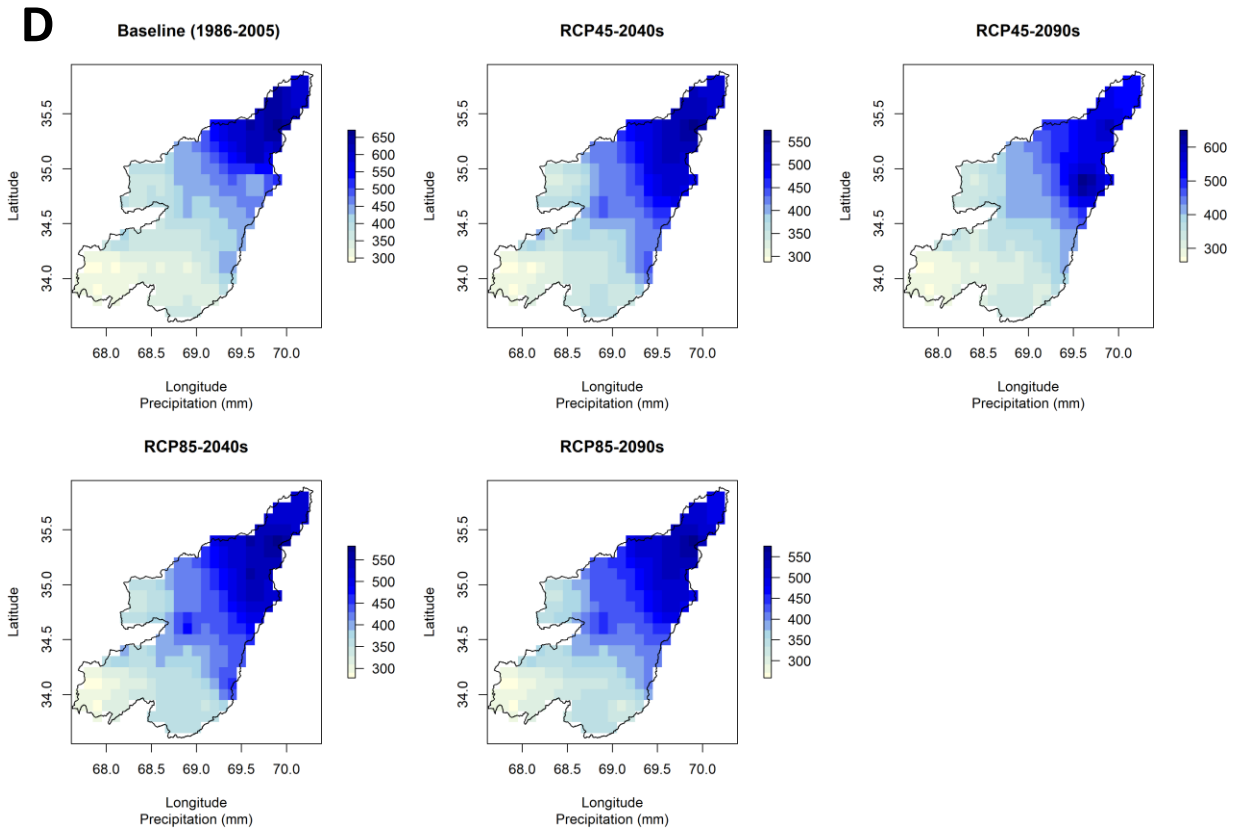
D
Baseline (1986-2005)
RCP45-2040s
RCP45-2090s
RCP85-2040s
RCP85-2090s
Latitude
Longitude
Precipitation (mm)

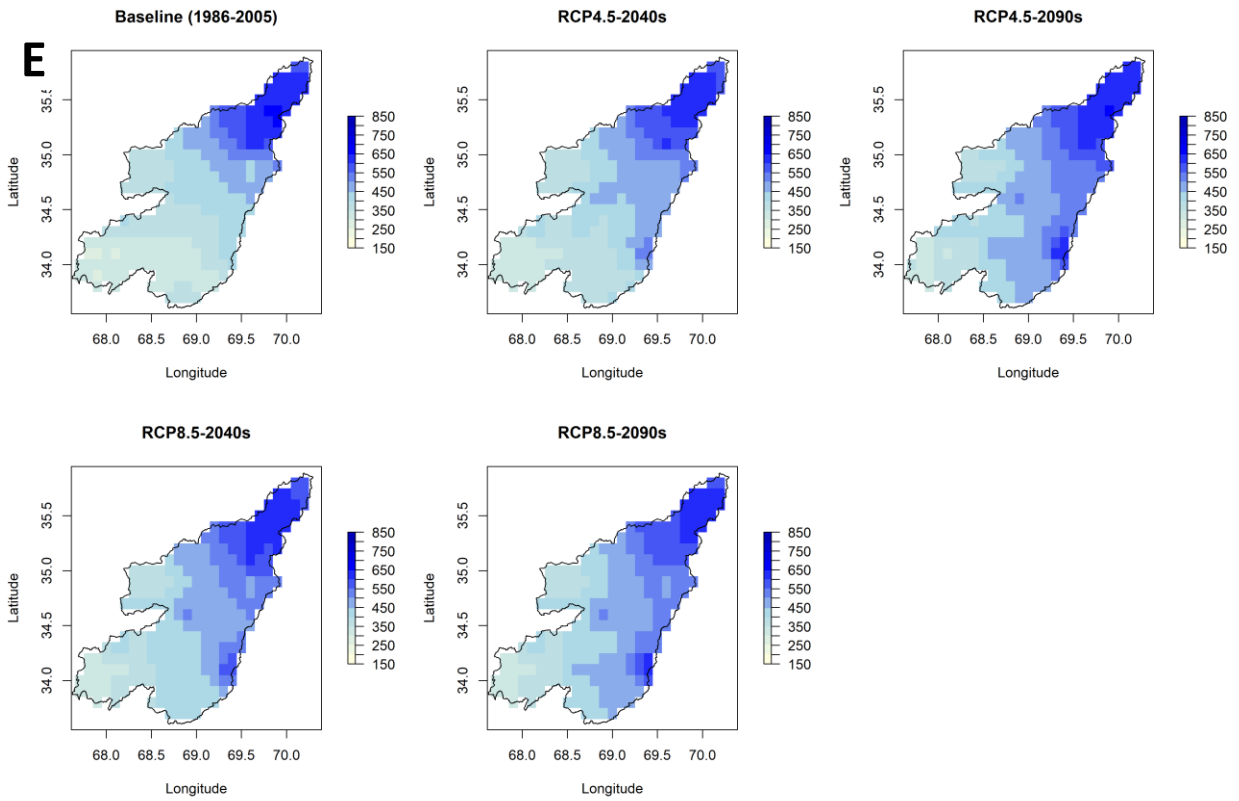

Figure 5-24:The baseline and future precipitation changes in the climate models including: A) CanESM2, B) Remo2009, C) RegCM4-4, D) Miroc5, and E) the ensemble of all 4 RCMs in the UKRB.

Also, the spatial changes in annual Tmax and annul Tmin indicate that the temperature will get warmer in the future (relative to the reference period- 1986-2005) under both RCP4.5 and RCP8.5 all over the UKRB (Figure 5-25). The Tmax obviously shows a higher temperature increase in the north part of the basin which is a mountinouse area of Hindukush. The annual Tmax increase is projected 6.1 °C in 2090s under the worse scenario of RCP8.5. In 2040s, the annual Tmin shows the higher temperature changes in the south part of the basin (Logar Watershed), while it shows the maximum changes in the northern and southern part of the basin in 2090s, in the UKRB (Figure 5-26).

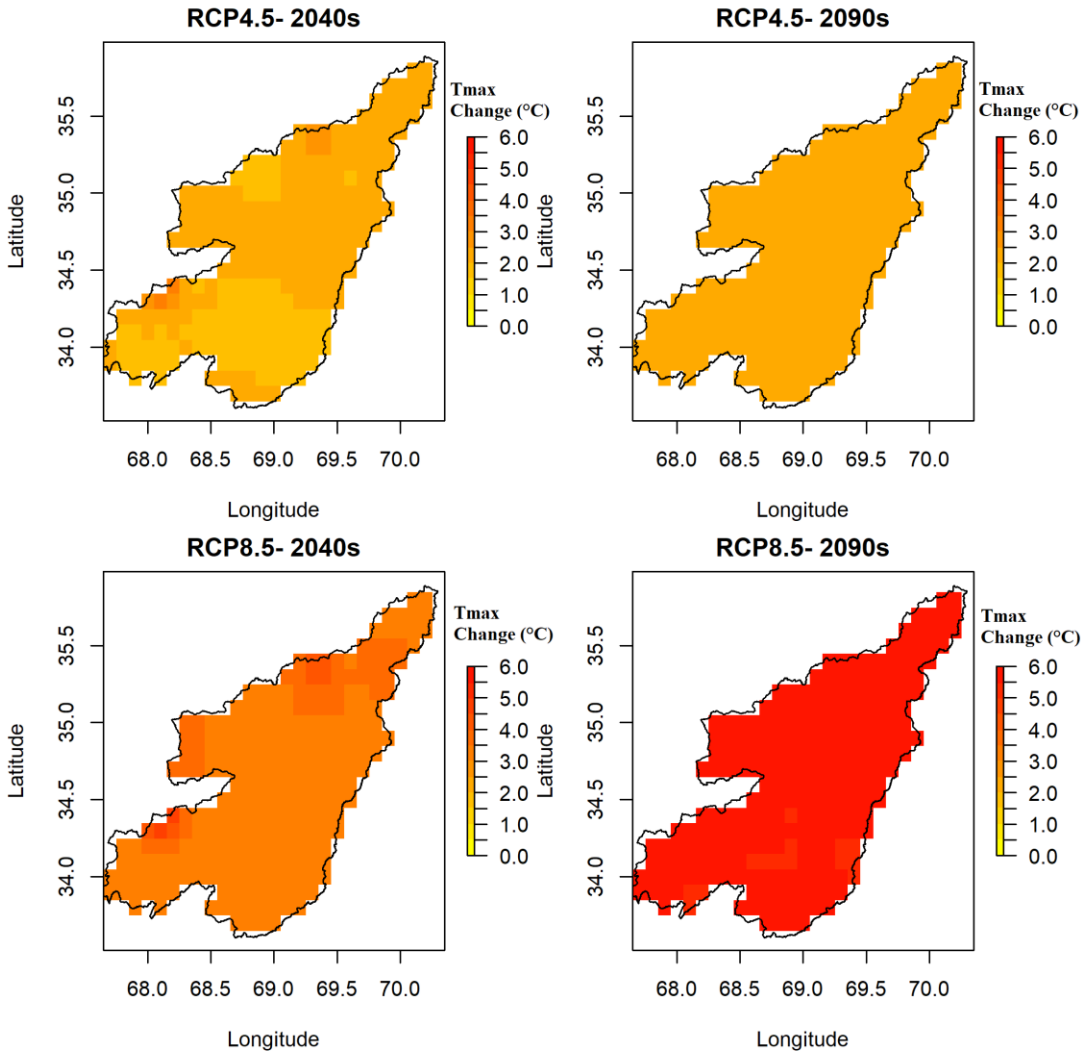

Figure 5-25: Changes in future spatial distribution of annual maximum temperature compared to the baseline period (1986–2005) over the upper Kabul river basin.

The temperature anomalies are calculated based on the equation 19.

Temperature anomaly = Baseline temperature - Future temperature *(19)*

Where, temperature anomaly represents the deviation from the reference temperature. Observed temperature is the actual temperature value at a specific time or location and reference temperature is a baseline temperature value used for comparison.

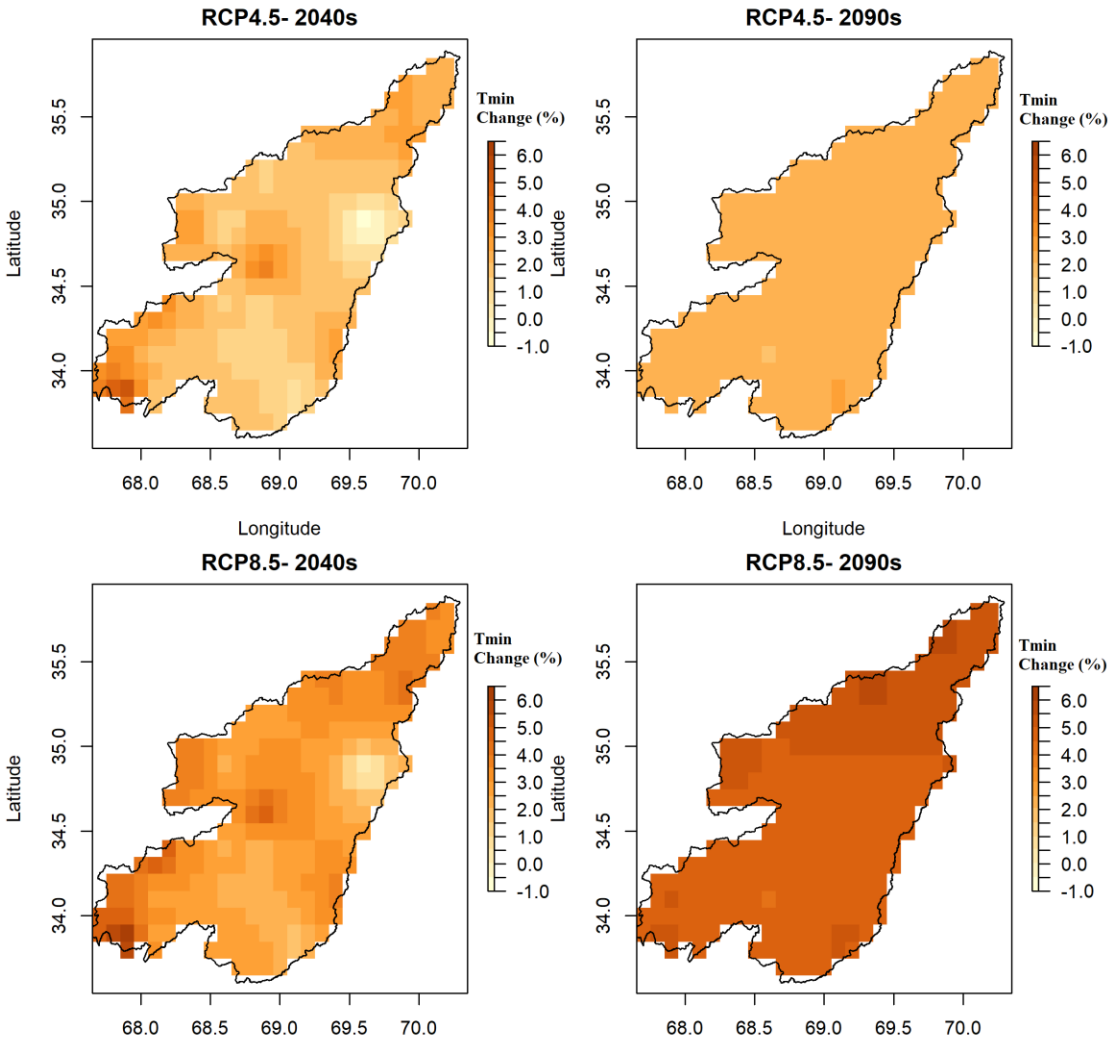

Figure 5-26: Changes in future spatial distribution of annual minimum temperature compared to the baseline period (1986–2005) over the upper Kabul river basin.

The figures 5-27 and 5-28 illustrate the spatial changes in future maximum and minimum temperatures from each RCM across the sub-catchments for the 2040s and 2090s compared to the baseline period (1986-2005), under RCP4.5 and RCP8.5 scenarios in the Upper Kabul River Basin (UKRB). The maps display outputs from four regional climate models (RCMs), includes: CanESM2, Remo2009, RegCM4-4, and Miroc5. In the maximum temperature maps, orange represents the highest temperatures, while light blue indicates the lowest. Similarly, in the minimum temperature maps, orange still denotes maximum temperatures, but green is used for the minimum values. These maps highlight clear differences in temperature and precipitation across the UKRB, especially in relation to the region's topography, which has a more pronounced

impact than the cardinal directions of the catchment area. Future maximum temperature changes are observed throughout the study area under both RCP4.5 and RCP8.5 scenarios, with the most extreme changes occurring under the worst-case scenario (RCP8.5) in all four models. The southern part of the basin, which consists of lower-elevation sub-catchments, shows a warmer temperature compared to the northern parts, which are at higher elevations.

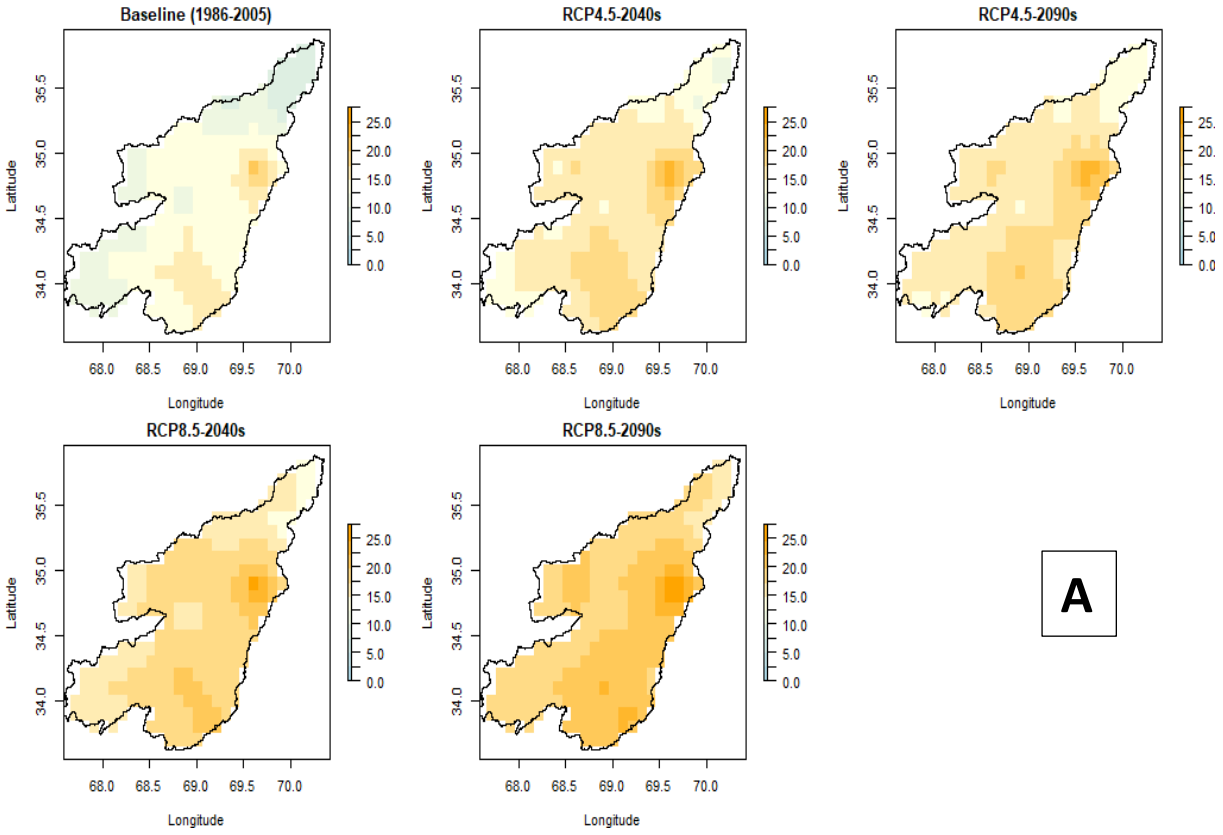

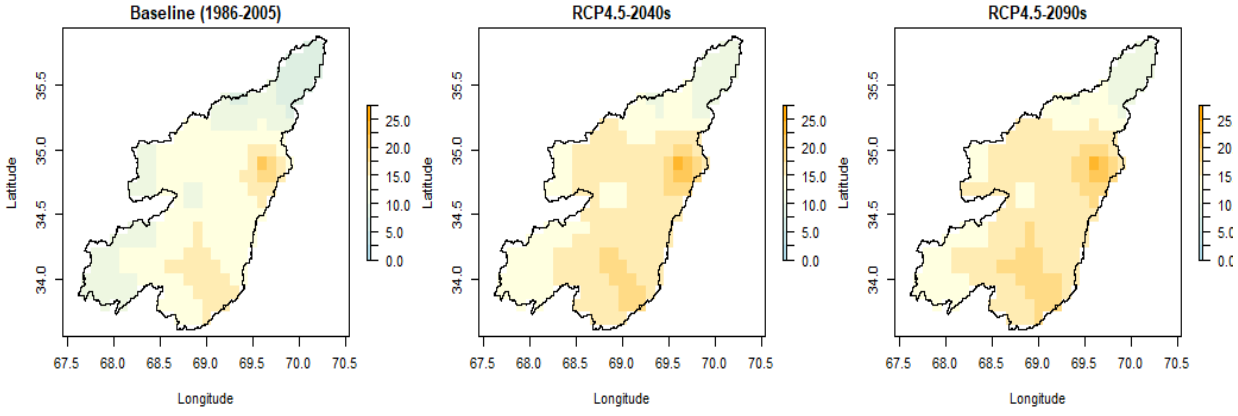
Baseline (1986-2005)
RCP4.5-2040s
RCP4.5-2090s
RCP8.5-2040s
RCP8.5-2090s
Latitude
Longitude
34.0
34.5
35.0
35.5
67.5
68.0
68.5
69.0
69.5
70.0
70.5
0.0
5.0
10.0
15.0
20.0
25.0

B

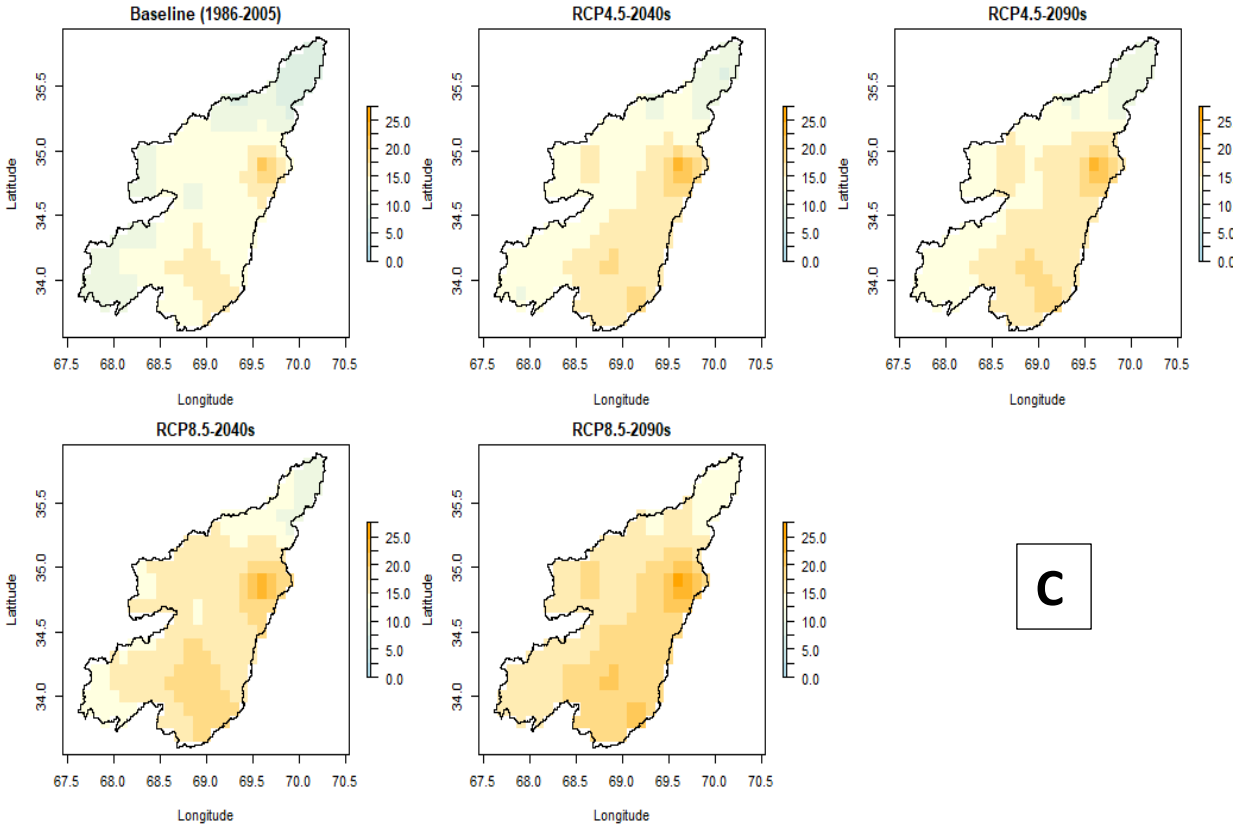
Baseline (1986-2005)
RCP4.5-2040s
RCP4.5-2090s
RCP8.5-2040s
RCP8.5-2090s
Latitude
Longitude
34.0
34.5
35.0
35.5
67.5
68.0
68.5
69.0
69.5
70.0
70.5
0.0
5.0
10.0
15.0
20.0
25.0

C

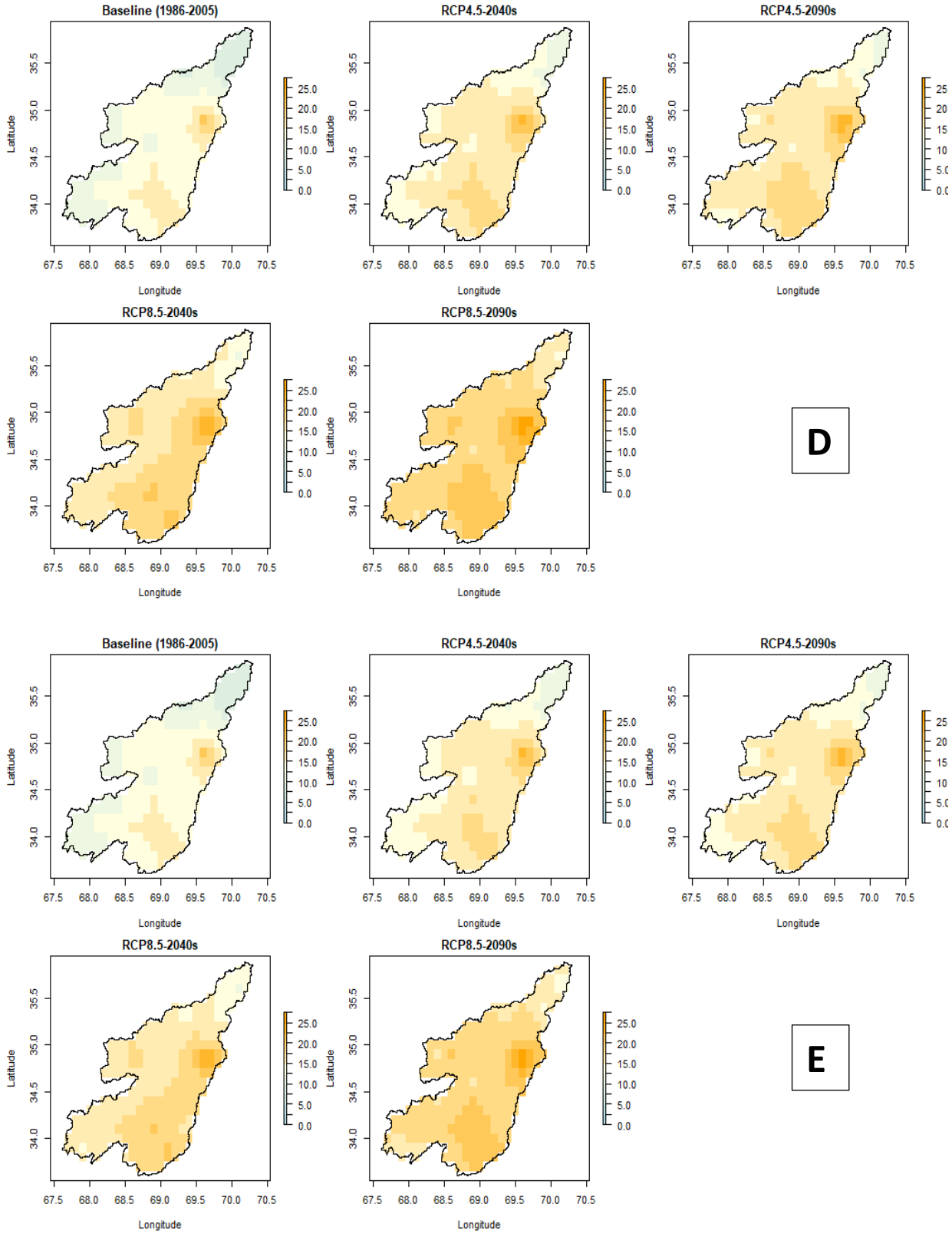

Figure 5-27: *The baseline and future maximum temperature changes in the climate models including: A) CanESM2, B) Remo2009, C) RegCM4-4, D) Miroc 5, and E) the ensemble of all 4 RCMs in the UKRB.*

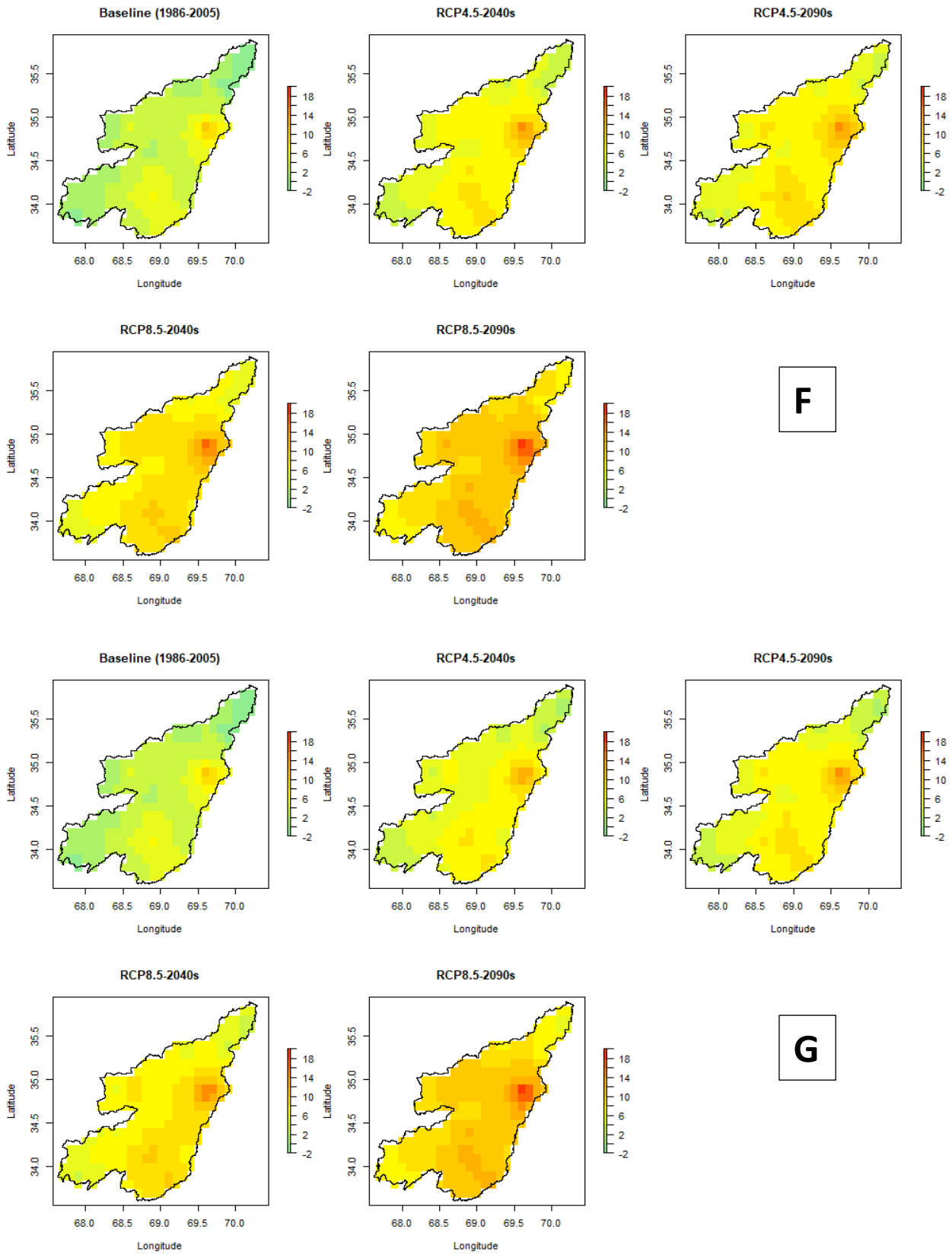
Baseline (1986-2005)
RCP4.5-2040s
RCP4.5-2090s
RCP8.5-2040s
RCP8.5-2090s
F
Baseline (1986-2005)
RCP4.5-2040s
RCP4.5-2090s
RCP8.5-2040s
RCP8.5-2090s
G
Latitude
Longitude
34.0
34.5
35.0
35.5
68.0
68.5
69.0
69.5
70.0
18
14
10
6
2
-2

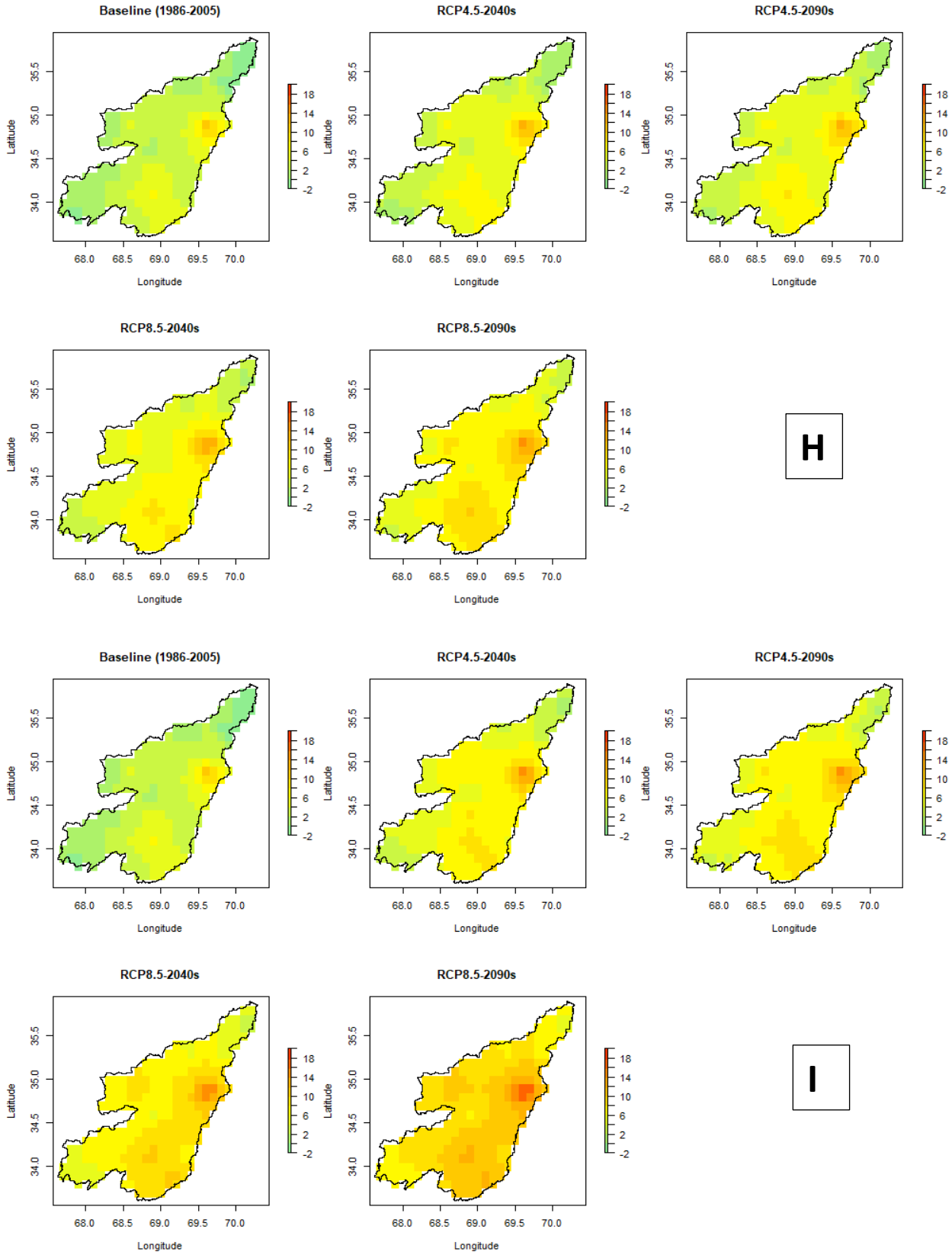
Baseline (1986-2005)
RCP4.5-2040s
RCP4.5-2090s
RCP8.5-2040s
RCP8.5-2090s
H
Baseline (1986-2005)
RCP4.5-2040s
RCP4.5-2090s
RCP8.5-2040s
RCP8.5-2090s
I
Latitude
Longitude
34.0
34.5
35.0
35.5
68.0
68.5
69.0
69.5
70.0
18
14
10
6
2
-2

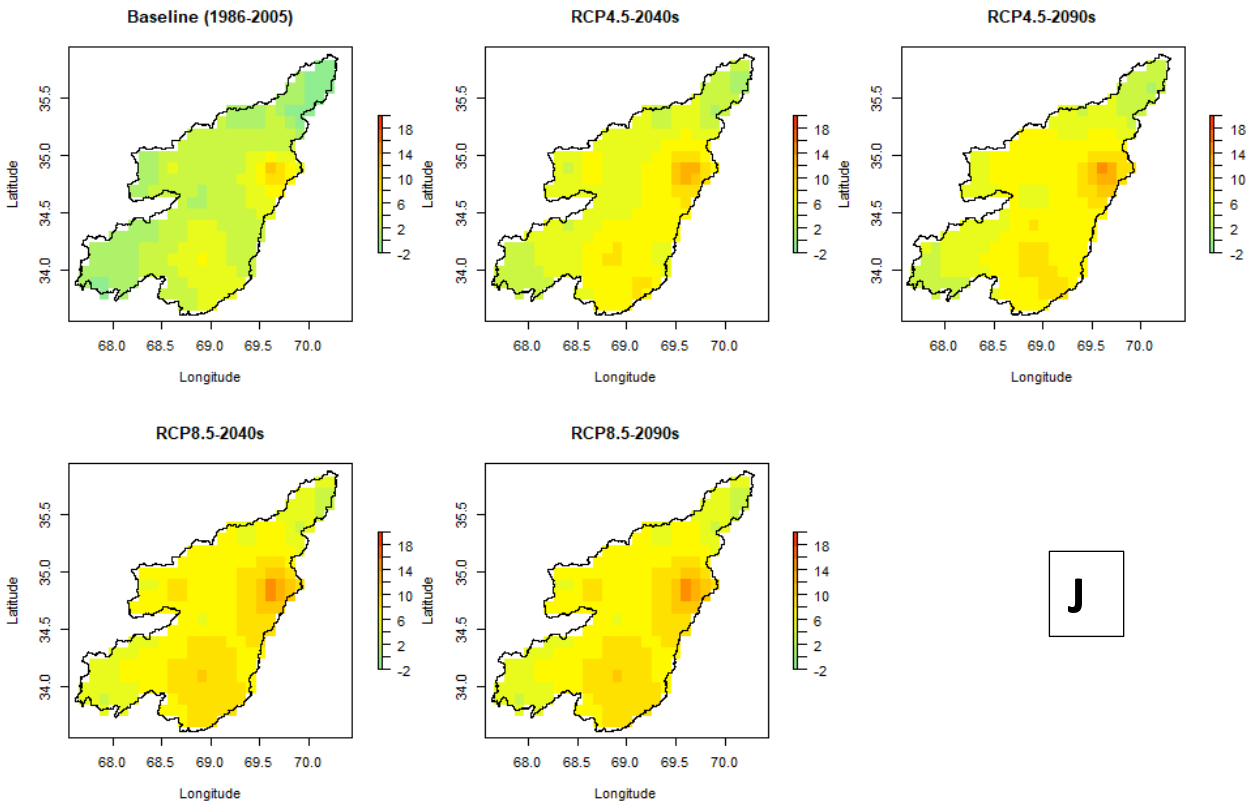

Figure 5-28: The baseline and future minimum temperature changes in the climate models including: F) CanESM2, G) Remo2009, H) RegCM4-4, I) Miroc5, and J) the ensemble of all 4 RCMs in the UKRB.

5.2.5 Extreme trend results

This study also examined how the trend of annual extreme temperature and precipitation might change in the future over the course of the 21st century (2006-2100) in UKRB, specifically looking at six indices: annual total wet day precipitation (PRCPTOT), extremely wet days (R99p), monthly minimum value of daily minimum temperature (TNn), monthly maximum value of daily maximum temperature (TXx), warm nights and warm days shown in Table 5-12 and Figure 5-29, and is defined by the Expert Team on Climate Change Detection Monitoring and Indices (ETCCDMI), jointly sponsored by World Meteorological Organization (WMO) commission of Climatology (CCI) and the Climate Variability and Predictability (CLIVAR) (Vincent *et al.*, 2005). The analyzed annual precipitation trend shows an insignificant decrease from 2006 to 2100, especially under RCP4.5 and after 2082, while the annual extremes of minimum and maximum temperature show a significant increase under both RCPs 4.5 and 8.5 scenarios with a p-value of 0, indicating that the climate is getting hotter. In addition, there was not a significant trend change in future extreme precipitation. The number of warm nights and warm days shows

an increase in the future, specifically the significant increase will occur in the end of the century (Figure 5-29).

Table 5.12: Extreme indices studied in this research. RR is the precipitation in the table.

ID	Indicator Name	Units	Indicator definitions
PRCPTOT	Annual total wet day precipitation	mm	Let RR_{ij} be the daily precipitation amount on day i in period j. If i represent the number of days in j, then PRCPTOTj = $\sum(RRij)$
R99P	Extremely wet days: Annual total PRCP when RR > 99th percentile	mm	Let RR_{wj} be the daily precipitation amount on a wet day w (RR $\geq$ 1.0mm) in period i and let $RR_{wn}99$ be the 99^{th} percentile of precipitation on wet days in the period. If W represents the number of wet days in the period, then: $R99Pj = \sum_{W=1}^{W} RRwj \text{ where } RRwj > RRwn99$
TNn	Min Tmin: Monthly minimum value of daily minimum temp	°C	Let TNij be the daily minimum temperatures in month i, period j. The minimum daily minimum temperature each month is then: TN_{ij} = min (Tn_{ij})
TXx	Max TMax: Monthly maximum value of daily maximum temp…	°C	Let TX_{ij} be the daily maximum temperatures in month i, period j. The maximum daily maximum temperature each month is then: TX_{ij}= max (Tx_{ij})
TN90p	Warm nights	%	Number of days when monthly value of daily minimum temperature TN > 90^{th} percentile
TX90p	Warm days	%	Number of days when monthly value of daily maximum temperature TX > 90^{th} percentile

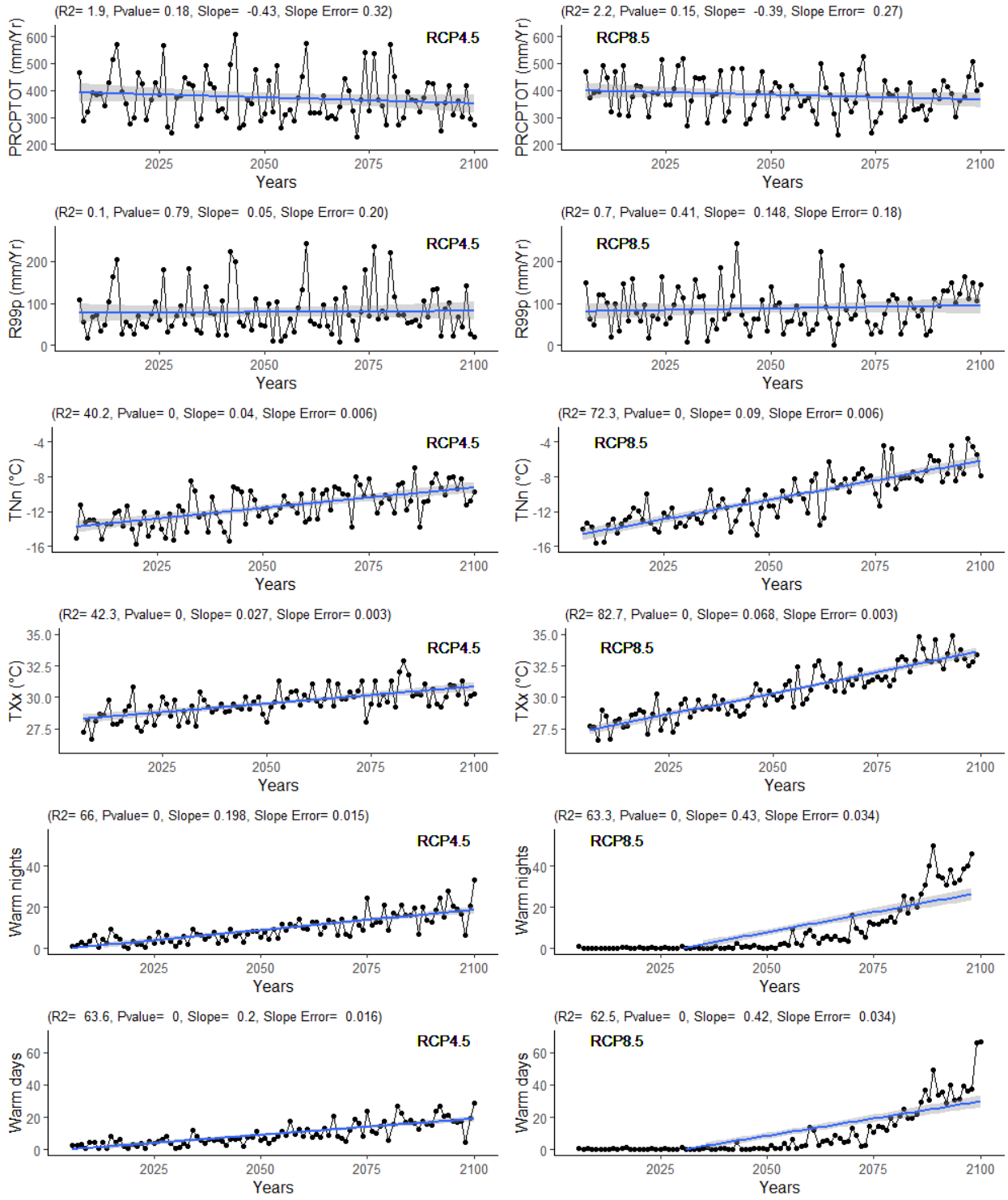

Figure 5-29. The six future annual indices; Precipitation in wet days (PRCPTOT), Extremely precipitation (R99p), Monthly minimum value of daily minimum temperature °C (TNn), Monthly maximum value of daily maximum temperature °C (TXx), Warm nights, and Warm days for the period of 2006-2100 from the ensemble of 4 RCMs in the upper Kabul River basin. The visualization of the plot is in an annual series along with trends computed by linear least square (solid blue line). The statistics of linear trend fitting are displayed on the top of the plots.

5.3 Climate change impacts on water resources

This section examines the results from the impact of future climate change on surface runoff and water availability in the UKRB under RCP 4.5 and RCP 8.5 scenarios. The study used the bias corrected precipitation and temperature results from the linear scaling method. The data were used from 24 grids (stations) in the SWAT hydrological model for analyzing the baseline and the future scenarios. Further details about the analyzed results are provided in the subsequent section below.

5.3.1 Monthly variation in streamflow under RCP4.5

Figure 5-26 illustrates the response of the climate change on the monthly surface runoff for the 2040s and 2090s under RCP4.5 and RCP8.5. The baseline (1968-2005) runoff is showed in black line and the models mean showed in the red lines. The results indicate how the temperature's increase had impacted the water flow in UKRB, subsequently causes a decrease in discharge in the summer season, while shows increases in flow peaks during the winter and spring seasons. The future monthly flow peak showed a backward shift to March and April instead of May and June in Tang-I-Gulbahar and Shukhi stations, while in Tang-i-Saidan station, the flow peaks shifted from April to March in both period of 2040s and 2090s.

In 2090s, the water availability is projected to reduce compared to 2040s under both RCPs 4.5 and 8.5 scenarios. The results from each RCM showed a different pattern of monthly runoff. The CanESM-2 and the RegCM4-4 models are wetter climate model, which shows higher discharge peaks compared to the baseline and the other models. In contrary the Miroc-5 and Remo-2009 showed a lower monthly discharge peaks compared to the historical period and other two aforementioned RCMs. Based on monthly discharge results, future seasonal water availability could be expected to vary in UKRB (Figure 5-30). In this study, the ET and the percolation both were not validated due to the unavailability of data.

5.3.2 Monthly variation in streamflow under RCP8.5

The monthly future surface runoff simulations are also depicted in the Figure 5-30 for the higher emission scenario (RCP8.5). The results indicate that, increases and decreases in hydrological variations tended to be more extreme under RCP 8.5 and in the end-century (2090s). In this scenario, the runoff values decreased further in summer months compared to RCP4.5. The monthly future discharge is projected to increase in the first four months of the year (January to

April), and decrease in the summer months (May to August). The magnitude of differences varies depending on the month and scenario. Comparing with the baseline's streamflow, the future monthly streamflow is projected to decrease over time in UKRB. Generally, the results showed that the overall patterns of streamflow changes in response to climate change are similar in RCP4.5 and RCP8.5. However, the magnitude of change is much higher under the RCP8.5 scenario, which assumes a higher greenhouse gas emissions and therefore more severe climate change impacts. Specifically, the period of 2090s is projected to be much drier under the RCP8.5 scenario compared to the RCP4.5 scenario, meaning a greater reduction in streamflow in that period.

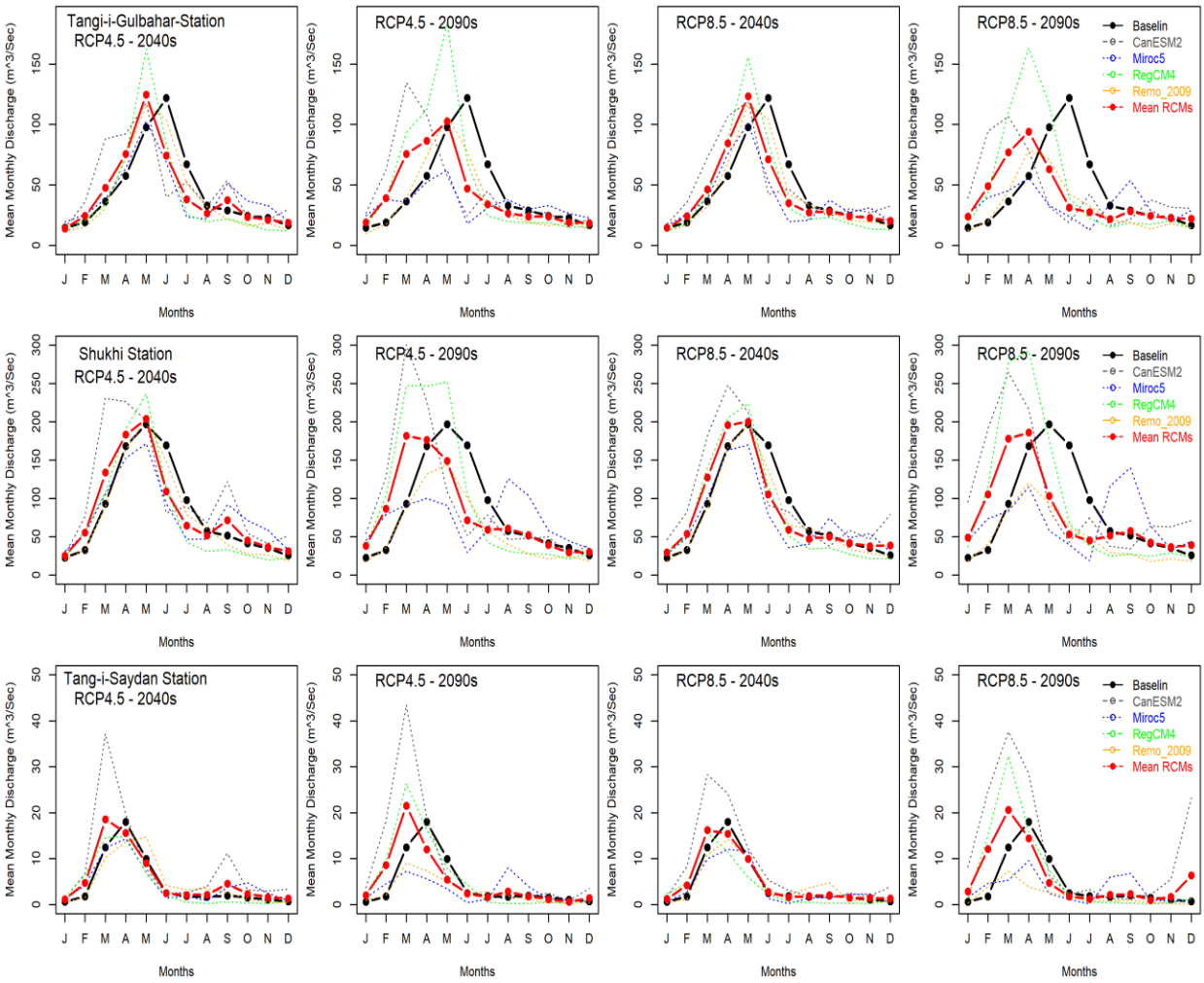

Figure 5-30: Future response of stream flow compared to the baseline under RCP 4.5 and RCP 8.5 for Tang-i-Gulbahar station (upper figure), Shukhi Station (Middle) and Tang-i-Saidan Station (lower). The black line shows the discharge for historic (1986-2005) and the red line shows discharge from Mean RCMs for two future periods 2040s and 2090s.

5.3.3 Annual variations in streamflow under climate change

The basin-wide projected annual changes in streamflow, percolation, green waterflow change (actual evapotranspiration), potential evapotranspiration, precipitation, snowfall and snowmelt for the 2040s and 2090s period are depicted in Figure 5-31. The results indicated that, there is an increase in annul streamflow and the total annual water yield in 2040s and 2090s compared to the baseline period in UKRB. The annual surface runoff throughout the UKRB is projected to increase 18 mm in 2040s, and 15 mm in 2090s based on RCP4.5. likewise, the annual surface runoff is projected to increase 15 mm in 2040s and 28 mm in 2090s under RCP8.5 (Figure 5-31). In contrary, the annual snowfall, snowmelt, sublimation from snow surface, percolation, and the groundwater recharge showed a decrease compared to the annual baseline in UKRB. The increment of annual surface runoff in UKRB is due to an increase in the annual precipitation and decrease in percolation, groundwater recharge, and the rapid glaciers and snow melt. The result also shows that, increases in temperature is impacting the actual evapotranspiration (ET) and potential evapotranspiration (PET) which will increase in the future.

The annual snowfall decrease includes -38.5 mm and -80 mm for 2040s and 2090s, respectively under RCP4.5. In addition, the snowfall is expected to decrease -48 mm, and -122 mm for 2040s and 2090s, respectively under RCP8.5. The annual snowmelt indicated to decrease -26 mm, and -57 mm for 2040s and 2090s based on RCP4.5. Under RCP8.5, the annual snowmelt indicated to decrease -34 mm, and -86 mm for the 2040s and 2090s. The decreasing of snowfall and snowmelt in the future could likely be due to impact of climate change, specifically the increase of higher temperature and changing the pattern of precipitation from snowfall to rainfall in UKRB. The snow and glaciers will be melting faster and in the earlier months of the year. Also, both the snowfall and snow melt show maximum decrease in the 2090s under both RCPs 4.5 and 8.5.

The results also show, the groundwater contribution is decreasing in the future. Under RCP4.5, the decrease in groundwater contribution is -7.5 mm and -15.8 mm for the 2040s and 2090s, respectively. Meanwhile, under RCP8.5, the decrease is larger with -9 mm and -20 mm for the same periods, respectively. Similarly, soil percolation is projected to decrease as well, with a decrease of -9 mm and -21 mm in 2040s and 2090s under RCP4.5, and a larger decrease of -12 mm and -27 mm in 2040s and 2090s under RCP8.5, respectively. These changes in groundwater and soil percolation have significant implications for the water resources in the UKRB, as they

can affect the overall water availability and contribute to the changes in surface runoff. The Annual actual evapotranspiration (ET) and potential evapotranspiration (PET) shows an increase in both RCPs compared to the baseline and in both periods of 2040s and 2090s in UKRB. The actual evapotranspiration (ET) has increased significantly under RCP4.5 by 12.6 mm in 2040s and by 11 mm in 2090s, while under RCP8.5 the ET significantly increased by 21 mm and 14 mm for the 2040s and 2090s, respectively. The increase in annual ET is more prominent in the 2090s under RCP8.5 (Figure 5-31). Additionally, the magnitude of the increase in PET is significantly higher by 2090s under RCP8.5. The annual PET shows an increase of 77 mm and 128 mm for the 2040s and 2090s under RCP4.5, while under RCP8.5 PET increases will be 92 mm and 244 mm for the 2040s and 2090s in UKRB. An increase in PET is primarily driven by the increases in temperature, which is the main factor affecting the future actual and potential evapotranspiration.

The lateral soil flow contribution is shown very low in UKRB and therefore in the future climate change analysis didn't show any significant changes under both RCPs. Our findings are similar to the findings of (Giang *et al.*, 2014; Lutz *et al.*, 2014). Overall, the annual discharge is projected to increase, consequently there will be more surface runoff in the basin annually, but there is also likely to face the problem with uneven seasonally and spatially distribution of water resources.

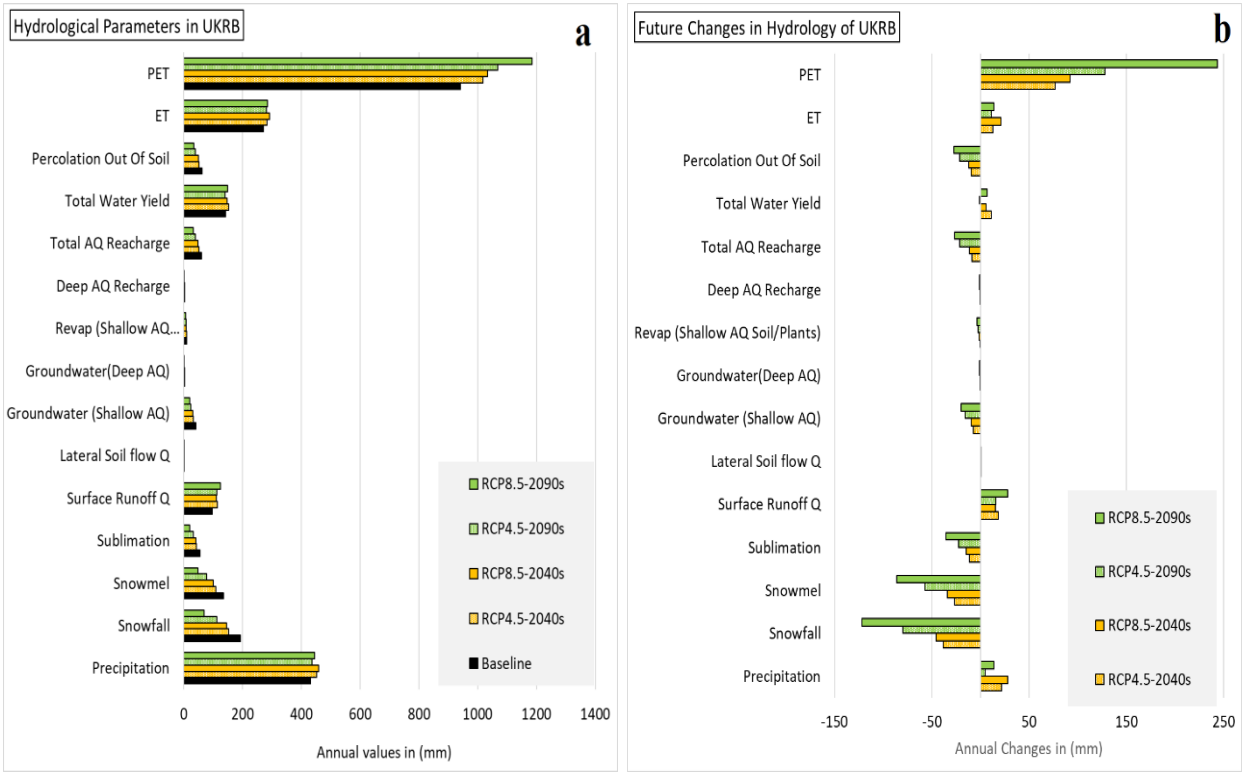

Figure 5-31: (a) The annual hydrological components for baseline and RCMs , (b) Changes of annual hydrological components for 2040s and 2090s compered to baseline, under RCP 4.5 and RCP 8.5.

Water yield is defined as the net amount of water flowing past a point on a stream during a given period (Villamizar, Pineda and Carrillo, 2019). The results suggest that water yield within UKRB will increase in the future, except in 2090s under RCP4.5. In the baseline period, the annual water yield shows 142 mm which changed to 153 mm and 148 mm under RCP4.5, and 141 mm and 149 mm under RCP8.5 for 2040s and 2090s, respectively. Based on the results, it appears that the UKRB may have sufficient annual water resources due to the projected increase in annual streamflow and total water yield. However, there may still be challenges with the seasonal and spatial distribution of water resources, particularly during the summer season when the runoff values are projected to decrease further under RCP8.5. This suggests that while overall annual water supply may be sufficient, there may still be issues with water availability during periods of high demand (Summer season).

5.3.4 Seasonal variations in streamflow under climate change

The future seasonal streamflow is presented in Figure 5-32. The seasonal streamflow in the UKRB shows larger variations during the rainy season (December to May) compared to the dry

season (June to November). Additionally, compared to the baseline period, there is an increase in the seasonal streamflow during the rainy season over time and decreases in dry season. This may indicate that the amount of water flowing in the rivers during the winter and early spring seasons are increasing however, decreasing in the summer and autumn seasons. These streamflow increments were more accentuated in rainy season and in the long term, with an increase of approximately 45 % of streamflow from December to May under RCP8.5 for the period of 2090s. Unlike to rainy season, there is a decrease in future dry season's streamflow compared to baseline, except the 2040s of RCP4.5.

Future projected hydrology results revealed that, the impact of climate change on the hydrology of UKRB is significant, as the results show an increase in the rainfall but a decrease in snowfall due to the changing precipitation pattern. This change in precipitation pattern will also affect the snow and glaciers melt which is expected to decrease in the future due to higher average temperatures. Specifically, the projected results indicate that there will be less snow and glacier melt in the 2090s under RCP8.5. These changes in precipitation patterns will have a significant impact on the water resources in the study area and may cause water scarcity in the summer season, which could lead to drought conditions.

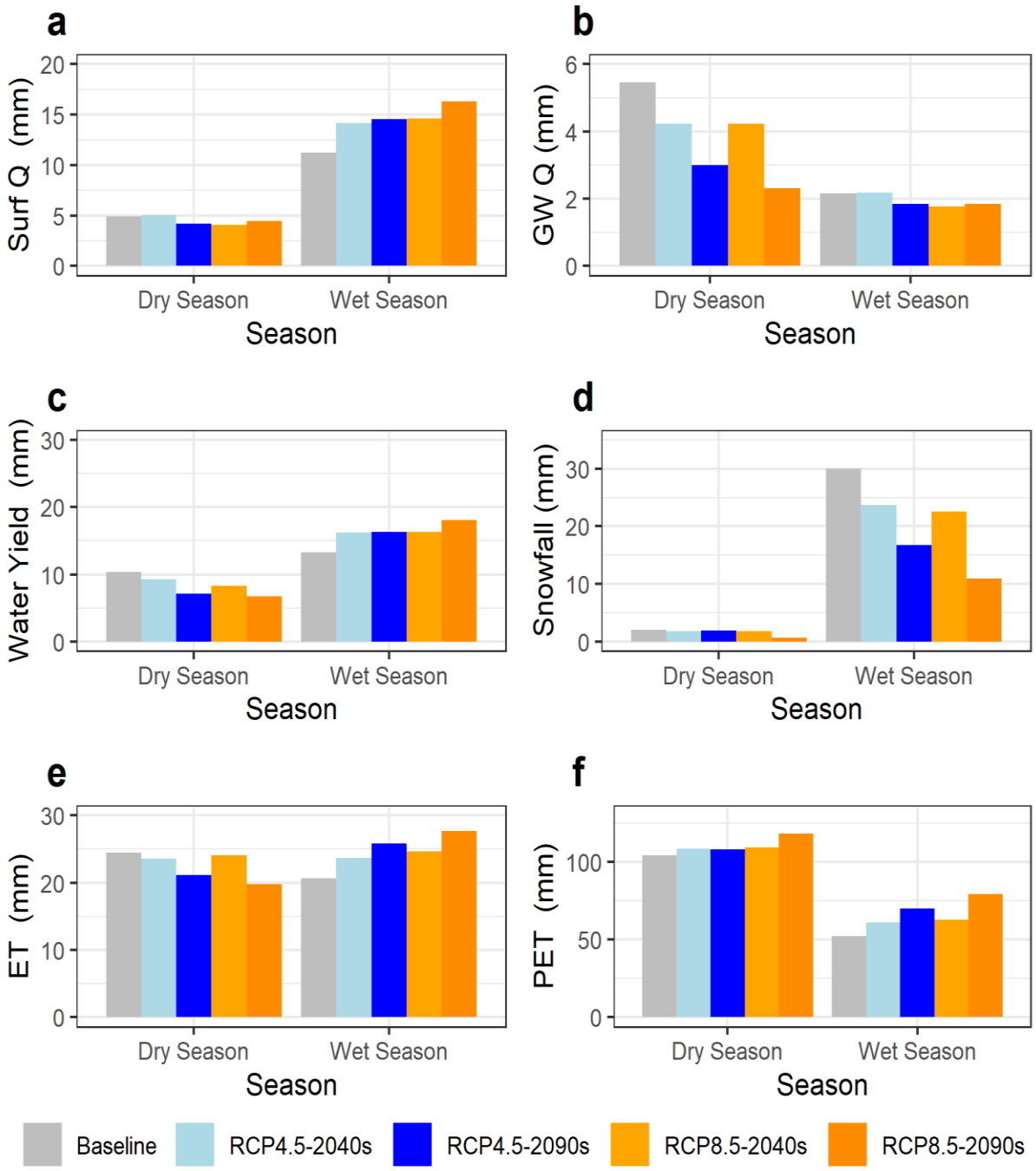

Figure 5-32: The seasonal changes in; (a) snowfall, (b) surface runoff, (c) lateral flow, (d) water yield, (e) evapotranspiration (ET), and (f) potential evapotranspiration (PET) for dry and wet seasons in UKRB. The results are showed for the baseline, 2040s and 2090s periods under RCP4.5 and RCP8.5.

6 DISCUSSION AND CONCLUSION

6.1 Discussion

The study utilized the regional climate models (RCMs) output to simulate and analyze the future climate in the UKRB. However, to improve the accuracy of the RCMs' precipitation and temperature projections, three bias correction methods were applied and the results validated with APHRODITE data due to lacking access of local historical data. The impact of climate change on water resources in the UKRB was then assessed using the soil and water assessment tool (SWAT) and GIS software. The details of discussion part of this study are explained in the below sections.

6.1.1 Discussion on bias correction

It is well established that precipitation and temperature simulations from RCMs often provide bias representation of observations, and hence making bias correction necessary before being used for climate impact studies (Gudmundsson *et al.*, 2012b; Teutschbein and Seibert, 2012). Previous studies found that different bias correction methods have relatively good performance in correcting the raw simulations to the observed in different aspects (Teutschbein and Seibert, 2012; Tadese, Kumar and Koech, 2020; Enayati *et al.*, 2021). For instance, the linear scaling (Ls) and local intensity scaling (Lis) methods performed well in reducing the mean and 90^{th} percentile, while the distribution mapping (Dm) and power transformation of precipitation (Pt) methods performed better in correcting the probability and intensity of wet days, additionally, the delta change (Dc) method matched observations of current conditions and consequently outperformed by definition (Teutschbein and Seibert, 2012). Likewise, the performance of non-parametric transformations (e.g., Empirical quantile mapping (Eqm)) was best in reducing biases of precipitation in the RCMs (Gudmundsson *et al.*, 2012b). Therefore, in this study the linear scaling (Ls), delta change (Dc) and empirical quantile mapping (Eqm) methods were selected. Each of these methods has its own strengths and weaknesses, and by using a combination of methods, we were able to account for different aspects of bias in the climate models. This approach helped to increase the accuracy and reliability of the data used to analyze the impacts of climate change on water resources in UKRB. On the other hand, the discussion highlights the importance of using bias correction methods to improve the accuracy and reliability of climate models output to use for future climate and hydrology assessment, and the importance of selecting appropriate method

for further climate change impact study on water resource in the UKRB. The result demonstrates that all methods could remove biases in RCM's precipitation and temperature. However, the Dc method indicated the best statistical and graphical correlation in this study, its limitations were also acknowledged. As noted by Teutschbein and Sebert (2012), the Dc does not adjust the RCM simulations themselves in the baseline period, but rather uses the observations and only the RCM change signals for the future projection. This implies that the delta change method cannot be evaluated for the control run, as it corresponds to the observed climate and thus provides a perfect match to the observations by definition. Therefore, the linear scaling method was selected as the better option for climate change impact study in this research. The selection considered both the statistical and graphical correlation between the corrected data and APHRODITE data.

Our findings indicate that the Ls method performed better than Eqm in capturing the distribution of monthly precipitation and temperature in the historical period. This suggests that the linear scaling method was able to correct the bias more accurately in precipitation and temperature of the RCMs. Additionally, the graphical correlation in long-term annual projected precipitation compared to APHRODITE data showed better results by linear scaling than quantile mapping in the historical period. The study findings also revealed that the bias correction methods had a higher degree of uncertainty in precipitation compared to temperature values in RCMs, as shown by RMSE statistics in Table 5-7. This could be due to using the remote sensing (APHRODITE) data for bias correction of RCMs instead of observed data. Our results are consistent with previous studies Lutz et al., (2014) which has reported significant variations in precipitation and low variations in temperature values between RCMs in five larger river basins in Asia. Additionally, there results indicated that the Kabul river basin has a higher degree of uncertainty than other river basins in Asia (Lutz *et al.*, 2014).

According to the data presented in Table 5-7, under the RCP4.5 scenario, the annual temperature is expected to increase by 1.9 °C in the 2040s and 2.3 °C in the 2090s. However, under the RCP8.5 scenario, the increase in mean annual temperature is projected to be more severe with an increase of 3.2 °C in the 2040s and 6.1 °C in the 2090s. These projections suggest a significant warming trend in the UKRB which could have worse implications for the region's seasonal water resources including the surface runoff and ground water flow contributions (*Figure 5-32*). The several key climate indicators and trends with a focus on total annual precipitation, extreme precipitation, temperature extremes, and the frequency of warm nights and

warm days are also discussed in this study. The analysis reveals an insignificant decrease in annual total wet day precipitation trend and there is no significant change in the future extreme precipitations and remains relatively stable over the analyzed period. The minimum and maximum temperature extremes indicate a highly statistically significant increase under both RCP4.5 and RCP8.5. This implies that the climate is getting hotter in the UKRB, with more extreme temperatures in the future (Figure 5-29). The results suggest that the impacts of climate change on temperature extremes are likely to be more significant than those on precipitation, at least in the region and period covered by the study. The number of warm nights and warm days is also projected to increase significantly in the future and is expected to be most pronounced after 2050 and toward the end of the century. The analysis reveals that while annual precipitation trend may see a slight decrease in the mountainous north part of the basin, the climate is experiencing significant warming trends with more extreme temperatures, and an increase in the number of warm nights and warm days trend. These findings are indicative of the ongoing impact of climate change on weather patterns and temperature extremes.

Previous studies in Hindu Kush Himalaya region including the KRB suggested an increase in precipitation and temperature which are expected to lead to more snow melt and glacier melt in the region (Iqbal *et al.*, 2018). So, our findings are also in line with some prior researches conducted in the KRB (Wi *et al.*, 2015; Sidiqi, Shrestha and Ninsawat, 2018). The rise in air temperature projected in the UKRB will lead to increase in actual and potential evapotranspiration, increased runoff in a shorter period, droughts mainly in the summer season resulting to a greater water stress in the study area, particularly in the lower parts of the basin including the Kabul city. Also, the interannual shifts of temperature will affect the precipitation pattern and snowmelt in UKRB. Also, the increasing extreme temperature will intensify the droughts in the summer months which will accelerate the water stress process in the study area.

6.1.2 Discussion on current hydrology (2010-2019)

Hydrological modeling performance refers to how accurately a model predicts the behavior of the system being studied compared to actual observations. The performance of SWAT hydrological model is done by comparing the simulated results to the real-world discharge observations in the Upper Kabul River Basin (UKRB). The model was built, calibrated and validated on daily and monthly time intervals to provide a comprehensive analysis of the model's

accuracy. This type of evaluation is essential in ensuring that models are reliable tools for predicting the behavior of natural systems and can be used to make informed decisions. The statistical Nash-Sutcliffe (NS) efficiency performance of runoff was generally satisfactory to very good agreement between the simulated and observed discharge over the UKRB during calibration and validation. However, we noticed that there was uncertainty in the model's ability to simulate flow peaks, with underestimations occurring in some years at the calibrated stations (Figure 5-1). The simulated baseflow was in a reasonable fit in all calibrated stations except for the Pul-i-Ashawa station on Ghurband river, where there was higher baseflow in August and September compared to the observations. According to previous studies, underestimation occurs in hydrological modeling due to observation errors, biases in precipitation inputs, and hydrological modeling uncertainties (D. N. Moriasi *et al.*, 2007).

The monthly results showed that the model performance was good to very good in most of the stations, with monthly NS values ranging from 66% to 91% of correlations between simulations and observation flow. However, the Sang-i-Nawishta station had a lower NS value of 54% indicating that the model's performance was only satisfactory in that station. The possible reasons behind the lower values of NS in Sang-i-Nawishta station between observed and simulated runoff could be due to errors in the input precipitation or observed discharge data used in the model. The Shukhi station in Panjshir river had the highest annual peak flows in June 2015 and 2016 (Figure 5-4). This information provides an indication of the variability of the water flow in the region and can be used to validate the results of the hydrological model used in the study. The statistical results of SWAT showed small differences, indicating that the model is adequate for simulating the hydrology and runoff. The text concludes that the SWAT model has demonstrated its quality and potential as a numerical tool for water resources management in this study. By inserting an input of 406 mm average precipitation, the model simulation showed the output as 148 mm total water yield that accounts for 39 % of the basin water balance. While due to larger potential evapotranspiration of 1,790 mm, the average ET was estimated greater than the total water yields as 246.6 mm or 61 % of the total hydrological parameters that goes back to atmosphere rather than contributing to the water yield. The surface runoff accounts for 24 % and the total aquifer recharge accounts 15.1 % of the annual hydrological cycle in UKRB, figure 5-7.

The study showed that between 2010 and 2019, the evapotranspiration is the major water loses component in the study area. In this study, the ET and ground water were not validated during

the hydrological model processing due to lacking access to observed data. This means that the accuracy of the model's representation of these processes is uncertain, as there was no comparison between the model's prediction and actual measurements or observations for these two variables in UKRB. Thus, it seems reasonable to assume that these two critical components were well simulated but obviously consists some minor uncertainty. Despite this, "very favorable" runoff results were achieved at multiple locations by SWAT model.

The Upper Kabul River Basin (UKRB) is characterized by a significant variation in altitude, with elevations ranging from 995 meters above sea level (msl) at its lowest point to 5,694 meters msl in the glaciated and snow-covered northern areas. This vast difference in altitude, along with the alpine topography, plays a critical role in shaping the hydrological dynamics of the basin. The altitude may impact the hydrology and climate in the UKRB by the orographic and climatic influences, glacier and snowmelt contribution. The steep topography, with sharp peaks and deep valleys in the UKRB, creates a pronounced orographic effect, where moist air masses are forced upward over mountains, cooling and condensing to form precipitation (Minder, 2010). This leads to substantial differences in weather patterns between the higher-altitude northern regions and the lower-altitude southern regions. The climatic contrasts in deferent altitudes significantly influence the timing and distribution of water resources throughout. The northern regions, with peaks covered by permanent snow and glaciers are also crucial for sustaining streamflow in the UKRB. Glaciers act as natural reservoirs, storing water during winter and releasing it as meltwater during the warmer summer months. This meltwater is essential in maintaining the river's flow during dry periods, stabilizing water supplies, and supporting agriculture and ecosystems in downstream regions. The presence of glaciers at such high altitudes ensures a steady streamflow, even during periods of reduced rainfall. The role of elevation in water flow dynamics are very significant in the basin (Barnett, Adam and Lettenmaier, 2005). The steep slopes increase the velocity of water runoff, contributing to faster-moving streams that converge in the lower, flatter parts of the basin. This transition from steep, mountainous terrain to gentler foothills and plains influences both the quantity of water available downstream. In contrast, the southern, lower-altitude areas, while still contributing to water flow, rely more heavily on rainfall and lack the buffering effect provided by glaciers and snowpack.

6.1.3 Discussion on future water availability under climate change

This section discusses the impact of climate change on the future runoff estimation and other hydrological parameters in UKRB. The study compared the baseline period (1986-2005) with that of the future periods of 2040s and 2090s under RCP4.5 and RCP8.5 scenarios.

The future runoff shows that, seasonally a decrease in summer discharge is shown, while increasing discharge peak occurred during winter and spring seasons due to temperature increase (Figure 5-30). The results also revealed a backward shift in the monthly runoff peaks from May and June to March and April in Tang-i-Gulbahar and Shukhi stations, while in Tang-i-Saidan station, the runoff peak will shift from April to March in both periods of 2040s and 2090s. These shifts in the timing of runoff can have significant impacts on the availability of water resources for various related sectors such as agriculture, industry, and domestic use, which may further exacerbate water stress in the region. For instance, the shifts suggest that the snowmelt will occur earlier in the year, resulting in a rapid increase and a larger runoff for a shorter period, which may lead to more floods in the spring and droughts in the summer months. Our research highlights the seasonal shifts in runoff which is consistent with findings from (Mohammad Tayib Bromand, 2015). This study similarly reports that rising temperatures will lead to earlier snowmelt, shifting runoff peaks to earlier months and resulting in reduced summer flow. Also, the backward shift in runoff peaks observed in our study, resonates with findings from (Iqbal et al., 2018). This earlier snowmelt, coupled with increased winter and spring runoff, could exacerbate spring flooding, while the reduced summer flows could lead to droughts later in the year. Consiquently, the study highlights the climate change increases the risk of more frequent and intense floods during the wet season and potential droughts during the dry season. Additionally, (Baig and Hasson, 2023) suggests that these altered streamflow patterns could increase flood inundation risks, especially in low-lying areas during the peak snowmelt seasons. Our findings align with this, indicating that more rapid snowmelt during spring could result in flash floods, further complicating water resource management in the basin.

Our study suggests that the annual total water yield in the UKRB is expected to increase in the 2040s and 2090s of RCP4.5 due to precipitation increase, while it shows a decline in the 2040s and increase in the 2090s under higher emission scenario (RCP8.5). Our study also showed that under the RCP8.5, the changes in hydrological parameters tend to be more extreme. In particular, the monthly runoff shows a further decrease during summer months compared to the RCP4.5

scenario, indicating that the effects of climate change are expected to be more sever in the future if we continue with the high greenhouse gas emissions. Additionally, our study suggests that the annual total water yiled is expected to increase in the future under both RCP4.5 and RCP8.5 scenarios, but with variations across seasons. This aligns with study of (Hashmi et al., 2020) wich similarily predicts an increase in overall annual runoff. The increment of annual surface runoff is due increased in the annual precipitation, and there are other factors that may offset this increase, for instance, decreased in percolation and groundwater. Other factors such as changes in land use, soil moisture, and temperature could also potentially impact the hydrological cycle and contribute to changes in streamflow patterns. However, while annual runoff may increase, it is not uniformly distributed, with potential decreases during critical dry periods. This suggests that even though total runoff increases, water availability during summer months may still be constrained, leading to seasonal water stress.

Morover, our research shows a projected decrease in snowmelt, snowpack sublimation, and percolation in both future scenarios, which would impact both surface and groundwater resources. This finding is supported by (Azizi and Asaoka, 2020) which also highlights the importance of snowmelts in regulating river flows and ground water recharge in the KRB. The reduction in snowmelt will decrease groundwater recharge and further exacerbate water scarcity during the summer months in the UKRB, when water demand is highest. Moreover, there will be a decrease in future annual percolation and groundwater recharge, which could further reduce the water availability in the summer season. Similarly, (Sidiqi, Shrestha and Ninsawat, 2018) predicted the reduced percolation which could offset the benefits of increased precipitation, reducing groundwater availability and negatively impacting water supplies in the summer season in the KRB.

Our research also notes a significant increase in actual and potential evapotranspiration (ET and PET) under both RCP4.5 and RCP8.5 scenarios, particularly under RCP8.5 in the 2090s. This is consistent with (Akhtar *et al.*, 2022), which also identifies rising ET as a major factor influencing water availability in the KRB. The increased evapotranspiration reduces the amount of water available for surface runoff and groundwater recharge, compounding the challenges posed by climate change in the study area. The rising ET rates suggest that even with increased precipitation, less water will remain available for human use, exacerbating water shortages. . Increasing in the rate of ET meaning that more water is being lost from the land surface, resulting

in a decrease in the amount of water available for surface runoff, groundwater recharge, and other hydrological processes. This is an important finding as ET plays a crucial role in the water cycle, and the increase in the ET can have significant impacts on the hydrological balance of the region. This information is important in understanding the impacts of climate change on the hydrological cycle in the region and can aid in developing effective water management strategies. Also, Our research findings are align with previous hydrology studies referenced as (Giang et al., 2014; Lutz et al., 2014).

Additionally, the large elevation variation within the UKRB ranging from 995 msl to 5,694 msl defines the basin's hydrological processes. The glaciated peaks in the north of the basin play a crucial role in water storage and release, while the lowland areas depend on this meltwater for a stable water supply. Understanding these dynamics is essential for effective water management, especially in the face of changing climatic conditions. The higher-elevation areas, which experience prolonged snow and glacier melt are crucial for ensuring water availability during the summer months when precipitation is low (Huss and Hock, 2018). However, climate change poses a risk to these glaciated regions, with rising temperatures threatening to reduce snowmelt and accelerate glacial retreat (Huss and Hock, 2018). This could lead to diminished water supplies in the future, particularly for lower-elevation areas that depend on this seasonal meltwater. Therefore, the stark altitude difference within the UKRB necessitates careful water resource management in the basin. As a conclution of the discussion, our research findings align closely with previous studies on the impacts of climate change on surface runoff and the water availability in the Kabul River Basin. The common threads across all studies include the shifts in runoff timing, the increased risk of floods and droughts, and the complex interplay between rising precipitation and temperature, reduced snowmelt, and increased evapotranspiration. Together, these studies underscore the urgent need for integrated water resource management strategies in the Kabul River Basin to address the challenges posed by changing hydrological patterns, particularly in the face of high greenhouse gas emissions and future climate scenarios.

6.1.4 Limitation of the study

Throughout the research study, several limitations were encountered, such as the issue of spatial variability in weather data for building the current hydrological model.In developing countries such as Afghanistan, obtaining realistic time series observed data is difficult due to limited resources. Only a few stations which managed by the government, provide the data

making it difficult to obtain long-term historical daily data, including precipitation, temperature, wind, solar radiation, and humidity which are essential for achieving accurate hydrological results. Another major limitation is the unavailability of dependable historical daily weather data that could be considered representative for all elevations within the basin. The Ministry of Energy and Water (MEW) in Afghanistan started collecting and analyzing water level data at a few hydrology stations in the Helmand River Basin in 1946 (MEW and JICA, 2019). By 1976, 153 hydrological stations had been installed and operated until 1980 with data collected, analyzed, stored and published in annual water-year books. However, after the civil war, these services stopped until 2000 (MEW and JICA, 2019). When the new government developed, MEW installed 29 hydro-meteorological stations across the Kabul river basin from 2004 (Ayoubi, 2017). However, most of these stations were not unable to record data due to technical difficulties and insecurity, resulting in missing values for months or even years. Furthermore, the majority of the stations installed in the plain areas cannot provide a representative picture of the hydro-meteorological conditions in the high elevations of the mountainous areas. This is due to the large variation in elevation between the upstream and downstream areas of the basin.

To compensate for missing data, particularly for precipitation and temperature, two methods were employed in this study. The first method used was the Inverse Distance Weighting (IWD) interpolation technique in GIS, which utilized the elevation and distance of each station to calculate average values from nearby stations. The second method involved calculating the average daily values from previous years for stations where surrounding stations also had missing data for the same time period. Another limitation of the study is the lack of future landcover change which can have a significant impact on hydrological processes in the future. Landcover change can impact soil properties, vegetation cover, and surface runoff which in turn can impact the water availability. However, due to the unavailability of data on future landcover change, this study did not consider its impact on the hydrological model. Furthermore, the study did not consider the impact of potential future changes in population and water demand on water resources. As the population in the KRB is expected to increase in the future, it is important to consider the impact of this on water resource and to plan for future water demand in future studies. Finally, the study only considered two greenhouse gas emission scenarios (RCP4.5 and RCP8.5), and did not consider other potential future scenarios. It is important to consider a range of scenarios in order to fully understand the potential impacts of climate change on water resources.

6.2 CONCLUSIONS

The research investigated the impact of climate change on surface runoff and water resources availability in Upper Kabul River Basin (UKRB) by comparing the baseline period with two future period under RCP4.5 and RCP8.5 scenarios using the SWAT. The study presented the capability of SWAT model for simulation of surface runoff by performing calibration and validation of the model. Three statistical methods were used for correcting bias in climate model outputs namely linear scaling, delta change and empirical quantile mapping. By applying bias correction techniques to RCM's output, the accuracy of the historical and future precipitation and temperature data was improved and the discrepancies between the RCM's data and APHRODITE data (e.g., precipitation and temperature) were significantly reduced, leading to a better understanding of the future changes in climate and hydrology in UKRB. The linear scaling method performed better in terms of reducing uncertainty and matching the projected and APHRODITE data in this study, and its results were used in hydrological analysis. The study focused on how changes in surface runoff, evapotranspiration (ET), and groundwater occurs on monthly and annual basis. The study predicts a significant increase in mean annual temperature in 2040s and 2090s based on the RCP4.5 and RCP8.5 scenarios in UKRB. The increase in temperature is likely expected to be higher under RCP8.5 than RCP4.5.

Moreover, the projections show a backward shift in temperatures peak, and the temperature peaks in June instead of July. The study predicts an increase in mean annual temperature by +1.9 °C in 2040s, and +3 °C in 2090s based on RCP4.5 compared to the baseline. Similarly, the projected annual temperature increase is expected to be +2.4 °C in 2040, and almost +6 °C in 2090s based on RCP8.5 scenario compared to the baseline. There is a 95 % confidence that a significant increase in the trend of future temperature projection during 21st century (2006-2100) in the upper Kabul river basin exist. The study found that under RCP4.5, there will be an increase in mean annual precipitation of about +5% (21mm) in 2040s, and an increase of about +1% (3.2 mm) in 2090s. Moreover, under RCP8.5, the mean annual precipitation is expected to increase by +9 % (37mm) in 2040s and about +2 % (10mm) in 2090s compared to the baseline. Unlike the annual precipitation, the trend of future annual precipitation for the period of 2006-2100 shows an insignificant decrease with P-value= 0.35, and P-value=0.63 (based on Mann-Kendall trend test) under RCP4.5 and RCP8.5, respectively in UKRB.

The SWAT model was built, calibrated, and validated using real-world discharge observations, and the Nash-Sutcliffe efficiency was used to evaluate the performance of the model. The

predicted results from the SWAT model between the 2010 to 2018 showed a good agreement between the simulated and observed runoff across the UKRB during calibration and validation. There were some uncertainties in simulating flow peaks, as well as some discrepancies in the baseflows of some stations. The good performance of the SWAT hydrological model in a mountainous area like UKRB highlights its potential for accurately assessing the water resource, and the impact of climate change on water resources in other river basins in Afghanistan. Overall, the results demonstrate the potential of the SWAT model as a reliable tool for water resources estimation and management. However, some uncertainty remains regarding the accuracy of the model's representation of groundwater due to a lack of observed data. The study showed that evapotranspiration is the major water loss of the water balance component in the study area during the period of 2010-2019.

The future hydrological results show that there will be an increase in mean annual runoff in 2040s and 2090s compared to the baseline period in UKRB. This increase is due to increase in annual precipitation; however, the study predicts a decrease in annual snowfall, snowmelt, sublimation from snow surface, percolation, and the groundwater recharge. The decrease in snowmelt and glacier melt could also lead to changes in the timing and volumes of river flow which can impact the seasonal water availability for agriculture, urban water consumption, and hydropower generation. The monthly runoff peaks also revealed a backward shift to March and April instead of May and June in Tang-i-Gulbahar and Shukhi stations, while in Tang-i-Saidan station the runoff peak shifted from April to March in both periods of 2040s and 2090s in UKRB. However, the shifts in the timing of runoff will lead to significant impacts on water availability for various sectors, exacerbating water stress in the region. Seasonally, the UKRB will experience a decrease in summer runoff, but an increase in winter and spring runoff peaks due to climate change. Also, the runoff seasonal variations in the future will increase the gaps between water availability and demand, particularly during the dry season.

As a conclusion drawn from the findings of this study, climate change is expected to have significant impacts on future water availability in the UKRB. Increase in temperature is likely to lead to changes in precipitation patterns which could result in more frequent floods (high peaks in runoff) in the winter and spring, and droughts in the summer. The projected decrease in water availability during the dry season could lead to negative consequences on agriculture, livestock, and food security in the future in UKRB, if it’s not managed. This imbalance in the seasonal availability of water resources can have significant implications for the management of water

resources, including the need for appropriate infrastructures (e.g., check dams, ponds and reservoirs), careful management and planning strategies, and effective water conservation practices to ensure sustainable water use, and to address the climate change risk. The findings also highlight the need and importance of implementing effective climate adaptation and mitigation strategies to help mitigate the impact of climate change on water resources in the study area. Overall, these findings can aid the policymakers and researchers who are working in climate change implication studies and water resources management in the region. Additionally, this study contributes to the growing body of knowledge on climate change impacts on water resources and emphasizes the need for continued research in this field.

6.3 RECOMMENDATIONS

The findings indicated that climate change is likely to impact a range of sections as critical variables such as precipitation (both in quantity and intensity), temperature, surface runoff, ground water recharge, evapotranspiration, snowfall and snowmelt. In particular, the projected changes in surface runoff showed a high and low flow conditions in the river network of UKRB, which can challenge the water resources management. The application of SWAT hydrological modeling approach in this study provides valuable insights into historical and future climate projections impact on water resources in Kabul river basin and water sustainability. In light of the findings, the study underscores the urgent need for effective water resource management strategies and climate change adaptation plans/polices, mitigate the consequences of climate changes on water resources, ecosystems and the local communities, and to increase the resilience under climate change in the KRB. Key measures or strategies to consider includes:

1. Nature based solutions are recommended for both climate changes mitigation and adaptation.
    - Controlling the land degradation by limiting and monitoring the human activities, for instance deforestation, and increase the reforestation to reduce the surface runoff and flooding, increase the groundwater recharge, and mitigate the soil erosions.
    - Initiate and increase the grassland restoration activities in the heavily degraded grasslands.
    - Maintain intact ecosystem such as the existing wetlands for water storage, ground water recharge, and retain carbon stocks, and prevent the land grabbing by local communities around to prevent the land use change. The good example of this can be the Kol-i-Hashmat Khan wetland located in the Kabul city.

2. Institutional and public strengthening regarding water consumption and climate change adaptation:
    - Initiate and conduct the public awareness programs among local communities at schools and mosques regarding water conservation and climate change impacts. Engaging the local communities in water management decisions can foster more sustainable water management. For example, emphasize the role of individuals in reducing water waste and encourage responsible water use habits.
    - Enhancing institutional capacities for water management & conservation practices, and climate change adaptation is crucial.
    - Coordination among the government agencies involved in water and agriculture sectors, stakeholders, and communities to develop integrated water management approaches. This can lead to more effective water resources management and conservation efforts.

3. Long-term monitoring and forecasting systems

Strengthening the basin's monitoring infrastructure to better predict hydrological changes and implement timely responses.

- Deploy and increase the hydro-met stations at different elevations in KRB to record and monitor the local climate change such as; precipitation, temperature, solar radiations, humidity, wind speed, discharges etc.
- Establish a glacier monitoring system to regularly assess and monitor the water availability in KRB.
- Establish/or develop the early warning systems for droughts and floods can minimize their impacts in the future.

4. Establish and Enhance the Water Storage Conservations
    - Developing additional water storage facilities, such as rain harvesting systems (check dams and ponds), reservoirs to buffer against the variability in water availability.
    - Promote sustainable agricultural practices to maximize water-use efficiency during dry seasons in Kabul river basin. developing more efficient irrigation methods, like drip or sprinkler irrigation systems, which can reduce water loses and improve crop yields.

5. Climate Resilient Agriculture

- Encouraging the adoption of drought-resistant crop varieties, and farming practices (crop rotation) that are less water-intensive. This will help water savings, mitigate the impact of water scarcity on food security in the future in KRB.

6. Policy Strengthening;
    - Formulate policies and procedures at regional scale that promote sustainable water use and protect critical water resources. These plans should include strategies for water allocation, drought management, flood control, and groundwater recharge. The climate changes projections should also integrate to ensure resilience of changing conditions in the future.

By implementing these strategies, it is possible that KRB can ensure the long-term sustainability of its water resources and enhance its resilience to the impacts of climate change. These insights, with the international significance of the Kabul River basin, contribute to the global understanding of hydrological processes and are of interest to a broad international audience.

7 REFERENCES

1. Aawar, T. and Khare, D. (2020) 'Assessment of climate change impacts on streamflow through hydrological model using SWAT model: a case study of Afghanistan', *Modeling Earth Systems and Environment*, 6(3), pp. 1427–1437. Available at: https://doi.org/10.1007/s40808-020-00759-0.
2. Abbaspour, K.C. (2015) *SWAT-Calibration and Uncertainty Programs (CUP)—A User Manual.*
3. Abbaspour, K.C., Johnson, C.A. and van Genuchten, M.T. (2004) 'Estimating Uncertain Flow and Transport Parameters Using a Sequential Uncertainty Fitting Procedure', *Vadose Zone Journal*, 3(4), pp. 1340–1352. Available at: https://doi.org/10.2136/vzj2004.1340.
4. Abbaspour, K.C., Rouholahnejad, E., Vaghefi, S., Srinivasan, R., Yang, H. and Kløve, B. (2015) 'A continental-scale hydrology and water quality model for Europe: Calibration and uncertainty of a high-resolution large-scale SWAT model', *Journal of Hydrology*, 524, pp. 733–752. Available at: https://doi.org/10.1016/j.jhydrol.2015.03.027.
5. Adib, M.N.M., Rowshon, M.K., Mojid, M.A. and Habibu, I. (2020) 'Projected Streamflow in the Kurau River Basin of Western Malaysia under Future Climate Scenarios', *Scientific Reports*, 10(1). Available at: https://doi.org/10.1038/s41598-020-65114-w.

6. Ahmad, I., Tang, D., Wang, T., Wang, M. and Wagan, B. (2015) 'Precipitation trends over time using Mann-Kendall and spearman's Rho tests in swat river basin, Pakistan', *Advances in Meteorology*, 2015. Available at: https://doi.org/10.1155/2015/431860.
7. Ahmad, M. and Wasiq, M. (2004) *Water resource development in Northern Afghanistan and its implications for Amu Darya basin, World Bank Working Paper*.
8. Aich, V., Akhundzadah, N., Knuerr, A., Khoshbeen, A., Hattermann, F., Paeth, H., Scanlon, A. and Paton, E. (2017) 'Climate Change in Afghanistan Deduced from Reanalysis and Coordinated Regional Climate Downscaling Experiment (CORDEX)—South Asia Simulations', *Climate*, 5(2), p. 38. Available at: https://doi.org/10.3390/cli5020038.
9. Aich, V., Akhundzadah, N.A., Knuerr, A., Khoshbeen, A.J., Hattermann, F., Paeth, H., Scanlon, A. and Paton, E.N. (2017a) 'Climate change in Afghanistan deduced from reanalysis and coordinated regional climate downscaling experiment (CORDEX)-South Asia simulations', *Climate*, 5(2). Available at: https://doi.org/10.3390/cli5020038.
10. Aich, V., Akhundzadah, N.A., Knuerr, A., Khoshbeen, A.J., Hattermann, F., Paeth, H., Scanlon, A. and Paton, E.N. (2017b) 'Climate Change in Afghanistan Deduced from Reanalysis and Coordinated Regional Climate Downscaling Experiment (CORDEX)—South Asia Simulations', *Climate 2017, Vol. 5, Page 38*, 5(2), p. 38. Available at: https://doi.org/10.3390/CLI5020038.
11. Aich, V. and Khoshbeen, A.J. (2016) *Afghanistan: Climate Change Science Perspectives. Kabul: National Environmental Protection Agency & UN Environment.*
12. Akhtar, F. (2017) *Water availability and demand analysis in the Kabul River Basin , Afghanistan (Ph.D Thesis).* Rheinischen Friedrich-Wilhelms-Universität Bonn.
13. Akhtar, F., Awan, U.K., Borgemeister, C. and Tischbein, B. (2021) 'Coupling remote sensing and hydrological model for evaluating the impacts of climate change on streamflow in data-scarce environment', *Sustainability (Switzerland)*, 13(24). Available at: https://doi.org/10.3390/su132414025.
14. Akhtar, F., Awan, U.K., Tischbein, B. and Liaqat, U.W. (2018) 'Assessment of irrigation performance in large river basins under data scarce environment-A case of Kabul River basin, Afghanistan', *Remote Sensing*, 10(6). Available at: https://doi.org/10.3390/rs10060972.
15. Akhtar, F., Borgemeister, C., Tischbein, B. and Awan, U.K. (2022) 'Metrics Assessment and Streamflow Modeling under Changing Climate in a Data-Scarce Heterogeneous Region: A Case Study of the Kabul River Basin', *Water (Switzerland)*, 14(11). Available at:

https://doi.org/10.3390/w14111697.

16. Arian, H., Kayastha, R.B., Bhattarai, B.C., Shresta, A., Rasouli, H. and Armstrong, R. (2016) 'Application of the Snowmelt Runoff Model in the Salang River Basin, Afghanistan Using MODIS Satellite Data', *Journal of Hydrology and Meteorology*, 9(1), pp. 109–118. Available at: https://doi.org/10.3126/jhm.v9i1.15586.
17. Arnold, J.G., Allen, P.M. and Bernhardt, G. (1993) 'A comprehensive surface-groundwater flow model', *Journal of Hydrology*, 142(1–4), pp. 47–69. Available at: https://doi.org/10.1016/0022-1694(93)90004-S.
18. Arnold, J.G., Kiniry, J.R., Srinivasan, R., Williams, J.R., Haney, E.B. and Neitsch, S.L. (2012) *Soil & Water Assessment Tool: Input/Output Documentation*.
19. Arnold, J.G., Srinivasan, R., Muttiah, R.S. and Williams, J.R. (1998) 'LARGE AREA HYDROLOGIC MODELING AND ASSESSMENT PART I: MODEL DEVELOPMENT 1', *JAWRA Journal of the American Water Resources Association*, 34(1), pp. 73–89. Available at: https://doi.org/10.1111/j.1752-1688.1998.tb05961.x.
20. Ayoubi, T. (2017) *Simulation of Surface Runoff Using SWAT Model and GIS : A Case Study of Panjshir Watershed (M.Sc. Thesis)*. University of the Ryukyus.
21. Ayoubi, T. and Dongshik, K. (2016) 'Panjshir Watershed Hydrologic Model Using Integrated GIS and ARCSWAT Interface', *International Journal of Geology, Earth and Environmental Sciences*, 6(1), pp. 145–161. Available at: https://www.cibtech.org/J-GEOLOGY-EARTH-ENVIRONMENT/PUBLICATIONS/2016/VOL_6_NO_1/JGEE-06-01-Contents.htm.
22. Azizi, A.H. and Asaoka, Y. (2020) 'Assessment of the impact of climate change on snow distribution and river flows in a snow-dominated mountainous watershed in the western hindukush–himalaya, afghanistan', *Hydrology*, 7(4), pp. 1–24. Available at: https://doi.org/10.3390/hydrology7040074.
23. Baig, S. and Hasson, S. ul (2023) 'Flood Inundation and Streamflow Changes in the Kabul River Basin under Climate Change', *Sustainability*, 16(1), p. 116. Available at: https://doi.org/10.3390/su16010116.
24. Barnett, T.P., Adam, J.C. and Lettenmaier, D.P. (2005) 'Potential impacts of a warming climate on water availability in snow-dominated regions', *Nature*, 438(7066), pp. 303–309. Available at: https://doi.org/10.1038/nature04141.
25. Bjelica, J. (2021) *Shrinking, Thinning, Retreating: Afghan glaciers under threat from climate change, Afghanistan Analysts Network*. Available at: https://www.afghanistan-analysts.org.

26. Bokhari, S.A.A., Ahmad, B., Ali, J., Ahmad, S., Mushtaq, H. and Rasul, G. (2018) 'Future Climate Change Projections of the Kabul River Basin Using a Multi-model Ensemble of High-Resolution Statistically Downscaled Data', *Earth Systems and Environment*, 2(3), pp. 477–497. Available at: https://doi.org/10.1007/s41748-018-0061-y.
27. Brati, M.Q., Ishihara, M.I. and Higashi, O. (2019) 'Groundwater level reduction and pollution in relation to household water management in Kabul, Afghanistan', *Sustainable Water Resources Management*, 5(3), pp. 1315–1325. Available at: https://doi.org/10.1007/s40899-019-00312-7.
28. Calvin, K., Dasgupta, D., Krinner, G., Mukherji, A., Thorne, P.W., Trisos, C., Romero, J., Aldunce, P., Barrett, K., Blanco, G., Cheung, W.W.L., Connors, S., Denton, F., Diongue-Niang, A., Dodman, D., Garschagen, M., Geden, O., Hayward, B., Jones, C., Jotzo, F., Krug, T., Lasco, R., Lee, Y.-Y., Masson-Delmotte, V., Meinshausen, M., Mintenbeck, K., Mokssit, A., Otto, F.E.L., Pathak, M., Pirani, A., Poloczanska, E., Pörtner, H.-O., Revi, A., Roberts, D.C., Roy, J., Ruane, A.C., Skea, J., Shukla, P.R., Slade, R., Slangen, A., Sokona, Y., Sörensson, A.A., Tignor, M., van Vuuren, D., Wei, Y.-M., Winkler, H., Zhai, P., Zommers, Z., Hourcade, J.-C., Johnson, F.X., Pachauri, S., Simpson, N.P., Singh, C., Thomas, A., Totin, E., Alegría, A., Armour, K., Bednar-Friedl, B., Blok, K., Cissé, G., Dentener, F., Eriksen, S., Fischer, E., Garner, G., Guivarch, C., Haasnoot, M., Hansen, G., Hauser, M., Hawkins, E., Hermans, T., Kopp, R., Leprince-Ringuet, N., Lewis, J., Ley, D., Ludden, C., Niamir, L., Nicholls, Z., Some, S., Szopa, S., Trewin, B., van der Wijst, K.-I., Winter, G., Witting, M., Birt, A. and Ha, M. (2023) *IPCC, 2023: Climate Change 2023: Synthesis Report. Contribution of Working Groups I, II and III to the Sixth Assessment Report of the Intergovernmental Panel on Climate Change [Core Writing Team, H. Lee and J. Romero (eds.)]. IPCC, Geneva, Switzerland.* Edited by P. Arias, M. Bustamante, I. Elgizouli, G. Flato, M. Howden, C. Méndez-Vallejo, J.J. Pereira, R. Pichs-Madruga, S.K. Rose, Y. Saheb, R. Sánchez Rodríguez, D. Ürge-Vorsatz, C. Xiao, N. Yassaa, J. Romero, J. Kim, E.F. Haites, Y. Jung, R. Stavins, A. Birt, M. Ha, D.J.A. Orendain, L. Ignon, S. Park, Y. Park, A. Reisinger, D. Cammaramo, A. Fischlin, J.S. Fuglestvedt, G. Hansen, C. Ludden, V. Masson-Delmotte, J.B.R. Matthews, K. Mintenbeck, A. Pirani, E. Poloczanska, N. Leprince-Ringuet, and C. Péan. Available at: https://doi.org/10.59327/IPCC/AR6-9789291691647.
29. Cao, W., Zhang, Z., Liu, Y., Band, L.E., Wang, S. and Xu, H. (2021) 'Seasonal differences in future climate and streamflow variation in a watershed of Northern China', *Journal of*

Hydrology: Regional Studies, 38, p. 100959. Available at: https://doi.org/10.1016/j.ejrh.2021.100959.

30. Chaubey, I., Cotter, A.S., Costello, T.A. and Soerens, T.S. (2005) 'Effect of DEM data resolution on SWAT output uncertainty', *Hydrological Processes*, 19(3), pp. 621–628. Available at: https://doi.org/10.1002/hyp.5607.
31. CMIP5-DKRZ (2021) *CMIP5-DKRZ Data Search | CMIP5-DKRZ | ESGF-CoG, https://cordex.org*. Available at: https://esgf-data.dkrz.de/search/cmip5-dkrz/ (Accessed: 10 April 2021).
32. D. N. Moriasi, J. G. Arnold, M. W. Van Liew, R. L. Bingner, R. D. Harmel and T. L. Veith (2007) 'Model Evaluation Guidelines for Systematic Quantification of Accuracy in Watershed Simulations', *American Society of Agricultural and Biological Engineers, St. Joseph, Michigan www.asabe.org*, 50(3), pp. 885–900. Available at: https://doi.org/10.13031/2013.23153.
33. Dutta, D. and Bhattacharjya, R.K. (2022) 'A statistical bias correction technique for global climate model predicted near-surface temperature in India using the generalized regression neural network', *Journal of Water and Climate Change*, 13(2), pp. 854–871. Available at: https://doi.org/10.2166/WCC.2022.214.
34. Enayati, M., Bozorg-Haddad, O., Bazrafshan, J., Hejabi, S. and Chu, X. (2021) 'Bias correction capabilities of quantile mapping methods for rainfall and temperature variables', *Journal of Water and Climate Change*, 12(2), pp. 401–419. Available at: https://doi.org/10.2166/WCC.2020.261.
35. Eqrar, N. and Shroder, J. (2016) *Development of Water Resources in the Kabul River Basin, Transboundary Water Resources in Afghanistan: Climate Change and Land-Use Implications*. Elsevier Inc. Available at: https://doi.org/10.1016/B978-0-12-801886-6.00004-5.
36. FAO (1971) *Soil Map of the World (FAO/UNESCO), Food and Agriculture Organization of the United Nations*. Available at: https://www.fao.org/soils-portal/soil-survey/soil-maps-and-databases/faounesco-soil-map-of-the-world/en/ (Accessed: 2 May 2020).
37. FAO (2010) *Landcover Atlas of the Islamic Rebulic of Afghanistan: Food and Agriculture Organization of the United Nations and Ministry of Agriculture, Irrigation and Livestock, FAO/MAIL*.
38. Favre, R. and Kamal, G.M. (2004) *Watershed atlas of Afghanistan: FIRST EDITION - WORKING DOCUMENT FOR PLANNERS., Ministry of Irrigation, Water Resources and*

Environment and the Food and Agriculture Organization of the United Nations (FAO) in Afganistan.

39. Ficklin, D.L., Luo, Y., Luedeling, E. and Zhang, M. (2009) 'Climate change sensitivity assessment of a highly agricultural watershed using SWAT', *Journal of Hydrology*, 374(1–2), pp. 16–29. Available at: https://doi.org/10.1016/j.jhydrol.2009.05.016.
40. Forero-Ortiz, E., Martínez-Gomariz, E. and Monjo, R. (2020) 'Climate Change Implications for Water Availability: A Case Study of Barcelona City', *Sustainability*, 12(5), p. 1779. Available at: https://doi.org/10.3390/su12051779.
41. Fuka, D.R., Walter, M.T., MacAlister, C., Degaetano, A.T., Steenhuis, T.S. and Easton, Z.M. (2014) 'Using the Climate Forecast System Reanalysis as weather input data for watershed models', *Hydrological Processes*, 28(22), pp. 5613–5623. Available at: https://doi.org/10.1002/hyp.10073.
42. Gassman, P.W., Reyes, M.R., Green, C.H. and Arnold, J.G. (2007) 'The Soil and Water Assessment Tool: Historical Development, Applications, and Future Research Directions', *Transactions of the ASABE*, 50(4), pp. 1211–1250. Available at: https://doi.org/10.13031/2013.23637.
43. Ghulami, M., Babel, M.S. and Shrestha, M.S. (2017) 'Evaluation of gridded precipitation datasets for the Kabul Basin, Afghanistan', *International Journal of Remote Sensing*, 38(11), pp. 3317–3332. Available at: https://doi.org/10.1080/01431161.2017.1294775.
44. Ghulami, M., Gourbesville, P., Audra, P. and Shie-Yui, L. (2022) 'Performance evaluation of CORDEX South Asia models for projections of precipitation over the Kabul basin, Afghanistan', *LHB: Hydroscience Journal*, 108(1). Available at: https://doi.org/10.1080/27678490.2022.2095936.
45. Giang, P.Q., Toshiki, K., Sakata, M., Kunikane, S. and Vinh, T.Q. (2014) 'Modelling climate change impacts on the seasonality of water resources in the upper Ca river watershed in Southeast Asia', *Scientific World Journal*, 2014. Available at: https://doi.org/10.1155/2014/279135.
46. Golmohammadi, G., Prasher, S., Madani, A. and Rudra, R. (2014) 'Evaluating three hydrological distributed watershed models: MIKE-SHE, APEX, SWAT', *Hydrology*, 1(1), pp. 20–39. Available at: https://doi.org/10.3390/hydrology1010020.
47. Gudmundsson, L., Bremnes, J.B., Haugen, J.E. and Engen-Skaugen, T. (2012a) 'Technical Note: Downscaling RCM precipitation to the station scale using statistical transformations – a

comparison of methods', *Hydrology and Earth System Sciences*, 16(9), pp. 3383–3390. Available at: https://doi.org/10.5194/hess-16-3383-2012.

48. Gudmundsson, L., Bremnes, J.B., Haugen, J.E. and Engen-Skaugen, T. (2012b) 'Technical Note: Downscaling RCM precipitation to the station scale using statistical transformations – A comparison of methods', *Hydrology and Earth System Sciences*, 16(9), pp. 3383–3390. Available at: https://doi.org/10.5194/hess-16-3383-2012.
49. Gupta, H. V., Kling, H., Yilmaz, K.K. and Martinez, G.F. (2009) 'Decomposition of the mean squared error and NSE performance criteria: Implications for improving hydrological modelling', *Journal of Hydrology*, 377(1–2), pp. 80–91. Available at: https://doi.org/10.1016/j.jhydrol.2009.08.003.
50. Guse, B., Reusser, D.E. and Fohrer, N. (2014) 'How to improve the representation of hydrological processes in SWAT for a lowland catchment - temporal analysis of parameter sensitivity and model performance', *Hydrological Processes*, 28(4), pp. 2651–2670. Available at: https://doi.org/10.1002/hyp.9777.
51. Hashmi, M.Z.U.R., Masood, A., Mushtaq, H., Bukhari, S.A.A., Ahmad, B. and Tahir, A.A. (2020) 'Exploring climate change impacts during first half of the 21st century on flow regime of the transboundary kabul river in the hindukush region', *Journal of Water and Climate Change*, 11(4), pp. 1521–1538. Available at: https://doi.org/10.2166/wcc.2019.094.
52. Hoegh-Guldberg, O., Jacob, D., Taylor, M., Bindi, M., Brown, S., Camilloni, I., Diedhiou, A., Djalante, R., Ebi, K.L., Engelbrecht, F., Guiot, J., Hijioka, Y., Mehrotra, S., Payne, A., Seneviratne, S.I., Thomas, A., Warren, R. and Zhou, G. (2022) 'Impacts of 1.5°C Global Warming on Natural and Human Systems', in *Global Warming of 1.5°C*. Cambridge University Press, pp. 175–312. Available at: https://doi.org/10.1017/9781009157940.005.
53. Houben, G. and Tunnermeier, T. (2005) *Hydrogeology of the Kabul Basin, Part I: Geology, aquifer characteristics, climate and hydrology, Federal Institute for Geosciences and Natural Resources (BGR)*. Hannover.
54. Hu, Z., Zhang, C., Hu, Q. and Tian, H. (2014) 'Temperature Changes in Central Asia from 1979 to 2011 Based on Multiple Datasets*', *Journal of Climate*, 27(3), pp. 1143–1167. Available at: https://doi.org/10.1175/JCLI-D-13-00064.1.
55. Huss, M. and Hock, R. (2018) 'Global-scale hydrological response to future glacier mass loss', *Nature Climate Change*, 8(2), pp. 135–140. Available at: https://doi.org/10.1038/s41558-017-0049-x.

56. ICIMOD (2012) *Soil and Terrain Database for Afghanistan. Kathmandu: International Centre for Integrated Mountain Development (ICIMOD)*.
57. ICIMOD (2018) *Learning from a disaster event: Investigating the 2018 Panjshir flood in Afghanistan, mountain environment regional enformation system-ICIMOD*. Available at: https://www.icimod.org/success-stories/learning-from-a-disaster-event-investigating-the-2018-panjshir-flood-in-afghanistan/.
58. Immerzeel, W.W., van Beek, L.P. and Bierkens, M.F. (2010) 'Climate Change Will Affect the Asian Water Towers', *Science*, 328(5984)(July), pp. 1382–1385.
59. Intergovernmental Panel on Climate Change (IPCC) (2023) *Climate Change 2022 – Impacts, Adaptation and Vulnerability, O., Roberts, DC, Tignor, M., Poloczanska, ES, Mintenbeck, K., Ale, A., Eds*. Cambridge University Press. Available at: https://doi.org/10.1017/9781009325844.
60. Iqbal, M., Dahri, Z., Querner, E., Khan, A. and Hofstra, N. (2018) 'Impact of Climate Change on Flood Frequency and Intensity in the Kabul River Basin', *Geosciences*, 8(4), p. 114. Available at: https://doi.org/10.3390/geosciences8040114.
61. Jha, M., Arnold, J.G., Gassman, P.W., Giorgi, F. and Gu, R.R. (2006) 'Climate change sensitivity assessment on Upper Mississippi River Basin streamflows using SWAT', *Journal of the American Water Resources Association*, 42(4), pp. 997–1015. Available at: https://doi.org/10.1111/j.1752-1688.2006.tb04510.x.
62. Jones, A., Caon, L. and Yigini, Y. (2023) *Soil Atlas of Asia*. Luxembourg: Publications Office of the European Union, Luxembourg. Available at: https://doi.org/10.2760/044457.
63. Khatiwada, K.R., Pradhananga, S. and Nepal, S. (2024) 'Inferring the impacts of climate extreme in the Kabul River Basin', *Regional Environmental Change*, 24(1), p. 17. Available at: https://doi.org/10.1007/s10113-023-02167-3.
64. Kouchi, D.H., Esmaili, K., Faridhosseini, A., Sanaeinejad, S.H., Khalili, D. and Abbaspour, K.C. (2017) 'Sensitivity of Calibrated Parameters and Water Resource Estimates on Different Objective Functions and Optimization Algorithms', *Water*, 9(6), p. 384. Available at: https://doi.org/10.3390/w9060384.
65. Kreft, S., Eckstein, D., Dorsch, L. and Fischer, L. (2015) *GLOBAL CLIMATE RISK INDEX 2016, Germanwatch e.V.* Bonn. Available at: https://germanwatch.org/sites/default/files/publication/13503.pdf.
66. Liu, Y., Cui, G. and Li, H. (2020) 'Optimization and Application of Snow Melting Modules

in SWAT Model for the Alpine Regions of Northern China', *Water*, 12(3), p. 636. Available at: https://doi.org/10.3390/w12030636.

67. Lukas, G. (2016) 'Package " qmap ": Statistical Transformations for Post-Processing Climate Model'. Available at: https://doi.org/10.5194/hess-16-3383-2012.bernexp.
68. Lutz, A.F., Immerzeel, W.W., Shrestha, A.B. and Bierkens, M.F.P. (2014) 'Consistent increase in High Asia's runoff due to increasing glacier melt and precipitation', *Nature Climate Change*, 4(7), pp. 587–592. Available at: https://doi.org/10.1038/nclimate2237.
69. Mack, T.J., Chornack, M.P. and Taher, M.R. (2013) 'Groundwater-level trends and implications for sustainable water use in the Kabul Basin, Afghanistan', *Environment Systems and Decisions*, 33(3), pp. 457–467. Available at: https://doi.org/10.1007/s10669-013-9455-4.
70. Maharjan, S.B., Shrestha, F., Azizi, F., Joya, E., Bajracharya, B., Bromand, M.T. and Rahimi, M.M. (2021) 'Monitoring of Glaciers and Glacial Lakes in Afghanistan', in *Earth Observation Science and Applications for Risk Reduction and Enhanced Resilience in Hindu Kush Himalaya Region*. Cham: Springer International Publishing, pp. 211–230. Available at: https://doi.org/10.1007/978-3-030-73569-2_11.
71. MAIL (2019) 'Ministry of Agriculture, Irrigation and Livestock (MAIL), Department of statistics'. Available at: https://mail.gov.af (Accessed: 10 May 2019).
72. Masson-Delmotte, V., Zhai, P., Chen, Y., Goldfarb, L., Gomis, M.I., Matthews, J.B.R., Berger, S., Huang, M., Yelekçi, O., Yu, R., Zhou, B., Lonnoy, E., Maycock, T.K., Waterfield, T., Leitzell, K. and Caud, N. (2021) *Working Group I Contribution to the Sixth Assessment Report of the Intergovernmental Panel on Climate Change*. Available at: www.ipcc.ch.
73. McElroy, A.D., Chiu, S.Y., Nebgen, J.W., Aleti, A. and Bennett, F.W. (1976) *Loading functions for assessment of water pollution from nonpoint sources*. Available at: https://inis.iaea.org (Accessed: 9 September 2024).
74. McSweeney, C., New, M., Lizcano, G. and Lu, X. (2010) 'The UNDP Climate Change Country Profiles', *Bulletin of the American Meteorological Society*, 91(2), pp. 157–166. Available at: https://doi.org/10.1175/2009BAMS2826.1.
75. Mendez, M., Maathuis, B., Hein-Griggs, D. and Alvarado-Gamboa, L.-F. (2020) 'Performance Evaluation of Bias Correction Methods for Climate Change Monthly Precipitation Projections over Costa Rica', *Water*, 12(2), p. 482. Available at: https://doi.org/10.3390/w12020482.
76. Mengistu, A.G., van Rensburg, L.D. and Woyessa, Y.E. (2019) 'Techniques for calibration and validation of SWAT model in data scarce arid and semi-arid catchments in South Africa',

Journal of Hydrology: Regional Studies, 25(May), p. 100621. Available at: https://doi.org/10.1016/j.ejrh.2019.100621.

77. Mengistu, D.T. and Sorteberg, A. (2012) 'Sensitivity of SWAT simulated streamflow to climatic changes within the Eastern Nile River basin', *Hydrology and Earth System Sciences*, 16(2), pp. 391–407. Available at: https://doi.org/10.5194/hess-16-391-2012.
78. MEW and JICA (2019) *Long-and Short-Term Plan (WRD)-Appemdix 1 of the Project for Capacity Enhancement on Hydro-Meteorological Information Management in the Ministry of Energy and Water in the Islamic Republic of Afghanistan*.
79. Mills, L. (2013) *Afghanistan Water Resources Development (AWARD) Technical Assistance Project - Technical and Implementation Support Consultancy (TISC)*.
80. Minder, J.R. (2010) 'The Sensitivity of Mountain Snowpack Accumulation to Climate Warming', *Journal of Climate*, 23(10), pp. 2634–2650. Available at: https://doi.org/10.1175/2009JCLI3263.1.
81. Mohammad Tayib Bromand (2015) *IMPACT ASSESSMENT OF CLIMATE CHANGE ON WATER RESOURCES IN THE KABUL RIVER BASIN, AFGHANISTAN, Graduate School of Science and Engineering, Ritsumeikan University, Shiga, Japan.* Ritsumeikan University.
82. Mohanty, A., Mishra, M., Sharma, D. and Waheed Ibrahimzada, M. (2012) 'Chapter 3 Assessing the Hydrological Impacts of Climate Change on the Amu Darya River, Afghanistan', in, pp. 33–52. Available at: https://doi.org/10.1108/S2040-7262(2012)0000011009.
83. Mukhopadhyay, B. and Khan, A. (2014) 'A quantitative assessment of the genetic sources of the hydrologic flow regimes in Upper Indus Basin and its significance in a changing climate', *Journal of Hydrology*, 509, pp. 549–572. Available at: https://doi.org/10.1016/j.jhydrol.2013.11.059.
84. Narsimlu, B., Gosain, A.K. and Chahar, B.R. (2013) 'Assessment of Future Climate Change Impacts on Water Resources of Upper Sind River Basin, India Using SWAT Model', *Water Resources Management*, 27(10), pp. 3647–3662. Available at: https://doi.org/10.1007/s11269-013-0371-7.
85. Nash, J.E. and Sutcliffe, J.V. (1970) 'River flow forecasting through conceptual models part I — A discussion of principles', *Journal of Hydrology*, 10(3), pp. 282–290. Available at: https://doi.org/10.1016/0022-1694(70)90255-6.
86. Nasiri, S., Ansari, H. and Ziaei, A.N. (2020) 'Simulation of water balance equation

components using SWAT model in Samalqan Watershed (Iran)', *Arabian Journal of Geosciences*, 13(11), p. 421. Available at: https://doi.org/10.1007/s12517-020-05366-y.

87. NAWARA (2019) *Daily precipitation and temperature data obtained from the National Water Affairs Authority (NAWARA), National Water Affairs Authority*. Kabul-Afghnistan.
88. Neitsch, S.L., Arnold, J.G., Kiniry, J.R. and Williams, J.R. (2011) *Soil and Water Assessment Tool Theoretical Documentation Version 2009, Texas Water Resources Institute*. Available at: http://hdl.handle.net/1969.1/128050.
89. Nikulin, G. and Legutke, S. (2016) 'Data Reference Syntax (DRS) for bias-adjusted CORDEX simulations'.
90. Ougahi, J.H., Karim, S. and Mahmood, S.A. (2022) 'Application of the SWAT model to assess climate and land use/cover change impacts on water balance components of the Kabul River Basin, Afghanistan', *Journal of Water and Climate Change*, 13(11), pp. 3977–3999. Available at: https://doi.org/10.2166/wcc.2022.261.
91. Prein, A.F., Liu, C., Ikeda, K., Trier, S.B., Rasmussen, R.M., Holland, G.J. and Clark, M.P. (2017) 'Increased rainfall volume from future convective storms in the US', *Nature Climate Change*, 7(12), pp. 880–884. Available at: https://doi.org/10.1038/s41558-017-0007-7.
92. Qian, W. and Chang, H.H. (2021) 'Projecting Health Impacts of Future Temperature: A Comparison of Quantile-Mapping Bias-Correction Methods', *International Journal of Environmental Research and Public Health*, 18(4), p. 1992. Available at: https://doi.org/10.3390/ijerph18041992.
93. Rathjens, H., Bieger, K., Srinivasan, R., Chaubey, I. and Arnold, J.G. (2016) *CMhyd User Manual*. Available at: https://swat.tamu.edu/media/115265/bias_cor_man.pdf.
94. Reyer, C.P.., Otto, I.M., Adams, S., Albrecht, T., Baarsch, F., Cartsburg, M., Coumou, D., Eden, A., Ludi, E., Marcus, R., Mengel, M., Mosello, B., Robinson, A., Schleussner, C.-F., Serdeczny, O. and Stagl, J. (2017) 'Climate change impacts in Central Asia and their implications for development', *Regional Environmental Change*, 17(6), pp. 1639–1650. Available at: https://doi.org/10.1007/s10113-015-0893-z.
95. Rosario Klautau de Araujo Gomes, R. and Lima Fernandes, L. (2017) 'Hydrological characterization of the Araguaia River through reference flows', *Applied Water Science*, 7(8), pp. 4605–4614. Available at: https://doi.org/10.1007/s13201-017-0622-5.
96. Schad, P. (2016) 'The International Soil Classification System WRB, Third Edition, 2014', in *Springer Water*, pp. 563–571. Available at: https://doi.org/10.1007/978-3-319-24409-9_25.

97. Sediqi, M.N. and Komori, D. (2023) ‘Assessing Water Resource Sustainability in the Kabul River Basin: A Standardized Runoff Index and Reliability, Resilience, and Vulnerability Framework Approach’, *Sustainability*, 16(1), p. 246. Available at: https://doi.org/10.3390/su16010246.
98. Selvakumar, R. and Gunavathi, S. (2021) ‘Assessment of Various Bias Correction Methods on Precipitation of Regional Climate Model and Future Projection’. Available at: https://doi.org/10.21203/rs.3.rs-339080/v1.
99. Shiru, M.S., Shahid, S., Shiru, S., Chung, E.S., Alias, N., Ahmed, K., Dioha, E.C., Sa’adi, Z., Salman, S., Noor, M., Nashwan, M.S., Idlan, M.K., Khan, N., Momade, M.H., Houmsi, M.R., Iqbal, Z., Ishanch, Q. and Sediqi, M.N. (2020) ‘Challenges in water resources of Lagos mega city of Nigeria in the context of climate change’, *Journal of Water and Climate Change*, 11(4), pp. 1067–1083. Available at: https://doi.org/10.2166/wcc.2019.047.
100. Shrestha, M., Acharya, S.C. and Shrestha, P.K. (2017) ‘Bias correction of climate models for hydrological modelling – are simple methods still useful?’, *Meteorological Applications*, 24(3), pp. 531–539. Available at: https://doi.org/10.1002/met.1655.
101. Shroder, J.F., Ahmadzai, S.J. and Ellis, W.. (2007) *Hydrologic Investigations of the Glacial Systems of Afghanistan and Their Impact on Soil Formation. U.S. Geological Survey Professional Paper 1757*.
102. Sidiqi, M. and Shrestha, S. (2021) ‘Assessment of Climate Change Impact on the Hydrology of the Kabul River Basin, Afghanistan’, *Journal of Water Engineering and Management*, 2(1), pp. 1–21. Available at: https://doi.org/10.47884/jweam.v2i1pp01-21.
103. Sidiqi, M., Shrestha, S. and Ninsawat, S. (2018) ‘Projection of climate change scenarios in the Kabul River Basin, Afghanistan’, *Current Science*, 114(6), pp. 1304–1310. Available at: https://doi.org/10.18520/cs/v114/i06/1304-1310.
104. Singh, V., Kumar Goyal, M., Surampalli, R.Y. and Munoz-Arriola, F. (2017) ‘Sub catchment Assessment of snowpack and snowmelt change by analyzing elevation bands and parameter sensitivity in the high Himalayas’, *Hydrology and Earth System Sciences Discussions*, pp. 1–31. Available at: https://doi.org/10.5194/hess-2016-689.
105. Srinivasan, R. and Arnold, J.G. (1994) ‘INTEGRATION OF A BASIN-SCALE WATER QUALITY MODEL WITH GIS’, *JAWRA Journal of the American Water Resources Association*, 30(3), pp. 453–462. Available at: https://doi.org/10.1111/j.1752-1688.1994.tb03304.x.

106. Srinivasan, R., Ramanarayanan, T.S., Arnold, J.G. and Bednarz, S.T. (1998) 'LARGE AREA HYDROLOGIC MODELING AND ASSESSMENT PART II: MODEL APPLICATION 1', *JAWRA Journal of the American Water Resources Association*, 34(1), pp. 91–101. Available at: https://doi.org/10.1111/j.1752-1688.1998.tb05962.x.

107. Sun, Q., Miao, C., Duan, Q., Ashouri, H., Sorooshian, S. and Hsu, K. (2018) 'A Review of Global Precipitation Data Sets: Data Sources, Estimation, and Intercomparisons', *Reviews of Geophysics*, 56(1), pp. 79–107. Available at: https://doi.org/10.1002/2017RG000574.

108. Tadese, M.T., Kumar, L. and Koech, R. (2020) 'Climate change projections in the Awash River Basin of Ethiopia using Global and Regional Climate Models', *International Journal of Climatology*, 40(8), pp. 3649–3666. Available at: https://doi.org/10.1002/joc.6418.

109. Taylor, K.E. (2001) 'Summarizing multiple aspects of model performance in a single diagram', *Journal of Geophysical Research: Atmospheres*, 106(D7), pp. 7183–7192. Available at: https://doi.org/10.1029/2000JD900719.

110. Teutschbein, C. and Seibert, J. (2012) 'Bias correction of regional climate model simulations for hydrological climate-change impact studies: Review and evaluation of different methods', *Journal of Hydrology*, 456–457, pp. 12–29. Available at: https://doi.org/10.1016/j.jhydrol.2012.05.052.

111. Thomann, R.V. and Mueller, J.A. (1987) *Principles of Surface Water Quality Modeling and Control*. New York: Harper & Row.

112. Tuo, Y., Marcolini, G., Disse, M. and Chiogna, G. (2018) 'Calibration of snow parameters in SWAT: comparison of three approaches in the Upper Adige River basin (Italy)', *Hydrological Sciences Journal*, 63(4), pp. 657–678. Available at: https://doi.org/10.1080/02626667.2018.1439172.

113. U.S. Geological Survey (2014) *Shuttle Radar Topography Mission-Digital Elevation Model (SRTM-DEM), U.S. Geological Survey's Earth Resources Observation and Science (EROS) Center*. Available at: https://earthexplorer.usgs.gov/ (Accessed: 5 March 2020).

114. UC Louvain (2020) *EM-DAT website Atlas - Afghanistan, Brussels, Belgium*. Available at: https://www.emdat.be/emdat_atlas/sub_html_pages/sub_html_AFG.html.

115. Villamizar, S.R., Pineda, S.M. and Carrillo, G.A. (2019) 'The Effects of Land Use and Climate Change on the Water Yield of a Watershed in Colombia', *Water*, 11(2), p. 285. Available at: https://doi.org/10.3390/w11020285.

116. Vincent, L.A., Peterson, T.C., Barros, V.R., Marino, M.B., Rusticucci, M., Carrasco, G.,

Ramirez, E., Alves, L.M., Ambrizzi, T., Berlato, M.A., Grimm, A.M., Marengo, J.A., Molion, L., Moncunill, D.F., Rebello, E., Anunciação, Y.M.T., Quintana, J., Santos, J.L., Baez, J., Coronel, G., Garcia, J., Trebejo, I., Bidegain, M., Haylock, M.R. and Karoly, D. (2005) 'Observed Trends in Indices of Daily Temperature Extremes in South America 1960–2000', *Journal of Climate*, 18(23), pp. 5011–5023. Available at: https://doi.org/10.1175/JCLI3589.1.

117. Viviroli, D., Archer, D.R., Buytaert, W., Fowler, H.J., Greenwood, G.B., Hamlet, A.F., Huang, Y., Koboltschnig, G., Litaor, M.I., López-Moreno, J.I., Lorentz, S., Schädler, B., Schreier, H., Schwaiger, K., Vuille, M. and Woods, R. (2011) 'Climate change and mountain water resources: overview and recommendations for research, management and policy', *Hydrology and Earth System Sciences*, 15(2), pp. 471–504. Available at: https://doi.org/10.5194/hess-15-471-2011.

118. Wi, S., Yang, Y.C.E., Steinschneider, S., Khalil, A. and Brown, C.M. (2015) 'Calibration approaches for distributed hydrologic models in poorly gaged basins: implication for streamflow projections under climate change', *Hydrology and Earth System Sciences*, 19(2), pp. 857–876. Available at: https://doi.org/10.5194/hess-19-857-2015.

119. Williams, J.R. (1975) 'SEDIMENT ROUTING FOR AGRICULTURAL WATERSHEDS', *JAWRA Journal of the American Water Resources Association*, 11(5), pp. 965–974. Available at: https://doi.org/10.1111/j.1752-1688.1975.tb01817.x.

120. Winchell, M., Srinivasan, R., Di Luzio, M. and Arnold, J.G. (2013) *ArcSWAT Interface for SWAT2012 (A user manual)*.

121. World Bank (2010) *Scoping Strategic Options for Development of the Kabul River Basin: A Multisectoral Decision Supporting System Approach*.

122. X. Zhang, R. Srinivasan and M. Van Liew (2008) 'Multi-Site Calibration of the SWAT Model for Hydrologic Modeling', *Transactions of the ASABE*, 51(6), pp. 2039–2049. Available at: https://doi.org/10.13031/2013.25407.

123. Yapo, P.O., Gupta, H.V. and Sorooshian, S. (1996) 'Automatic calibration of conceptual rainfall-runoff models: sensitivity to calibration data', *Journal of Hydrology*, 181(1–4), pp. 23–48. Available at: https://doi.org/10.1016/0022-1694(95)02918-4.

124. Yatagai, A., Kamiguchi, K., Arakawa, O., Hamada, A., Yasutomi, N. and Kitoh, A. (2012) 'APHRODITE: Constructing a Long-Term Daily Gridded Precipitation Dataset for Asia Based on a Dense Network of Rain Gauges', *Bulletin of the American Meteorological Society*, 93(9), pp. 1401–1415. Available at: https://doi.org/10.1175/BAMS-D-11-00122.1.

125. Zaryab, A., Reza Noori, A., Wegerich, K. and Kløve, B. (2017) 'Special Issue on Water Use Management Challenges in Central Assessment of water quality and quantity trends in Kabul aquifers with an outline for future drinking water supplies', *Central Asian Journal of Water Research*, 3(2), pp. 3–11.
126. Zhang, X., Yang, F. and Canada, E. (2004) *RClimDex (1.0) User Manual*.

8 APPENDIXES

8.1 The climate trend statistical results

The Mann-Kendall and Shapiro Wilk trend test statistical results for bias corrected annual and seasonal precipitation and temperature in the baseline period is showed in tables A-1 and A-2.

Table A-1: The Man-Kendall and Shapiro wilk trend results for the annual precipitation, maximum and minimum temperature in UKRB.

	Annual -Mann-Kendall (MK) Trend						**Annual -Shapiro Wilk Trend**			
	MK (S)	*K's Tau*	*V (S)*	*P Value*	*NS (Z)*	*Sen's slope*	beta (Slope)	CI_low	CI_up	p-value
Precipitation	6.0	0.0316	950.0	0.8711	0.1622	0.7700	-1.04	-8.97	6.89	0.88
T Max	68.0	0.3579	950.0	**0.0297**	2.1738	0.1150	0.0816	0.0061	0.1571	**0.0483**
T Min	64.0	0.3368	950.0	**0.0410**	2.0440	0.0775	0.0661	-0.0062	0.1384	0.09

Table A-2: The Man-Kendall and Shapiro wilk trend results for the seasonal precipitation, maximum and minimum temperature in UKRB.

	Seasonal -Mann-Kendall (MK) Trend						**Seasonal -Shapiro Wilk Trend**			
	MK (S)	*K's Tau*	*V (S)*	*P Value*	*NS (Z)*	*Sen's slope*	beta (Slope)	CI_low	CI_up	p-value
Spring Precipitation	-34	-0.18	950	0.284	-1.07	-3.07	-2.89	-8.56	2.77	0.33
Winter Precipitation	18	0.09	950	0.581	0.55	0.83	0.8	-3	4.61	0.683
Summer TMax	68	0.36	950	**0.030**	2.17	0.09	0.08	0.01	0.15	**0.032**
Winter TMin	46	0.24	950	0.144	1.46	0.08	0.06	-0.02	0.15	0.173

The positive Kendall's tau value denotes the positive trend and the negative Kendall's tau value express the negative or decreasing trend. The bold values in cells shows the significance of p-va lue which is less than 0.05.

8.2 Extreme climatic indices

Extreme climatic indices result for precipitation and temperature during the historical period (1986-2005), and future period (2006-2100) under RCP 4.5 and RCP8.5 in UKRB in Afghanistan. The results are the output from linear scaling method using the RClimDex software.

RClimDex is developed and maintained at Climate Research Branch of Meteorological Service of Canada (Zhang, Yang and Canada, 2004). The initial development was funded by the Canadian International Development Agency through the Canada-China Climate Change Cooperation (C5) project (Zhang, Yang and Canada, 2004). The RClimDex is designed to provide a user-friendly interface to compute indices of climate extremes. It computes all 27 core indices recommended by the Expert Team for Climate Change Detection Monitoring and Indices (ETCCDMI) as well as some other temperature and precipitation indices with user defined thresholds. A main objective of constructing climate extremes indices is to use for climate change monitoring and detection studies. The RClimDex includes a data quality control procedure, before the indices can be computed (Zhang, Yang and Canada, 2004). The RClimDex has tree steps including; the preprocessing of data, Quality control of data and calculation of core indices for climate variables.

In this study we focused on following indices for the climate change evaluation in UKRB and the statistical results shown in Table A-3.

1. Total wet day annual precipitation (prcptot)
2. Extremely wet days (r99p)
3. Warm nights (tn90p)
4. Warm days (tx90p)
5. Minimum value of daily minimum temperature (°C) (tnn)
6. Maximum value of daily maximum temperature (°C) (txx)
7. Mean Maximum temperature (°C) (TMAXmean)
8. Mean Minimum temperature (°C) (TMINmean)

Table A-3: The p-value results and slope of the 27 climatic indices in UKRB.

			Slope			STD of Slope			P_Value		
	Indices	**Indicator Name**	**Baseline**	**RCP4.5**	**RCP8.5**	**Baseline**	**RCP4.5**	**RCP8.5**	**Baseline**	**RCP4.5**	**RCP8.5**
1	cdd	Consecutive dry days (Days)	0.41	0.018	0.034	0.4	0.046	0.03	0.32	0.697	0.258
2	csdi	Cold spell duration indicator (Days)	-0.3	-0.277	-0.533	0.35	0.048	0.065	0.41	0	0
3	cwd	Consecutive wet days (Days)	0	-0.042	-0.035	0.08	0.015	0.015	0.96	0.005	0.019
4	dtr	Diurnal temperature range (°C)	0.02	0.004	0.008	0.02	0.001	0.001	0.35	0	0
5	fd0	Frost days (Days)	-0.77	-0.401	-1.031	0.41	0.032	0.04	0.08	0	0
6	gsl	Growing season Length (Days)	0.11	0.409	0.992	0.37	0.044	0.048	0.77	0	0
7	id0	Ice days (Days)	-0.68	-0.363	-0.356	0.72	0.033	0.027	0.36	0	0
8	***prcptot***	***Annual total wet-day precipitation (mm)***	***-0.85***	***-0.432***	***-0.396***	***3.96***	***0.32***	***0.274***	***0.83***	***0.181***	***0.151***
9	r10mm	Number of heavy precipitation days	-0.09	0.007	0.007	0.14	0.009	0.008	0.5	0.451	0.404
10	r20mm	Number of very heavy precipitation days	0.04	0.001	0.001	0.06	0.004	0.004	0.47	0.866	0.766
11	r95p	Very wet days (mm)	1.09	0.054	0.148	2.14	0.204	0.181	0.62	0.793	0.417
12	***r99p***	***Extremely wet days (mm)***	***0.71***	***0.037***	***0.062***	***1.33***	***0.146***	***0.169***	***0.6***	***0.802***	***0.715***
13	rx1day	Max 1-day precipitation amount (mm)	0.14	-0.021	0.022	0.31	0.055	0.081	0.66	0.704	0.788
14	rx5day	Max 5-day precipitation amount (mm)	0.42	0.033	0.035	0.84	0.091	0.117	0.62	0.716	0.766
15	sdii	Simple daily intensity index (mm/day)	0.01	0.001	0.002	0.02	0.002	0.002	0.53	0.669	0.117
16	su25	Summer days	1.12	0.398	1.06	0.69	0.047	0.038	0.12	0	0
17	***TMAXmean***	***Mean Tmax (°C)***	***0.08***	***0.035***	***0.075***	***0.04***	***0.002***	***0.002***	***0.05***	***0***	***0***
18	***TMINmean***	***Mean Tmin (°C)***	***0.07***	***0.031***	***0.066***	***0.04***	***0.001***	***0.001***	***0.09***	***0***	***0***
19	tn10p	Cool nights	-0.45	-0.217	-0.375	0.24	0.023	0.025	0.08	0	0
20	***tn90p***	***Warm nights***	***0.51***	***0.198***	***0.435***	***0.33***	***0.015***	***0.034***	***0.15***	***0***	***0***
21	***tnn***	***Minimum value of daily Tmin (°C)***	***0.05***	***0.048***	***0.092***	***0.06***	***0.006***	***0.006***	***0.38***	***0***	***0***
22	tnx	Max Tmin (°C)	0.04	0.02	0.063	0.05	0.002	0.003	0.44	0	0
23	tx10p	Cool days	-0.52	-0.206	-0.361	0.22	0.022	0.023	0.03	0	0

24	***tx90p***	***Warm days***	***0.51***	***0.2***	***0.427***	***0.33***	***0.016***	***0.034***	***0.14***	***0***	***0***
25	txn	Min Tmax (°C)	0.09	0.043	0.084	0.06	0.007	0.006	0.17	0	0
26	***txx***	***Maximum value of daily Tmax (°C)***	***0.03***	***0.027***	***0.068***	***0.06***	***0.003***	***0.003***	***0.62***	***0***	***0***
27	wsdi	Warm spell duration indicator (days)	0.75	0.235	0.717	0.33	0.032	0.096	0.03	0	0

The graphical results of the trend assessment for the 27 climatic indices are showen in the folowing figure A-16 for the baseline (1986-2005) and the future period of 2006-2100 under two RCPs (4.5 and 8.5) scenarios.

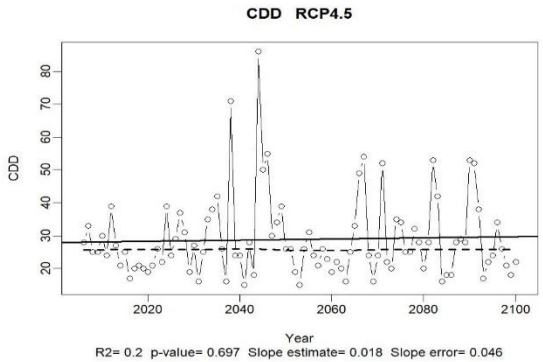

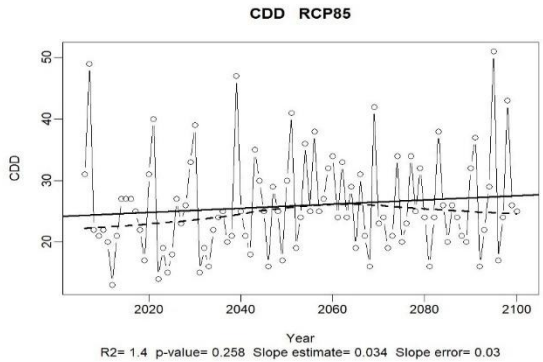

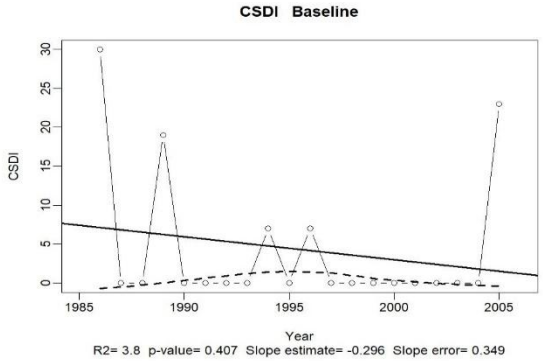

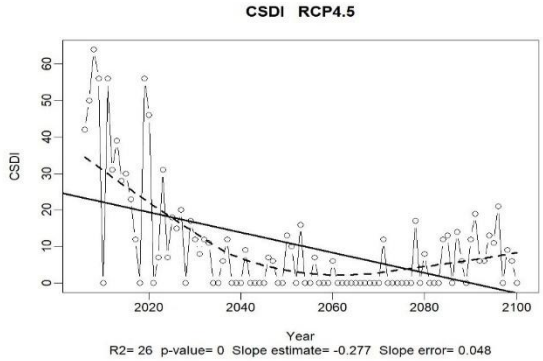

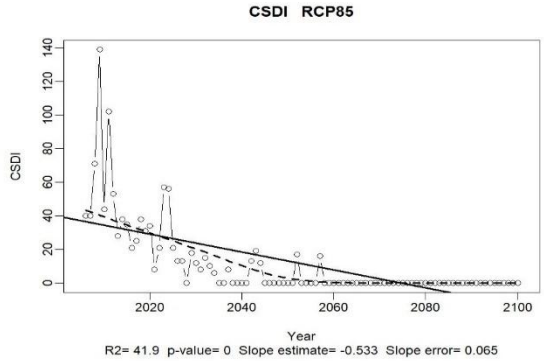

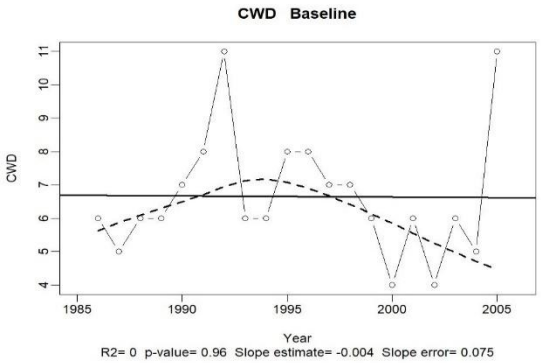
CWD Baseline
CWD
Year
R2= 0 p-value= 0.96 Slope estimate= -0.004 Slope error= 0.075

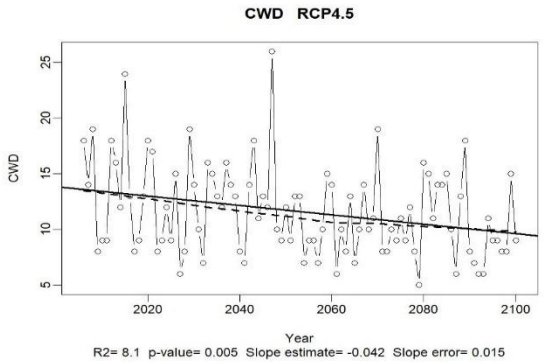
CWD RCP4.5
CWD
Year
R2= 8.1 p-value= 0.005 Slope estimate= -0.042 Slope error= 0.015

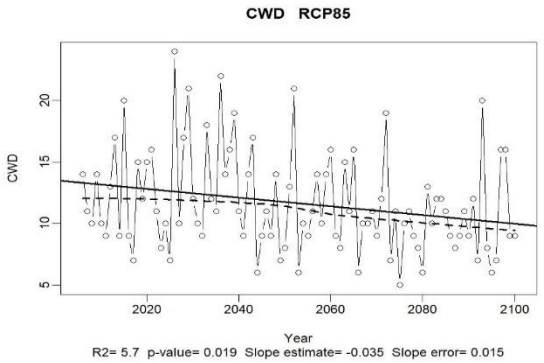
CWD RCP85
CWD
Year
R2= 5.7 p-value= 0.019 Slope estimate= -0.035 Slope error= 0.015

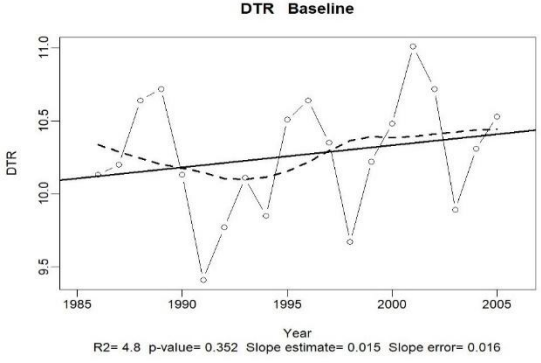
DTR Baseline
DTR
Year
R2= 4.8 p-value= 0.352 Slope estimate= 0.015 Slope error= 0.016

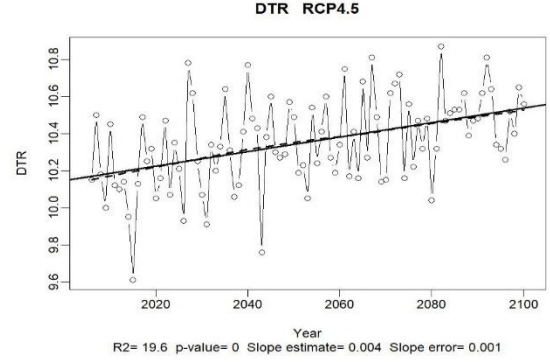
DTR RCP4.5
DTR
Year
R2= 19.6 p-value= 0 Slope estimate= 0.004 Slope error= 0.001

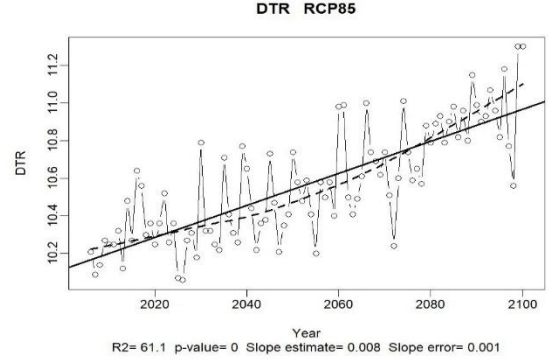
DTR RCP85
DTR
Year
R2= 61.1 p-value= 0 Slope estimate= 0.008 Slope error= 0.001

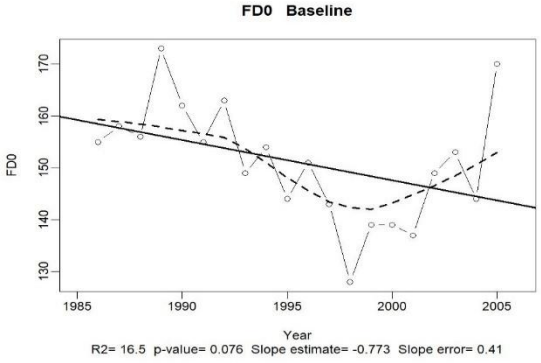
FD0 Baseline
FD0
Year
R2= 16.5 p-value= 0.076 Slope estimate= -0.773 Slope error= 0.41

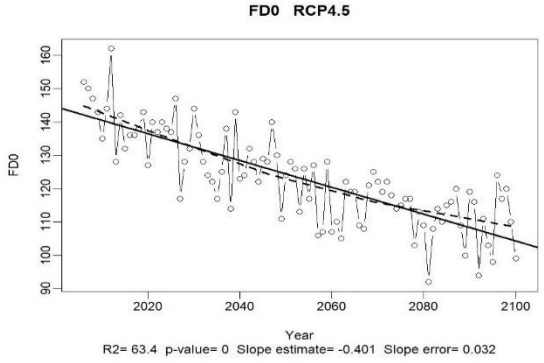
FD0 RCP4.5
FD0
Year
R2= 63.4 p-value= 0 Slope estimate= -0.401 Slope error= 0.032

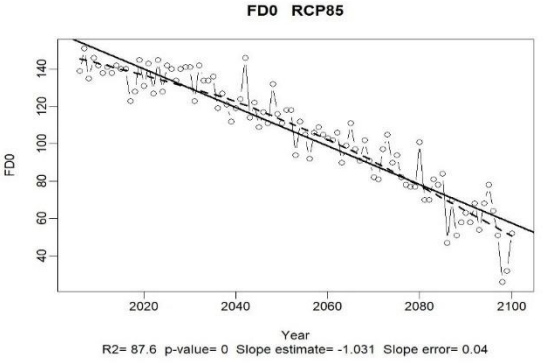
FD0 RCP85
FD0
Year
R2= 87.6 p-value= 0 Slope estimate= -1.031 Slope error= 0.04

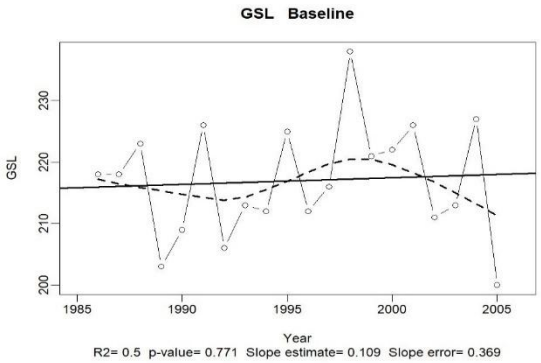
GSL Baseline
GSL
Year
R2= 0.5 p-value= 0.771 Slope estimate= 0.109 Slope error= 0.369

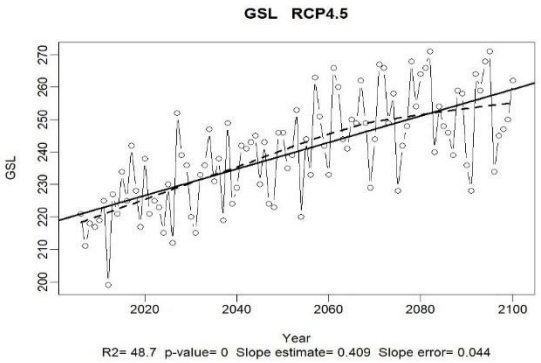
GSL RCP4.5
GSL
Year
R2= 48.7 p-value= 0 Slope estimate= 0.409 Slope error= 0.044

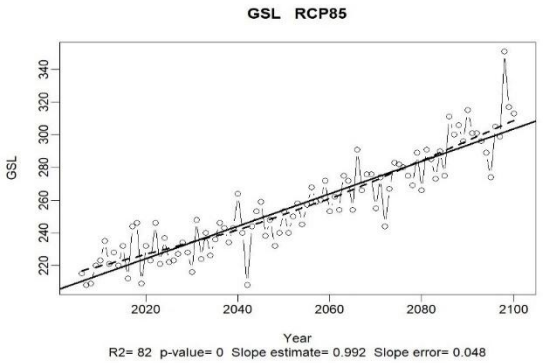
GSL RCP85
GSL
Year
R2= 82 p-value= 0 Slope estimate= 0.992 Slope error= 0.048

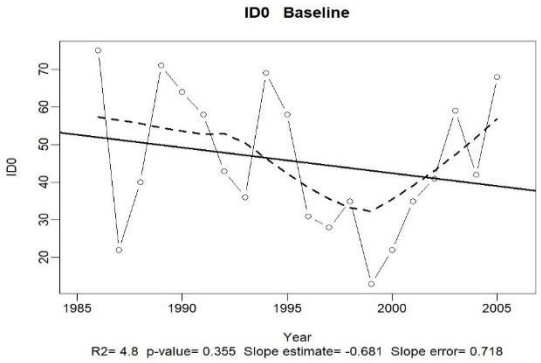
ID0 Baseline
ID0
Year
R2= 4.8 p-value= 0.355 Slope estimate= -0.681 Slope error= 0.718

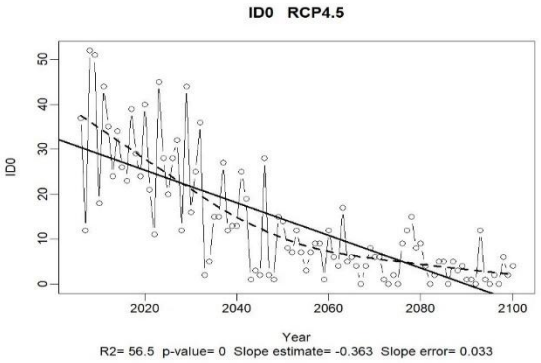
ID0 RCP4.5
ID0
Year
R2= 56.5 p-value= 0 Slope estimate= -0.363 Slope error= 0.033

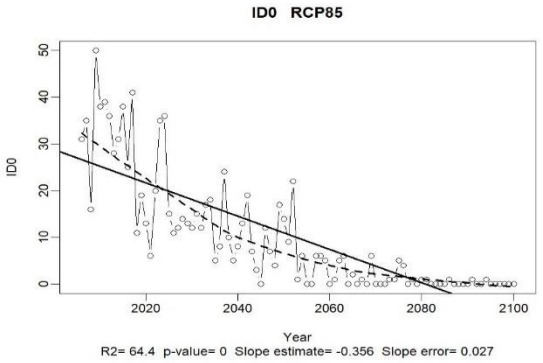
ID0 RCP85
ID0
Year
R2= 64.4 p-value= 0 Slope estimate= -0.356 Slope error= 0.027

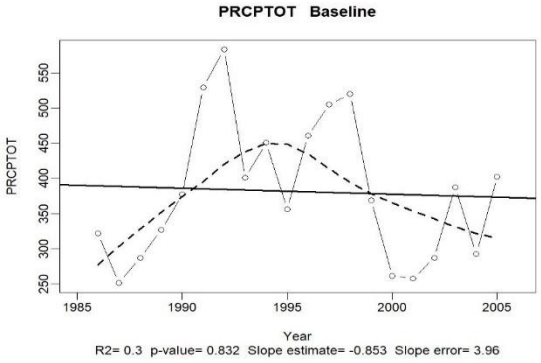
PRCPTOT Baseline
PRCPTOT
Year
R2= 0.3 p-value= 0.832 Slope estimate= -0.853 Slope error= 3.96

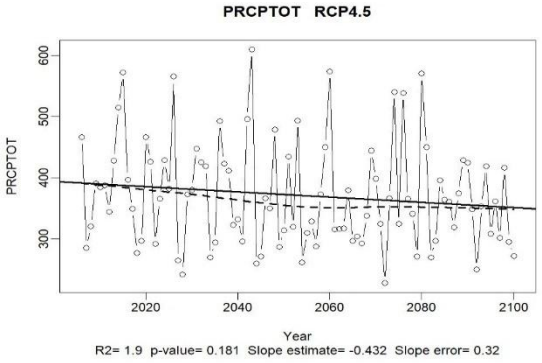
PRCPTOT RCP4.5
PRCPTOT
Year
R2= 1.9 p-value= 0.181 Slope estimate= -0.432 Slope error= 0.32

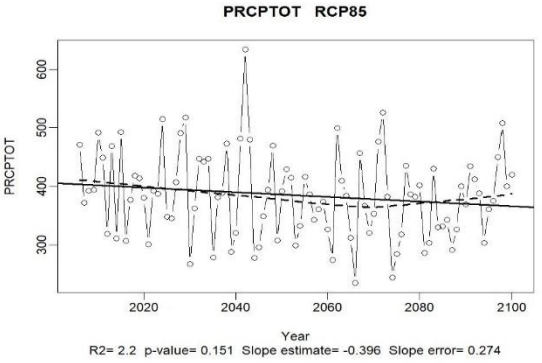
PRCPTOT RCP85
PRCPTOT
Year
R2= 2.2 p-value= 0.151 Slope estimate= -0.396 Slope error= 0.274

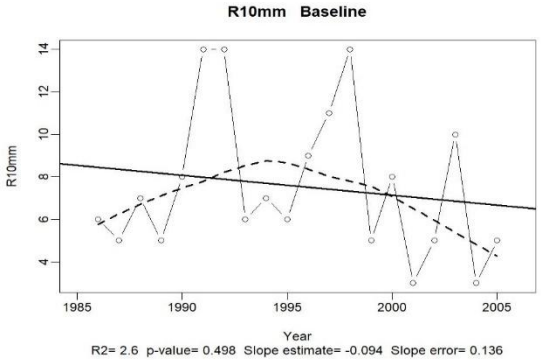
R10mm Baseline
R10mm
Year
R2= 2.6 p-value= 0.498 Slope estimate= -0.094 Slope error= 0.136

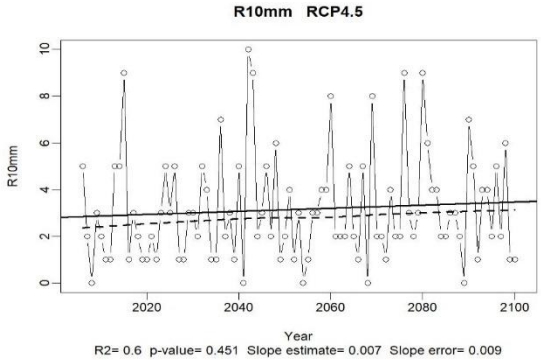
R10mm RCP4.5
R10mm
Year
R2= 0.6 p-value= 0.451 Slope estimate= 0.007 Slope error= 0.009

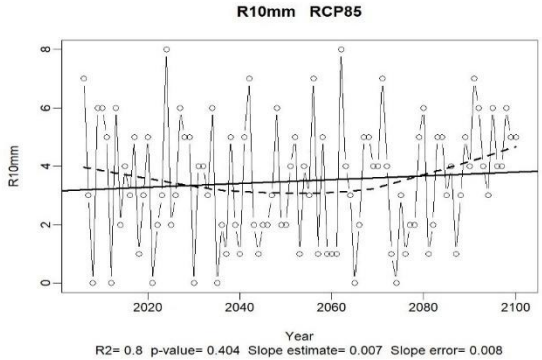
R10mm RCP85
R10mm
Year
R2= 0.8 p-value= 0.404 Slope estimate= 0.007 Slope error= 0.008

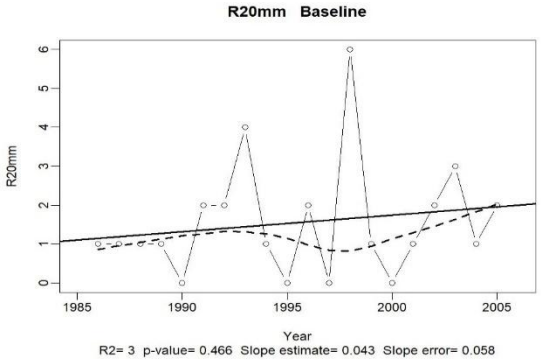
R20mm Baseline
R20mm
Year
R2= 3 p-value= 0.466 Slope estimate= 0.043 Slope error= 0.058

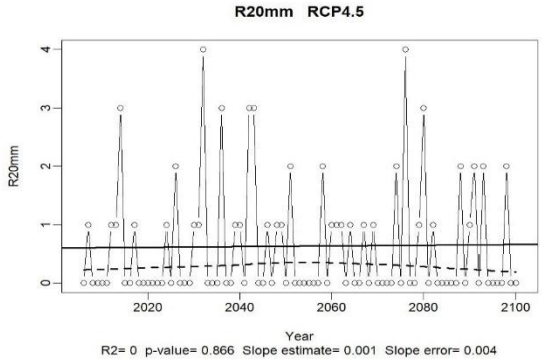
R20mm RCP4.5
R20mm
Year
R2= 0 p-value= 0.866 Slope estimate= 0.001 Slope error= 0.004

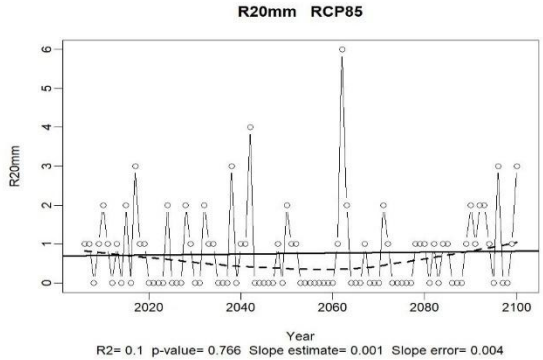
R20mm RCP85
R20mm
Year
R2= 0.1 p-value= 0.766 Slope estimate= 0.001 Slope error= 0.004

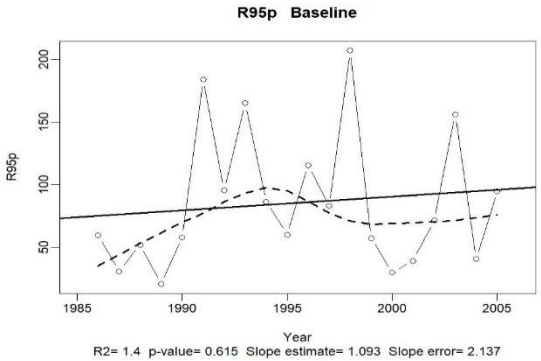
R95p Baseline
R95p
Year
R2= 1.4 p-value= 0.615 Slope estimate= 1.093 Slope error= 2.137

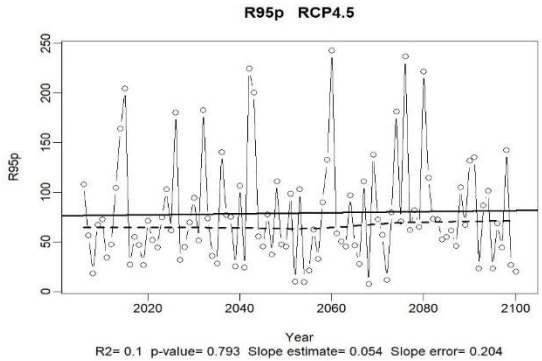
R95p RCP4.5
R95p
Year
R2= 0.1 p-value= 0.793 Slope estimate= 0.054 Slope error= 0.204

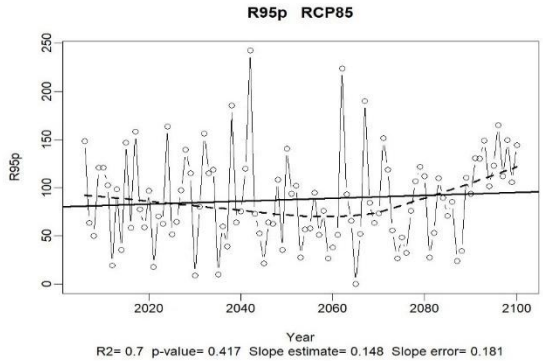
R95p RCP85
R95p
Year
R2= 0.7 p-value= 0.417 Slope estimate= 0.148 Slope error= 0.181

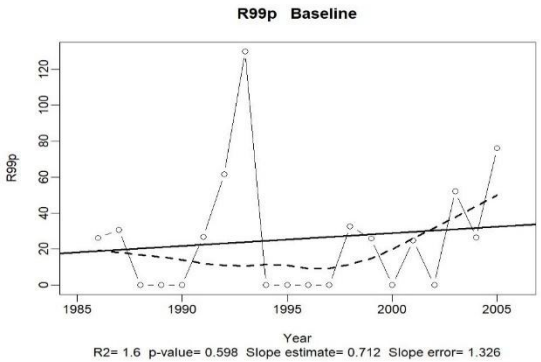
R99p Baseline
R99p
Year
R2= 1.6 p-value= 0.598 Slope estimate= 0.712 Slope error= 1.326

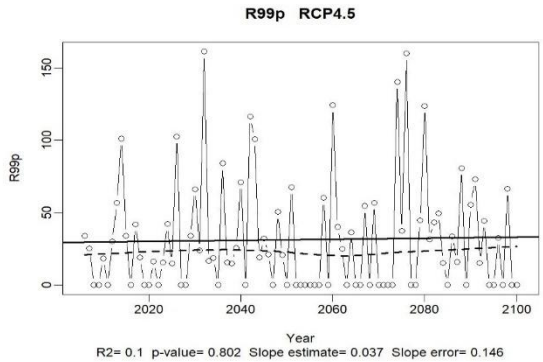
R99p RCP4.5
R99p
Year
R2= 0.1 p-value= 0.802 Slope estimate= 0.037 Slope error= 0.146

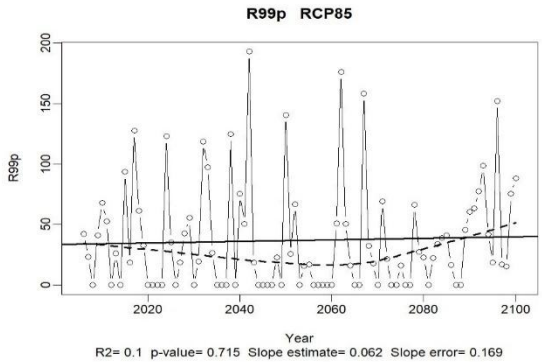
R99p RCP85
R99p
Year
R2= 0.1 p-value= 0.715 Slope estimate= 0.062 Slope error= 0.169

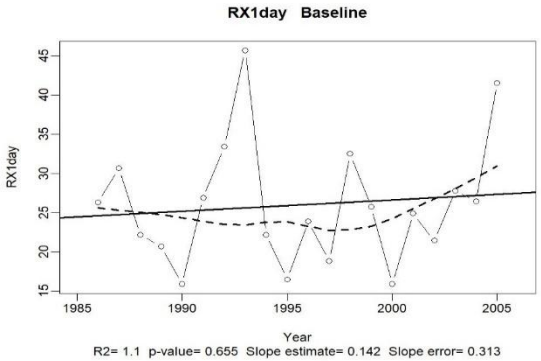
RX1day Baseline
RX1day
Year
R2= 1.1 p-value= 0.655 Slope estimate= 0.142 Slope error= 0.313

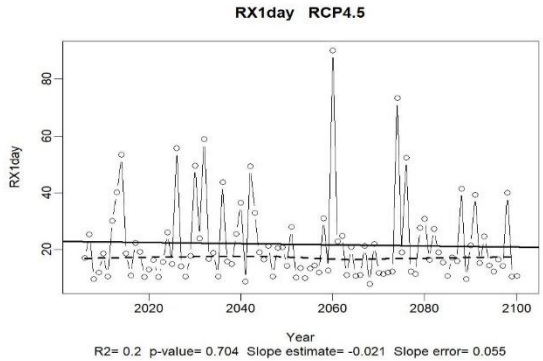
RX1day RCP4.5
RX1day
Year
R2= 0.2 p-value= 0.704 Slope estimate= -0.021 Slope error= 0.055

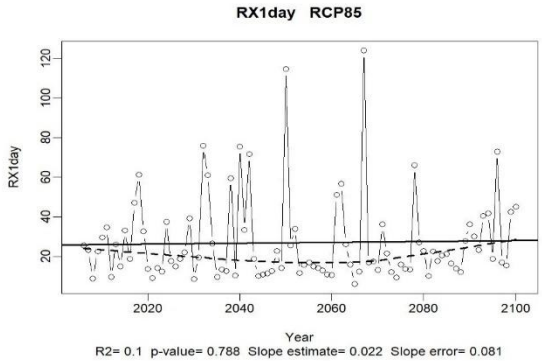
RX1day RCP85
RX1day
Year
R2= 0.1 p-value= 0.788 Slope estimate= 0.022 Slope error= 0.081

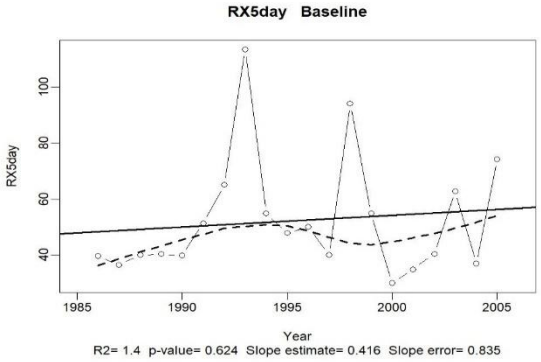
RX5day Baseline
RX5day
Year
R2= 1.4 p-value= 0.624 Slope estimate= 0.416 Slope error= 0.835

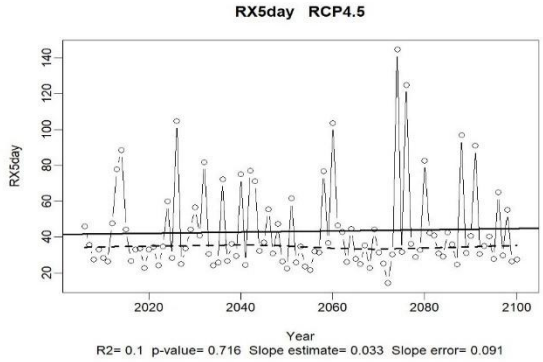
RX5day RCP4.5
RX5day
Year
R2= 0.1 p-value= 0.716 Slope estimate= 0.033 Slope error= 0.091

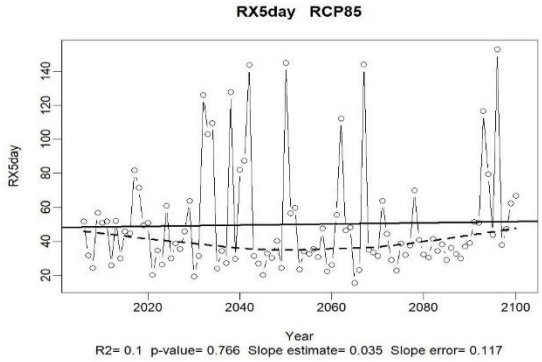
RX5day RCP85
RX5day
Year
R2= 0.1 p-value= 0.766 Slope estimate= 0.035 Slope error= 0.117

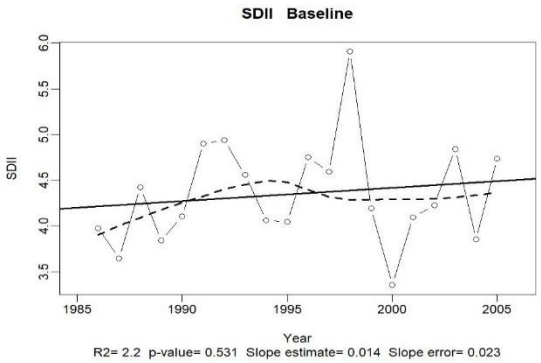
SDII Baseline
SDII
Year
R2= 2.2 p-value= 0.531 Slope estimate= 0.014 Slope error= 0.023

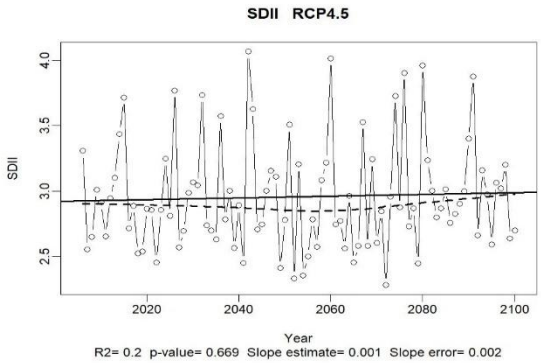
SDII RCP4.5
SDII
Year
R2= 0.2 p-value= 0.669 Slope estimate= 0.001 Slope error= 0.002

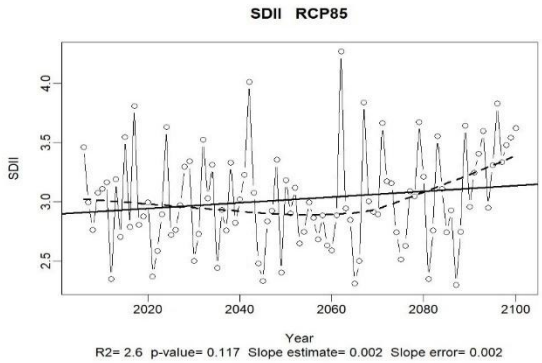
SDII RCP85
SDII
Year
R2= 2.6 p-value= 0.117 Slope estimate= 0.002 Slope error= 0.002

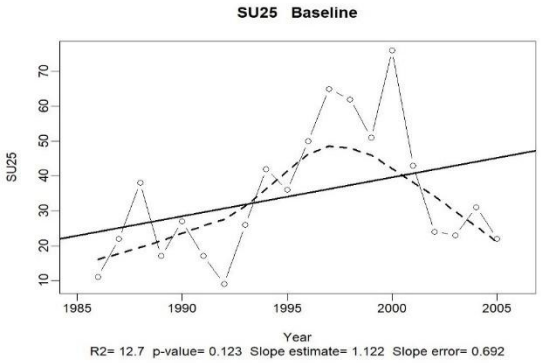
SU25 Baseline
SU25
Year
R2= 12.7 p-value= 0.123 Slope estimate= 1.122 Slope error= 0.692

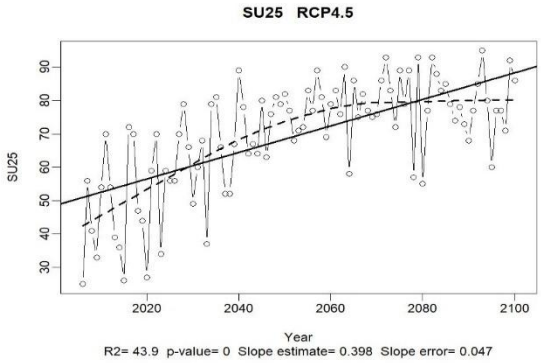
SU25 RCP4.5
SU25
Year
R2= 43.9 p-value= 0 Slope estimate= 0.398 Slope error= 0.047

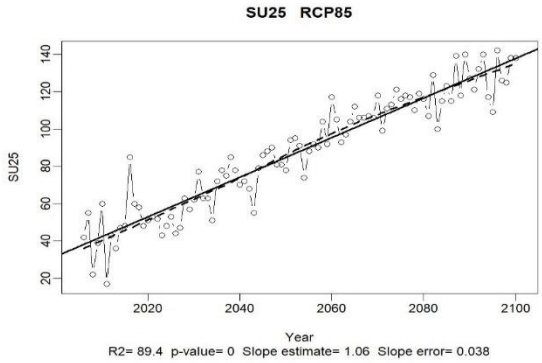
SU25 RCP85
SU25
Year
R2= 89.4 p-value= 0 Slope estimate= 1.06 Slope error= 0.038

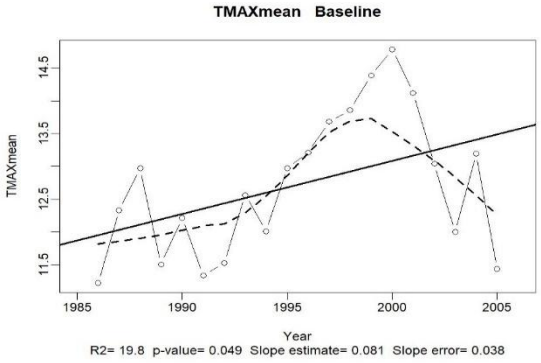
TMAXmean Baseline
TMAXmean
Year
R2= 19.8 p-value= 0.049 Slope estimate= 0.081 Slope error= 0.038

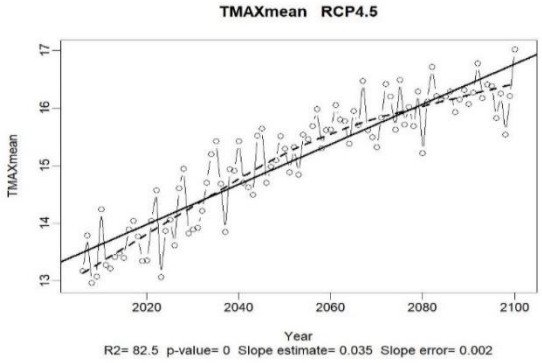
TMAXmean RCP4.5
TMAXmean
Year
R2= 82.5 p-value= 0 Slope estimate= 0.035 Slope error= 0.002

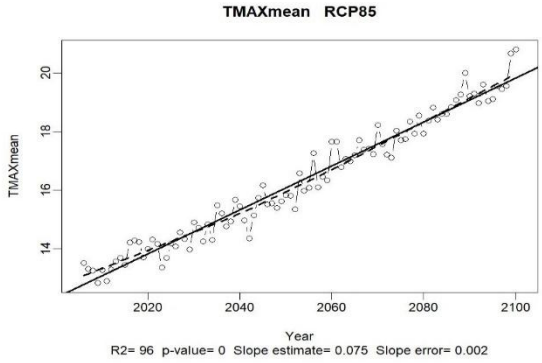
TMAXmean RCP85
TMAXmean
Year
R2= 96 p-value= 0 Slope estimate= 0.075 Slope error= 0.002

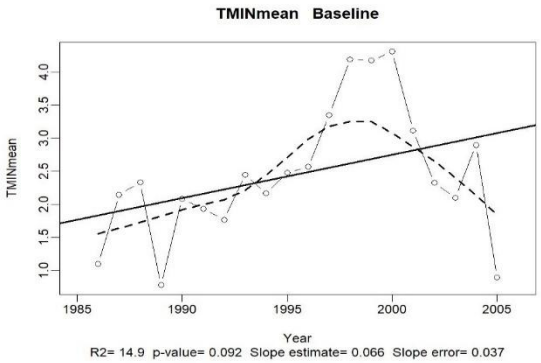
TMINmean Baseline
TMINmean
Year
R2= 14.9 p-value= 0.092 Slope estimate= 0.066 Slope error= 0.037

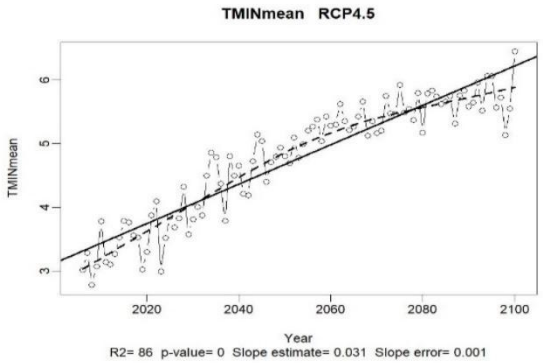
TMINmean RCP4.5
TMINmean
Year
R2= 86 p-value= 0 Slope estimate= 0.031 Slope error= 0.001

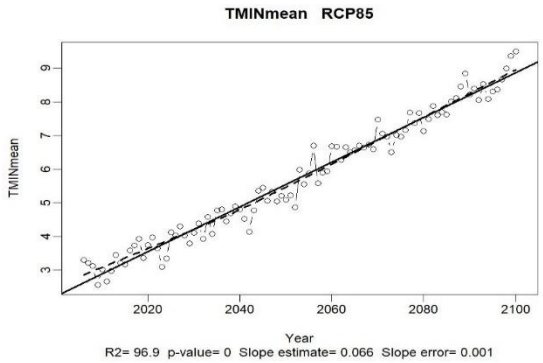
TMINmean RCP85
TMINmean
Year
R2= 96.9 p-value= 0 Slope estimate= 0.066 Slope error= 0.001

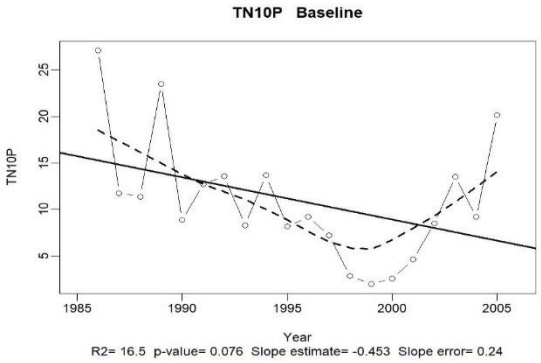
TN10P Baseline
TN10P
Year
R2= 16.5 p-value= 0.076 Slope estimate= -0.453 Slope error= 0.24

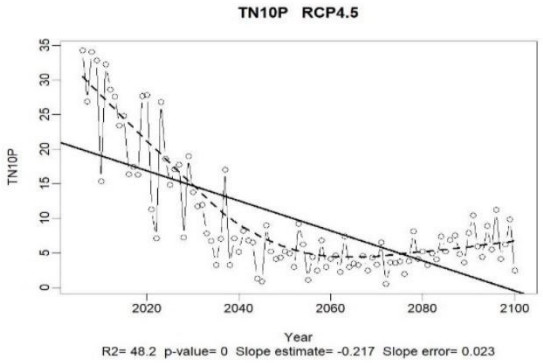
TN10P RCP4.5
TN10P
Year
R2= 48.2 p-value= 0 Slope estimate= -0.217 Slope error= 0.023

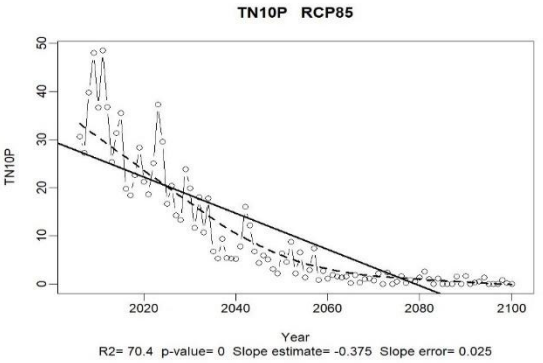
TN10P RCP85
TN10P
Year
R2= 70.4 p-value= 0 Slope estimate= -0.375 Slope error= 0.025

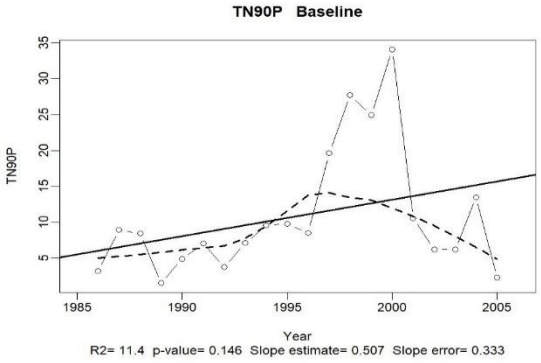
TN90P Baseline
TN90P
Year
R2= 11.4 p-value= 0.146 Slope estimate= 0.507 Slope error= 0.333

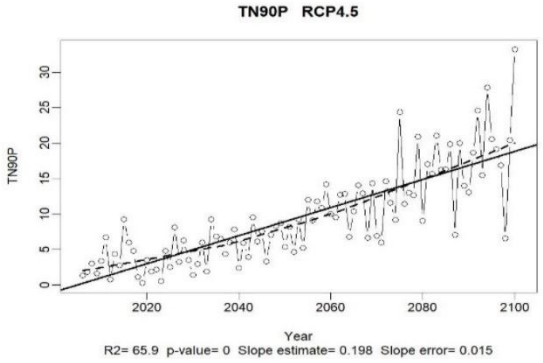
TN90P RCP4.5
TN90P
Year
R2= 65.9 p-value= 0 Slope estimate= 0.198 Slope error= 0.015

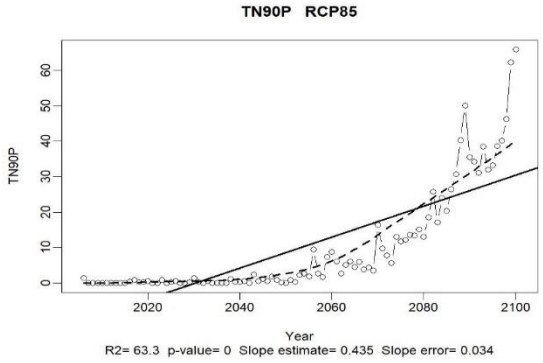
TN90P RCP85
TN90P
Year
R2= 63.3 p-value= 0 Slope estimate= 0.435 Slope error= 0.034

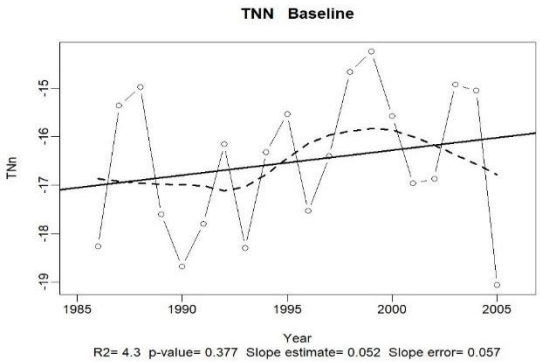
TNN Baseline
TNn
Year
R2= 4.3 p-value= 0.377 Slope estimate= 0.052 Slope error= 0.057

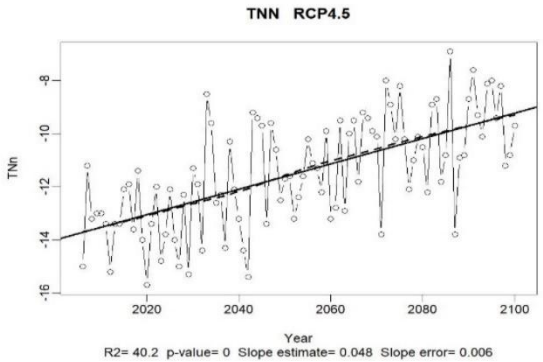
TNN RCP4.5
TNn
Year
R2= 40.2 p-value= 0 Slope estimate= 0.048 Slope error= 0.006

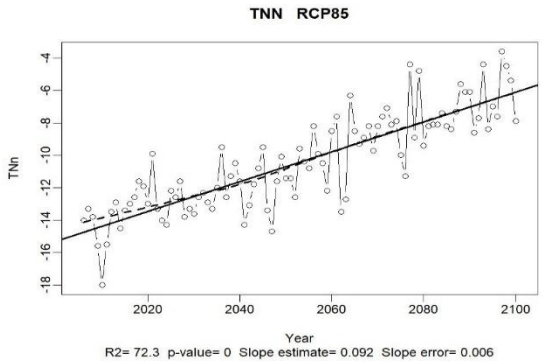
TNN RCP85
TNn
Year
R2= 72.3 p-value= 0 Slope estimate= 0.092 Slope error= 0.006

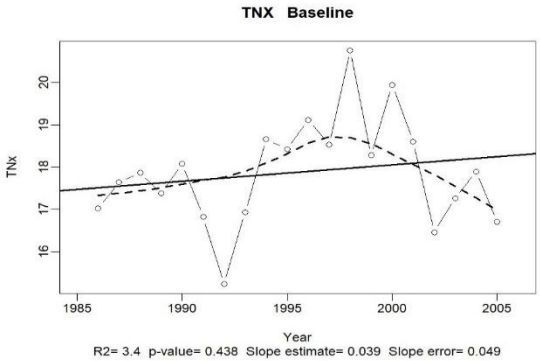
TNX Baseline
TNx
Year
R2= 3.4 p-value= 0.438 Slope estimate= 0.039 Slope error= 0.049

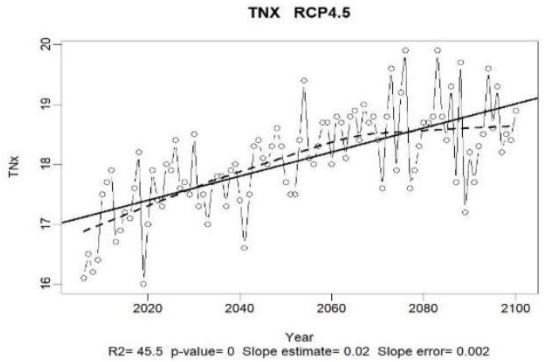
TNX RCP4.5
TNx
Year
R2= 45.5 p-value= 0 Slope estimate= 0.02 Slope error= 0.002

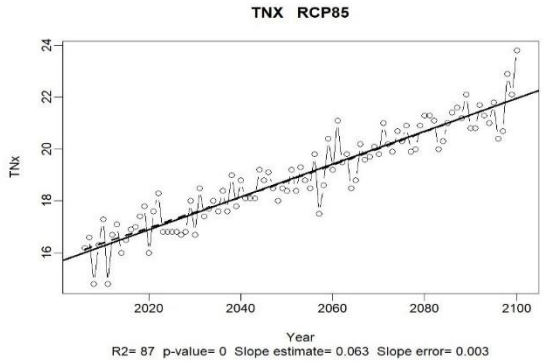
TNX RCP85
TNx
Year
R2= 87 p-value= 0 Slope estimate= 0.063 Slope error= 0.003

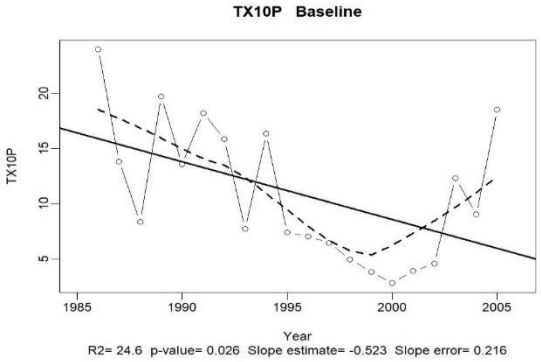
TX10P Baseline
TX10P
Year
R2= 24.6 p-value= 0.026 Slope estimate= -0.523 Slope error= 0.216

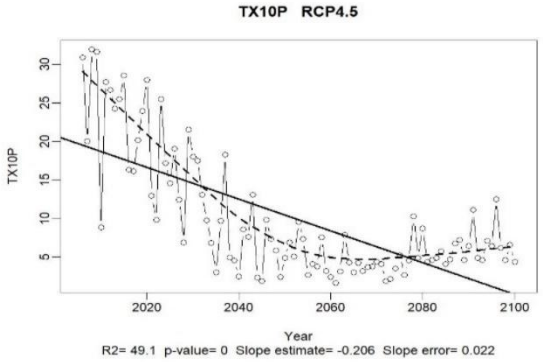
TX10P RCP4.5
TX10P
Year
R2= 49.1 p-value= 0 Slope estimate= -0.206 Slope error= 0.022

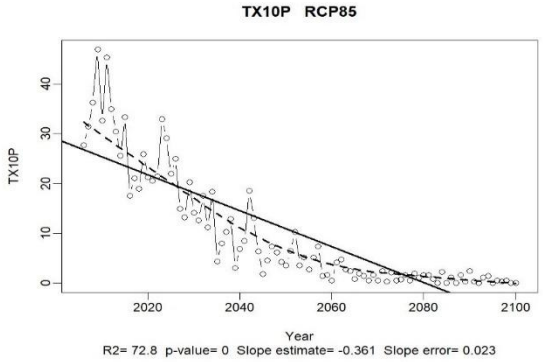
TX10P RCP85
TX10P
Year
R2= 72.8 p-value= 0 Slope estimate= -0.361 Slope error= 0.023

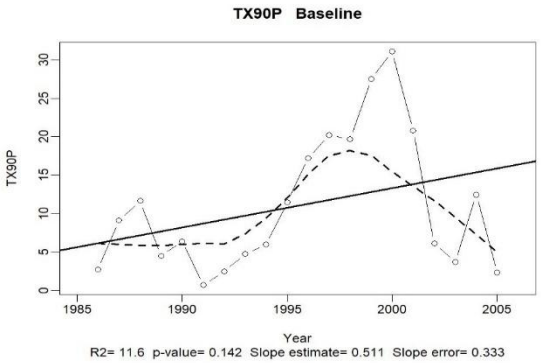
TX90P Baseline
TX90P
Year
R2= 11.6 p-value= 0.142 Slope estimate= 0.511 Slope error= 0.333

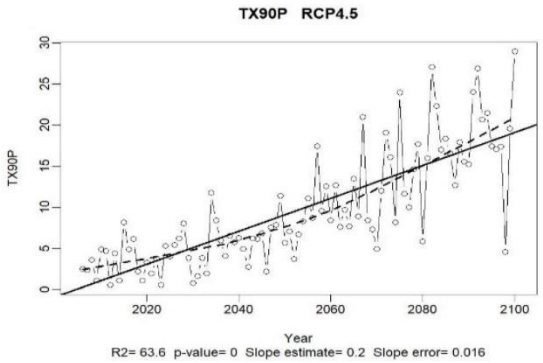
TX90P RCP4.5
TX90P
Year
R2= 63.6 p-value= 0 Slope estimate= 0.2 Slope error= 0.016

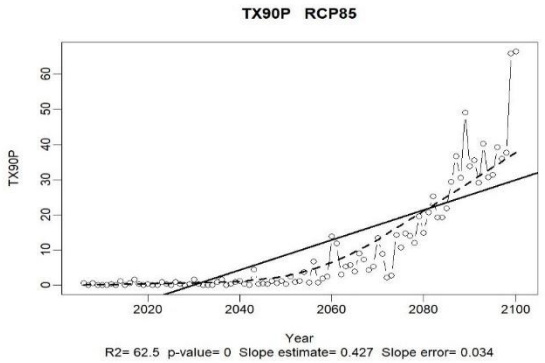
TX90P RCP85
TX90P
Year
R2= 62.5 p-value= 0 Slope estimate= 0.427 Slope error= 0.034

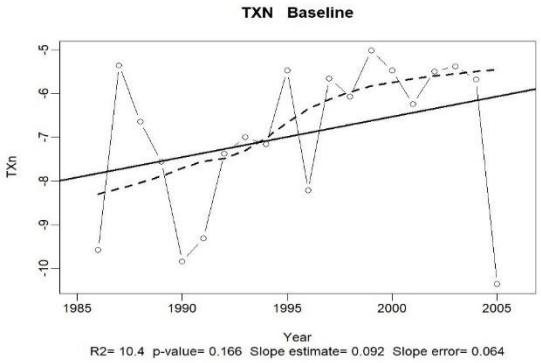
TXN Baseline
TXn
Year
R2= 10.4 p-value= 0.166 Slope estimate= 0.092 Slope error= 0.064

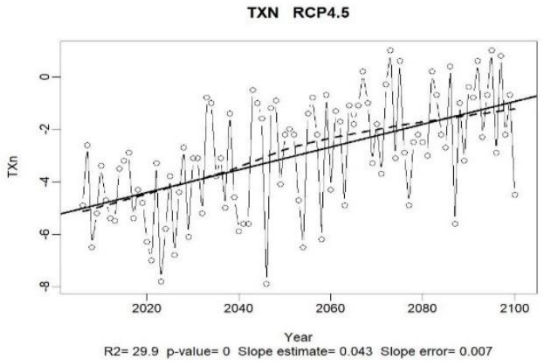
TXN RCP4.5
TXn
Year
R2= 29.9 p-value= 0 Slope estimate= 0.043 Slope error= 0.007

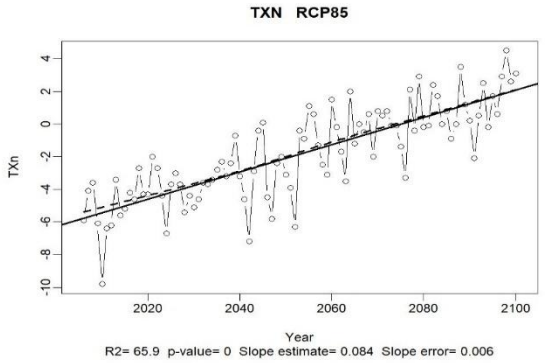
TXN RCP85
TXn
Year
R2= 65.9 p-value= 0 Slope estimate= 0.084 Slope error= 0.006

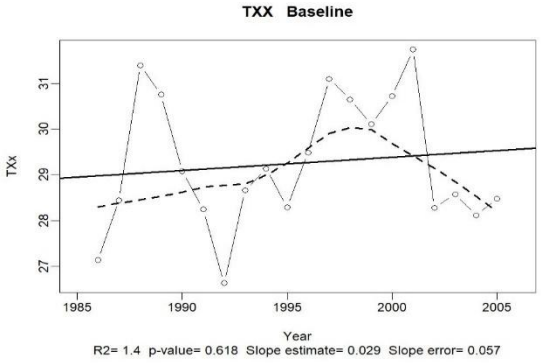
TXX Baseline
TXx
Year
R2= 1.4 p-value= 0.618 Slope estimate= 0.029 Slope error= 0.057

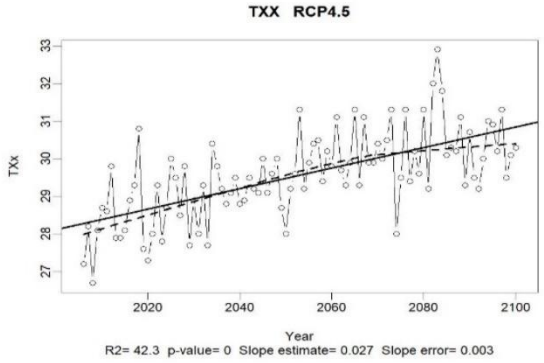
TXX RCP4.5
TXx
Year
R2= 42.3 p-value= 0 Slope estimate= 0.027 Slope error= 0.003

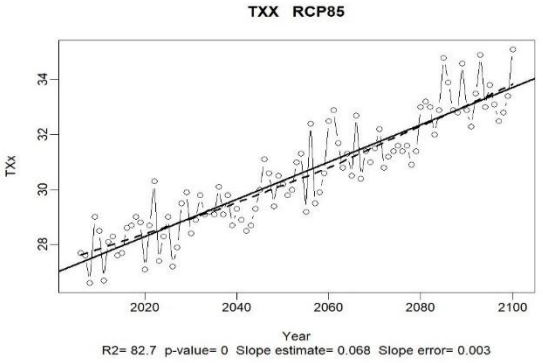
TXX RCP85
TXx
Year
R2= 82.7 p-value= 0 Slope estimate= 0.068 Slope error= 0.003

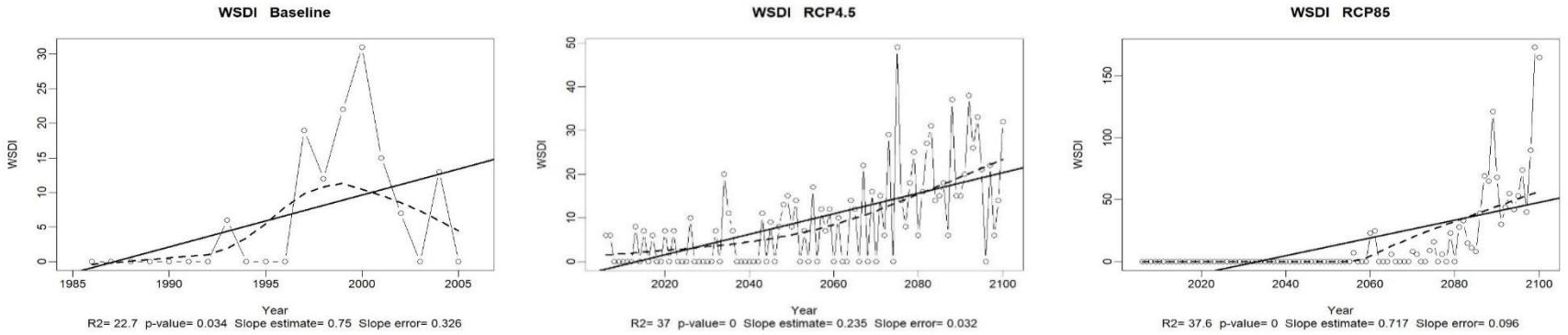

Figure A-16: Extreme indices during the base period (1986-2005) and future (2006-2100) in UKRB. The visualization of the plots is in annual series, along with trends computed by linear least square (solid line) and locally weighted linear regression (dashed line). The statistics of linear trend fitting are displayed on the plots.

This page is intentionally left blank